Roles of DNA polymerase η and replication protein A (RPA) in undamaged and platinum-treated human cells

A thesis presented to the National University of Ireland, Galway,
for the degree of Doctor of Philosophy

by

Anna Magdalena Sokol, M.Sc.

DNA Damage Response Laboratory,
Centre for Chromosome Biology,
Discipline of Biochemistry, School of Natural Sciences,
National University of Ireland, Galway

Head of School: Dr. Heinz-Peter Nasheuer
Head of Discipline: Dr. Michael P. Carty
Supervisor: Dr. Michael P. Carty

September 2012

"Nothing in life is to be feared, it is only to be understood.
Now is the time to understand more, so that we may fear less."

Maria Skłodowska-Curie

I dedicate this thesis to my fearless husband, Wojtek.

TABLE OF CONTENTS

LIST OF FIGURES

Supplementary Figures

Appendix Figures

LIST OF TABLES

ACKNOWLEDGMENTS

I would like to thank my supervisor, Dr. Michael Carty for his vast knowledge, advice and constant motivation during my PhD. Thank you for your help with this thesis. I hope you are as gone on it as I am!

To all the members of the CCB in Galway, for their imput during the weekly meetings and for sharing their resources. I would like to thank Dr. Philippe Pasero and his lab for making my stay in Montpellier an unforgettable experience. Big THANK YOU to Prof. Romuald Kondys, a gifted Physics teacher, for preventing me from becoming a German tutor!

My PhD would have been impossible to complete if it were not for the DDR team. Séverine you gave me the science bug when I first came to Ireland to do my Masters Thesis research project. I promise to keep it alive. Áine, my dear brain-twin, thank you for being such a wonderful friend that I could always count on. Thank you for throwing shoes at me and making me buy so many. Giant thanks to my bench buddy Sarah, for tolerating me by her side through all these years. You deserve the biggest RESPECT! I am also grateful for your help during the writing time, you are a friend in need and indeed. A very special message to my friend Kathleen: It is done! Thank you to former DDR team members, Elaine and Mitra. To our neighbour Laura, for her humongous heart. I will miss you all!

Thanks to all the people that made my Ireland adventure such a wonderful time. To my TC friends and writing room buddies. Special mention to THE POLISH GANG, for being a fantastic distraction from bench work. To my dear friend mitosis... I mean Aga. I know our friendship will last for at least as long as our cells will cycle.

Thanks to my homeys in Rybnik. Guys, despite the time and the distance between Poland and Ireland, despite the fact that some have gotten married, some have had children, some have cats, some have BMWs - we are the same group of people that met over a decade ago! And I love it! Jerzolu I made figure 4.2 the day you were born and I dedicate it to you. Your mum certainly did a better job than me.

I would like to sincerely thank my family, my parents, grand parents and the Karwots. Your constant motivation, support, encouragement and love has helped me become who I am today. Mum you are my biggest hero!

And finally, the biggest (most humongous) thanks to my husband Wojtek. For his love, sacrifice and tolerance throughout our life together. I appreciate it most sincerely. Thank you for making me complete.

THESIS STRUCTURE AND DECLARATION OF CONTRIBUTIONS

Thesis structure

This thesis is written in the article-based style. It consists of a short Introductory Chapter (Chapter 1: General Introduction) which leads on to the research questions and is followed by a Methodology Chapter (Chapter 2: Materials and Methods). The Results Chapters (Chapter 3 and 4) are written in the form of stand-alone manuscripts with a view to submitting these to international, peer-reviewed journals for publication. The Results Chapters are followed by a concluding Chapter summarising the findings and outlining future research directions based on these findings. Each Chapter contains references relevant to the topic. The Appendix contains (i) a short research report which provides important findings relevant to both Results Chapters; (ii) a published manuscript and (iii) one published review and one review being prepared for submission to a peer-reviewed journal.

Declaration of contributions

I declare that I have not obtained a previous qualification from the National University of Ireland, Galway or elsewhere based on this work. I conducted the experiments presented here and wrote the thesis under the supervision of Dr. Michael P. Carty. Dr. Séverine Cruet-Hennequart (NUI, Galway, Ireland) and Dr. Philippe Pasero (IGH, Montpellier, France) contributed intellectually to the research presented in Chapter 3. The experiments and data analysis presented in Figure 3.2 and Supplementary Figure 3.2 were carried out in collaboration with Dr. Philippe Pasero (IGH, Montpellier, France). My contributions to the manuscript and reviews included as Appendices are as follows:

Appendix B: I have made a substantial contribution to the published manuscript having designed, performed and analysed the experiments which constitute Figure 5 of the manuscript.

Appendix C: I have contributed to the published review by writing the section 'Role of Polη in bypass of lesions induced by platinum-based chemotherapeutic drugs'.

Appendix D: I have major contribution to the review which is in preparation for submission to *The International Journal of Molecular Sciences*. I wrote the Sections 3.2 – 5 and both designed and generated the Figures included in this manuscript.

All contributors have been acknowledged on the title page of each Chapter by the inclusion of the contributors as co-authors.

AUTHORS ABSTRACT

Platinum-based drugs are widely used in cancer therapy. Bypass of platinum-induced DNA adducts during DNA replication by specialised DNA polymerases may contribute to drug tolerance and tumour cell resistance. Human cells lacking the *POLH* gene product, DNA polymerase η (polη), are characterized by increased sensitivity to cisplatin and related platinum-based chemotherapeutic drugs. To directly investigate the role of polη in bypass of platinum-induced lesions during DNA replication *in vivo*, DNA combing was used to compare the length of individual nascent DNA strands in polη-deficient XP30RO cells and in a derivative cell line, TR30-2, in which wild-type polη is expressed from a *POLH* transgene. Following treatment with cisplatin or carboplatin, nascent DNA strands were on average up to 39% shorter in cells lacking polη than in cells expressing polη, consistent with a role for polη in bypass of platinum-induced lesions during DNA replication *in vivo*. This provides direct evidence at the level of individual DNA strands that polη modulates nascent strand length in human cells exposed to platinum-based chemotherapeutic drugs. Consistent with checkpoint activation, cisplatin and carboplatin induced phosphorylation of Chk1 on serine 317. Moreover, damage-dependent phosphorylation of histone 2AX on serine 139 was significantly increased in cells lacking polη, indicating enhanced DNA damage signalling. Phosphorylation of replication protein A (RPA), the main ssDNA binding protein was also investigated. RPA, a heterotrimeric protein, involved in most aspects of normal DNA metabolism including replication, recombination and repair, is regulated by phosphorylation of the N-terminal domain of the 34kDa RPA2 subunit. Phosphorylation is carried out in a cell-cycle-dependent manner by cyclin-dependent kinases, and following DNA damage by PIK kinases. Using EdU labelling and immunofluorescence, cisplatin- and carboplatin-induced phosphorylation of RPA2 on Ser4/Ser8 was directly correlated with the severity of replication inhibition in individual, polη-deficient cells. This data provides novel insights into the role of polη and RPA in DNA replication and the DNA damage response in human cells following treatment with platinum-based chemotherapeutic drugs. Phosphorylation of Ser4/Ser8 of RPA2 is associated with induction of DNA damage. Further investigation of RPA2 phosphorylation revealed that phosphorylation on Ser4/Ser8 could also be detected in mitotic cells. Durig mitosis the majority of the RPA2 protein is excluded from the chromatin. However, using the phospho-Ser4/Ser8 RPA2 specific antibody in immunofluorescence it was found that during normal mitosis, a fraction of RPA2 protein localised to the centrosome, near the centromere and to the midbody at various mitotic stages. RPA2 is dephosphorylated during late cytokinesis, before cells enter the G1-phase. These data may indicate a novel role for RPA in mitosis and cytokinesis in human cells.

Chapter 1: Cellular responses to platinum-based chemotherapeutics

GENERAL INTRODUCTION

Sokol A.M.[1], Carty M.P.[1]

[1] DNA Damage Response Laboratory, Centre for Chromosome Biology, Biochemistry, School of Natural Sciences, National University of Ireland, Galway, Ireland

Key words: cell cycle, cancer, chemotherapeutics, DNA damage responses, DNA repair, translesion synthesis, replication protein A (RPA)

1.1 The cell cycle

All new cells arise by the division of cells that already exist. A single cell that existed about 4 billion years ago is regarded as the ancestor for every living cell today (Nasmyth, 1995). Since that time, evolution of cells and organisms has depended on genetic information transmitted by cell division (Nasmyth, 1995). Between one division and the next, a cell must pass through a precise sequence of stages known as the cell cycle. The basic function of the cell cycle is to duplicate DNA which carries the genetic information written in a biochemical code and divide the two copies into two genetically identical daughter cells (Vermeulen et al., 2003). The eukaryotic cell cycle is divided morphologically into mitotic phase (M) and interphase (I) (Norbury and Nurse, 1992). The interphase consists of G_1, S and G_2 phases (Figure 1.1) (Norbury and Nurse, 1992). G_1 and G_2 represent gaps in the cell cycle between DNA synthesis and cell division (Figure 1.1). With the onset of G_1 phase, the cell starts protein synthesis in preparation for DNA replication, or enters the quiescent G_0 phase in the presence of inhibitory signals or unfavourable growth conditions. During S (synthesis) phase the DNA is duplicated. In G_2, the cell prepares for the mitotic phase where it undergoes nuclear and cytoplasmic divisions, referred to as mitosis and cytokinesis, respectively (Figure 1.1) (Norbury and Nurse, 1992; Vermeulen et al., 2003).

1.1.1 S-phase

A daughter cell inherits one copy of the genome which needs to be faithfully duplicated during S-phase in the dividing cell. Accurate and complete replication of DNA is essential for maintaining genome stability and for cell survival (Jones and Petermann, 2012). In eukaryotes, replication is initiated at specific sites of the genome called origins of replication. Replication origins are activated at various sites and times during S-phase (Jackson and Pombo, 1998). In late mitosis, during the process of origin licensing, replication initiation proteins localise to the chromatin and form the pre-replication complex (pre-RC). The pre-RC is composed of the origin recognition complex (ORC), cell division cycle 6 protein (CDC6) and CDC-10-dependent transcript 1 (CDT1) which then recruit six minichromosomal maintenance protein helicases (MCM2-7) (reviewed in Jones and Petermann, 2012; Maiorano et al., 2006). In *Saccharomyces cerevisiae*, the ORC complex binds to specific conserved sequences termed autonomously replicating sequences (ARS), at which replication initiation takes place (Alabert and Groth, 2012; Dhar et al., 2012). In contrast, origin firing in higher eukaryotes is not dependent on DNA sequence but is influenced by chromatin structure, nuclear organisation, gene expression and developmental stage (Alabert and Groth, 2012; Maiorano et al., 2006). Replication is initiated at the onset of S-phase by the specific phosphorylation of the pre-RC complex by CDK2-cyclinE and

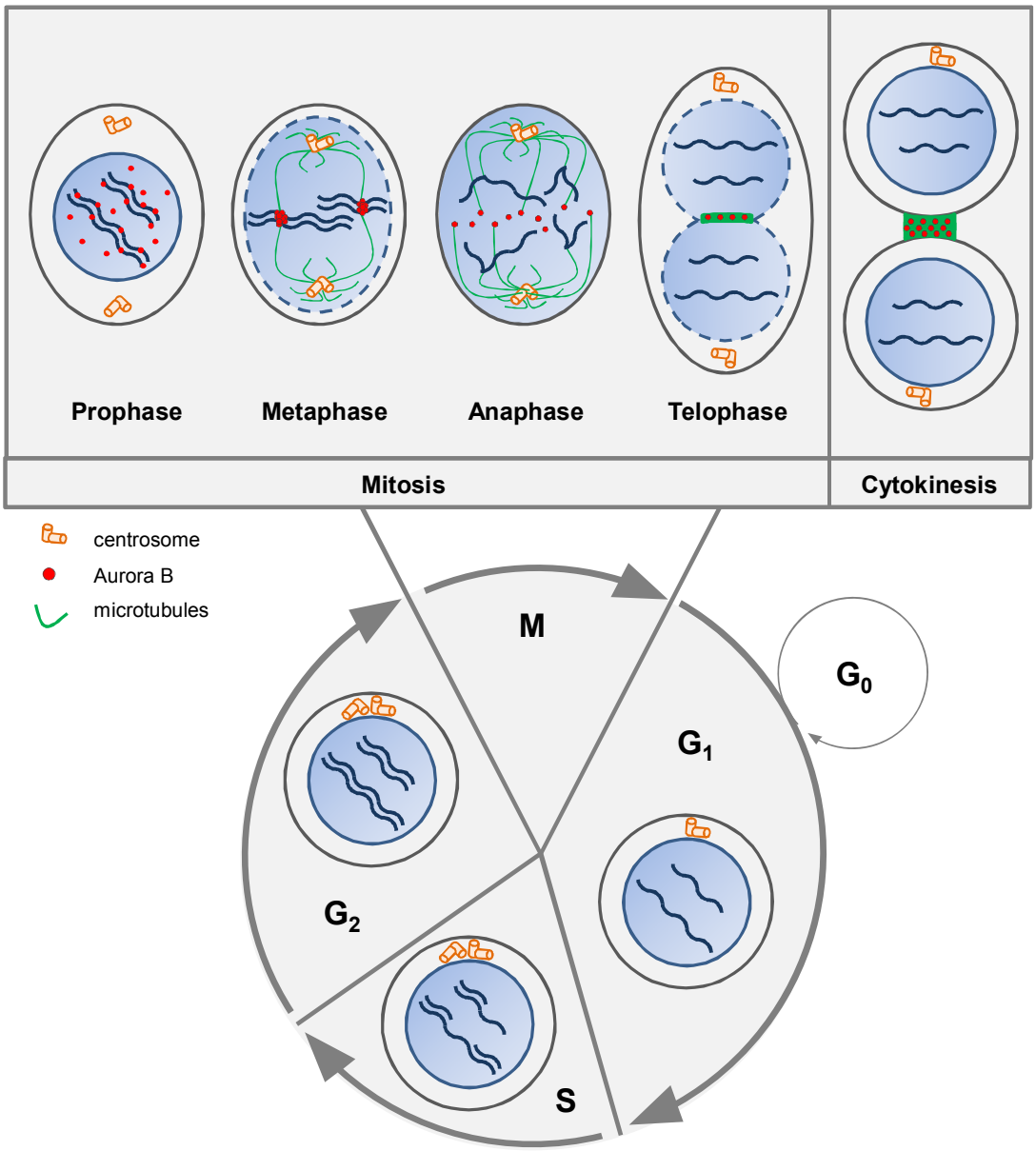

Figure 1.1 The cell cycle. The eukaryotic cell cycle comprises of two phases: interphase and mitotic phase (M). Interphase is further divided into G_1 and G_2 phases, which separate S-phase, where DNA replication occurs, from mitosis. During G_1 phase, when growth conditions are unfavourable the cell can exit the cell cycle and become senescent (G_0). The mitotic phase is further subdivided into mitosis and cytokinesis, during which nuclear and cytoplasmic division takes place. Different phases of mitosis can be distinguished by differential localisation of the chromosomes, Aurora B protein and microtubules (adapted from Carmena and Earnshaw, 2003; Morgan, 2008).

cell division cycle 7 protein (CDC7). Phosphorylation of the pre-RC complex promotes recruitment of other proteins, including cell division cycle 45 (CDC45) and the GINS (go-ichi-ni-san (five-one-two-three)) complex, activating the replicative MCM2-7 helicase in order to fully initiate origin activation, termed origin firing (reviewed in Alabert and Groth, 2012; Bell and Dutta, 2002; Jones and Petermann, 2012; Maiorano et al., 2006). Additionally, initiation of DNA synthesis requires CDC45-dependent recruitment of DNA polymerase-α-primase (Bell and Dutta, 2002). CDC45, GINS and MCM2-7 form an active

helicase which unwinds the DNA and facilitates the progression of two functional units of DNA synthesis, called replication forks (RFs) (Bell and Dutta, 2002; Maiorano et al., 2006). RF stability is ensured by claspin and the fork protection complex (FPC), composed of Timeless and Tipin proteins (Leman and Noguchi, 2012; Sercin and Kemp, 2012). The FPC serves as a connection platform between the MCM2-7 helicase and DNA polymerase α. Upon activation of MCM2-7 helicase, ssDNA regions are generated, which are bound by replication protein A (RPA) (Bell and Dutta, 2002; Maiorano et al., 2006). DNA synthesis starts with RNA primer synthesis by the DNA polymerase-α-primase holoenzyme (Bell and Dutta, 2002). These replication intermediates are substrates for replication factor C (RFC) which is involved in ATP-dependent recruitment of the DNA polymerase δ accessory factor, proliferating cell nuclear antigen (PCNA). RPA, RFC and PCNA mediate the polymerase switch from DNA polymerase-α-primase to the more processive DNA polymerases, δ or ε (Bell and Dutta, 2002; Mossi et al., 2000). Upon replication initiation, replication forks move away from the origin in a bi-directional manner (Bell and Dutta, 2002; Jones and Petermann, 2012) and each fork carries out DNA synthesis on the leading and lagging strand templates (Bell and Dutta, 2002). DNA replication terminates when opposing replication forks meet (Jones and Petermann, 2012).

1.1.2 M-phase

M-phase is the terminal phase of each normal cell cycle. Here, the cell and the previously duplicated DNA undergo dynamic processes that lead to eventual cell division. Changes in the morphology of the dividing nucleus have allowed for the distinction of the following stages in karyokinesis: prophase, metaphase, anaphase and telophase (Figure 1.1) (Norbury and Nurse, 1992; Vermeulen et al., 2003). Eukaryotic mitosis starts with the onset of prophase, during which the duplicated chromosomes condense (Figure 1.1). Prophase terminates with breakdown of the nuclear envelope (Norbury and Nurse, 1992). Metaphase is characterised by alignment of the chromosomes on the nuclear equator, called the spindle (Figure 1.1). The two identical sister chromatids that form chromosomes are separated in anaphase, and relocate to opposite spindle poles (Figure 1.1). Cells exit M-phase during telophase, upon formation of two daughter nuclei connected by the intranuclear bridge (Figure 1.1) (Norbury and Nurse, 1992; Pines and Rieder, 2001). Progression through mitosis requires major rearrangements of the cellular cytoskeleton, driven by the centrosome and associated microtubules (Kellogg et al., 1994; Mardin and Schiebel, 2012). The centrosome, also known as the microtubule organizing centre (MTOC), consists of a pair of centrioles surrounded by the pericentriolar material (PCM) and undergoes characteristic changes during the cell cycle. In proliferating cells, the centrosome duplicates once per cell cycle, in S-phase, and with the onset of mitosis, the duplicated centrosomes move to

opposite poles to form the bipolar mitotic spindle (Mardin and Schiebel, 2012). The importance of faithful centrosome duplication and function is underlined by the fact that centrosome abnormalities characterise many types of human cancers (Doxsey et al., 2005; Duensing, 2005; Kline-Smith and Walczak, 2004). The main role of the centrosome during normal mitosis is to govern microtubule function. Microtubules (MT) are polymers composed of α- and β-tubulin heterodimers, and their growth is initiated in the PCM of the centrosome by a complex containing γ-tubulin (Doxsey et al., 2005; Kline-Smith and Walczak, 2004). MTs constitute crucial elements of the cytoskeleton, and the arrangement of MTs around the centrosome dictates intracellular protein trafficking, the assembly of the mitotic spindle, cell polarity and cytokinesis. Centrosome-mediated microtubule elongation is initiated upon centrosome separation in prophase. The spindle microtubules attach to kinetochores, specialised protein structures formed at the centromere of sister chromatids, and play a role in chromosome bi-orientation during metaphase, and in the relocation of sister chromatids towards the opposite poles during anaphase. In telophase, the microtubules remain localised between the newly-formed nuclei and will form the intracellular bridge during cytokinesis (Kline-Smith and Walczak, 2004).

The central region of the intercellular bridge, where overlapping antiparallel bundles of microtubules are covered by an electron-dense matrix, is termed the midbody (Figure 1.1). Here, abscission, the final step in cytokinesis, takes place, during which the post-mitotic cells are physically separated (Fededa and Gerlich, 2012; Steigemann and Gerlich, 2009). The Aurora B kinase plays a key role in ensuring tight temporal and spatial control of mitosis and cytokinesis (Fededa and Gerlich, 2012). The Aurora B kinase, a serine/threonine kinase and member of the chromosome passenger complex, is involved in accurate attachment of microtubules to the kinetochores, and therefore in chromosome segregation to the two daughter cells (Carmena and Earnshaw, 2003). In metaphase, Aurora B relocates from the kinetochore, through the central spindle during anaphase and finally to the midbody at the onset of telophase and during cytokinesis (Figure 1.1) (Carmena and Earnshaw, 2003; Fededa and Gerlich, 2012). Aurora B is kept active by unsegregated chromatin at the spindle plane, to prevent abscission until the midbody region is chromatin-free (Fededa and Gerlich, 2012).

1.1.3 Cell cycle regulation

In eukaryotic cells, progression through each stage of the cell cycle is regulated by complexes of cyclin-dependent kinases (CDK) and cyclins (Vermeulen et al., 2003). So far, five mammalian CDKs have been identified which regulate specific phases of the cell cycle: in G1 phase: CDK4, CDK6 and CDK2; in S phase: CDK2; and in M-phase: CDK1

(Vermeulen et al., 2003). In order for CDKs to be active, the kinase must associate with the proper regulatory subunit from the cyclin protein family (Pines, 1995). While CDK levels remain stable during the cell cycle, cyclins levels change due to regulated proteolytic degradation, dictating that CDKs are only active at specific times of the cell cycle (Pines, 1991). For example, expression and degradation of cyclin B, which binds to CDK1, controls mitotic entry and exit (King et al., 1994). As mentioned before, CDK2/cyclin E activity is required for initiation of DNA replication during S-phase (Jones and Petermann, 2012; Vermeulen et al., 2003). Additionally, cyclin/CDK complex activity is regulated by phosphorylation (Vermeulen et al., 2003). The most active state is achieved when a conserved threonine residue in the CDK is phosphorylated by the CAK (CDK7–cyclin H complex) and undergoes structural rearrangements that enhance cyclin binding. In contrast, activation can be suppressed by phosphorylation on a conserved tyrosine near the N-terminal of CDKs carried out by Wee1 and Myt1 kinases. This inhibitory phosphorylation is removed by CDC25 family phosphatases (Vermeulen et al., 2003). The activity of CDC25 family proteins is influenced by cell cycle checkpoints (Kastan and Bartek, 2004), as will be discussed later.

1.2 Cancer

The importance of cell cycle and cell proliferation control is underlined by the fact that cells undergoing rapid and uncontrolled division give rise to masses of genetically abnormal tissue, called tumours, the typical symptom of cancer (Cree, 2011). Based on the ability of human tumours to metastasise and invade surrounding tissue, they are subdivided into benign and malignant, with the latter often being fatal to the entire organism (Cree, 2011; Hanahan and Weinberg, 2011). Cancer is one of the leading causes of death in the human population, in all age groups among both males and females, with the death toll being higher in developing countries (Siegel et al., 2012, http://www.who.int/cancer/en/). According to recent studies, only 5-10% of cancer cases are due to known inherited genetic abnormalities, while the rest of the cases may be potentiated by unhealthy lifestyle or diet (Anand et al., 2008). The best example is the strong relationship between cigarette smoking and lung cancer (Proctor, 2001). Cancer is a heterogeneous disease and tumours of different tissues behave different. Despite the fact that there are more than 100 distinct types of cancer, they all share common features. In 2000, Weinberg and Hannahan proposed the six hallmarks of cancer that normal cells acquire in the process of tumourogenesis and malignancy transformation (Hanahan and Weinberg, 2000). These are (i) self-sufficiency in growth signals, (ii) insensitivity to anti-growth signals, (iii) evasion of apoptosis, (iv) limitless replicative potential, (v) sustained angiogenesis and (vi) tissue invasion and

metastasis (Hanahan and Weinberg, 2000). Recently, due to advances in the field of cancer research, additional characteristics have been added to the six hallmarks of cancer cells. These include avoidance of immune destruction, and deregulation of cellular energetic pathways, with both features supporting cancer cell survival, proliferation and dissemination (Hanahan and Weinberg, 2011). All cancer hallmarks are underpinned by the genomic instability of cancer cells (Hanahan and Weinberg, 2011).

1.2.1 Cancer treatment

Cancer cells in malignant tumours can be heterogeneous in terms of their genetic instability and the precise mechanisms that allow them to undergo uncontrolled division. Understanding these specific variations at the molecular level has important implications for cancer treatment (Loeb et al., 2003). Anti-cancer strategies depend on the histological nature of the tumour and the general disease state. Surgical elimination of the tumour and neighbouring tissue remains the main treatment option for solid tumours, while radiotherapy and chemotherapy using relatively non-specific therapeutics, including platinum-based drugs, are still the widely used. While ionizing radiation is a carcinogen, as shown by the increase in thyroid cancer in children exposed following the Chernobyl nuclear accident in 1986 (Moysich et al., 2002), radiotherapy continues to be the most frequently used cancer treatment (Baskar et al., 2012).

Cancer chemotherapy constitutes the major anticancer strategy, and comprises a vast library of drugs that preferably target more than one cancer hallmark, most commonly aiming at inhibition of the cancer cell cycle and activation of cell death pathways. Chemotherapeutics can be subdivided into drugs that (i) inhibit specific cell cycle phases, (ii) induce DNA damage and (iii) inhibit DNA replication (Schmidt and Bastians, 2007). Cell division can be targeted directly by inhibitors of the mitotic spindle, thus preventing equal division of chromosomes to the two daughter cells. Anti-mitotic agents, including monastrol, are used in treatment of a variety of human solid tumours, including breast and ovarian cancer (Schmidt and Bastians, 2007; Weaver and Cleveland, 2005). Among others, platinum-based drugs constitute a group of chemotherapeutics with anti-cancer properties, which damage DNA and severely inhibit DNA replication and transcription (Table 1.1). Attempts to replicate or transcribe damaged DNA results in increased cytotoxicity, especially in rapidly dividing cancer cells (Helleday et al., 2008).

Treatment type	Drug name	DNA lesions induced
Radiotherapy and radiomimetics	Ionizing radiation	SSBs, DSBs, base damage
	Bleomycin	
Monofunctional alkylators	Alkylosulphonates	Base damage, bulky DNA adducts
	Nitrosourea compounds	
	Temozolomide	
Bifunctional alkylators	Nitrogen mustard	**DNA crosslinks, bulky DNA adducts, DBSs**
	Mitomycin C	
	Cisplatin, Carboplatin	
Anti-metabolites	5-Fluorouracil	Cytotoxic metabolite, base pairing inhibition: base damage
	Thiopurines	
	Folate analogues	
Topoisomerase inhibitors	Camptothecins (Topo I)	SSBs, DSBs
	Etoposide (Topo II)	
	Anthracyclines (doxorubicin, TopoII)	
Replication inhibitors	Aphidicolin	Replication lesions, DSBs
	Hydroxyurea	

Table 1.1 Examples of direct and indirect DNA-damaging agents used in cancer therapy. In bold, compounds used in this study (adapted from Jackson and Bartek, 2009).

1.2.2 Platinum based-chemotherapeutic drugs

Over 40 years ago, the biological activity of cis-diamminedichloroplatinum (II) or cisplatin was discovered as an unexpected outcome of an investigation into the influence of electromagnetic radiation on cell division. Exposure of *Escherichia coli* to cisplatin, derived from platinum electrodes placed in the growth chamber, resulted in a 300-fold increase in bacterial cell size, without cell division (Rosenberg et al., 1965). Further *in vivo* experiments conducted on sarcomas in mice revealed a significant influence of cisplatin on tumour regression (Rosenberg et al., 1969). Since then, cisplatin has been widely and successfully used in treatment of variety of human tumours, including germ cell tumours (in particular testicular cancer), small cell lung cancer and lymphomas. However, cisplatin treatment causes severe side effects, primarily due to nephrotoxicity, neuorotoxicity and ototocixity (Kelland, 2007; Rybak et al., 2007) Studies on cancer resistance and improvement of drug selectivity towards cancer cells led to synthesis and biological evaluation of many cisplatin analogues such as carboplatin [*cis*-diammine(1,1-cyclobutanedicarboxylate)-platinum(II)], a second-generation platinum drug used in head and neck and ovarian cancer treatment (Aabo et al., 1998; Kelland, 2007). Carboplatin has a more stable leaving group than chloride (1,1-cyclobutane-dicarboxylate). Carboplatin treatment results in lower toxicity without affecting anti-tumour efficacy and it is devoid of nephrotoxicity, neurotoxicity and toxicity towards the gastrointestinal tract (Kelland, 2007). Oxaliplatin, the third generation platinum anti-

tumour compound having a diaminocyclohexane carrier ligand, is successfully used in colorectal cancer treatment (Chaney et al., 2005; Woynarowski et al., 2000) and is among the most widely used anti-cancer drugs (Arnesano and Natile, 2009). Satraplatin, picoplatin and other drugs developed to improve the effect of cisplatin constitute the rest of the platinum-based chemotherapeutic drug family (Kelland, 2007); however, these are not in wide clinical use.

1.2.2.1 Cellular uptake

Platinum-based compounds enter the cell both by passive diffusion, driven by the difference in Cl^- concentration between the extracellular matrix (>100 mM) and cytoplasm (4–20 mM) (Arnesano and Natile, 2009; Kelland, 2007), and by active transport, using the major plasma membrane transporter, copper transporter-1 (CTR1) (Figure 1.2). Loss of CTR1 in mouse embryonic fibroblasts leads to a 65% decrease in cellular platinum accumulation when compared to wild type cells, and is accompanied by a 2-3 fold increase in drug resistance (Holzer et al., 2006). Moreover, it was found that *CTR1* expression was down-regulated in cisplatin-resistant cancer cell lines (Holzer et al., 2004; Ishida et al., 2002), thus the increase of *CTR1* expression can potentially enhance the sensitivity of cancer cells to platinum-based chemotherapy (Howell et al., 2010). Furthermore, platinum uptake was reported to depend on the activity of an as yet unidentified Na^+, K^+-ATPase, involved in maintaining a proper sodium gradient across the cell membrane (Ahmad, 2010; Andrews et al., 1991). Additionally, organic cation transporters (OCTs) are expressed in tissues that are sensitive to platinum-based drugs, and have been proposed to be involved in the cellular uptake of these agents (Figure 1.2) (Ahmad, 2010; Nelson et al., 1984).

1.2.2.2 Mechanism of action

Platinum-based chemotherapeutic drugs are biotransformed intracellularly by aquation of the leaving group (Figure 1.2) (Ahmad, 2010; Kelland, 2007). Once activated, the compounds can covalently bind to the main biological target, nuclear DNA (Wang and Lippard, 2005). Even though only 1% of total intracellular platinum reaches the DNA, the cytotoxic effects of treatment are attributed to DNA-alkylation by platinum-based drugs (Gonzalez et al., 2001). Platinum-based chemotherapeutic drugs damage DNA by covalent binding primarily at the nucleophilic N7-site of purine bases, leading to formation of monoadducts, intra- and interstrand adducts, and DNA-protein cross-links (Figure 1.2) (Eastman, 1987). Intrastrand adducts between two adjacent guanines are the most abundant adducts formed by cisplatin (Kelland, 2007; Kelland et al., 1993). The most cytotoxic adducts, interstrand cross-links (ICLs), constitute less then 1% of all adducts formed (Eastman, 1987; Kelland, 2007). Cisplatin and carboplatin share the same carrier ligand and

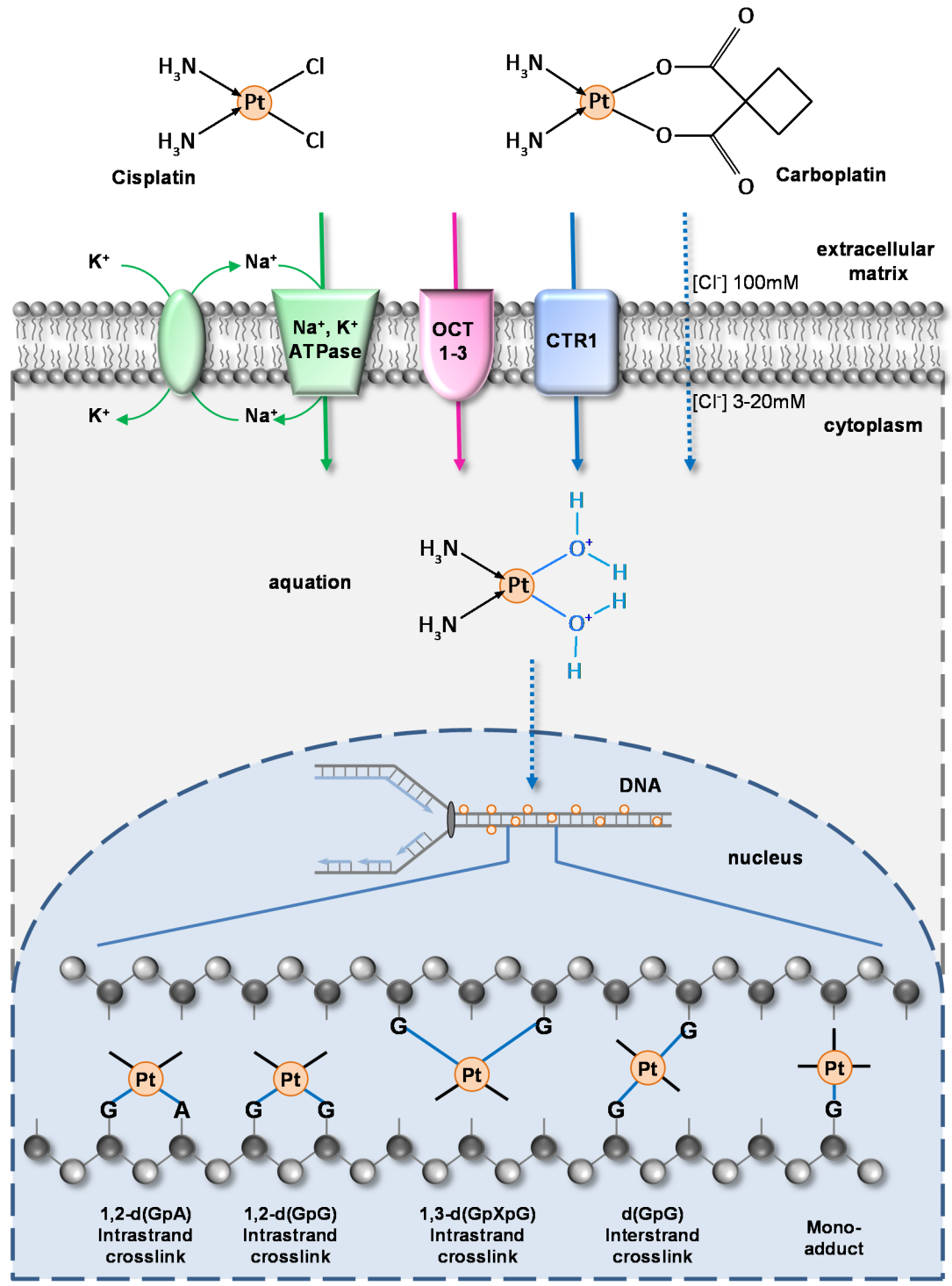

Figure 1.2 Cisplatin and carboplatin: celluar uptake and adduct formation. Drugs are transported inside the cell by active transport or passive diffusion. Upon aquation, platinum-based chemotherapeutics can form intra- and inter-strand crosslinks between the platinum atom and the N7 position of guanine or adenine (adapted from Hall et al., 2008; Kartalou and Essigmann, 2001b).

form the same type of DNA lesions, with similar frequencies *in vitro* (Table 1.2).

However, it was found that a 20-40 times higher concentration of carboplatin is needed to achieve the cytotoxicity levels induced by cisplatin (Kelland, 2007). This could be

partially explained by limited carboplatin aquation (Hongo et al., 1994) which leads to ten-fold slower DNA lesion formation compared to cisplatin. Interestingly, it was observed upon treatment of Chinese hamster ovarian (CHO) cells with equitoxic doses of cisplatin and carboplatin, that the most common DNA lesion formed was the 1,2-d(GpG)-intrastrand crosslink in the case of cisplatin treatment (Table 1.2, reviewed in Kartalou and Essigmann, 2001b), whereas in the case of carboplatin, the 1,3-d(pGpXpG) intrastrand crosslink was formed most frequently (Table 1.2, (Blommaert et al., 1995). Platinum-DNA adducts cause both bending and unwinding the DNA double helix. Various platinum-DNA lesions affect DNA structure differently. For example, the most abundant cisplatin-induced adduct, the 1,2-d(GpG) intrastrand crosslink, unwinds the double-helix by 13° and bends it by 35° towards the major grove (Bellon et al., 1991). DNA platination severely impairs DNA replication and transcription, critical processes especially for rapidly dividing cancer cells, and leads to cell death.

Adduct type	**Percentage of adduct formed**			
	In vitro		In cultured CHO cells	
	cisplatin	carboplatin	cisplatin	carboplatin
Mono-adduct	13%	22%	9%	17%
1,2-d(GpA)	19%	11%	15%	16%
1,2-d(GpG)	65%	58%	**57%**	28%
1,3-d(GpXpG)	3%	9%	18%	**38%**

Table 1.2 Frequency of platinum-DNA adducts. The percentage of DNA adducts in *in vitro* studies were obtained by atomic absorption spectroscopy (AAS). ELISA approach was used to determine platination in DNA isolated from cisplatin- or carboplatin-treated Chinese hamster ovarian (CHO) cells (adapted from Blommaert et al., 1995). In bold: the lesion formed most frequently *in vivo*.

1.3 The DNA Damage Response (DDR)

DNA damaging agents include those of exogenous origin, such as solar UV-irradiation (Pattison and Davies, 2006) or chemicals, for example, platinum-based drugs (Figure 1.3; see previous paragraph). In addition, there are endogenous sources of DNA damage, the best example being the generation of reactive origin species (ROS) as a consequence of oxidative respiration (Figure 1.3) (Valko et al., 2006). Recently, misincorporation of ribonucleotides into DNA was reported to be the most commonly occurring, endogenous nucleotide base lesion in replicating cells (Figure 1.3) (Reijns et al., 2012). While DNA damaging agents are widely used in cancer chemotherapy, in normal cells DNA lesions which block genome replication and transcription need to be processed as they constitute a severe threat to genome integrity, and to the viability of the entire organism

(Jackson and Bartek, 2009). This is mediated by a signalling cascade of DNA damage sensors, mediators, transducers and effector proteins which activate downstream cellular responses, including damage repair, cell cycle inhibition or ultimate cell death, collectively called the DNA damage response (DDR) (Figure 1.3).

1.3.1 Cell cycle checkpoints

In order to maintain genetic stability, the dividing cell must, for example, complete DNA replication before the sister chromatids are separated into two daughter cells. DNA duplication can however be inhibited by various DNA lesions, including platinum-based chemotherapeutic drugs. The cell needs therefore additional time to accurately complete S-phase before progressing further through the cell cycle. Checkpoints are critical elements of DNA damage response which evolved in response to constant exposure of cells to endogenous and exogenous sources of DNA damage (Hartwell and Weinert, 1989; Lukas et al., 2004; Vermeulen et al., 2003; Zhou and Elledge, 2000). Checkpoints operate in each phase of cell cycle and checkpoint activation in response to DNA damage is mediated by post-translational modification of proteins in the signalling cascade (Huen and Chen, 2008). Protein phosphorylation by PI-3 kinase-related protein kinases (PIKKs) plays a central role in the damage response. PIKKs are a family of eukaryotic proteins which include ataxia telangiectasia mutated (ATM), ataxia telangiectasia and Rad-3-related (ATR) and DNA protein kinase (DNA-PK) (Abraham, 2004; Kim et al., 1999). ATM, ATR and DNA-PK are high molecular weight proteins (over 300kDa), and each phosphorylates target substrates on serine or threonine residues found in SQ/TQ consensus sites (Abraham, 2004). ATM and DNA-PK are often associated with signalling from DSBs, while ATR is activated at sites of ssDNA and stalled replication forks (Huen and Chen, 2008). Another important group of protein kinases are the checkpoint kinases Chk1 and Chk2. Chk1 is activated by ATR-mediated phosphorylation whereas Chk2 activation is ATM-dependent (Stracker et al., 2009). Once active, Chk1 and Chk2 phosphorylate and downregulate the activity of CDC25 proteins, which directly regulates cell cycle progression (Section 1.1.1; Kastan and Bartek, 2004; Stracker et al., 2009).

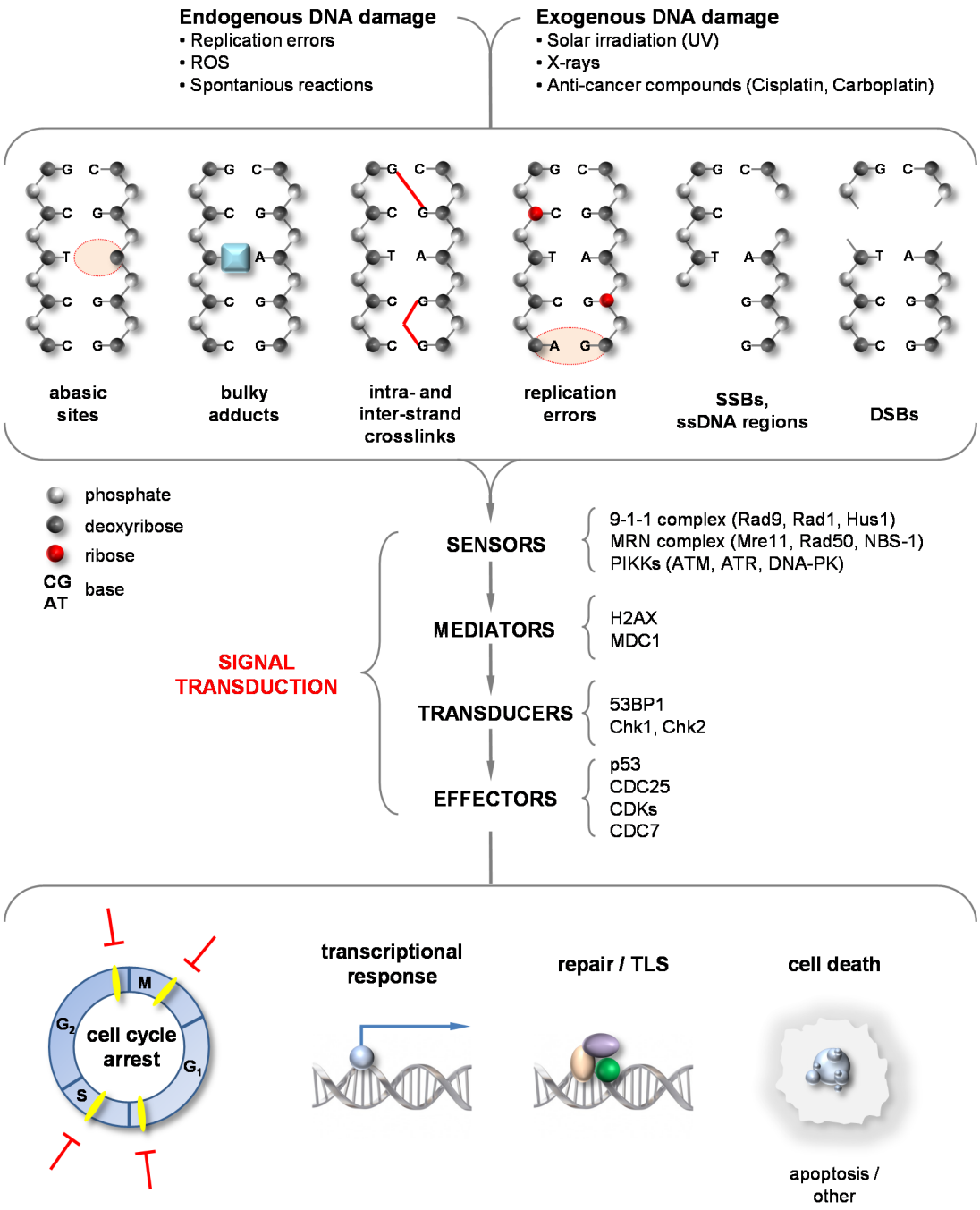

Figure 1.3 Overview of DNA damage and the DNA damage response. DNA can be damaged from both endogenous and exogenous sources. Following DNA damage, cells activate a cascade of signalling events in which a series of damage sensor, mediator, transducer and effector proteins dictate cellular fate (adapted from (Hoeijmakers, 2001; Niida and Nakanishi, 2006; Zhou and Elledge, 2000).

1.3.1.1 The DNA replication checkpoint

In S-phase, the ongoing replication fork (RF) can be compromised by DNA lesions induced by exogenous DNA damaging agents such as platinum-based chemotherapeutic drugs (Hoffmann et al., 1995; Lindahl, 1993; Villani et al., 1988). Naturally occurring barriers to ongoing replication include DNA binding proteins, late replication zones and

transcription units (Branzei and Foiani, 2010). Collectively, these unusual DNA structures modulate RF dynamics and can activate replication checkpoints to prevent DNA damage (Branzei and Foiani, 2010; Jones and Petermann, 2012). The replication checkpoint is proposed to play a role in (i) inhibition of new origin firing, (ii) down-regulation of the rate of DNA synthesis and (iii) replication fork (RF) stabilization in order to allow repair the DNA damage and prevent fork collapse (Jones and Petermann, 2012). However, a recent study has shown that the checkpoint function is not required for fork stabilisation in *Saccharomyces pombe* (De Piccoli et al., 2012). It was found that the DNA damage-dependent S-phase checkpoint response and the subsequent phosphorylation of proteins involved in DNA replication, controls the function of the replisome rather than its' stability, since RFs were found to be stable in the absence of the checkpoint kinases Mec1 and Rad53 (homologues of human ATR and Chk2) (De Piccoli et al., 2012).

Alterations in DNA structure, such as adducts that block the activity of replicative DNA polymerases, can lead to uncoupling of polymerase and helicase activities at the replication fork (Byun et al., 2005), generating of regions of ssDNA (Zou and Elledge, 2003). ssDNA is a substrate for replication protein A (RPA) binding. ATR is recruited to the sites of stalled forks by the interaction of ATRIP (ATR-interacting protein) with ssDNA-bound RPA (Zou and Elledge, 2003). ATR activation requires Rad17-mediated loading of the 9-1-1 (Rad1-Rad9-Hus1) complex which recruits TopBP1 (topoisomerase IIb binding protein 1) (Figure 1.4) (reviewed in (Allen et al., 2011). Then, the Timeless-Tipin (TIM-Tipin) complex is recruited through the interaction of Tipin with RPA2, which allows association of Claspin-Chk1 with the damage site (Figure 1.4). Interaction of ATR with Claspin is essential for efficient phosphorylation of Chk1 by ATR, and, therefore, for checkpoint activation (Kemp et al., 2010). Activated ATR phosphorylates a number of other proteins involved in downstream signalling and stabilisation of the inhibited replication fork, including RPA and H2AX (Figure 1.4) (Matsuoka et al., 2007).

In mammalian cells, activated Chk1 phosphorylates CDC25A, a phosphotyrosine phosphatase. Phosphorylated CDC25A is excluded from the nucleus, and targeted for subsequent ubiquitination and degradation (Sanchez et al., 1997; Sorensen et al., 2003). Down-regulation of CDC25A suppresses CDK function thus inhibiting both cell cycle progression and origin firing (see Section 1.1.1; Section 1.1.3) (Maya-Mendoza et al., 2007; Petermann et al., 2010; Sanchez et al., 1997). Chk1-mediated inhibition of cell cycle progression provides time for DNA repair to occur (Speroni et al., 2012; Zhou and Elledge, 2000). Moreover, Chk1 activity has been recently proposed to play a role in fork progression past UV-induced DNA lesions mediated by translesion synthesis (TLS) (Figure 1.4) (Elvers et al., 2012; Speroni et al., 2012).

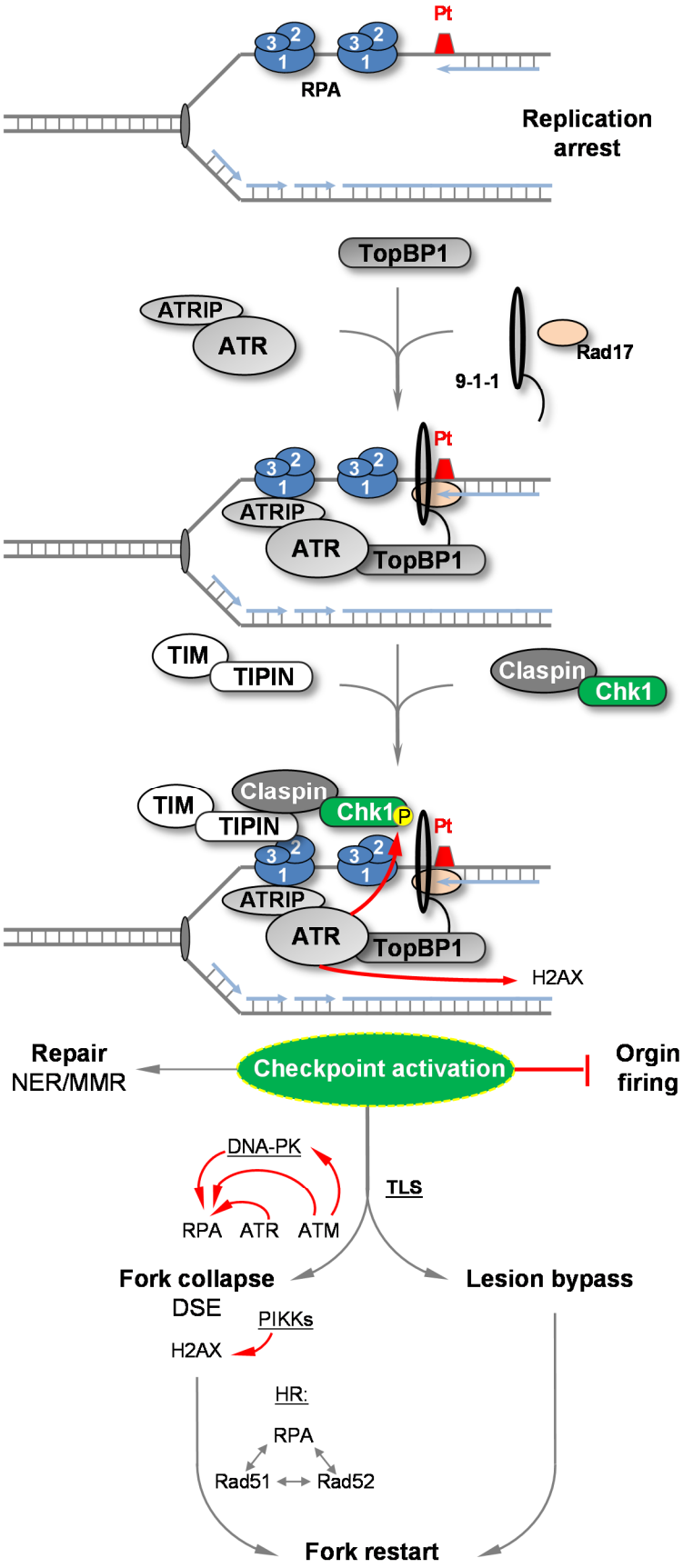

Figure 1.4 Platinum-induced replication checkpoint activation. Stalling of ongoing replication fork at the sites of platinum-induced DNA lesions generates ssDNA that is coated by RPA, leading to

recruitment of the ATR-ATRIP complex. ATR activation recruits TopBP1, mediated by the 9-1-1 complex. Interaction of the RPA2 subunit of RPA with the Tipin subunit of the Timeless-Tipin complex faciliates association of Claspin-Chk1 with ATR. Phosphorylation of Chk1 by ATR at the DNA damage site activates the replication checkpoint. The checkpoint inhibits cell cycle progression, prevents new origins from firing, provides more time for damage repair and allows for lesion bypass in TLS-mediated manner. In the case of fork collapse the DSE that is generated must be repaired before the fork restarts (adapted from Allen et al., 2011; Kemp et al., 2010).

DNA replication resumes following removal of the DNA lesion or following bypass synthesis. If DNA repair or lesion bypass is deficient, delayed restart of the replication fork can lead to fork collapse and to the generation of double-strand ends (DSE) (Allen et al., 2011). DSE can be also generated when an ongoing replication fork encounters a ssDNA break. Homologous recombination-mediated DSE repair in S-phase is necessary for the stalled fork to restart (Figure 1.4) (Allen et al., 2011).

Arrested replication forks can also be restarted by repriming of DNA synthesis downstream from the lesion. In fact, studies in bacteria have revealed that lesion-compromised replication can be directly restarted by DNA primase-dependent, *de novo* synthesis of an RNA primer on the leading strand template (Heller and Marians, 2006; Yeeles and Marians, 2011). Moreover, discontinuous DNA synthesis on the leading strand was also observed in UV-treated budding yeast, suggesting that re-priming occurs on the leading strand in eukaryotes (Lopes et al., 2006). The remaining gaps are proposed to be repaired post-replicatively, for example by translesion synthesis (Branzei and Foiani, 2010; Lehmann and Fuchs, 2006). In higher eukaryotes there is evidence that that both lesion bypass at arrested forks, and repriming downstream from the lesion may occur.

1.3.2 DNA repair

Checkpoint activity throughout the cell cycle provides additional time for DNA repair. More then 150 genes in human cells encode proteins involved in DNA repair (Wood et al., 2005). These genes can be subdivided into two groups. The first group consists of genes encoding proteins involved in DNA damage signalling and regulation of DNA repair, while genes in the second group encode proteins that directly carry out DNA repair, via mismatch repair (MMR), base excision repair (BER), nucleotide excision repair (NER) and DSB repair (Wood et al., 2005).

BER is the major repair pathway for minor chemical alteration of bases and for DNA SSBs, which mostly arise from endogenous origin (Branzei and Foiani, 2008). NER plays an important role in repair of a wide range of helix-distorting lesions, including platinum-induced lesions (Figure 1.4). Base-pair mismatches and insertion/deletion mispairs,

generated by errors during DNA replication or as result of recombination, are repaired by MMR, which operates primarily in S-phase (Li, 2008). Mutations in genes encoding repair proteins underlie a number of human cancer-prone diseases (Table 1.3; Christmann et al., 2003; Hoeijmakers, 2001). The choice of which repair pathway is employed depends on the type of DNA damage and on the cell cycle phase (Branzei and Foiani, 2008).

Disease	Deficiecy in process/mutated gene(s)	Major cancer predisposition
Hereditary non-polyposis colon cancer (HNPCC)	MMR: *MSH2 PMS1, PMS2 MLH1*	Colorectal cancer
Xeroderma pigmentosum	NER: *XPA-XPG*	UV-induced skin cancer
Xeroderma pigmentosum variant	TLS: *POLH*	UV-induced skin cancer
Familial breast, ovarian carcinoma syndrome	HR:*BRCA1/BRCA2*	Breast/ovarian cancer
Nijmegen breakage syndrome (NBS)	DSBs repair: *NBS1*	Lymphomas

Table 1.3 Examples of human cancer-prone disorders resulting from mutations in DNA repair genes (Christmann et al., 2003; Hoeijmakers, 2001; Hoeijmakers, 2009).

1.3.2.1 Translesion synthesis (TLS) and DNA polymerase η (polη)

Not all lesions are repaired before cells enter the S-phase. Some of these remaining lesions, including platinum-DNA lesions, constitute an obstacle for the major replicative DNA polymerases, α, δ and ε (Hoffmann et al., 1995; Villani et al., 1988). The process of translesion synthesis (TLS) plays an important role in preventing replication fork collapse at the sites of replication arrest, by allowing DNA synthesis to continue past unrepaired lesion in the DNA (Masutani et al., 2000; Vaisman et al., 2000). Therefore, in the context of anti-cancer drugs, TLS is considered to play an important role in DNA damage tolerance and resistance (Masutani et al., 2000; Vaisman et al., 2000), as well as in the mutagenicity of DNA adducts in dividing cells (Chaney et al., 2005; Vaisman et al., 2000). Translesion synthesis is carried out by specialised DNA polymerases, including DNA polymerase η (polη). Polη, a 78kDa protein encoded by the human *POLH* gene belongs to the Y family of DNA polymerases,is primarily involved in accurate bypass of UV-induced dithymine cyclobutane pyrimidine dimers (CPD) (Johnson et al., 1999a; Masutani et al., 1999). Mutations in *POLH* have been found in all patients with the skin cancer-prone, genetic disease, xeroderma pigmentosum variant (Table 1.3) (for review see attached Appendix C; Cruet-Hennequart et al., 2010; Johnson et al., 1999a; Masutani et al., 1999). In the absence

of polη in XPV patients, mutations accumulate at sites of UV-induced CPDs, ultimately leading to increased skin cancer incidence (Cleaver, 1972; Johnson et al., 1999b; McCulloch et al., 2004).

In addition to the major role of polη in error-free replication at sites of UV-induced CPDs, *in vitro* studies show that polη exhibits the highest efficiency in carrying out DNA synthesis past Pt-DNA 1,2-d-(GpG)-intrastrand adducts, compared to other eukaryotic DNA polymerases (Masutani et al., 2000; Vaisman et al., 2000). Whereas platinum adducts completely block synthesis by DNA polymerases α, ε and δ polymerases (Hoffmann et al., 1995; Villani et al., 1988) even in the presence of accessory proteins including PCNA or RPA (Hoffmann et al., 1995), polη could bypass these lesions more efficiently than other X, B and Y family polymerases (Vaisman et al., 1999; Vaisman et al., 2000).

1.3.2.1.1 Translesion synthesis by polη on platinum-damaged DNA

Translesion synthesis (TLS) polymerases are recruited to sites of damaged DNA by Rad6-Rad18 mediated mono-ubiquitination of PCNA (for review see attached Appendix C; Cruet-Hennequart et al., 2010; Kannouche and Lehmann, 2004; Lehmann et al., 2007; Strzalka and Ziemienowicz, 2011). During this process, called the polymerase switch, the normal replicative polymerase is replaced by the specialised TLS DNA polymerase at the lesion site (Cruet-Hennequart et al., 2010; Lehmann et al., 2007). Following bypass, the TLS polymerase dissociates, and processive synthesis by pol δ or ε resumes. Polη interacts with PCNA through a C-terminal PCNA-interaction domain, and it further interacts with ubiquitinated PCNA through a separate ubiquitin-binding domain also located in the C-terminus (Acharya et al., 2008; Cruet-Hennequart et al., 2010; Kannouche et al., 2004). Interaction of polη with ubiquitinated PCNA stabilises the protein at the replication fork (Acharya et al., 2008). PCNA can also be further ubiquitinated, and PCNA polyubiquitination was found to play a role in the bypass of damaged DNA by the process of template switching (Lee and Myung, 2008; Strzalka and Ziemienowicz, 2011). The function of PCNA can also by modified by SUMOylation (Lee and Myung, 2008). Studies is yeast revealed that PCNA is SUMOylated upon loading of the protein onto DNA during normal DNA replication in S-phase, and this modification was found to suppress recombination and the establishment of cohesion (Lee and Myung, 2008; Strzalka and Ziemienowicz, 2011). However the role of PCNA SUMOylation in DNA synthesis in vertebrate cells is less well understood.

Recent biochemical and structural analyses have provided insights into the unique structural features of polη, that allow for bypass of platinum-DNA adducts (Alt et al., 2007; Biertumpfel et al., 2010; Ummat et al., 2012; Zhao et al., 2012). The catalytic core of yeast

pol η was crystallized in a ternary complexes with an oligonucleotide template containing 1,2 d(GpG)-Pt lesion, along with incoming dNTPs, and two different primers (Alt et al., 2007). A series of crystals were generated in which the protein was crystallised in the 'pre-elongation' and the 'elongation' step of lesion bypass. It was found that, as polη encounters the Pt-DNA adduct in the 'pre-elongation' complex, the adduct is situated outside the active site. The first guanine residue (3'dG) of the cisplatin adduct, is positioned away from the incoming dCTP that is situated in the active site even in the absence of template. In addition to dCTP, two metal ions are also present in the active site (Alt et al., 2007). The metal ions are coordinated by catalytically essential residues, Asp30, Asp155 and Glu156 residues (catalytic triad) (Figure 1.5). When the template-primer complex rotates to initiate the 3'dG elongation step, the 1,2 d(GpG)-Pt adduct is partially situated in the active site. The 3'dG of the lesion forms a standard Watson-Crick base pair with the incoming dCTP. The α-phosphate of the incoming dCTP is coordinated by Arg73, and the decrease in the distance between this group and the 3'OH nucleophile enables nucleotidyl transfer to take place (Alt et al., 2007). Consistent with this, mutation of Arg73 to leucine reduced bypass of Pt-DNA adducts by polη by slowing down the first step and inhibiting of the second step of the process (Alt et al., 2007; Washington et al., 2001). This first step of TLS is efficient and accurate, and is guided by the H-bonds and by the backbone of polη at Phe35 (Figure 1.5). In contrast to the first step in lesion bypass, the second step, which involves incorporation of a nucleotide opposite the second guanine residue, is slower and can result in incorporation of dCTP or dATP (Alt et al., 2007; Masutani et al., 2000). The decrease in specificity is caused by the influence of the cross-linking Pt-bond on the orientation of the 5'dG in the active site. Because of the Pt-crosslink, only one H-bond can be formed, and the distance between 3'OH nucleophile and the α-phosphate of the incoming nucleotide is therefore significantly larger than in the first step (Alt et al., 2007). This allows for incorporation of either dATP and dCTP opposite the 5'dG residue of the adduct (Alt et al., 2007). Overall, the results obtained from the crystallographic studies are consistent with data generated *in vitro* from bypass of oligonucleotide templates by purified polη (Masutani et al., 2000). Recently, human polη was crystallised in four different steps in the process of DNA replication on either undamaged DNA or on a template containing a cisplatin-1,2-d(GpG)cross-link (Zhao et al., 2012). Consistent with the results from structural analysis of yeast polη described above, it was found that, during TLS bypass of platinum-damaged DNA, incorporation of the first nucleotide occurred in an error-free manner and with the highest efficiency (Zhao et al., 2012). The catalytic triad was found to be conserved, and Arg61 (corresponding to yeast Arg73) was found to interact with the phosphate and the base of the incoming nucleotide (Figure 1.5) (Ummat et al., 2012; Zhao et al., 2012). The importance of the conserved Gln38

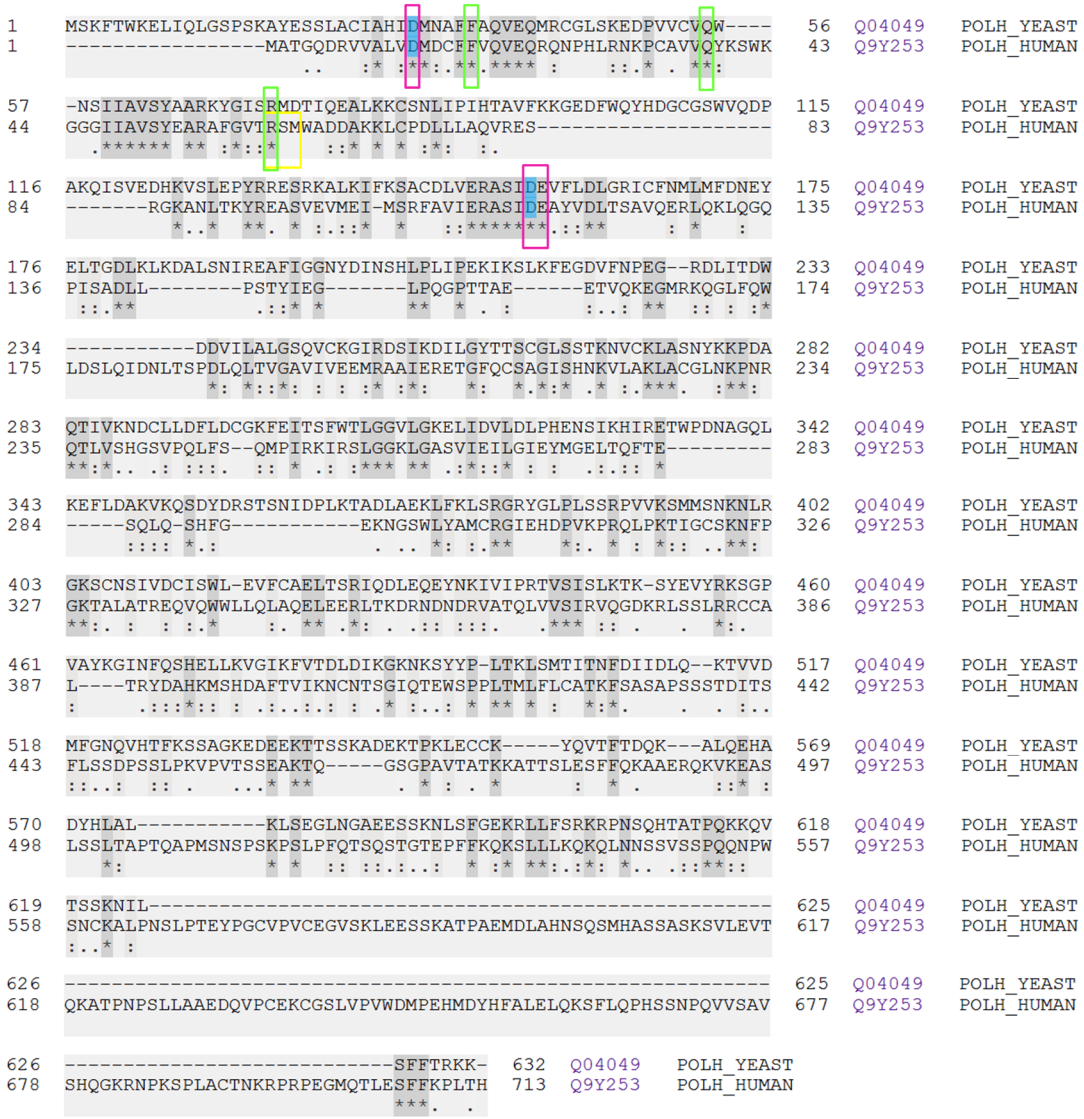

Figure 1.5 Alignment of yeast *RAD30* and human *POLH* gene products. Analysis was carried out using the www.uniprot.org website. Identical residues are shown in a dark gray background and marked with an asterisk (*). The catalytic triad is marked in pink, and amino acids directly interacting with metal ions are marked in blue. Conserved residues, responsible for proper positioning of the damaged DNA template and the incoming nucleotide are marked in green. The dynamic loop, unique for human polη marked in yellow.

(corresponding to yeast Gln55) in stabilising the damaged template within the active site was underlined by the fact that mutation of Gln38 to alanine resulted in a 70% decrease in the *in vitro* catalytic activity of human polη for the incorporation of dCTP opposite the 3'dG in the 1,2-d(GpG)-Pt crosslink (Figure 1.5) (Ummat et al., 2012). Interestingly, human polη was found to undergo a unique conformational change during translesion synthesis. In order to accommodate the large 1,2- d(GpG)-Pt adduct, a protein loop containing Arg61-Ser62-Met63 (Arg61-Met63, Figure 1.5) shifts, opening the active site, which allows the lesion to be accommodated in the stacked-in conformation, and maintains dCTP binding (Zhao et al., 2012).

As already noted, purified polη efficiently bypasses the 3'dG of the 1,2-d(GpG)-Pt crosslink, with 82% catalytic efficiency relative to undamaged DNA (Zhao et al., 2012). However, the catalytic activity drops to 35% during insertion of a dCTP opposite the 5'dG of the lesion (Zhao et al., 2012). It has been proposed that translesion synthesis operates in two steps and is carried out by two translesion polymerases, the 'inserter' and the 'extender' (Prakash et al., 2005). In this model, polη inserts the incoming nucleotides across from dinucleotide lesions in damaged DNA, while elongation from the resulting primer-terminus is carried out by other DNA polymerases. Pol ζ, a member of B-family polymerases, has been proposed to carry out extension of platinum-DNA lesions that are bypassed by polη (Shachar et al., 2009; Ummat et al., 2012).

The biochemical and structural studies described here provide good evidence that polη can bypass cisplatin-induced intrastrand 1,2-d(GpG)-adducts. Coupled with evidence that polη-deficient cell lines are sensitive to platinum-based drugs, this indicates that polη plays a role in bypass of platinum-DNA adducts in genomic DNA *in vivo* (Bassett et al., 2004; Chen et al., 2006; Cruet-Hennequart et al., 2008; Cruet-Hennequart et al., 2009). However, to date there is no direct evidence that polη expression modulates the length of nascent strands in cells exposed to cisplatin or related agents.

To conclude, due to unique structural features including a very open active site, polη can play a dual role in human cells. While the major role of polη is to protect against mutagenesis at UV-induced cyclobutane pyrimidine dimers, it may also contribute to the resistance of tumours to platinum-based chemotherapy, by carrying out bypass of platinum-induced lesions in DNA (Ceppi et al., 2009; Teng et al., 2010).

Apart from its role in intrastrand DNA lesion bypass, polη has been reported to play a role in HR-mediated ICL repair (Ho et al., 2011; Ho and Schärer, 2010; Zheng et al., 2003). Consistent with this, there is *in vitro* (McIlwraith et al., 2005) and *in vivo* (Kawamoto et al., 2005) evidence that polη can play a role in homologous recombination, by extending the D-loop upon Rad51-mediated sequence homology search and invasion. This suggests that, polη may modulate the outcome to platinum-induced DNA damage through its activity in more than one cellular process. However, given that intrastrand crosslink constitute more than 90% of platinum-induced adducts in DNA, and the strong biochemical evidence for polη-mediated bypass of these lesions, further investigation of the role of polη in replication of platinum-damage in genomic DNA in human cells is warranted.

1.3.2.2 DNA double-strand break (DSB) repair

Prolonged arrest of replication forks at platinum-induced DNA damage sites can eventually lead to fork collapse, generating DNA double strand ends (DSEs) (Branzei and Foiani, 2007). DSEs and DSBs constitute a serious threat to genome integrity, and can result in gene deletions, loss of heterozygosity, translocations and chromosome loss (Shrivastav et al., 2008). These lesions are sensed rapidly and provoke an extensive response in chromatin flanking the break, highlighted by PIKK-dependent phosphorylation of histone H2AX on Ser139, generating γH2AX (Chanoux et al., 2009; Revet et al., 2011) and 53-binding protein 1 (53BP1) recruitment (Schultz et al., 2000). In human cells, there are two major pathways for repair of DSBs: non-homologous end joining (NHEJ) and homologous recombination (HR) (Hartlerode and Scully, 2009; Shrivastav et al., 2008). While NHEJ is an error-prone pathway due to the potential loss of sequence information during end resection, HR is generally considered to be error-free since homologous DNA sequences are used as templates for repair. Thus, accessibility of homologous sequences, for example in sister chromatids, restricts HR activity to the S- and G_2 phases of the cell cycle (Hartlerode and Scully, 2009; Shrivastav et al., 2008). Consistent with this, DSB repair by NHEJ pathway is more important in the G_1, G_0 and early S-phases (Hartlerode and Scully, 2009; Shrivastav et al., 2008).

1.3.2.2.1 Non-homologous end joining (NHEJ)

The first step of non-homologous end-joining (NHEJ) requires DSB detection by the Ku70/Ku80 heterodimer. Ku70/Ku80 binds to broken DNA ends with high affinity, in a structure-specific but sequence-independent manner (Cary et al., 1997; Walker et al., 2001). Following binding, the Ku heterodimer recruits and activate the catalytic subunit, DNA-PK_{cs}. Ku70/Ku80 and DNA-PK_{cs} comprise the PIK kinase, DNA-PK (Yaneva et al., 1997)., The protein Artemis is then recruited, a 5'-3' exonuclease, which upon binding to the site of DSB is phosphorylated in a DNA-PK-dependent manner and processes DSB ends (Hartlerode and Scully, 2009; Ma et al., 2002). NHEJ-mediated resolution of DSBs requires ligation of the DNA ends mediated by the X4-L4, protein complex comprising of XRCC4 (X-ray repair complementing defective repair in Chinese hamster cells 4), DNA ligase IV and XLF (XRCC4-like factor) (Hartlerode and Scully, 2009).

1.3.2.2.2 Homologous recombination (HR)

The homologous recombination (HR) pathway repairs double-strand breaks (DSBs) and double-strand ends (DSEs), in particular in S phase. In addition, 'chicken foot'-type structures arising from reversed forks resulting from replication arrest may also be substrates

for HR (Helleday, 2003). HR is initiated with damage recognition by MRN complex, consisting of Mre11-Rad50-NBS1 (Meiotic recombination 11-Radiation sensitive 50-Nijmegen breakage syndrome 1). This is followed by degradation of one end of the DNA by the 5'-3' exonuclease activity of MRN complex, resulting in the formation of a 3' ssDNA overhang. RPA binds the ssDNA overhang, while radiation-sensitive 52 recombinase (Rad52) binds to the 3' ssDNA end (Bernstein and Rothstein, 2009; Hartlerode and Scully, 2009). Next, upon RPA phosphorylation, radiation sensitive 51recombinase (Rad51), binds to the site of damage in a process mediated by Rad52- and BRCA-2 (breast cancer 2). Rad51 forms a nucleofilament on the DNA and initiates the search for a homologous sequence (Bernstein and Rothstein, 2009; Deng et al., 2009; Hartlerode and Scully, 2009). Once a homologous region is located, Rad51 mediates strand invasion, leading to D-loop formation. The 3' end of the damaged DNA is extended and information is copied from the undamaged strand (possibly by polη, see Section 1.3.2.1.1). This results in formation of a Holliday junction which must be resolved in order for HR to terminate (Bernstein and Rothstein, 2009; Hartlerode and Scully, 2009).

1.3.3 Replication Protein A – a key player in the DNA damage response

Replication protein A (RPA), is heterotrimeric complex of 70, 34 and 14 kDa subunits (RPA1, RPA2, RPA3, respectively), is the main ssDNA binding protein in mammalian cells (Wold and Kelly, 1988). The single-stranded DNA binding activity is mainly due to the RPA1 subunit. RPA plays a key role in all aspects of DNA metabolism in which single-stranded DNA is generated, including DNA replication, repair and recombination.

RPA is required for both the initiation and elongation phases of DNA replication. RPA associates with origins of replication in a CDC45-dependent manner, and is required for the replication activity of processive polymerases (Section 1.1.1) (Kenny et al., 1989; Tsurimoto and Stillman, 1991a; Tsurimoto and Stillman, 1991b). Additionally, RPA has an key role in recruitment of ATR to DNA damage sites and ATR-mediated checkpoint activation and further DNA damage responses (Figure 1.4) (Section 1.3.1.1) (Wu et al., 2005a; Zou and Elledge, 2003; Zou et al., 2006).

RPA function appears to be regulated by post-translational modification (PTM). Both the RPA1 and RPA2 subunits are known to be modified by phosphorylation (Figure 1.6) (Nuss et al., 2005). RPA1 is also modified by SUMOylation (Figure 1.6) (Dou et al., 2010) while RPA2 has been shown to be poly-(ADP-ribosylated) (Figure 1.6) (Eki and Hurwitz, 1991). The best studied post-translational modification of RPA is the phosphorylation of the RPA2 subunit. The N-terminal domain of RPA2 is an established

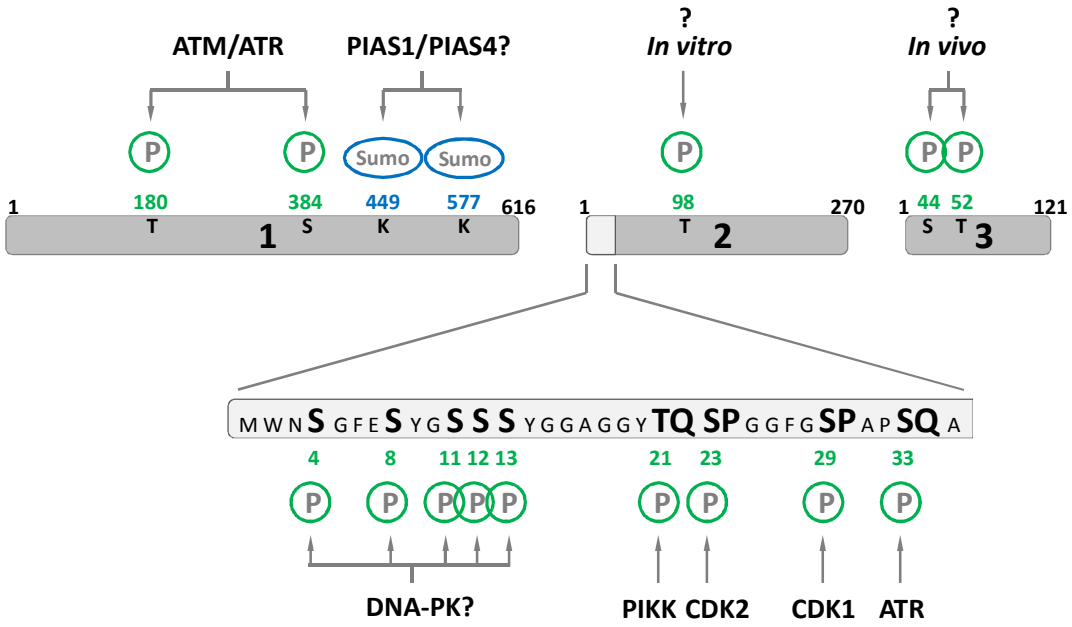

Figure 1.6 Diagram of the three RPA subunits with established and potential sites of post-translational modification.

target for phosphorylation *in vitro* and *in vivo* (Nuss et al., 2005). This RPA2 domain contains a number of serine and threonine residues which are phosphorylated in a cell cycle-dependent manner by CDKs (Anantha et al., 2007; Din et al., 1990; Dornreiter et al., 1992; Fotedar and Roberts, 1992; Niu et al., 1997; Stephan et al., 2009), as well as by PIK kinases in response to DNA damage (Figure 1.6) (Binz et al., 2004; Carty et al., 1994; Cruet-Hennequart et al., 2008; Liu and Weaver, 1993; Oakley et al., 2001). 2D-phosphopeptide mapping and mass spectrometry analysis revealed that in total, there are nine potential phosphorylation sites within the 33 amino acid N-terminal tail of RPA2 (Figure 1.6) (Niu et al., 1997; Nuss et al., 2005; Zernik-Kobak et al., 1997). Deletion of the first 33 amino acid residues from human RPA2 abolishes RPA phosphorylation (Henricksen et al., 1996). Interestingly, attempts to reveal the crystal structure of the N-terminal region of human RPA2 were not fully successful. Deng *et al*. (2007) reported that, based on structural analysis of the soluble RPA2-RPA3 heterodimer, the N-terminal domain of RPA2 was attached by a flexible linker to the rest of the protein and was intrinsically disordered while in the non-phosphorylated state (Deng et al., 2007). This disordered N-terminus of RPA2, found to be characteristic of phosphoryalation domains (Iakoucheva et al., 2004), may regulate the participation of RPA2 in high-specificity and low-affinity interactions with structurally variable partner proteins, including kinases and other DNA damage response proteins (Deng et al., 2007; Iakoucheva et al., 2004). Phosphorylation of the N-terminal domain of RPA2 is crucial for the function of RPA in the DNA damage response, and in DNA recombination and repair rather than in DNA synthesis. For example, expression and purification of an RPA2 hybrid protein that contained the N-terminal domain of RPA4, an

alternative form of RPA2 that does not support DNA synthesis, show wild-type levels of DNA replication *in vitro* (Mason et al., 2009). RPA1,by binding non-specifically and tightly to ssDNA, can substitute for the RPA heterotrimer in unwinding a new replication origin *in vitro* (Borowiec et al., 1990; Wold et al., 1987), specific protein-protein interactions between various DNA replication factors and the two other RPA subunits are crucial in proper assembly and function of the DNA synthesis initiation complex (Dornreiter et al., 1992; Lee and Kim, 1995; Mason et al., 2009; Melendy and Stillman, 1993). The conformational alterations in the heterotrimer induced by phosphorylation include (i) intersubunit interaction between the negative charges present on the N-terminal of RPA2 as a result of phosphorylation and the basic cleft of the DNA binding domain F (DBD-F) of RPA1 (Binz et al., 2004) and (ii) re-arrangements resulting from interaction of hyperphosphorylated RPA2 with the DBD-B motif located within RPA1 (Liu et al., 2005). As noted, the N-terminal domain of RPA2 may act as a flexible hinge region that, upon phosphorylation, interacts with DNA binding motifs present within the heterotrimer and reduces the single-stranded DNA-binding (Liu et al., 2005; Patrick et al., 2005) and double helix destabilisation activities of RPA (Binz et al., 2003; Liu et al., 2005). There is evidence that the phosphorylation-derived negative charge on the N-terminal of RPA2 changes the DNA binding mode of the heterotrimer, from compact to extended (Fanning et al., 2006). It has been proposed that this RPA conformation would favour DNA repair, where RPA, tightly bound to long stretches of ssDNA, functions to protect the DNA against nucleases and resolves DNA secondary structures until the repair process is complete. This RPA conformation would account for RPA extraction from replicating chromatin as during replication, RPA would preferably bind in the compact mode, favouring the fast RPA cycling on and off the replicating DNA (Fanning et al., 2006). These predictions are supported by studies where hyperphosphorylated RPA was found to bind equally tightly to ssDNA (Binz et al., 2003; Oakley et al., 2003).

In vitro phosphorylation of threonine 98, located outside the N-terminus of RPA2, has also been described. However, little is known on how this modification impacts RPA function (Nuss et al., 2005).

1.3.3.1 DNA damage-induced phosphorylation of the N-terminal domain of RPA2

As described above, it is well established that exposure of cells to DNA damaging agents such as UV-C irradiation (UV-C) (Carty et al., 1994; Cruet-Hennequart et al., 2006), ionizing radiation (IR) (Stephan et al., 2009) and cisplatin (Cruet-Hennequart et al., 2008) or replication inhibitors like hydroxyurea (HU) (Manthey et al., 2007) and camptothecin (CPT) (Shao et al., 1999), results in the generation of additional forms of RPA2, detectable

upon SDS-PAGE as bands of even lower mobility compared to the mitotic form. These forms of RPA2 correspond to protein phosphorylation on at least four of the residues located in the N-terminal domain, at Ser4, Ser8, Ser 11-13, Thr21, Ser23, Ser29 or Ser33 (Nuss et al., 2005; Oakley et al., 2001; Zernik-Kobak et al., 1997). This form has been termed hyperphosphorylated RPA2 (Nuss et al., 2005; Oakley et al., 2001).

While serines 23 and 29 are phosphorylated by CDK-cyclin complexes. Ser33 and Thr21 constitute consensus sites for phosphatidylinositol 3-kinases (PIKK) including ATM, ATR and DNA-PK (Figure 1.6) (Kim et al., 1999). It is established that following genotoxic stress ATR phosphorylates RPA2 on Ser33 (Anantha et al., 2007; Olson et al., 2006). Thr21 was reported to be phosphorylated primarily by ATM and DNA-PK, and to a lesser extent by ATR (Block et al., 2004; Zernik-Kobak et al., 1997). While little is known about phosphorylation of serines 11-13, DNA-PK can phosphorylate Ser4 and Ser8 *in vitro* (Zernik-Kobak et al., 1997). *In vivo*, this phosphorylation event was reported to be DNA-PK-dependent following UV-C and cisplatin treatment (Cruet-Hennequart et al., 2006; Cruet-Hennequart et al., 2008).

It has been proposed that in response to DNA damage in interphase cells, RPA2 is primarily phosphorylated on Ser33 by the ATR-ATRIP complex early in the damage response, and that this phosphorylation is required for subsequent phosphorylation of other N-terminally located sites (Anantha et al., 2007). Even though multiple phosphorylation events are needed to generate the hyperphosphorylated form of RPA2 , the actual residues, responsible kinases and the sequence of phosphorylation events can vary depending on the type of DNA damage and the cell cycle phase (Anantha et al., 2007; Cruet-Hennequart et al., 2008; Sakasai et al., 2006; Stephan et al., 2009). In addition to its role during the normal cell cycle, CDK-cyclin-dependent phosphorylation of RPA2 on Ser23 and Ser29 was found to play a role in DSB repair in interphase cells treated with bleomycin or CPT (Anantha et al., 2007). In contrast, phosphorylation of Ser23 and Ser29 was dispensable for IR-induced RPA2 hyperphosphorylation in interphase cells, suggesting that the type of DNA damage affects which sites on RPA2 are modified (Stephan et al., 2009).

RPA2 can also be phosphorylated in response to DNA damage in mitotic cells. Anantha et al. (2007) reported that in mitotic cells, phosphorylation of Ser23 and Ser29 is required for the N-terminal domain of RPA2 to undergo additional phosphorylation events when cells are exposed to bleomycin. The importance of RPA2 hyperphosphorylation in DNA damage processing, cell cycle progression and viability has been emphasised by the fact that in response to mitotic DNA damage, cells in which endogenous RPA2 was replaced with a RPA2 mutant, where Ser23 and Ser29 were both mutated to alanine, showed a severe

delay in exiting mitosis into G1 phase, increased spindle assembly checkpoint (SAC) activation and elevated apoptosis (Anantha et al., 2008). It was proposed that DNA damage-induced RPA2 hyperphosphorylation in mitosis can be governed through the SAC, and enhanced mitotic exit can function to allow damaged DNA to be repaired by mechanisms operating in G1 phase (Anantha and Borowiec, 2009). This hypothesis is consistent with the idea that as a result of chromatin condensation, DNA breaks may not be repaired efficiently in mitotic cells.

As RPA function is indispensible for DNA replication, there is growing evidence supporting the hypothesis that RPA is most rapidly hyperphosphorylated in response to inhibition of DNA replication (Anantha et al., 2007; Liaw et al., 2011; Rodrigo et al., 2000; Shi et al., 2010). DNA polymerase eta-deficient cells, treated with a chemotherapeutic drug cisplatin, accumulate hyperphosphorylated RPA2 under conditions where replication is strongly inhibited (Cruet-Hennequart et al., 2006; Cruet-Hennequart et al., 2008). Recent studies show that a novel RPA inhibitor, TDLR-505, synergistically increases the toxicity of cisplatin, supporting a role for RPA in rescuing cells from the cytotoxic effects of replication-blocking lesions (Shuck and Turchi, 2010). Sakasai et al. (2006) reported that differences in the kinase-dependence and dynamics of RPA2 hyperphosphorylation when DNA synthesis is inhibited can be explained by the ability of specific drugs to cause direct or indirect replication-coupled DSBs (or DSEs) (Sakasai et al., 2006). Thus, while both ATR and DNA-PK were reported to participate in RPA2 hyperphosphorylation in response to CPT, a drug that causes direct, replication-coupled DSBs, RPA2 hyperphosphorylation induced by hydroxyurea, which induces DSBs indirectly, was found to be independent of DNA-PK (Sakasai et al., 2006). The hypothesis that hyperphosphorylated RPA2 further inhibits DNA replication is supported by findings that hyperphosphorylated RPA2 (i) binds less efficiently to ssDNA (Binz et al., 2003; Liu et al., 2005; Patrick et al., 2005), (ii) has decreased ability to interact with DNA polymerase α *in vitro* (Patrick et al., 2005) and (iii) is excluded from DNA replication foci (Vassin et al., 2004). Conversly, *in vitro* experiments show that RPA2 hyperphosphorylation has no impact on interaction with some proteins involved in nucleotide excision repair (XPA) (Oakley et al., 2003; Patrick et al., 2005) or recombination (Rad51, Rad52) (Jackson et al., 2002). There is increasing evidence that hyperphosphorylation of RPA2 can modualte the function of RPA in DNA damage signalling and repair, both through a change in RPA-DNA binding and in RPA-protein interactions (Mer et al., 2000). Additionally, DNA-PK- and CDK -dependent RPA2 hyperphosphorylation occurs on a subset of the RPA present in cells in the early stages of apoptosis (O'Meara et al., 2010; Treuner et al., 1999).

1.3.3.2 Role of post-translational modifications of RPA2 in regulating protein function in DSB repair by homologous recombination.

Generation of single-stranded DNA is a common feature of most aspects of DNA metabolism, and RPA therefore plays a central in the biochemical pathways that carry out these transactions. One of these is DNA double-strand repair by homologous recombination (HR) (Section 1.3.2.2.2). The role of RPA in HR is complex, and is determined in part by its strong affinity for ssDNA as well as through interaction of RPA with other HR proteins, including Rad51, Rad52 and BRCA2 (Deng et al., 2009; Sugiyama and Kowalczykowski, 2002). There is increasing evidence that the function of RPA in HR is regulated by damage-dependent phosphorylation of RPA2. Thus, RPA2 hyperphosphorylation was found to occur predominantly in S and G2 phase cells, where HR preferentially occurs (Anantha et al., 2007; Cruet-Hennequart et al., 2009). Additionally, hyperphosphorylated RPA preferentially localised to repair foci following treatment of A549 human lung adenocarcinoma cells with UV-C or camptothecin (Wu et al., 2005a).

A key step in HR-mediated DSB repair is the formation of a Rad51 nucleofilament in order for the recombinase to initiate a homologous strand search (San Filippo et al., 2008). RPA, as the most abundant ssDNA-binding protein in the nucleus, plays an important role in the early stages of HR, by binding to ssDNA generated during DNA strand resection, thereby reducing the secondary structure of the ssDNA. At this stage, RPA outcompetes Rad51 for binding to ssDNA ends, and initially inhibits presynaptic complex formation (Deng et al., 2009). This inhibition is alleviated by the recruitment of Rad52 to the site of damage where it acts as a mediator between RPA-coated ssDNA and Rad51, since Rad52 interacts with both Rad51 and RPA as well as with ssDNA (Deng et al., 2009). RPA2 hyperphosphorylation facilitates the displacement of RPA from ssDNA by Rad51 and the activation of further HR steps (Deng et al., 2009; Golub et al., 1998). Hyperphosphorylated RPA was reported to directly interact with Rad51 *in vitro* (Wu et al., 2005b). Upon Rad51 nucleofilament formation, RPA was found to accelerate the later steps in HR, including homologous pairing and strand exchange *in vitro* (Golub et al., 1998).

Although there is increasing evidence that damage-dependent RPA2 hyperphosphorylation is specifically required for replication arrest-coupled HR, its precise role in this process is still not completely clear. Recently, Shi et al. (2010) reported that RPA2 hyperphosphorylation is essential in HR in response to DNA strand breaks resulting from replication arrest rather than DSBs arising directly from IR exposure (Shi et al., 2010). In support of this model, expression of an RPA2 mutant that cannot undergo N-terminal phosphorylation resulted in (i) decreased Rad51 foci formation, (ii) increased chromosomal

aberrations and (iii) loss of cell viability when cells were exposed to chemotherapeutic agents that inhibit DNA replication, but not when DSBs were directly induced (Shi et al., 2010). Additionally, it was found that hyperphosphorylation of RPA2 during HR-at sites of DNA replication arrest was dependent on functional BRCA1. This BRCA1-related modification of RPA2 provides further evidence that RPA2 hyperphosphorylation functions in efficient resolution of stalled forks by HR (Feng and Zhang, 2011).

DNA damage-induced hyperphosphorylation of RPA2 leads to disassociation of RPA from complexes formed with various protein partners, and possibly directs the heterotrimer to sites of HR-mediated repair. A recent report by Serrano et al. (2012) revealed that checkpoint-mediated RPA2 hyperphosphorylation severely impairs the interaction of the heterotrimer with p53 (Serrano et al., 2012). In the normal cell environment, RPA binds to and sequesters p53 (Dutta et al., 1993). In response to replication stress induced by CPT treatment, RPA2 is hyperphosphorylated by PIK kinases, no longer binds to p53 and is able to relocate to lesion sites and facilitate HR-mediated lesion processing (Serrano et al., 2012). Additionally, RPA2 phosphorylation releases p53 to orchestrate the DNA damage response (Serrano et al., 2012).

In addition to phosphorylation of RPA2, recent evidence indicates that additional PTMs also modulate RPA activity in response to DNA damage. As noted above, in response to genotoxins which directly induce DSBs (CPT and IR), RPA1 is SUMOylated *in vivo* (Dou et al., 2010). While SUMOylation did not affect hererotrimer stability or ssDNA binding, this modification was found to be critical for Rad51 recruitment to repair foci and for the displacement of RPA from the ssDNA allowing for efficient HR (Dou et al., 2010). Thus, in addition to RPA2 phosphorylation, SUMOylation of the RPA1 subunit of RPA also regulates DNA repair by HR. Since, in contrast to RPA2 phosphorylation, RPA1 SUMOylation appears to occur only in response to IR and CPT, it is hypothesised that the nature of lesion, by activating different signalling pathways, might dictate which type of post-translational modification of RPA occurs, and thereby how the protein functions in HR (Dou et al., 2010).

1.3.3.3 Role of RPA2 dephosphorylation

While the role of damage-induced phosphorylation of RPA2 in DNA lesion detection, DNA damage signal transduction, cell cycle regulation and final lesion repair was the focus of many reviews (Binz et al., 2004; Patrick et al., 2005), less is known about the biological significance of RPA dephosphorylation. Recently, damage-induced RPA2 phosphorylation was reported to be reversed by a dimeric complex of PP4 (protein phosphatase 4) and PP4R2 (regulatory subunit 2). Lee et al. (2010) reported that RPA can

interact with this PP4 complex *in vitro*, and that, *in vivo*, the level of hyperphosphorylated RPA2 is elevated upon silencing of PP4 activity using siRNA (Lee et al., 2010). The authors provide evidence for the importance of RPA2 dephosphorylation in effective DNA damage signalling, HR and normal cell cycle resumption. Firstly, cells with impaired RPA dephosphorylation show increased G2/M checkpoint signalling in response to IR. Secondly, premature RPA2 hyperphosphorylation led to a delay in RPA localisation to repair foci and impaired HR as a result of inefficient formation of Rad51 nucleofilaments. Thirdly, expression of hyperphospho-mimetic RPA2 mutants significantly impedes DNA synthesis upon DNA damage induction by IR. This suggests that dephosphorylation of RPA is necessary for resumption of DNA replication post-damage and for release of cell cycle arrest (Lee et al., 2010). Fourthly, cells with persistent levels of damage-induced, hyperphosphorylated RPA show increased sensitivity to DNA damaging agents (Feng et al., 2009; Lee et al., 2010). Additionally, PP2A-mediated RPA2 dephosphorylation was reported for efficient repair of replication-coupled DSEs (Feng et al., 2009).

There is increasing evidence that specific and sequential RPA phosphorylation and dephosphorylation events regulate efficient DNA repair by HR. Premature hyperphosphorylation of RPA2 in response to DNA damage impedes RPA localisation to repair centres, consistent with delayed RPA localisation to repair foci when the PP4 complex is inactive (Lee et al., 2010). One possible scenario for the role of RPA2 phosphorylation and dephosphorylation in regulation of HR are as follows. In response to DNA damage, pools of hyperphosphorylated RPA available from, for example, RPA disassociation from protein complexes, including XPA and p53 requires dephosphorylation for its efficient association with HR repair foci where it binds to DNA and eliminates secondary DNA structures. Next, RPA2 is phosphorylated to facilitate Rad52-mediated exchange for Rad51 on the DNA and in this form RPA participates in later HR steps until it is dephosphorylated when DNA synthesis is ready to restart.

1.4 Research objectives

Successful treatment with platinum-based chemotherapeutic drugs is based on induction of cancer cell death by apoptosis or necrosis, if the damage is severe (Figure 1.7) (Eastman, 1990; O'Meara et al., 2010). One way by which cancer cells can escape death post-exposure to platinum-based chemotherapeutic drugs is by DNA damage response (DDR)-mediated activation of DNA repair pathways (Figure 1.7) (Zorbas and Keppler, 2005). However, not all platinum-DNA lesions are repaired before the onset of S-phase and DNA replication can occur even in the presence of damage (Chang and Cimprich, 2009; Masutani et al., 2000). This in turn can lead to drug tolerance and the development of resistant tumours (Figure 1.7). In addition, mutagenesis at the sites of adducts in dividing cells could contribute to secondary tumour development (Figure 1.7) (Chaney et al., 2005; Kartalou and Essigmann, 2001a; Kartalou and Essigmann, 2001b). Continuation of DNA synthesis on platinum-damaged DNA can occur by activation of translesion synthesis (TLS), which involves recruitment of specialised DNA polymerases, including DNA polymerase η (polη) (Masutani et al., 2000; Vaisman et al., 2000).

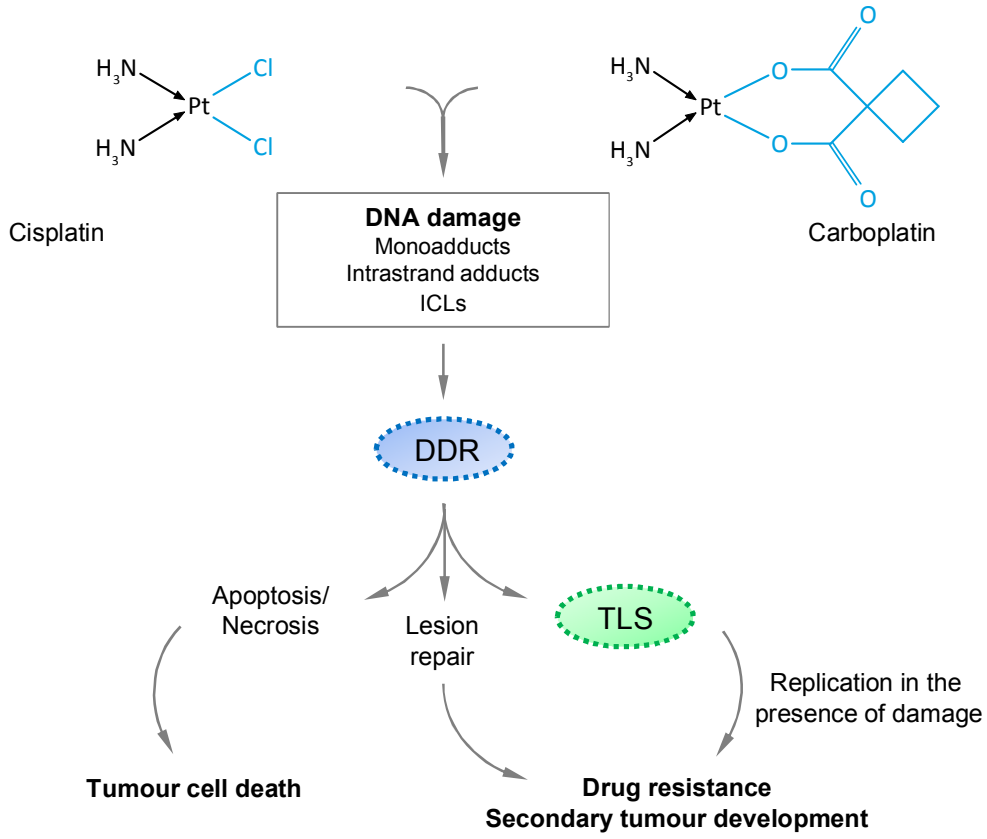

Figure 1.7 Possible cellular outcomes from treatment with platinum-based chemotherapeutic drugs.

The objectives of this research are to:

(i) investigate the polη-dependence of DNA synthesis in response to DNA damage by platinum-based chemotherapeutic drugs;

(ii) characterise PIK kinase-mediated signalling events following replication arrest, with a focus on phosphorylation of the replication protein A subunit, RPA2;

(iii) study DNA damage-independent functions of RPA2 phosphorylation

1.5 References

Aabo, K., M. Adams, P. Adnitt, D.S. Alberts, A. Athanazziou, V. Barley, D.R. Bell, U. Bianchi, G. Bolis, M.F. Brady, H.S. Brodovsky, H. Bruckner, M. Buyse, R. Canetta, V. Chylak, C.J. Cohen, N. Colombo, P.F. Conte, D. Crowther, J.H. Edmonson, C. Gennatas, E. Gilbey, M. Gore, D. Guthrie, B.Y. Yeap, and et al. 1998. Chemotherapy in advanced ovarian cancer: four systematic meta-analyses of individual patient data from 37 randomized trials. Advanced Ovarian Cancer Trialists' Group. *Br J Cancer*. 78:1479-87.

Abraham, R.T. 2004. PI 3-kinase related kinases: 'big' players in stress-induced signaling pathways. *DNA Repair (Amst)*. 3:883-7.

Acharya, N., J.H. Yoon, H. Gali, I. Unk, L. Haracska, R.E. Johnson, J. Hurwitz, L. Prakash, and S. Prakash. 2008. Roles of PCNA-binding and ubiquitin-binding domains in human DNA polymerase eta in translesion DNA synthesis. *Proc Natl Acad Sci U S A*. 105:17724-9.

Ahmad, S. 2010. Platinum–DNA Interactions and Subsequent Cellular Processes Controlling Sensitivity to Anticancer Platinum Complexes. *Chemistry & Biodiversity*. 7:543-566.

Alabert, C., and A. Groth. 2012. Chromatin replication and epigenome maintenance. *Nat Rev Mol Cell Biol*. 13:153-67.

Allen, C., A.K. Ashley, R. Hromas, and J.A. Nickoloff. 2011. More forks on the road to replication stress recovery. *J Mol Cell Biol*. 3:4-12.

Alt, A., K. Lammens, C. Chiocchini, A. Lammens, J.C. Pieck, D. Kuch, K.P. Hopfner, and T. Carell. 2007. Bypass of DNA lesions generated during anticancer treatment with cisplatin by DNA polymerase eta. *Science*. 318:967-70.

Anand, P., A.B. Kunnumakkara, C. Sundaram, K.B. Harikumar, S.T. Tharakan, O.S. Lai, B. Sung, and B.B. Aggarwal. 2008. Cancer is a preventable disease that requires major lifestyle changes. *Pharm Res*. 25:2097-116.

Anantha, R.W., and J.A. Borowiec. 2009. Mitotic crisis: the unmasking of a novel role for RPA. *Cell Cycle*. 8:357-61.

Anantha, R.W., E. Sokolova, and J.A. Borowiec. 2008. RPA phosphorylation facilitates mitotic exit in response to mitotic DNA damage. *Proc Natl Acad Sci U S A*. 105:12903-8.

Anantha, R.W., V.M. Vassin, and J.A. Borowiec. 2007. Sequential and synergistic modification of human RPA stimulates chromosomal DNA repair. *J Biol Chem*. 282:35910-23.

Andrews, P.A., S.C. Mann, H.H. Huynh, and K.D. Albright. 1991. Role of the Na+, K(+)-adenosine triphosphatase in the accumulation of cis-diamminedichloroplatinum(II) in human ovarian carcinoma cells. *Cancer Res*. 51:3677-81.

Arnesano, F., and G. Natile. 2009. Mechanistic insight into the cellular uptake and processing of cisplatin 30 years after its approval by FDA. *Coordination Chemistry Reviews*. 253:2070-2081.

Baskar, R., S.P. Yap, K.L. Chua, and K. Itahana. 2012. The diverse and complex roles of radiation on cancer treatment: therapeutic target and genome maintenance. *Am J Cancer Res*. 2:372-82.

Bassett, E., N.M. King, M.F. Bryant, S. Hector, L. Pendyala, S.G. Chaney, and M. Cordeiro-Stone. 2004. The role of DNA polymerase eta in translesion synthesis past platinum-DNA adducts in human fibroblasts. *Cancer Res*. 64:6469-75.

Bell, S.P., and A. Dutta. 2002. DNA replication in eukaryotic cells. *Annu Rev Biochem*. 71:333-74.

Bellon, S.F., J.H. Coleman, and S.J. Lippard. 1991. DNA unwinding produced by site-specific intrastrand cross-links of the antitumor drug cis-diamminedichloroplatinum(II). *Biochemistry*. 30:8026-35.

Bernstein, K.A., and R. Rothstein. 2009. At loose ends: resecting a double-strand break. *Cell*. 137:807-10.

Biertumpfel, C., Y. Zhao, Y. Kondo, S. Ramon-Maiques, M. Gregory, J.Y. Lee, C. Masutani, A.R. Lehmann, F. Hanaoka, and W. Yang. 2010. Structure and mechanism of human DNA polymerase eta. *Nature*. 465:1044-1048.

Binz, S.K., Y. Lao, D.F. Lowry, and M.S. Wold. 2003. The phosphorylation domain of the 32-kDa subunit of replication protein A (RPA) modulates RPA-DNA interactions. Evidence for an intersubunit interaction. *J Biol Chem*. 278:35584-91.

Binz, S.K., A.M. Sheehan, and M.S. Wold. 2004. Replication protein A phosphorylation and the cellular response to DNA damage. *DNA Repair (Amst)*. 3:1015-24.

Block, W.D., Y. Yu, and S.P. Lees-Miller. 2004. Phosphatidyl inositol 3-kinase-like serine/threonine protein kinases (PIKKs) are required for DNA damage-induced phosphorylation of the 32 kDa subunit of replication protein A at threonine 21. *Nucleic Acids Res*. 32:997-1005.

Blommaert, F.A., H.C.M. van Dijk-Knijnenburg, F.J. Dijt, L. den Engelse, R.A. Baan, F. Berends, and A.M.J. Fichtinger-Schepman. 1995. Formation of DNA Adducts by the Anticancer Drug Carboplatin: Different Nucleotide Sequence Preferences in Vitro and in Cells. *Biochemistry*. 34:8474-8480.

Borowiec, J.A., F.B. Dean, P.A. Bullock, and J. Hurwitz. 1990. Binding and unwinding--how T antigen engages the SV40 origin of DNA replication. *Cell*. 60:181-4.

Branzei, D., and M. Foiani. 2007. Interplay of replication checkpoints and repair proteins at stalled replication forks. *DNA Repair (Amst)*. 6:994-1003.

Branzei, D., and M. Foiani. 2008. Regulation of DNA repair throughout the cell cycle. *Nat Rev Mol Cell Biol*. 9:297-308.

Branzei, D., and M. Foiani. 2010. Maintaining genome stability at the replication fork. *Nat Rev Mol Cell Biol*. 11:208-19.

Byun, T.S., M. Pacek, M.C. Yee, J.C. Walter, and K.A. Cimprich. 2005. Functional uncoupling of MCM helicase and DNA polymerase activities activates the ATR-dependent checkpoint. *Genes Dev*. 19:1040-52.

Carmena, M., and W.C. Earnshaw. 2003. The cellular geography of Aurora kinases. *Nat Rev Mol Cell Biol*. 4:842-854.

Carty, M.P., M. Zernik-Kobak, S. McGrath, and K. Dixon. 1994. UV light-induced DNA synthesis arrest in HeLa cells is associated with changes in phosphorylation of human single-stranded DNA-binding protein. *EMBO J*. 13:2114-23.

Cary, R.B., S.R. Peterson, J. Wang, D.G. Bear, E.M. Bradbury, and D.J. Chen. 1997. DNA looping by Ku and the DNA-dependent protein kinase. *Proc Natl Acad Sci U S A*. 94:4267-72.

Ceppi, P., S. Novello, A. Cambieri, M. Longo, V. Monica, M. Lo Iacono, M. Giaj-Levra, S. Saviozzi, M. Volante, M. Papotti, and G. Scagliotti. 2009. Polymerase eta mRNA expression predicts survival of non-small cell lung cancer patients treated with platinum-based chemotherapy. *Clin Cancer Res*. 15:1039-45.

Chaney, S.G., S.L. Campbell, E. Bassett, and Y. Wu. 2005. Recognition and processing of cisplatin- and oxaliplatin-DNA adducts. *Critical reviews in oncology/hematology*. 53:3-11.

Chang, D.J., and K.A. Cimprich. 2009. DNA damage tolerance: when it's OK to make mistakes. *Nat Chem Biol*. 5:82-90.

Chanoux, R.A., B. Yin, K.A. Urtishak, A. Asare, C.H. Bassing, and E.J. Brown. 2009. ATR and H2AX Cooperate in Maintaining Genome Stability under Replication Stress. *Journal of Biological Chemistry*. 284:5994-6003.

Chen, Y.-w., J.E. Cleaver, F. Hanaoka, C.-f. Chang, and K.-m. Chou. 2006. A Novel Role of DNA Polymerase eta in Modulating Cellular Sensitivity to Chemotherapeutic Agents. *Molecular Cancer Research*. 4:257-265.

Christmann, M., M.T. Tomicic, W.P. Roos, and B. Kaina. 2003. Mechanisms of human DNA repair: an update. *Toxicology*. 193:3-34.

Cleaver, J.E. 1972. Xeroderma pigmentosum: variants with normal DNA repair and normal sensitivity to ultraviolet light. *J Invest Dermatol*. 58:124-8.

Cree, I.A. 2011. Cancer biology. *Methods Mol Biol*. 731:1-11.

Cruet-Hennequart, S., S. Coyne, M.T. Glynn, G.G. Oakley, and M.P. Carty. 2006. UV-induced RPA phosphorylation is increased in the absence of DNA polymerase eta and requires DNA-PK. *DNA Repair (Amst)*. 5:491-504.

Cruet-Hennequart, S., K. Gallagher, A.M. Sokol, S. Villalan, A.M. Prendergast, and M.P. Carty. 2010. DNA polymerase eta, a key protein in translesion synthesis in human cells. *Subcell Biochem*. 50:189-209.

Cruet-Hennequart, S., M.T. Glynn, L.S. Murillo, S. Coyne, and M.P. Carty. 2008. Enhanced DNA-PK-mediated RPA2 hyperphosphorylation in DNA polymerase eta-deficient human cells treated with cisplatin and oxaliplatin. *DNA Repair (Amst)*. 7:582-96.

Cruet-Hennequart, S., S. Villalan, A. Kaczmarczyk, E. O'Meara, A.M. Sokol, and M.P. Carty. 2009. Characterization of the effects of cisplatin and carboplatin on cell cycle progression and DNA damage response activation in DNA polymerase eta-deficient human cells. *Cell Cycle*. 8:3039-50.

De Piccoli, G., Y. Katou, T. Itoh, R. Nakato, K. Shirahige, and K. Labib. 2012. Replisome stability at defective DNA replication forks is independent of S phase checkpoint kinases. *Mol Cell*. 45:696-704.

Deng, X., J.E. Habel, V. Kabaleeswaran, E.H. Snell, M.S. Wold, and G.E. Borgstahl. 2007. Structure of the full-length human RPA14/32 complex gives insights into the mechanism of DNA binding and complex formation. *J Mol Biol*. 374:865-76.

Deng, X., A. Prakash, K. Dhar, G.S. Baia, C. Kolar, G.G. Oakley, and G.E. Borgstahl. 2009. Human replication protein A-Rad52-single-stranded DNA complex: stoichiometry and evidence for strand transfer regulation by phosphorylation. *Biochemistry*. 48:6633-43.

Dhar, M.K., S. Sehgal, and S. Kaul. 2012. Structure, replication efficiency and fragility of yeast ARS elements. *Res Microbiol*. 163:243-53.

Din, S., S.J. Brill, M.P. Fairman, and B. Stillman. 1990. Cell-cycle-regulated phosphorylation of DNA replication factor A from human and yeast cells. *Genes Dev*. 4:968-77.

Dornreiter, I., L.F. Erdile, I.U. Gilbert, D. von Winkler, T.J. Kelly, and E. Fanning. 1992. Interaction of DNA polymerase alpha-primase with cellular replication protein A and SV40 T antigen. *EMBO J*. 11:769-76.

Dou, H., C. Huang, M. Singh, P.B. Carpenter, and E.T. Yeh. 2010. Regulation of DNA repair through deSUMOylation and SUMOylation of replication protein A complex. *Mol Cell*. 39:333-45.

Doxsey, S., W. Zimmerman, and K. Mikule. 2005. Centrosome control of the cell cycle. *Trends Cell Biol*. 15:303-11.

Duensing, S. 2005. A tentative classification of centrosome abnormalities in cancer. *Cell Biol Int*. 29:352-9.

Dutta, A., J.M. Ruppert, J.C. Aster, and E. Winchester. 1993. Inhibition of DNA replication factor RPA by p53. *Nature*. 365:79-82.

Eastman, A. 1987. The formation, isolation and characterization of DNA adducts produced by anticancer platinum complexes. *Pharmacol Ther*. 34:155-66.

Eastman, A. 1990. Activation of programmed cell death by anticancer agents: cisplatin as a model system. *Cancer Cells*. 2:275-80.

Eki, T., and J. Hurwitz. 1991. Influence of poly(ADP-ribose) polymerase on the enzymatic synthesis of SV40 DNA. *J Biol Chem*. 266:3087-100.

Elvers, I., A. Hagenkort, F. Johansson, T. Djureinovic, A. Lagerqvist, N. Schultz, I. Stoimenov, K. Erixon, and T. Helleday. 2012. CHK1 activity is required for continuous replication fork elongation but not stabilization of post-replicative gaps after UV irradiation. *Nucleic Acids Res*. 40:8440-8.

Fanning, E., V. Klimovich, and A.R. Nager. 2006. A dynamic model for replication protein A (RPA) function in DNA processing pathways. *Nucleic Acids Res*. 34:4126-37.

Fededa, J.P., and D.W. Gerlich. 2012. Molecular control of animal cell cytokinesis. *Nat Cell Biol*. 14:440-7.

Feng, J., T. Wakeman, S. Yong, X. Wu, S. Kornbluth, and X.F. Wang. 2009. Protein phosphatase 2A-dependent dephosphorylation of replication protein A is required for the repair of DNA breaks induced by replication stress. *Mol Cell Biol*. 29:5696-709.

Feng, Z., and J. Zhang. 2011. A dual role of BRCA1 in two distinct homologous recombination mediated repair in response to replication arrest. *Nucleic Acids Res*. 40:726-38.

Fotedar, R., and J.M. Roberts. 1992. Cell cycle regulated phosphorylation of RPA-32 occurs within the replication initiation complex. *EMBO J*. 11:2177-87.

Golub, E.I., R.C. Gupta, T. Haaf, M.S. Wold, and C.M. Radding. 1998. Interaction of human rad51 recombination protein with single-stranded DNA binding protein, RPA. *Nucleic Acids Res*. 26:5388-93.

Gonzalez, V.M., M.A. Fuertes, C. Alonso, and J.M. Perez. 2001. Is cisplatin-induced cell death always produced by apoptosis? *Mol Pharmacol*. 59:657-63.

Hall, M.D., M. Okabe, D.W. Shen, X.J. Liang, and M.M. Gottesman. 2008. The role of cellular accumulation in determining sensitivity to platinum-based chemotherapy. *Annu Rev Pharmacol Toxicol*. 48:495-535.

Hanahan, D., and R.A. Weinberg. 2000. The hallmarks of cancer. *Cell*. 100:57-70.

Hanahan, D., and R.A. Weinberg. 2011. Hallmarks of cancer: the next generation. *Cell*. 144:646-74.

Hartlerode, A.J., and R. Scully. 2009. Mechanisms of double-strand break repair in somatic mammalian cells. *Biochem J*. 423:157-68.

Hartwell, L.H., and T.A. Weinert. 1989. Checkpoints: controls that ensure the order of cell cycle events. *Science*. 246:629-34.

Helleday, T. 2003. Pathways for mitotic homologous recombination in mammalian cells. *Mutat Res*. 532:103-15.

Helleday, T., E. Petermann, C. Lundin, B. Hodgson, and R.A. Sharma. 2008. DNA repair pathways as targets for cancer therapy. *Nat Rev Cancer*. 8:193-204.

Heller, R.C., and K.J. Marians. 2006. Replication fork reactivation downstream of a blocked nascent leading strand. *Nature*. 439:557-62.

Henricksen, L.A., T. Carter, A. Dutta, and M.S. Wold. 1996. Phosphorylation of human replication protein A by the DNA-dependent protein kinase is involved in the modulation of DNA replication. *Nucleic Acids Res*. 24:3107-12.

Ho, T.V., A. Guainazzi, S.B. Derkunt, M. Enoiu, and O.D. Scharer. 2011. Structure-dependent bypass of DNA interstrand crosslinks by translesion synthesis polymerases. *Nucleic Acids Res*. 39:7455-64.

Ho, T.V., and O.D. Schärer. 2010. Translesion DNA synthesis polymerases in DNA interstrand crosslink repair. *Environmental and Molecular Mutagenesis*. 51:552-566.

Hoeijmakers, J.H. 2001. Genome maintenance mechanisms for preventing cancer. *Nature*. 411:366-74.

Hoeijmakers, J.H. 2009. DNA damage, aging, and cancer. *N Engl J Med*. 361:1475-85.

Hoffmann, J.S., M.J. Pillaire, G. Maga, V. Podust, U. Hubscher, and G. Villani. 1995. DNA polymerase beta bypasses in vitro a single d(GpG)-cisplatin adduct placed on codon 13 of the HRAS gene. *Proc Natl Acad Sci U S A*. 92:5356-60.

Holzer, A.K., G.H. Manorek, and S.B. Howell. 2006. Contribution of the major copper influx transporter CTR1 to the cellular accumulation of cisplatin, carboplatin, and oxaliplatin. *Mol Pharmacol*. 70:1390-4.

Holzer, A.K., G. Samimi, K. Katano, W. Naerdemann, X. Lin, R. Safaei, and S.B. Howell. 2004. The copper influx transporter human copper transport protein 1 regulates the uptake of cisplatin in human ovarian carcinoma cells. *Mol Pharmacol*. 66:817-23.

Hongo, A., S. Seki, K. Akiyama, and T. Kudo. 1994. A comparison of in vitro platinum-DNA adduct formation between carboplatin and cisplatin. *Int J Biochem*. 26:1009-16.

Howell, S.B., R. Safaei, C.A. Larson, and M.J. Sailor. 2010. Copper transporters and the cellular pharmacology of the platinum-containing cancer drugs. *Mol Pharmacol*. 77:887-94.

Huen, M.S., and J. Chen. 2008. The DNA damage response pathways: at the crossroad of protein modifications. *Cell Res*. 18:8-16.

Iakoucheva, L.M., P. Radivojac, C.J. Brown, T.R. O'Connor, J.G. Sikes, Z. Obradovic, and A.K. Dunker. 2004. The importance of intrinsic disorder for protein phosphorylation. *Nucleic Acids Res*. 32:1037-49.

Ishida, S., J. Lee, D.J. Thiele, and I. Herskowitz. 2002. Uptake of the anticancer drug cisplatin mediated by the copper transporter Ctr1 in yeast and mammals. *Proc Natl Acad Sci U S A*. 99:14298-302.

Jackson, D., K. Dhar, J.K. Wahl, M.S. Wold, and G.E. Borgstahl. 2002. Analysis of the human replication protein A:Rad52 complex: evidence for crosstalk between RPA32, RPA70, Rad52 and DNA. *J Mol Biol*. 321:133-48.

Jackson, D.A., and A. Pombo. 1998. Replicon clusters are stable units of chromosome structure: evidence that nuclear organization contributes to the efficient activation and propagation of S phase in human cells. *J Cell Biol*. 140:1285-95.

Jackson, S.P., and J. Bartek. 2009. The DNA-damage response in human biology and disease. *Nature*. 461:1071-8.

Johnson, R.E., C.M. Kondratick, S. Prakash, and L. Prakash. 1999a. hRAD30 mutations in the variant form of xeroderma pigmentosum. *Science*. 285:263-5.

Johnson, R.E., S. Prakash, and L. Prakash. 1999b. Efficient Bypass of a Thymine-Thymine Dimer by Yeast DNA Polymerase, Pol. *Science*. 283:1001-1004.

Jones, R.M., and E. Petermann. 2012. Replication fork dynamics and the DNA damage response. *Biochem J*. 443:13-26.

Kannouche, P.L., and A.R. Lehmann. 2004. Ubiquitination of PCNA and the Polymerase Switch in Human Cells. *Cell Cycle*. 3:1009-1011.

Kannouche, P.L., J. Wing, and A.R. Lehmann. 2004. Interaction of Human DNA Polymerase eta with Monoubiquitinated PCNA: A Possible Mechanism for the Polymerase Switch in Response to DNA Damage. *Molecular cell*. 14:491-500.

Kartalou, M., and J.M. Essigmann. 2001a. Mechanisms of resistance to cisplatin. *Mutation Research/Fundamental and Molecular Mechanisms of Mutagenesis*. 478:23-43.

Kartalou, M., and J.M. Essigmann. 2001b. Recognition of cisplatin adducts by cellular proteins. *Mutation Research/Fundamental and Molecular Mechanisms of Mutagenesis*. 478:1-21.

Kastan, M.B., and J. Bartek. 2004. Cell-cycle checkpoints and cancer. *Nature*. 432:316-23.

Kawamoto, T., K. Araki, E. Sonoda, Y.M. Yamashita, K. Harada, K. Kikuchi, C. Masutani, F. Hanaoka, K. Nozaki, N. Hashimoto, and S. Takeda. 2005. Dual roles for DNA polymerase eta in homologous DNA recombination and translesion DNA synthesis. *Mol Cell*. 20:793-9.

Kelland, L. 2007. The resurgence of platinum-based cancer chemotherapy. *Nat Rev Cancer*. 7:573-584.

Kelland, L.R., G. Abel, M.J. McKeage, M. Jones, P.M. Goddard, M. Valenti, B.A. Murrer, and K.R. Harrap. 1993. Preclinical antitumor evaluation of bis-acetato-ammine-dichloro-cyclohexylamine platinum(IV): an orally active platinum drug. *Cancer Res*. 53:2581-6.

Kellogg, D.R., M. Moritz, and B.M. Alberts. 1994. The centrosome and cellular organization. *Annu Rev Biochem*. 63:639-74.

Kemp, M.G., Z. Akan, S. Yilmaz, M. Grillo, S.L. Smith-Roe, T.H. Kang, M. Cordeiro-Stone, W.K. Kaufmann, R.T. Abraham, A. Sancar, and K. Unsal-Kacmaz. 2010. Tipin-replication protein A interaction mediates Chk1 phosphorylation by ATR in response to genotoxic stress. *J Biol Chem*. 285:16562-71.

Kenny, M.K., S.H. Lee, and J. Hurwitz. 1989. Multiple functions of human single-stranded-DNA binding protein in simian virus 40 DNA replication: single-strand stabilization and stimulation of DNA polymerases alpha and delta. *Proc Natl Acad Sci U S A*. 86:9757-61.

Kim, S.T., D.S. Lim, C.E. Canman, and M.B. Kastan. 1999. Substrate specificities and identification of putative substrates of ATM kinase family members. *J Biol Chem*. 274:37538-43.

King, R.W., P.K. Jackson, and M.W. Kirschner. 1994. Mitosis in transition. *Cell*. 79:563-71.

Kline-Smith, S.L., and C.E. Walczak. 2004. Mitotic spindle assembly and chromosome segregation: refocusing on microtubule dynamics. *Mol Cell*. 15:317-27.

Lee, D.H., Y. Pan, S. Kanner, P. Sung, J.A. Borowiec, and D. Chowdhury. 2010. A PP4 phosphatase complex dephosphorylates RPA2 to facilitate DNA repair via homologous recombination. *Nat Struct Mol Biol*. 17:365-72.

Lee, K.Y., and K. Myung. 2008. PCNA modifications for regulation of post-replication repair pathways. *Mol Cells*. 26:5-11.

Lee, S.H., and D.K. Kim. 1995. The role of the 34-kDa subunit of human replication protein A in simian virus 40 DNA replication in vitro. *J Biol Chem*. 270:12801-7.

Lehmann, A.R., and R.P. Fuchs. 2006. Gaps and forks in DNA replication: Rediscovering old models. *DNA Repair (Amst)*. 5:1495-8.

Lehmann, A.R., A. Niimi, T. Ogi, S. Brown, S. Sabbioneda, J.F. Wing, P.L. Kannouche, and C.M. Green. 2007. Translesion synthesis: Y-family polymerases and the polymerase switch. *DNA Repair (Amst)*. 6:891-9.

Leman, A.R., and E. Noguchi. 2012. Local and global functions of Timeless and Tipin in replication fork protection. *Cell Cycle*. 11:3945-55.

Li, G.M. 2008. Mechanisms and functions of DNA mismatch repair. *Cell Res*. 18:85-98.

Liaw, H., D. Lee, and K. Myung. 2011. DNA-PK-Dependent RPA2 Hyperphosphorylation Facilitates DNA Repair and Suppresses Sister Chromatid Exchange. *PLoS ONE*. 6:e21424.

Lindahl, T. 1993. Instability and decay of the primary structure of DNA. *Nature*. 362:709-15.

Liu, V.F., and D.T. Weaver. 1993. The ionizing radiation-induced replication protein A phosphorylation response differs between ataxia telangiectasia and normal human cells. *Mol Cell Biol*. 13:7222-31.

Liu, Y., M. Kvaratskhelia, S. Hess, Y. Qu, and Y. Zou. 2005. Modulation of replication protein A function by its hyperphosphorylation-induced conformational change involving DNA binding domain B. *J Biol Chem*. 280:32775-83.

Loeb, L.A., K.R. Loeb, and J.P. Anderson. 2003. Multiple mutations and cancer. *Proc Natl Acad Sci U S A*. 100:776-81.

Lopes, M., M. Foiani, and J.M. Sogo. 2006. Multiple mechanisms control chromosome integrity after replication fork uncoupling and restart at irreparable UV lesions. *Mol Cell*. 21:15-27.

Lukas, J., C. Lukas, and J. Bartek. 2004. Mammalian cell cycle checkpoints: signalling pathways and their organization in space and time. *DNA Repair (Amst)*. 3:997-1007.

Ma, Y., U. Pannicke, K. Schwarz, and M.R. Lieber. 2002. Hairpin opening and overhang processing by an Artemis/DNA-dependent protein kinase complex in nonhomologous end joining and V(D)J recombination. *Cell*. 108:781-94.

Maiorano, D., M. Lutzmann, and M. Mechali. 2006. MCM proteins and DNA replication. *Curr Opin Cell Biol*. 18:130-6.

Manthey, K.C., S. Opiyo, J.G. Glanzer, D. Dimitrova, J. Elliott, and G.G. Oakley. 2007. NBS1 mediates ATR-dependent RPA hyperphosphorylation following replication-fork stall and collapse. *J Cell Sci*. 120:4221-9.

Mardin, B.R., and E. Schiebel. 2012. Breaking the ties that bind: new advances in centrosome biology. *J Cell Biol*. 197:11-8.

Mason, A.C., S.J. Haring, J.M. Pryor, C.A. Staloch, T.F. Gan, and M.S. Wold. 2009. An alternative form of replication protein a prevents viral replication in vitro. *J Biol Chem*. 284:5324-31.

Masutani, C., R. Kusumoto, S. Iwai, and F. Hanaoka. 2000. Mechanisms of accurate translesion synthesis by human DNA polymerase [eta]. *EMBO J*. 19:3100-3109.

Masutani, C., R. Kusumoto, A. Yamada, N. Dohmae, M. Yokoi, M. Yuasa, M. Araki, S. Iwai, K. Takio, and F. Hanaoka. 1999. The XPV (xeroderma pigmentosum variant) gene encodes human DNA polymerase eta. *Nature*. 399:700-4.

Matsuoka, S., B.A. Ballif, A. Smogorzewska, E.R. McDonald, 3rd, K.E. Hurov, J. Luo, C.E. Bakalarski, Z. Zhao, N. Solimini, Y. Lerenthal, Y. Shiloh, S.P. Gygi, and S.J. Elledge. 2007. ATM and ATR substrate analysis reveals extensive protein networks responsive to DNA damage. *Science*. 316:1160-6.

Maya-Mendoza, A., E. Petermann, D.A. Gillespie, K.W. Caldecott, and D.A. Jackson. 2007. Chk1 regulates the density of active replication origins during the vertebrate S phase. *EMBO J*. 26:2719-31.

McCulloch, S.D., R.J. Kokoska, C. Masutani, S. Iwai, F. Hanaoka, and T.A. Kunkel. 2004. Preferential cis-syn thymine dimer bypass by DNA polymerase eta occurs with biased fidelity. *Nature*. 428:97-100.

McIlwraith, M.J., A. Vaisman, Y. Liu, E. Fanning, R. Woodgate, and S.C. West. 2005. Human DNA polymerase eta promotes DNA synthesis from strand invasion intermediates of homologous recombination. *Mol Cell*. 20:783-92.

Melendy, T., and B. Stillman. 1993. An interaction between replication protein A and SV40 T antigen appears essential for primosome assembly during SV40 DNA replication. *J Biol Chem*. 268:3389-95.

Mer, G., A. Bochkarev, R. Gupta, E. Bochkareva, L. Frappier, C.J. Ingles, A.M. Edwards, and W.J. Chazin. 2000. Structural basis for the recognition of DNA repair proteins UNG2, XPA, and RAD52 by replication factor RPA. *Cell*. 103:449-56.

Morgan, D.O. 2008. SnapShot: cell-cycle regulators I. *Cell*. 135:764-764 e1.

Mossi, R., R.C. Keller, E. Ferrari, and U. Hubscher. 2000. DNA polymerase switching: II. Replication factor C abrogates primer synthesis by DNA polymerase alpha at a critical length. *J Mol Biol*. 295:803-14.

Moysich, K.B., R.J. Menezes, and A.M. Michalek. 2002. Chernobyl-related ionising radiation exposure and cancer risk: an epidemiological review. *Lancet Oncol*. 3:269-79.

Nasmyth, K. 1995. Evolution of the cell cycle. *Philos Trans R Soc Lond B Biol Sci*. 349:271-81.

Nelson, J.A., G. Santos, and B.H. Herbert. 1984. Mechanisms for the renal secretion of cisplatin. *Cancer Treat Rep*. 68:849-53.

Niida, H., and M. Nakanishi. 2006. DNA damage checkpoints in mammals. *Mutagenesis*. 21:3-9.

Niu, H., H. Erdjument-Bromage, Z.Q. Pan, S.H. Lee, P. Tempst, and J. Hurwitz. 1997. Mapping of amino acid residues in the p34 subunit of human single-stranded DNA-binding protein phosphorylated by DNA-dependent protein kinase and Cdc2 kinase in vitro. *J Biol Chem*. 272:12634-41.

Norbury, C., and P. Nurse. 1992. Animal cell cycles and their control. *Annu Rev Biochem*. 61:441-70.

Nuss, J.E., S.M. Patrick, G.G. Oakley, G.M. Alter, J.G. Robison, K. Dixon, and J.J. Turchi. 2005. DNA damage induced hyperphosphorylation of replication protein A. 1. Identification of novel sites of phosphorylation in response to DNA damage. *Biochemistry*. 44:8428-37.

O'Meara, E., S.v. Cruet-Hennequart, and M.P. Carty. 2010. Analysis of Protein Phosphorylation in Cisplatin-Treated Human Cells Following Annexin V-based Separation and Multi-Antibody Screening. *Cancer Genomics - Proteomics*. 7:279-286.

Oakley, G.G., L.I. Loberg, J. Yao, M.A. Risinger, R.L. Yunker, M. Zernik-Kobak, K.K. Khanna, M.F. Lavin, M.P. Carty, and K. Dixon. 2001. UV-induced hyperphosphorylation of replication protein a depends on DNA replication and expression of ATM protein. *Mol Biol Cell*. 12:1199-213.

Oakley, G.G., S.M. Patrick, J. Yao, M.P. Carty, J.J. Turchi, and K. Dixon. 2003. RPA phosphorylation in mitosis alters DNA binding and protein-protein interactions. *Biochemistry*. 42:3255-64.

Olson, E., C.J. Nievera, V. Klimovich, E. Fanning, and X. Wu. 2006. RPA2 is a direct downstream target for ATR to regulate the S-phase checkpoint. *J Biol Chem*. 281:39517-33.

Patrick, S.M., G.G. Oakley, K. Dixon, and J.J. Turchi. 2005. DNA damage induced hyperphosphorylation of replication protein A. 2. Characterization of DNA binding activity, protein interactions, and activity in DNA replication and repair. *Biochemistry*. 44:8438-48.

Pattison, D.I., and M.J. Davies. 2006. Actions of ultraviolet light on cellular structures. *EXS*:131-57.

Petermann, E., M. Woodcock, and T. Helleday. 2010. Chk1 promotes replication fork progression by controlling replication initiation. *Proc Natl Acad Sci U S A*. 107:16090-5.

Pines, J. 1991. Cyclins: wheels within wheels. *Cell Growth Differ*. 2:305-10.

Pines, J. 1995. Cyclins and cyclin-dependent kinases: theme and variations. *Adv Cancer Res*. 66:181-212.

Pines, J., and C.L. Rieder. 2001. Re-staging mitosis: a contemporary view of mitotic progression. *Nat Cell Biol*. 3:E3-6.

Prakash, S., R.E. Johnson, and L. Prakash. 2005. Eukaryotic translesion synthesis DNA polymerases: specificity of structure and function. *Annu Rev Biochem*. 74:317-53.

Proctor, R.N. 2001. Tobacco and the global lung cancer epidemic. *Nat Rev Cancer*. 1:82-6.

Reijns, M.A., B. Rabe, R.E. Rigby, P. Mill, K.R. Astell, L.A. Lettice, S. Boyle, A. Leitch, M. Keighren, F. Kilanowski, P.S. Devenney, D. Sexton, G. Grimes, I.J. Holt, R.E. Hill, M.S. Taylor, K.A. Lawson, J.R. Dorin, and A.P. Jackson. 2012. Enzymatic removal of ribonucleotides from DNA is essential for mammalian genome integrity and development. *Cell*. 149:1008-22.

Revet, I., L. Feeney, S. Bruguera, W. Wilson, T.K. Dong, D.H. Oh, D. Dankort, and J.E. Cleaver. 2011. Functional relevance of the histone H2Ax in the response to DNA damaging agents. *Proceedings of the National Academy of Sciences*. 108:8663-8667.

Rodrigo, G., S. Roumagnac, M.S. Wold, B. Salles, and P. Calsou. 2000. DNA replication but not nucleotide excision repair is required for UVC-induced replication protein A phosphorylation in mammalian cells. *Mol Cell Biol*. 20:2696-705.

Rosenberg, B., L. Vancamp, and T. Krigas. 1965. Inhibition of Cell Division in Escherichia Coli by Electrolysis Products from a Platinum Electrode. *Nature*. 205:698-9.

Rosenberg, B., L. VanCamp, J.E. Trosko, and V.H. Mansour. 1969. Platinum compounds: a new class of potent antitumour agents. *Nature*. 222:385-6.

Rybak, L.P., C.A. Whitworth, D. Mukherjea, and V. Ramkumar. 2007. Mechanisms of cisplatin-induced ototoxicity and prevention. *Hear Res*. 226:157-67.

Sakasai, R., K. Shinohe, Y. Ichijima, N. Okita, A. Shibata, K. Asahina, and H. Teraoka. 2006. Differential involvement of phosphatidylinositol 3-kinase-related protein kinases in hyperphosphorylation of replication protein A2 in response to replication-mediated DNA double-strand breaks. *Genes Cells*. 11:237-46.

San Filippo, J., P. Sung, and H. Klein. 2008. Mechanism of eukaryotic homologous recombination. *Annu Rev Biochem*. 77:229-57.

Sanchez, Y., C. Wong, R.S. Thoma, R. Richman, Z. Wu, H. Piwnica-Worms, and S.J. Elledge. 1997. Conservation of the Chk1 checkpoint pathway in mammals: linkage of DNA damage to Cdk regulation through Cdc25. *Science*. 277:1497-501.

Schmidt, M., and H. Bastians. 2007. Mitotic drug targets and the development of novel anti-mitotic anticancer drugs. *Drug Resist Updat*. 10:162-81.

Schultz, L.B., N.H. Chehab, A. Malikzay, and T.D. Halazonetis. 2000. p53 binding protein 1 (53BP1) is an early participant in the cellular response to DNA double-strand breaks. *J Cell Biol*. 151:1381-90.

Sercin, O., and M.G. Kemp. 2012. Characterization of functional domains in human Claspin. *Cell Cycle*. 10:1599-606.

Serrano, M.A., Z. Li, M. Dangeti, P.R. Musich, S. Patrick, M. Roginskaya, B. Cartwright, and Y. Zou. 2012. DNA-PK, ATM and ATR collaboratively regulate p53-RPA interaction to facilitate homologous recombination DNA repair. *Oncogene*.

Shachar, S., O. Ziv, S. Avkin, S. Adar, J. Wittschieben, T. Reiszner, S. Chaney, E.C. Friedberg, Z. Wang, T. Carell, N. Geacintov, and Z. Livneh. 2009. Two-polymerase mechanisms dictate error-free and error-prone translesion DNA synthesis in mammals. *EMBO J*. 28:383-393.

Shao, R.G., C.X. Cao, H. Zhang, K.W. Kohn, M.S. Wold, and Y. Pommier. 1999. Replication-mediated DNA damage by camptothecin induces phosphorylation of RPA by DNA-dependent protein kinase and dissociates RPA:DNA-PK complexes. *EMBO J*. 18:1397-406.

Shi, W., Z. Feng, J. Zhang, I. Gonzalez-Suarez, R.P. Vanderwaal, X. Wu, S.N. Powell, J.L. Roti Roti, and S. Gonzalo. 2010. The role of RPA2 phosphorylation in homologous recombination in response to replication arrest. *Carcinogenesis*. 31:994-1002.

Shrivastav, M., L.P. De Haro, and J.A. Nickoloff. 2008. Regulation of DNA double-strand break repair pathway choice. *Cell Res*. 18:134-47.

Shuck, S.C., and J.J. Turchi. 2010. Targeted inhibition of Replication Protein A reveals cytotoxic activity, synergy with chemotherapeutic DNA-damaging agents, and insight into cellular function. *Cancer Res*. 70:3189-98.

Siegel, R., D. Naishadham, and A. Jemal. 2012. Cancer statistics, 2012. *CA Cancer J Clin*. 62:10-29.

Sorensen, C.S., R.G. Syljuasen, J. Falck, T. Schroeder, L. Ronnstrand, K.K. Khanna, B.B. Zhou, J. Bartek, and J. Lukas. 2003. Chk1 regulates the S phase checkpoint by coupling the physiological turnover and ionizing radiation-induced accelerated proteolysis of Cdc25A. *Cancer Cell*. 3:247-58.

Speroni, J., M.B. Federico, S.F. Mansilla, G. Soria, and V. Gottifredi. 2012. Kinase-independent function of checkpoint kinase 1 (Chk1) in the replication of damaged DNA. *Proc Natl Acad Sci U S A*. 109:7344-9.

Steigemann, P., and D.W. Gerlich. 2009. Cytokinetic abscission: cellular dynamics at the midbody. *Trends in Cell Biology*. 19:606-616.

Stephan, H., C. Concannon, E. Kremmer, M.P. Carty, and H.P. Nasheuer. 2009. Ionizing radiation-dependent and independent phosphorylation of the 32-kDa subunit of replication protein A during mitosis. *Nucleic Acids Res*. 37:6028-41.

Stracker, T.H., T. Usui, and J.H. Petrini. 2009. Taking the time to make important decisions: the checkpoint effector kinases Chk1 and Chk2 and the DNA damage response. *DNA Repair (Amst)*. 8:1047-54.

Strzalka, W., and A. Ziemienowicz. 2011. Proliferating cell nuclear antigen (PCNA): a key factor in DNA replication and cell cycle regulation. *Ann Bot*. 107:1127-40.

Sugiyama, T., and S.C. Kowalczykowski. 2002. Rad52 protein associates with replication protein A (RPA)-single-stranded DNA to accelerate Rad51-mediated displacement of RPA and presynaptic complex formation. *J Biol Chem*. 277:31663-72.

Teng, K.Y., M.Z. Qiu, Z.H. Li, H.Y. Luo, Z.L. Zeng, R.Z. Luo, H.Z. Zhang, Z.Q. Wang, Y.H. Li, and R.H. Xu. 2010. DNA polymerase eta protein expression predicts treatment response and survival of metastatic gastric adenocarcinoma patients treated with oxaliplatin-based chemotherapy. *J Transl Med*. 8:126.

Treuner, K., A. Okuyama, R. Knippers, and F.O. Fackelmayer. 1999. Hyperphosphorylation of replication protein A middle subunit (RPA32) in apoptosis. *Nucleic Acids Res*. 27:1499-504.

Tsurimoto, T., and B. Stillman. 1991a. Replication factors required for SV40 DNA replication in vitro. I. DNA structure-specific recognition of a primer-template junction by eukaryotic DNA polymerases and their accessory proteins. *J Biol Chem*. 266:1950-60.

Tsurimoto, T., and B. Stillman. 1991b. Replication factors required for SV40 DNA replication in vitro. II. Switching of DNA polymerase alpha and delta during initiation of leading and lagging strand synthesis. *J Biol Chem*. 266:1961-8.

Ummat, A., O. Rechkoblit, R. Jain, J. Roy Choudhury, R.E. Johnson, T.D. Silverstein, A. Buku, S. Lone, L. Prakash, S. Prakash, and A.K. Aggarwal. 2012. Structural basis for cisplatin DNA damage tolerance by human polymerase eta during cancer chemotherapy. *Nat Struct Mol Biol*. 19:628-32.

Vaisman, A., S.E. Lim, S.M. Patrick, W.C. Copeland, D.C. Hinkle, J.J. Turchi, and S.G. Chaney. 1999. Effect of DNA polymerases and high mobility group protein 1 on the carrier ligand specificity for translesion synthesis past platinum-DNA adducts. *Biochemistry*. 38:11026-39.

Vaisman, A., C. Masutani, F. Hanaoka, and S.G. Chaney. 2000. Efficient Translesion Replication Past Oxaliplatin and Cisplatin GpG Adducts by Human DNA Polymerase η *Biochemistry*. 39:4575-4580.

Valko, M., C.J. Rhodes, J. Moncol, M. Izakovic, and M. Mazur. 2006. Free radicals, metals and antioxidants in oxidative stress-induced cancer. *Chem Biol Interact*. 160:1-40.

Vassin, V.M., M.S. Wold, and J.A. Borowiec. 2004. Replication Protein A (RPA) Phosphorylation Prevents RPA Association with Replication Centers. *Mol. Cell. Biol.* 24:1930-1943.

Vermeulen, K., D.R. Van Bockstaele, and Z.N. Berneman. 2003. The cell cycle: a review of regulation, deregulation and therapeutic targets in cancer. *Cell Prolif*. 36:131-49.

Villani, G., U. Hubscher, and J.L. Butour. 1988. Sites of termination of in vitro DNA synthesis on cis-diamminedichloroplatinum(II) treated single-stranded DNA: a comparison between E. coli DNA polymerase I and eucaryotic DNA polymerases alpha. *Nucleic Acids Res*. 16:4407-18.

Walker, J.R., R.A. Corpina, and J. Goldberg. 2001. Structure of the Ku heterodimer bound to DNA and its implications for double-strand break repair. *Nature*. 412:607-14.

Wang, D., and S.J. Lippard. 2005. Cellular processing of platinum anticancer drugs. *Nat Rev Drug Discov*. 4:307-320.

Washington, M.T., R.E. Johnson, L. Prakash, and S. Prakash. 2001. Accuracy of lesion bypass by yeast and human DNA polymerase eta. *Proc Natl Acad Sci U S A*. 98:8355-60.

Weaver, B.A., and D.W. Cleveland. 2005. Decoding the links between mitosis, cancer, and chemotherapy: The mitotic checkpoint, adaptation, and cell death. *Cancer Cell*. 8:7-12.

Wold, M.S., and T. Kelly. 1988. Purification and characterization of replication protein A, a cellular protein required for in vitro replication of simian virus 40 DNA. *Proc Natl Acad Sci U S A*. 85:2523-7.

Wold, M.S., J.J. Li, and T.J. Kelly. 1987. Initiation of simian virus 40 DNA replication in vitro: large-tumor-antigen- and origin-dependent unwinding of the template. *Proc Natl Acad Sci U S A*. 84:3643-7.

Wood, R.D., M. Mitchell, and T. Lindahl. 2005. Human DNA repair genes, 2005. *Mutat Res*. 577:275-83.

Woynarowski, J.M., S. Faivre, M.C. Herzig, B. Arnett, W.G. Chapman, A.V. Trevino, E. Raymond, S.G. Chaney, A. Vaisman, M. Varchenko, and P.E. Juniewicz. 2000. Oxaliplatin-induced damage of cellular DNA. *Mol Pharmacol*. 58:920-7.

Wu, X., Z. Yang, Y. Liu, and Y. Zou. 2005a. Preferential localization of hyperphosphorylated replication protein A to double-strand break repair and checkpoint complexes upon DNA damage. *Biochem J*. 391:473-80.

Wu, X., Z. Yang, Y. Liu, and Y. Zou. 2005b. Preferential localization of hyperphosphorylated replication protein A to double-strand break repair and checkpoint complexes upon DNA damage. *Biochem. J*. 391:473-480.

Yaneva, M., T. Kowalewski, and M.R. Lieber. 1997. Interaction of DNA-dependent protein kinase with DNA and with Ku: biochemical and atomic-force microscopy studies. *EMBO J*. 16:5098-112.

Yeeles, J.T., and K.J. Marians. 2011. The Escherichia coli replisome is inherently DNA damage tolerant. *Science*. 334:235-8.

Zernik-Kobak, M., K. Vasunia, M. Connelly, C.W. Anderson, and K. Dixon. 1997. Sites of UV-induced phosphorylation of the p34 subunit of replication protein A from HeLa cells. *J Biol Chem*. 272:23896-904.

Zhao, Y., C. Biertumpfel, M.T. Gregory, Y.J. Hua, F. Hanaoka, and W. Yang. 2012. Structural basis of human DNA polymerase eta-mediated chemoresistance to cisplatin. *Proc Natl Acad Sci U S A*. 109:7269-74.

Zheng, H., X. Wang, A.J. Warren, R.J. Legerski, R.S. Nairn, J.W. Hamilton, and L. Li. 2003. Nucleotide excision repair- and polymerase eta-mediated error-prone removal of mitomycin C interstrand cross-links. *Mol Cell Biol*. 23:754-61.

Zhou, B.B., and S.J. Elledge. 2000. The DNA damage response: putting checkpoints in perspective. *Nature*. 408:433-9.

Zorbas, H., and B.K. Keppler. 2005. Cisplatin Damage: Are DNA Repair Proteins Saviors or Traitors to the Cell? *ChemBioChem*. 6:1157-1166.

Zou, L., and S.J. Elledge. 2003. Sensing DNA damage through ATRIP recognition of RPA-ssDNA complexes. *Science*. 300:1542-8.

Zou, Y., Y. Liu, X. Wu, and S.M. Shell. 2006. Functions of human replication protein A (RPA): from DNA replication to DNA damage and stress responses. *J Cell Physiol*. 208:267-73.

Chapter 2: Materials and Methods

2.1 Materials

2.1.1 Equipment

- Agarose gel imager – AlphaImager™ 3400, Alpha Innotech, Santa Clara, CA, USA
- Bacterial Culture Incubator/Shaker – Heraeus, Thermo Electron Corporation, Marietta, OH, USA and Innova® 44, New Brunswick Scientific, Edison, NJ, USA
- Cell culture hood – Nuaire ™ Biological Safety Cabinet, NU-437-400E, Nuaire, Plymouth, MN, USA
- Cell freezer – Nalgene™ Cryo 1°C, Rochester, NY, USA
- Cytofuge - Thermo Shandon Cytospin 3
- Humidified cell culture incubator – Nuaire™ US Autoflow CO_2 water-jacketed incubator with Class 100 HEPA Filtration System, Nuaire™, Plymouth, MN, USA
- Benchtop Centrifuges – Rotanta 460 centrifuge (Hettich Zentrifugen, Tuttlingen, Germany), Sigma1-15K (Sigma Laborzentrifugen, Osterode an Harz, Germany)
- Film developer – CP1000 Automatic Film Processor, Agfa, Mortsel, Belgium
- Flow cytometer – FACSCalibur™ and FACSCanto™; Cell Quest™ and Diva™ Software, Becton Dickinson, NJ, USA
- Fume hood –1200 standard, 4616-L, ChemFlow, San Jose, CA, USA
- Heating block – DB-2P, Dri-Block, Techne® Inc., Burlington, NJ, USA
- Isoelectric focusing machine – Investigator™ 5000, Genomic Solutions, Cambridgeshire, UK
- Laboratory oven – Shaw Scientific Limited, Greenhills Industrial Estate, Dublin, Ireland
- Liquid nitrogen container – Jencons-PLS, Bedfordshire,UK
- Microscopes - DeltaVision Core system (Applied Precision) controlling an interline charge-coupled device camera (Coolsnap HQ2; Roper) mounted on an inverted microscope (IX-71; Olympus); Leica DM6000B equipped with a CoolSNAP HQ CCD camera and controlled with MetaMorph (Roper Scientific).
- Power supply – PowerPack 3000, Bio-Rad, Hemel Hempstead, UK
- Platform shaker – Stuart Scientific, Surrey, UK
- Protein electophoresis system – Mini Protean 3® Cell System, Bio-Rad, Hemel Hempstead, UK
- Protein transfer system – Mini Trans-Blot® Cell System, Bio-Rad, Hemel Hempstead, UK
- Pulsed-Field Gel electrophoresis system – CHEF-DR II System Bio-Rad, Hemel Hempstead, UK

- Spectrophotometer – N-1000 NanoDrop® Technologies, Wilmington, DE, USA and Victor^2 1420 Multilabel Counter, Wallac, MA, USA
- Thermal cycler – Mastercycler, Eppendorf, Cambridge, UK
- UV-C source – 245nm, Mineralight lamp, model UVG 11, UVP Inc., CA, USA
- Vacuum sealer – Russell Hobbs Westerly, RI, USA
- Waterbath – Clifton unstirred bath, Bennett Scientific, Devon, UK

2.1.2 Services

- **Pre-designed primer synthesis** was carried out by Sigma-Aldrich Company (UK)
- **DNA sequencing analyses** were provided by LGC Genomics, AGOWA GmbH, Berlin, Germany

2.1.3 Chemicals and plastic/glass ware

- **All chemicals** were purchased from either Merck/Calbiochem/Novagen (UK & Germany), Sigma-Aldrich Chemical Company (UK) or Thermo Fisher Scientific (MA, USA), unless otherwise stated.
- **All DNA polymerases, restriction endonucleases and ligases** supplemented with reaction buffers and BSA solutions were purchased from Novagen (UK) or New England Biolabs (UK) unless otherwise stated.
- **All plasmid isolation kits and DNA gel extraction kit were** purchased from QIAgen (Germany), Sigma-Aldrich (UK) or Promega (USA).
- **All sterile plastic ware** was purchased from Corning; Sigma-Aldrich (UK), Sarstedt GmbH (Germany) or Thermo Fisher Scientific (Dublin, Ireland).

Table 2.1 Chemicals used in tissue culture:

Chemical name	Common Name	Supplier	Diluent	Stock Concentration	Dose Range
5-bromo-2'-deoxyuridine	**BrdU**	Sigma	MEM	1mM	10 µM
5-chloro-2'-deoxyuridine	**CldU**	MP Biomedicals	PBS, 10% DMSO	10mM	200 µM
Cis-Diammine (1,1Cyclobutanedicarboxy-lato) platinum	**Carboplatin**	Sigma	d.H_2O	20mM	50 – 100 µM
cis-Diammineineplatinum (II) dichloride	**Cisplatin**	Ebewe	d.H_2O	1mg/ml	0.5 – 5.0 µg/ml
5-ethynyl-2'-deoxyuridine	**EdU**	Berry & Associates, Inc.	DMSO	10mM	10 µM
5-iodo-2'-deoxyuridine	**IdU**	Sigma	PBS, 10% DMSO	2mM	20 µM
Paclitaxel	**Taxol**	Sigma	DMSO	5mg/ml	5- 20 µg/ml
Phallodin	**Phalloidin**	Sigma	MeOH	5mg/ml	5 µg/ml
Methyl N-(5-thenoyl-2-benzimidazolyl) carbamate	**Nocodazole**	Sigma	DMSO	1mM	0.1 µM
NU7441	**DNA-PKi**	AxonMedChem	DMSO	10mM	10 µM

2.1.4 Bacterial strains and human cell lines

Table 2.2 Bacterial strains:

Bacterial strains	Origin	Characteristics
DH5α	Invitrogen, (obtained from Prof. Robert Lahue, CCB, NUIG)	Plasmid DNA amplification
Top10	Invitrogen, (obtained from Dr. Andrew Flaus, CCB, NUIG)	Plasmid DNA amplification

Table 2.3 Human cell lines:

Cell line	Origin	Characteristics
GM00637	Coriell Institute for Medical Research, New Jersey	Normal human fibroblasts
GM0317A (XP30RO)	Coriell Institute for Medical Research, New Jersey	Human fibroblasts, deficient on DNA polη-expression human fibroblasts as a result of 13bp deletion in exon 2 of the *POLH* gene
HeLa (CCL2)	ATCC (obtained from Prof. Kevin Sullivan, CCB, NUIG)	Human cervical adenocarcinoma cells
NFF	Obtained from Prof. Martin Lavin, UQCCR, University of Queensland, Australia	Normal foreskin fibroblasts
TR30-2	Dr. Michael Carty	XP30RO derivative constitutively expressing DNA polη from a *POLH* transgene

2.1.5 DNA plasmids

Table 2.4 DNA plasmids:

Plasmid	Origin	Characteristics
pcDNA 3.1+	Invitrogen, (obtained from Dr. Ciaran Morrison, CCB, NUIG)	High-level stable and transient protein expression in mammalian cells
peGFP-C1	Clontech, (obtained from Dr. Ciaran Morrison, CCB, NUIG)	High-level stable and transient protein expression of N-terminally GFP-tagged protein in mammalian cells
peGFP-N1	Clontech, (obtained from Dr. Ciaran Morrison, CCB, NUIG)	High-level stable and transient protein expression of C-terminally GFP-tagged protein in mammalian cells
RPA2WT-eGFP-C1	Dr. Klaus Weisshart, (obtained from Dr. Heinz-Peter Nasheuer, CCB, NUIG)	Expression of wild-type EGFP-RPA2 in mammalian cells (tag located on the N-terminus of RPA2)
wtRPA2-eGFP-N1	Dr. Michael Carty	Expression of wild-type EGFP-RPA2 in mammalian cells (tag located on the C-terminus of RPA2)
S4A-RPA2-eGFP-N1	Dr. Michael Carty	Expression of EGFP-RPA2 containing a serine to alanine mutation at position 4, in mammalian cells (tag located on the C-terminus of RPA2)

S8A-RPA2-eGFP-N1	Dr. Michael Carty	Expression of EGFP-RPA2 containing a serine to alanine mutation at position 8, in mammalian cells (tag located on the C-terminus of RPA2)
S4A/S8A-RPA2-eGFP-N1	Dr. Michael Carty	Expression of EGFP-RPA2 containing a serine to alanine mutation at position 4 and 8, in mammalian cells (tag located on the C-terminus of RPA2)
FLAG-wtRPA2(N)	Dr. Michael Carty	Expression of wild-type, FLAG-tagged RPA2 in mammalian cells (tag located on the N-terminus of RPA2)
FLAG-S4A-RPA2(N)	Dr. Michael Carty	Expression of FLAG-tagged RPA2 containing a serine to alanine mutation at position 4, in mammalian cells (tag located on the N-terminus of RPA2)
FLAG-S8A-RPA2(N)	Dr. Michael Carty	Expression of FLAG-tagged RPA2 containing a serine to alanine mutation at position 8, in mammalian cells (tag located on the N-terminus of RPA2)
FLAG-S4A/A8A-RPA2(N)	Dr. Michael Carty	Expression of FLAG-tagged RPA2 containing a serine to alanine mutation at position 4 and 8, in mammalian cells (tag located on the N-terminus of RPA2)
wtRPA2(C)-FLAG	Dr. Michael Carty	Expression of wild-type, FLAG-tagged RPA2 in mammalian cells (tag located on the C-terminus of RPA2)
S4A-RPA2(C)-FLAG	Dr. Michael Carty	Expression of FLAG-tagged RPA2 containing a serine to alanine mutation at position 4, in mammalian cells (tag located on the C-terminus of RPA2)
S8A-RPA2(C)-FLAG	Dr. Michael Carty	Expression of FLAG-tagged RPA2 containing a serine to alanine mutation at position 8, in mammalian cells (tag located on the C-terminus of RPA2)
S4A/S8A-RPA2(C)-FLAG	Dr. Michael Carty	Expression of FLAG-tagged RPA2 containing a serine to alanine mutation at position 4 and 8, in mammalian cells (tag located on the C-terminus of RPA2)

2.2 Methods

2.2.1 Cell lines

The human cell lines used in the present study are listed in Table 2.3. The normal human fibroblast cell line (repository number GM00637) was obtained from the National Institute for General Medical Sciences (NIGMS) Human Genetic Cell Repository (Coriell Institute for Medical Research, New Jersey). The XP30RO cell (Volpe and Cleaver, 1995) was originally obtained from Prof. J. Cleaver (UCSF); subsequently XP30RO cells were obtained from the Coriell Institute (repository number GM0317A). The TR30-2 cell line is a clone derived from XP30RO cells stably transfected with the His-V5-RAD30-pcDNA4/TO-E/Uni (pMR30-V5) plasmid as previously described for the inducible TR30-9 clone (Cruet-Hennequart et al., 2006). TR30-2 cells are not inducible for polη, and constitutively express wild-type polη from the *POLH* transgene. All cell lines were SV40-transformed fibroblasts. The HeLa cell line was obtained from Prof. Kevin F. Sullivan (Cell Biology Laboratory, Biochemistry, Centre for Chromosome Biology, NUI Galway).

2.2.2 Cell culture

Fibroblasts were grown in Minimal Essential Media (MEM, Sigma) supplemented with 2X essential amino acids (Gibco, Gaithersburg, MD, USA), 2x non-essential amino acids (Sigma), 2X vitamins (Gibco), 2mM L-glutamine (Sigma), 10% (v/v) uninactivated foetal bovine serum (FBS) (Gibco) and 1% (v/v) penicillin-streptomycin (Sigma). Normal foreskin fibroblasts (NFF) were grown in Dulbecco's Modified Eagle's Media (DMEM, Sigma) containing 10% (v/v) heat-inactivated FBS (Gibco). HeLa cells were grown in Dulbecco's Modified Eagle's Media (DMEM, Sigma) with high glucose content (4,500mg/ml) (Sigma), supplemented with 2mM L-glutamine (Sigma), 10% (v/v) heat-inactivated FBS (Gibco), 2X essential and non-essential amino acids (Sigma) and 1% (v/v) penicillin-streptomycin (Sigma). All cells grew as adherent cultures.

Cell culture procedures were carried out in a Class III Bio-Safety Cabinet. Disposable sterile plasticware was used for all cell culture protocols. Surfaces were sprayed with 70% industrial methylated spirits (IMS) prior to carrying out cell culture procedures. Cells were normally grown in 75cm^2 flasks, at a density of 1 x 10^4/ml in 15ml of medium, and incubated in an autoflow CO_2 water-jacketed incubator (Nuaire, Plymouth, MN, USA) at 37˚C and 5% CO_2.

Cell culture medium was changed every three days. Cells were subcultured when approximately 80% confluent, as determined using light microscopy, by treatment for 5

minutes at 37°C with 2X trypsin-EDTA (Sigma) in Hanks balanced salt solution (HBSS, Sigma). Cells were centrifuged at 1,200rpm for 5 minutes in a Rotanta 460 centrifuge (Hettich Zentrifugen, Tuttlingen, Germany) and the cell pellet was gently resuspended in 10ml of pre-warmed, fresh cell culture medium. Total cell number was determined using a Kova® Glasstic® Slide 10 combination coverslip-microscope slide (Hycor Biomedical Ltd, CA, USA). 2 x 10^5 cells were added to 20ml of pre-warmed medium in a sterile 75cm^2 flask.

2.2.3 Cryopreservation

Cells were removed from flasks by treatment with 2X trypsin-EDTA in Hanks balanced salt solution (HBSS) for 5 minutes. Cells were centrifuged at 1,200rpm for 5 minutes, counted and resuspended at 1.5 x 10^6/ml in freezing medium. XP30RO and TR30-2 cells were stored in liquid nitrogen at 1.5 x 10^6/ml in culture freezing medium (excluding all amino acids, vitamin supplements and antibiotics), and containing 20% (v/v) un-inactivated FBS and 10% (v/v) dimethlysulfoxide (DMSO, Sigma). For cryopreservation of NFF and HeLa cells, heat-inactivated FBS was used. The cell suspension was transferred to pre-labelled 1.5ml cryovials (Nunc, Wiesbaden, Germany) in 1ml aliquots. In order to maintain cell membrane integrity, cells were cooled at a rate of approximately 1˚C/minute by placing the cryovials in a Cryo 1°C Freezing Container (Nalgene®, Rochester, NY, USA) containing 250ml of 100% isopropanol. Cells were stored at -70˚C overnight and then transferred to a liquid nitrogen storage system (Jencons-PLS, Bedfordshire, UK).

2.2.4 Resuscitation

All cell lines were resuscitated by rapid thawing of the cell suspension at 37˚C. 1ml of pre-warmed medium was placed in a 15ml sterile tube, and the cell suspension was added and incubated at 37°C for 1 minute. 3ml of culture medium was then added, followed by incubation at 37°C for 1 minute. Cells were pelleted by centrifugation at 1,000rpm for 3 minutes, resuspended in 5ml of pre-warmed culture medium and placed in a 25cm^2 flask. Cells were incubated at 37˚C and 5% CO_2. The culture medium was changed the following day.

2.2.5 Cell treatment

2.2.5.1 Treatment with platinum-based drugs

36h to 48h before treatment, cells were seeded on 60mm or 100mm dishes and grown to approximately 70% confluence. Media was changed directly prior to treatment. 1mg/ml cisplatin or 20mM carboplatin stock solutions, of the volume required to reach the desired final concentration was added directly to culture media. Controls were treated with

the appropriate volume of dH_2O. Unless otherwise stated, cells were maintained in media containing drug until harvested for analysis. Details on the stock solutions of platinum-based drugs used in the present study are presented in Table 2.1.

2.2.5.2 Ultraviolet light treatment

36h to 48h before treatment cells were seeded on 60mm or 100mm dishes and grown to approximately 70% confluence. Prior to treatment, media from cultured cells was collected in sterile 15ml tubes, and cells were washed twice with pre-warmed, sterile phosphate-buffer saline (PBS, 140mM NaCl, 2.5mM KCl, 10mM Na_2HPO_4, 1.8mM KH_2PO_4, pH 7.6). 2ml of PBS per 60mm dish, and 5ml of PBS per 100mm dish was added to the cells. Open dishes were exposed to a UV-C source (Mineralight lamp, model UVG 11, UVP Inc., CA, USA) for a time period to reach the desired exposure level (12 seconds for $20J/m^2$). Control cells were mock-irradiated by removing the media and washing the cells in PBS as above. After UV-C treatment, the original media was returned to the dishes and cells were further cultured until being harvested for analysis.

2.2.6 XTT cell viability assay

The XTT assay (Roche, Basel, Switzerland) is based on the cleavage of the yellow tetrazolium salt XTT to form an orange formazan dye by metabolically active cells. Therefore, the amount of formazan dye formed directly correlates to the number of metabolically active cells (Gerlier and Thomasset, 1986; Scudiero et al., 1988). Cells were seeded in triplicate on a 96-well plate, at 5×10^3 per well in 150µl of media. After 24 h of incubation in a humidified incubator at 37ºC and 5% CO_2, media was removed and cells were treated with indicated doses of cisplatin or carboplatin in fresh medium. After 24h incubation, media containing drugs was removed, cells were washed twice with fresh media and the cells were allowed to recover in 150µl of media for 4 days. Immediately before use, 151µl per well of XTT labelling mastermix solution was prepared as follows: 1µl of electron coupling reagent (PMS (N-methyl dibenzopyrazine methyl sulfates; 0.383 mg/ml [1.25mM] in PBS) and 50µl of labelling reagent (sodium 3´-[1- (phenylaminocarbonyl)- 3,4 tetrazolium]-bis (4-methoxy-6-nitro) benzene sulfonicacid hydrate in RPMI 1640, without phenol red) was added to 100µl of pre-warmed media. 150µl of the mastermix was pipetted into each well of the 96-well tissue culture plate and cells were incubated for a further four hours. Absorbance was then measured at 490nm using a Victor^2 1420 Multilabel Counter (Wallac, MA, USA). Results are expressed as the percentage viability relative to the viability of untreated cells.

2.2.7 Flow cytometry

2.2.7.1 BrdU incorporation and cell harvesting

36h to 48h before treatment cells were seeded on 60mm dishes and grown to approximately 70% confluence. Cells were treated with platinum-based chemotherapeutic drugs as indicated for particular experiments. 75 minutes prior to the time of harvesting, cells were pulse-labelled with 10μM 5-bromo-2'-deoxyuridine (BrdU), a thymidine analogue which can be incorporated into DNA during replication. BrdU was diluted directly in culture media according to Table 2.1. After labelling, cells were harvested by trypsinisation as outlined in Section 2.2.2. Cells were collected by centrifugation at 1,200 rpm for 5 minutes, washed in PBS and pelleted again prior to resuspension in 1ml of ice-cold PBS. Cells were fixed by the slow, dropwise, addition of 3ml ice-cold 100% ethanol, and stored at -20°C until the day of staining.

2.2.7.2 BrdU and propidium iodide staining

On the day of flow cytometric analysis, cells were allowed to thaw at room temperature prior to centrifugation at 2,000 rpm for 10 minutes in a Rotanta centrifuge. The supernatant was discarded and the cell pellet was disrupted. Cells were permeablised by dropwise addition of 1ml of 2N HCl-0.5% (v/v) Triton X-100. HCl was neutralised by the addition of 1ml of $Na_2B_40_7$ pH 8.5, followed by centrifugation at 1,000 rpm for 10 minutes. Following resuspension in 750μl of PBS containing 1% (w/v) BSA and 0.5% (v/v) Tween-100, 15μl of FITC-labelled anti-BrdU antibody (BD Biosciences, NJ, USA) was added. Tubes were rotated at room temperature in the dark for 1 hour prior to centrifugation at 1,000 rpm for 3 minutes. Cells were washed twice in PBS containing 1% (w/v) BSA and 0.5% (v/v) Tween-100 and centrifuged as described above. DNA was stained by resuspending the cell pellet in 500μl propidium iodide containing RNase (PI/RNase) (BD Biosciences) for 15 minutes at room temperature in the dark. Samples were acquired using a FACSCalibur flow cytometer (BD Biosciences), and analysed using Cell Quest™ software.

2.2.8 Cell synchronization in mitosis and mitotic release

XP30RO and HeLa cells were grown in T175 flasks (three flasks per condition) until approximately 70% confluent and were then treated with 0.1μM nocodazole, a known anti-mitotic agent which prevents metaphase spindle formation and therefore arrests cells in pro-metaphase (Harper, 2005). Mitotically-arrested cells change morphology and, in the case of HeLa and XP30RO cells, become less attached to the flask surface. This fact was used to shake off the mitotic cell population after treatment with nocodazole for 16 hours. Cells were pelleted by centrifugation at 1,000rpm for 2 minutes, washed in 10ml of pre-warmed

culture media to remove nocodazole, transferred to a 15ml tube (Sarstedt) and pelleted again. Cells were then re-suspended in 2ml of warm media, placed in a waterbath at 37°C for up to 3 hours. Under these conditions, cells can complete mitosis and undergo cytokinesis (Skop et al., 2004). Where indicated, at specific times, an aliquot sample of cells ($1x10^6$) was taken for western blotting and for immunofluorescence analysis.

2.2.9 Midbody isolation

Midbodies were isolated from XP30RO cells at specific times following mitotic release (described in Section 2.2.8) (Skop et al., 2004). To stabilize spindle microtubules and actin filaments respectively *in vivo*, taxol and phalloidin (prepared as described in Table 2.1) were each added to the cell suspension to achieve a final concentration of 5µg/ml. Cells were then collected by centrifugation for 1min at 1,000rpm and the supernatant was discarded. Pellets were gently washed once with sterile ddH_2O. The supernatant was aspirated and the cell pellets were re-suspended in 400µl of midbody isolation buffer (2mM Pipes, pH 6.9 containing 0.25% (v/v) Triton X-100 and 20µg/ml taxol). Cell membranes were disrupted by vortexing the samples for 20 minutes at room temperature, controlling midbody isolation process using a phase-contrast microscope (Skop et al., 2004). Midbodies were then sedimented by centrifugation for 20 minutes at 2,000rpm, at room temperature. At this point samples were taken for immunofluorescence analysis. 5µl of the pellet was applied to a slide and fixed as described in Section 2.2.17.2.

Midbodies were further purified from spindles and cell debris by chilling the pellets on ice and washing with 500µl of 50mM MES, pH 6.3. Midbodies were pelleted by centrifugation for 2min at 1,000rpm, at 4°C. The washing step was repeated twice. The pellet was re-suspended in 100µl MES buffer, layered over 300µl of a 40% (v/v) glycerol cushion and centrifuged at 14,000rpm for 5min, at 4°C. The supernatant was discarded and the pellet was washed once with MES buffer. At this point another sample for taken for immunofluorescence analysis, as described above.

2.2.10 Cell lysate preparation

All procedures were carried out on ice. Cells were washed twice with 2ml ice-cold PBS pH 7.6 and all PBS was carefully removed using a water pump. The appropriate volume (50µl per 60mm dish) of cell lysis buffer (PBS pH 7.6, 1% (v/v) Triton (Sigma), 0.5% (w/v) deoxycholic acid (DOC, Sigma), 0.1% (w/v) SDS (Bio-Rad Laboratories, CA, USA) containing protease and phosphatase inhibitors (obtained from Sigma and listed in Table 2.5) was added to the culture dishes. Cells were scraped into the lysis solution using 39cm cell scrapers (Serstedt) and left on ice for 5 minutes. The lysate on the dish was again

scraped and transferred into a 1.5ml tube (Eppendorf). Tubes were vortexed at high speed for 20 seconds, and cell lysis was allowed to proceed by incubation of tubes on ice for a further 15 minutes. Tubes were then centrifuged at 14,000rpm for 15 minutes in a Sigma 1-15K centrifuge. Supernatants containing protein lysates were stored at -20˚C.

Inhibitor class	Inhibitor name	Stock concentration	Working concentration
Protease inhibitors	**Aprotinin**	2mg/ml	2µg/ml
	Leupeptin	1mg/ml	1 µg/ml
	Phenylmethylsulfonyl fluoride (PMSF)	100mM	1mM
Phosphatase inhibitors	**Sodium orthovanadate (Na_3VO4)**	100mM	1mM
	Sodium fluoride (NaF)	500mM	5mM

Table 2.5 Protease and phosphatase inhibitors.

2.2.11 Determination of protein concentration

Protein concentrations in cell lysates were estimated using the DC Protein Assay (Bio-Rad Laboratories). A 2mg/ml bovine serum albumin (BSA, Sigma) stock solution, prepared in lysis buffer, was used to prepare protein standards ranging from 0 to 1mg/ml. 5 µl of each standard were placed in duplicate wells of a 96-well plate (Sarstedt). Protein samples were mixed using a vortex and 2µl of each sample was added to duplicate wells. DC protein assay reagent A' was prepared immediately prior to use by addition of 20µl of reagent S per 1ml of reagent A. 25µl of reagent A' was added to each well, followed by the addition of 200µl of reagent B. The colour was allowed to develop for 15 minutes before the absorbance of each well was read at 490nm on a Victor^2 1420 Multilabel Counter (Wallac, MA, USA). Using MS Excel software (Microsoft, WA, USA), a plot of absorbance versus BSA concentration was prepared, and a linear trend line was estimated using the plotted points. The R^2 value was calculated; any curves having a R^2 value below 0.95 were discarded, and the assay was repeated. Using MS Excel, the slope of the trend line was calculated, and the equation $y = mx + c$ (where y = absorbance, m = slope of the trend line, x = BSA concentration and c = trend line intercept on the y-axis) was used to calculate the protein concentration of individual cell lysates.

2.2.12 Sodium Dodecyl Sulphate Polyacrylamide Gel Electrophoresis (SDS-PAGE)

Protein lysates were separated by sodium dodecyl sulphate polyacrylamide gel electrophoresis (SDS-PAGE) using the Mini-Protean® 3 Cell System (Bio-Rad). SDS-PAGE

gels were prepared according to Table 2.6. Protein lysates were prepared as described in 0. 15-30µg of protein was mixed with 4X Laemmli SDS reducing buffer (62.5mM Tris-HCl pH 6.8, 20% (v/v) glycerol, 2% (w/v) SDS, 5% (v/v) β-mercaptoethanol, 1% (w/v) bromphenol blue). Samples were placed in boiling water for five minutes, briefly spun down and applied to the SDS-PAGE gel using Gel Saver II tips (Fisher Scientific, UK). Pre-stained broad-range protein markers (either from Fermentas or ThermoScientific) were loaded in adjacent wells. Empty wells were filled with 1X Laemmli SDS reducing buffer. The upper and lower buffer tanks were filled with 1X running buffer (19.2mM glycine, 2.5mM Tris, 0.01% (w/v) SDS, pH 8.3), and electrophoresis was carried out at 130V (current limit, 400mA) until the desired separation was reached.

Running gel (2 x 1mm gel or 1 x 1.5mm gel)		
Acrylamide % (w/v)	**10%**	**12%**
H_2O	4ml	3.3ml
30% (w/v) Acrylamide-Bis (Bio-Rad)	3.3ml	4ml
1.5M Tris-HCl pH 8.8	2.5ml	2.5ml
10% (w/v) SDS	0.1ml	0.1ml
10% (w/v) APS	0.1ml	0.1ml
TEMED	0.004ml	0.004ml
Stacking gel (2 x 1mm gel or 1 x 1.5mm gel)		
Acrylamide % (w/v)	**5%**	
H_2O	2.8ml	
30% (w/v) Acrylamide-Bis (Bio-Rad)	0.66ml	
1.0M Tris-HCl pH 6.8	0.5ml	
10% (w/v) SDS	0.04ml	
10% (w/v) APS	0.04ml	
TEMED	0.004ml	

Table 2.6 SDS-PAGE gel components.

2.2.13 Western Immunoblotting

2.2.13.1 Protein transfer

SDS-PAGE gels were soaked in 1X transfer buffer (19.2mM glycine, 2.5mM Tris, 20% (v/v) methanol) for 10 minutes. Immobilon-P polyvinylidene fluoride (PVDF, Millipore, MA, USA) membrane was cut to the correct size and pre-activated by submerging in methanol for three minutes, followed by d.H_2O, and transfer buffer. Sponge pads and filter paper (Whatman, UK) were also soaked in cold 1X transfer buffer for 10 minutes. The transfer cassettes were assembled with the PVDF membrane on the cathode side and the SDS-PAGE gel on the anode side. Three filter papers were placed on each side of the membrane and gel, and a sponge was then placed outside the filter papers. The Mini Trans-Blot® Cell System (Bio-Rad) transfer apparatus was assembled; an ice-pack was placed in the tank and the apparatus was filled with cold 1X transfer buffer. Transfer was carried out at 100V for 45 minutes.

2.2.13.2 Blocking and primary antibody probing

Following protein transfer, free protein-binding sites on the membranes were blocked by incubating the membranes in 5% blocking solution (10mM Tris base, 68 mM NaCl, pH 7.6, containing 0.05% (v/v) Tween-100, 5% (w/v) non-fat powered milk (Marvel, Premier Foods, UK) for 1 hour at room temperature on a platform shaker (Stuart Scientific, Surrey, UK) set on medium speed. The membranes were probed with primary antibody using the appropriate dilution of the antibody (according to Table 2.7) in 5% blocking solution.

Membranes to be blotted with anti-rat RPA2 were blocked with 10% foetal bovine serum (FBS), 5% (w/v) bovine serum albumin (BSA) T-TBS (10mM Tris base, 68 mM NaCl, pH 7.6) for 90 minutes.

Membranes with the primary antibody solution were placed in plastic bags, air bubbles were removed, bags were heat-sealed using a vacuum sealer (Russell Hobbs Westerly, RI, USA) and rocked on a platform shaker overnight at 4°C. Unbound primary antibody was then removed by washing the membranes in 25ml TBS-T (10mM Tris base, 68 mM NaCl, pH 7.6, containing 0.05% Tween-100) for 10 minutes, three times.

2.2.13.3 Detection

Detection of primary antibody binding was carried out by probing the membrane with horseradish peroxidase (HRP)-linked secondary antibodies (Jackson ImmunoResearch Laboratories, Inc., PA, USA). Membranes were incubated with the appropriate secondary antibody, diluted according to Table 2.7, in 3% blocking solution (100mM Tris, 68mM

PRIMARY ANTIBODIES			
Name	**Species**	**Dilution**	**Supplier; catalogue number**
Anti-AIM-1 (Aurora B)	Mouse	1/1000	BD Biosciences; #611082
Anti-actin	Rabbit	1/5000	Sigma; #2066
Anti-cleaved caspase-3 (Asp175)	Rabbit	1/1000	Cell Signalling; #9661
Anti-chk1 (clone DCS-310)	Mouse	1/1000	Sigma; #C 9358
Anti-phospho-chk1 (ser317)	Rabbit	1/1000	Cell Signalling; # 2344
Anti-GFP	Mouse	1/1000	Roche; #11814460001
Anti-phospho-H2AX (ser139) JBW301	Mouse	1/1000	Upstate; # 05-636
Anti-cleaved PARP (asp214) (19F4)	Mouse	1/2000	Cell Signalling; #9546
Anti-polymerase eta (B-7)	Mouse	1/100	Santa Cruz; # Sc-17770
Anti-polymerase eta	Rabbit	1/1000	Abcam; #ab17725 Lot 591998
Anti-RPA p34 (Ab-3)	Mouse	1/4000	Oncogene; #NA19L
Anti-RPA1; rat (hybridoma)	Rat	1/10	Dr. Heinz Peter Nasheuer (CCB, NUIG); Dr. Elisabeth Kremmer; clone RAC-4D9
Anti-RPA2; rat (hybridoma)	Rat	1/10	Dr. Heinz Peter Nasheuer (CCB,NUIG); Dr. Elisabeth Kremmer; clone RBF-4E4
Anti-phospho-Ser4/Ser8 RPA2	Rabbit	1/4000	Bethyl; # A300-245A-1
Anti-α tubulin	Mouse	1/5000	Prof. Kevin F. Sullivan (CCB, NUIG); Sigma; #T9026
SECONDARY ANTIBODIES			
Horseradish peroxidase (HRP) – conjugated goat anti-mouse IgG	Mouse	1/5000	Jackson ImmunoResearch; 115-035-003
Horseradish peroxidase (HRP) – conjugated goat anti-rabbit IgG	Rabbit	1/5000	Jackson ImmunoResearch; 111-035-003
Horseradish peroxidase (HRP) – conjugated donkey anti-rat IgG	Rat	1/10000	Dr. Heinz-Peter Nasheuer (CCB, NUIG); Jackson ImmunoResearch; 712-035-153

Table 2.7 Antibodies dilutions used in western immunoblotting.

NaCl, 0.05% (v/v) Tween-20, 3% (w/v) non-fat powered milk (Marvel, Premier Foods, UK), for 1 hour at room temperature on a platform shaker. Following incubation in secondary antibody, the membranes were washed five times in 25ml TBS-T for 10 minutes per wash with gentle rocking.

HRP activity was visualised using the ECL$^+$ or ECL Prime western blotting chemoluminescence detection systems (Amersham Biosciences, Buckinghamshire, UK). 2ml of detection solution was prepared for approximately 52cm^2 of membrane. Reagent A and reagent B from the ECL$^+$ kit were warmed to room temperature, and mixed at a ratio of 1:40 before being pipetted onto the membrane. When ECL Prime was used, reagent A and B were mixed at a ratio of 1:1. Membranes were incubated in ECL$^+$ or ECL Prime for five minutes and then transferred to a film cassette (Sigma). The remaining steps of the procedure were performed under dark room conditions using a safety light (Safe Light filter no. 6B, Kodak). The film was developed manually in Devalex® X-Ray Developer until bands appeared, rinsed in dH2O and then fixed in Fixaplus® X-Ray Fixer (Champion Photochemistry, Essex, UK). The film was rinsed in dH2O and allowed to dry. Alternatively, the film was developed using a CP1000 Automatic Film Processor (Agfa, Mortsel, Belgium) using the same reagents.

2.2.14 Two-dimensional (2D) gel electrophoresis

Protein samples were separated based on their isolectric point (IP) and molecular weight (MW) using two-dimensional (2D) gel electrophoresis (Gorg et al., 2009).

2.2.14.1 Sample preparation

XP30RO cells were harvested, lysed and protein concentration was determined as described in Sections 2.2.10 and 2.2.11. For each sample, lysates containing 400µg of protein were placed in separate 1.5ml tubes (Eppendorf) and 3X the volume of acetone was added to precipitate the proteins. Protein precipitation was carried out at -20°C, overnight. The following day, tubes were centrifuged at 14,000rpm for 15 minutes, supernatants were discarded and protein pellets were air-dried at 37°C for 15 minutes.

2.2.14.2 First dimension (1D) strip re-hydration

Rehydration solution was prepared by the addition of 4µl of pH 4-7 Isoelectric Point Gel (IPG) buffer (GE Healthcare) and 2.5mg of Dithiothreitol (DTT, Sigma) to 1ml of DeStreak rehydration buffer (GE Healthcare). Air-dried protein samples were rehydrated in 230µl of rehydration solution, vortexed for 2min and centrifuged at 14,000rpm for 10 minutes. Supernatants were transferred into fresh 1.5ml tubes. 220µl of the protein sample was pippeted into a clean well of the rehydration tray. Ready Strip rehydration strips, pH4-7

(11cm, Bio-Rad) were carefully placed in the well, with the gel side down, avoiding air-bubbles and the samples were covered with mineral oil (Sigma). Rehydration was carried out for 16h, at room temperature in the dark.

2.2.14.3 Isoelectric focusing

Isoelectric focusing was carried out using an Investigator 5000 apparatus (Genomic Solutions). Strips were removed from the rehydration tray and excess mineral oil was removed. Next, rehydrated strips were placed into the well of the isoelectric focusing apparatus so that that both ends of the strips touched the electrodes. Wells were covered with mineral oil. Protein separation based on pI was carried out at 500V (50µA per gel) for 27 hours. The strips were then removed from the wells, excess mineral oil was removed and strips were placed in milliQ-H_2O for 5 minutes. Strips were placed back into the rehydration tray and incubated in equilibration solution (ES1), containing 45mM Tris-HCl (pH 7.0), 6M Urea, 30% (v/v) glycerol, 2% (w/v) SDS, 10mg/ml DTT (all from Sigma) for 20min, at room temperature with gentle shaking. Next, ES1 was removed and strips were washed 2X with milliQ-H_2O and incubated with equilibration solution (ES2), containing 45mM Tris-HCl (pH 7.0), 6M Urea, 30% (v/v) glycerol, 2% (w/v) SDS, 25mg/ml Iodo-acetamide (all from Sigma) for 20min, at room temperature with gentle shaking.

2.2.14.4 Second dimension separation

Second dimension protein separation, based on protein molecular mass, was carried out using the Criterion System (Bio-Rad). 12% gels were prepared as described previously (Table 2.6 SDS-PAGE gel components), and 15ml of running gel solution was prepared per strip. Each strip was placed onto an individual Criterion gel. A clean piece of filter paper, onto which 5µl of broad-range molecular marker (Fermentas) had been added, was placed on the top of Criterion gel, at one side, and fixed in place using 0.8% (w/v) low melting agarose (Molecular Probes). Protein separation, transfer and antibody staining was carried out as described in Sections 2.2.12 - 2.2.13.3.

2.2.15 Immunoprecipitation

Immunoprecipitation was carried out using Dynabeads® M-270 Epoxy magnetic beads (Invitrogen). 1mg of Dynabeads® was weighed out into a 1.5ml test tube (Eppendorf) and the beads were washed 3 times in 500µl of 0.1M sodium phosphate buffer, pH 7.4 (Sigma). To remove the washing buffer, the tube was placed on a magnet in order to accumulate the beads at the side before removing the supernatant. Next, the beads were washed with 500µl of PBS, and the beads were coated by incubation with 1µg of the desired primary antibody in a final volume of 250µl PBS. 250µl of 3M ammonium sulphate (Sigma)

made up in 0.1M sodium phosphate buffer pH 7.4 was also added to the beads to give a final concentration of 1.5M ammonium sulphate. The mixture was incubated overnight at 37°C with rotation. The following day, using the magnet, the antibody-coupled beads were washed 4X with PBS, with the final wash carried out for 5 minutes at room temperature with rotation. Antibody-coupled beads were then washed once with 500µl of cell lysis buffer (provided in the Dynabeads® M-270 Epoxy kit). Next the beads were incubated with 400µg of protein lysate at a concentration of 1µg/ml, overnight at 4°C with rotation. Following overnight incubation, the supernatant was removed and the beads were washed three times with 200µl of cell lysis buffer. Bound protein was eluted by incubation of the beads with 60µl of 0.1M citrate (pH 3.1, Sigma) at room temperature for 5 minutes with rotation. The tube was then placed on a magnet and beads were collected at the side. The supernatant containing the isolated protein was transferred to a new tube and stored at -20°C.

2.2.16 λ phospohatase treatment

Cells were harvested and lysed in cell lysis buffer without the addition of phosphatase inhibitors, protein content was determined as described in Sections 2.2.10 and 2.2.11. An appriopriate volume of lysate, containing 30µg of protein was transferred into four separate 0.5ml tubes (Eppendorf). 2.4µl of 10X λ phosphatase reaction buffer and 2.4µl of 10X $MnCl_2$ (both from Sigma) were placed in each tube. Phosphatase inhibitor, Na_3VO_4 was added to specified tubes, to reach the final concentration of 1mM. 1µl of λ phosphatase (Sigma) was added to the appropriate tubes. Reactions were brought up to a final volume of 24µl with milliQ-H_2O and allowed to proceed for 45 minutes, at 30°C. The reaction was stopped by the addition of 5 µl of 4X Laemmli buffer and by then placing the tubes in boiling water for 5 minutes. The samples were stored at -20°C before analysis by SDS-PAGE and western blotting.

2.2.17 Immunofluorescence

2.2.17.1 Coverslip treatment

Φ15mm, No. 1.5 glass coverslips (VWR) were cleaned prior to use in tissue culture. Coverslips were placed in a jar and immersed in concentrated HCl overnight, in the fume hood. The next day the coverslips were rinsed extensively in ddH2O, followed by boiling in d.H2O for 15 minutes. Coverslips were allowed to cool and were then extensively washed: first, 5 times with ddH20, then 3 times with 95% (v/v) ethanol (Sigma) and finally, once in 100% (v/v) ethanol. Excess ethanol was removed and coverslips were then placed in single layers on paper and allowed to dry under UV light overnight, in a closed laminar flow hood. Coverslips were kept in sterile 100mm dishes (Sarstedt).

2.2.17.2 Sample preparation

On the day of the experiment, a drop of PBS (5µl) was placed in a tissue culture dish directly underneath the coverslip in order to minimize coverslip movement when applying the cell suspension. Cells were grown directly on coverslips for at least 36 hours before being treated as indicated in particular experiments. Following treatment for the indicated times, cells were gently washed twice with 2ml of PBS and fixed using 4% paraformaldehyde (PFA, 1.5ml of PFA per 30mm dish, Electron Microscopy Sciences) for 15 minutes at room temperature. Cells were then washed 3 times for 2min with PBS. At this point, either the staining procedure outlined below was followed, or the coverslips with fixed cells were stored at 4°C for subsequent processing.

In specific cases, cells were prepared for immunofluorescence analysis using a Thermo Shandon Cytospin 3 cytofuge. Using this approach, a sample can be obtained consisting of single layer of suspended cells (e.g. apoptotic cells or cells growing in suspension) deposited onto a clearly-defined area of a glass slide. Mitotically-enriched cell populations were obtained as described in Section 2.2.8. Cells were collected and resuspended in PBS at $2x10^5$ cells per ml. 200µl of this cell suspension was used per each funnel in the cytofuge, and cells were centrifuged onto poly-L-lysine coated slides (BDH) for 5 minutes at 800rpm. A liquid blocking pen (Sigma) was used to mark the sample area, the cells were fixed as described above and stored at 4°C until the day of staining.

Where indicated, a pre-permeablisation step was carried out prior to fixation. After two washes in PBS, cells were incubated for 15 minutes on ice with pre-permeabilisation buffer prepared according to Table 2.8 (Richard et al., 2008). Inhibitors and ATP were added just before use. Following incubation on ice, the pre-permeablisation buffer was aspirated and the cells were fixed on the coverslips as described above.

2.2.17.3 Immunostaining and detection

On the day of staining, coverslips were allowed to equilibrate to room temperature. Cells permeabilisation was performed by washing the coverslips twice for 10 minutes in PBS-TX (PBS pH7.4, 0.1% (v/v) Triton X-100), with gentle rocking. Non-specific antibody binding sites were blocked with PBS-TX containing 1% (w/v) bovine serum albumin (BSA, Sigma) for 30 minutes at room temperature, with gentle rocking. Coverslips to be stained with anti-γH2AX primary antibody were incubated in blocking solution consisting of PBS supplemented with 0.5% (w/v) BSA and 20% (v/v) normal goat serum (NGS, Sigma). Coverslips to be stained with rat serum-derived primary antibodies were blocked with PBS containing 0.05% (v/v) Tween-20, 5% (w/v) BSA and 10% (v/v) NGS.

Compound name	Stock concentration	Working concentration
HEPES buffer pH 8.0	200mM	20mM
Sodium chloride (NaCl)	2M	20mM
Magnesium Chloride ($MgCl_2$)	500mM	5mM
Igepal (NP-40)	100% (v/v)	0.5% (v/v)
Sodium orthovanadate (Na_3VO4)	100mM	0.1mM
Sodium fluoride (NaF)	500mM	1mM
Adenosine 5'-triphophate disodium salt (ATP)	100mM	1mM

Table 2.8 Pre-permeabilisation buffer components.

Primary antibodies were diluted in appropriate blocking solutions according to Table 2.9. Coverslips were transferred cell-side up onto a parafilm-coated, light-isolated cassette and incubated with 50µl of the diluted antibody for 1 hour, either at room temperature or at 37°C. Coverslips were then transferred to 4-well plates and washed 4 times, for 7 minutes each time, in PBS-TX, unless otherwise stated. The secondary antibody incubation step was performed by placing the coverslips in the dark cassette in secondary antibody-containing solution (prepared according to Table 2.9) for 1h at room temperature or at 37°C. After the washing steps, where dual-labelling was carried out, a second round of primary and secondary staining was performed according to protocol described above. In order to remove detergent and salt, coverslips were then washed in PBS followed by ddH_2O and air-dried. Coverslips were inverted and mounted onto SuperFrost glass slides (BDH) using 2µl of Slow Fade Gold mounting reagent (Invitrogene), containing 4',6-diamidino-2-phenylindole (DAPI, Sigma-Aldrich) to counterstain the DNA. The edges of the coverslips were secured onto the slides using nail varnish. Slides were stored in the dark at 4°C if required.

2.2.17.4 The use of blocking peptide against anti-phospho-Ser4/Ser8 RPA2 primary antibody

Where indicated, blocking peptide (Bethyl; BP 300-245P), which corresponds to epitopes recognised by the anti-phospho-Ser4/Ser8 RPA2 primary antibody was used to inhibit binding of the antibody to phospho-Ser4/Ser8 RPA2 antibody to bind cellular phospho-Ser4/Ser8 RPA2. Samples for immufluorescence staining were prepared as described in Section 2.2.17.2. Prior to applying the primary antibody solution onto samples, antibody was pre-incubated with the blocking peptide at the concentration of 12.5µg of blocking peptide per 1µg of primary antibody. The blocking reaction was allowed to proceed for 2h at 37°C, before being diluted to an appropriate concentration in PBS-TX containing

PRIMARY ANTIBODIES			
Name	**Species**	**Dilution**	**Supplier; catalogue number**
Anti-AIM-1 (Aurora B)	Mouse	1/100	BD Biosciences; #611082
Anti-53BP1	Rabbit	1/400	Prof. Noel Lowndes (CCB, NUIG); Novus; #NB100-904
Anti-BrdU clone B44	Mouse	1/20	Dr. Philippe Pasero (IGH); Becton Dickinson; # 347580
Anti-BrdU clone BU1/75	Rat	1/20	Dr. Philippe Pasero (IGH); AbCys SA; #ABC117 7513
Anti-ssDNA (poly dT)	Mouse	1/500	Dr. Philippe Pasero (IGH); Chemicon MAB3034
Anti-phospho-H2AX (ser139) JBW301	Mouse	1/8000	Upstate; # 05-636
Anti-RPA p34 (Ab-3)	Mouse	1/500	Oncogene; #NA19L
Anti-RPA2; rat (hybridoma)	Rat	1/5	Dr. Heinz-Peter Nasheuer (CCB, NUIG); Dr. Elisabeth Kremmer; clone RBF-4E4
Anti-phospho-Ser4/Ser8 RPA2	Rabbit	1/100 - 1/4000	Bethyl; # A300-245A-1
Anti-phospho-Ser23 RPA2; rat (hybridoma)	Rat	1/5	Dr. Heinz-Peter Nasheuer (CCB, NUIG); Dr. Elisabeth Kremmer; clone RBF-8H3
Anti-phospho-Ser29 RPA2; rat (hybridoma)	Rat	1/5	Dr. Heinz-Peter Nasheuer (CCB, NUIG); Dr. Elisabeth Kremmer; clone RBF-8C7
Anti-SJI; 6.24.83.12	Human	1/200	Prof. Kevin F. Sullivan (CCB, NUIG)
Anti-α tubulin	Mouse	1/1000	Prof. Kevin F. Sullivan (CCB, NUIG); Sigma; #T9026
SECONDARY ANTIBODIES			
Alexa Fluor 488-conjugated goat anti-mouse IgG	Mouse	1/100 - 1/2000	Invitrogen; #A-11001
Alexa Fluor 488-conjugated goat anti-rabbit IgG	Rabbit	1/100 - 1/2000	Invitrogen; #A-11008
Alexa Fluor 488-conjugated chicken anti-rat IgG	Rat	1/50	Dr. Philippe Pasero (IGH); Molecular Probes; #A21470
Alexa Fluor 546-conjugated goat anti-mouse IgG1	Mouse	1/50	Dr. Philippe Pasero (IGH); Molecular Probes; #A21123
Alexa Fluor 594-conjugated goat anti-mouse IgG	Mouse	1/100 - 1/2000	Invitrogen; #A-11005

Alexa Fluor 594-conjugated goat anti-mouse IgG	Rabbit	1/100 - 1/2000	Invitrogen; #A-11012
DyLight 594 AffiniPure donkey Anti-Rat IgG	Rat	1/200	Dr. Heinz-Peter Nasheuer (CCB, NUIG); Jackson ImmunoResearch; 712-525-153
Alexa Fluor 674-conjugated goat anti-mouse IgG2a	Mouse	1/50	Dr. Philippe Pasero (IGH); Molecular Probes; #A21241
Rhodamine-conjugated donkey anti-human IgG	Human	1/200	Prof. Kevin F. Sullivan (CCB, NUIG); Jackson ImmunoResearch; 109-025-003

Table 2.9 Antibodies and dilutions used in immunofluorescence procedures.

1% (w/v) bovine serum albumin (BSA) according to Table 2.9. The rest of the immunofluorescence procedure was carried out as described in Section 2.2.17.3.

2.2.17.5 Primary antibody labelling approach

In specific cases, where two antibodies of rabbit origin were to be used for dual-labelling immunofluorescence, the Zenon Alexa Fluor 488-conjugated rabbit IgG labelling kit (Invitrogen) was used to directly label one of the antibodies, as presented in Figure 2.1. As described above, cells were grown on glass coverslips, fixed and blocked in appropriate blocking solution. Immediately before use, 1µl (equal to 1µg) of anti-phospho-Ser4/Ser8 RPA2 primary antibody was incubated in a 1.5ml test tube with 5µl of the Zenon rabbit IgG labelling reagent (component A), which contains labelled Fab antibody fragment. The mixture was incubated for 5 minutes at room temperature. In order to neutralize the excess labelled Fab fragment, 5µl of the Zenon blocking reagent (component B), which contains nonspecific IgG, was added and the reaction was allowed to proceed for a further 5 minutes at room temperature. Following labelling, the Zenon Alexa Fluor 488-conjugated Rabbit IgG labelling complex was diluted to a give the appropriate concentration of the primary antibody (1/200 dilution in the case of anti-phospho-Ser4/Ser8 RPA2 primary antibody). 50µl of this solution was applied to coverslips placed on the parafilm coated surface of the light-isolated casette. Samples were incubated for 1 hour at room temperature and then washed in PBS-TX as described above. Samples were then exposed to the desired second primary antibody raised in rabbit, washed in PBS-TX and incubated with Alexa Fuor 594-conjugated anti-rabbit IgG secondary antibody as previously described, according to Table 2.9. Washing and mounting procedures were carried out as described in Section 2.2.17.3.

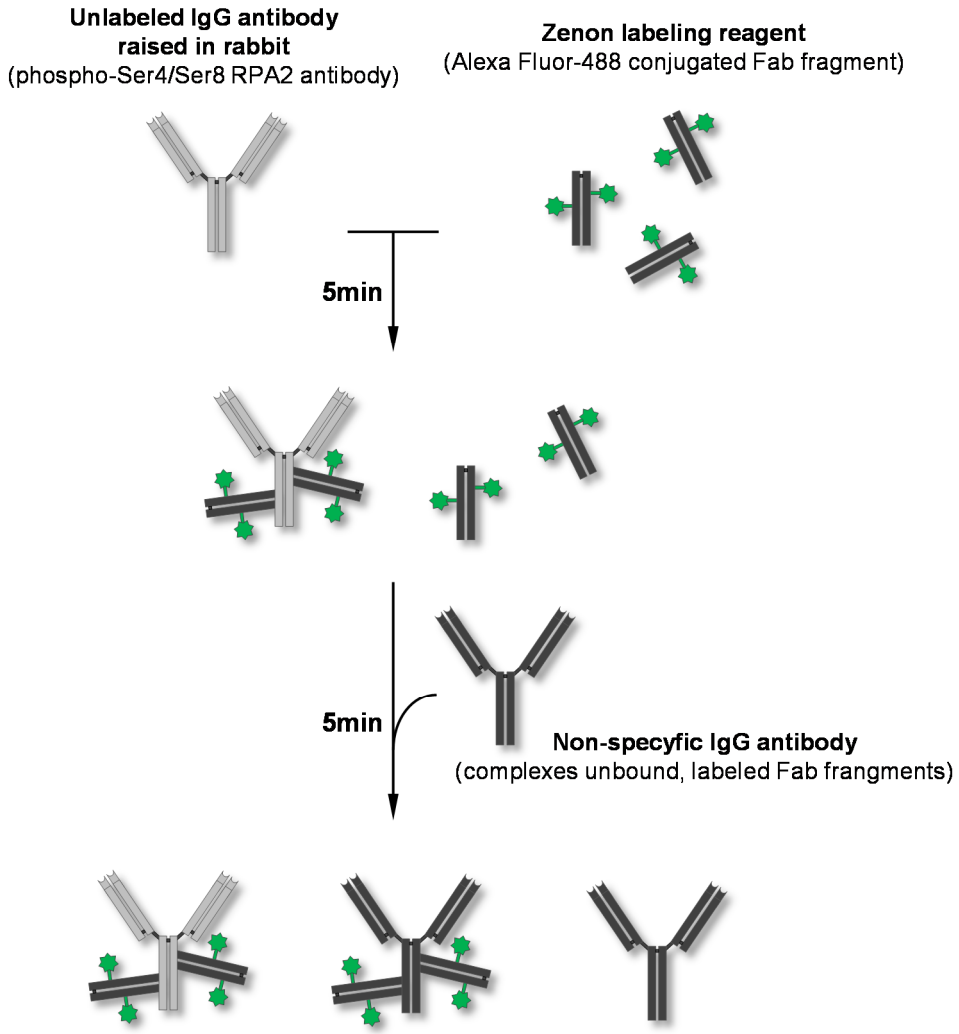

Figure 2.1 Zenon Alexa Fluor 488-conjugated Rabbit IgG kit labelling scheme (adapted from manufacturers Invitrogen protocol)

2.2.18 Analysis of DNA replication using the azide-alkyne Huisgen cycloaddition reaction ('Click chemistry')

DNA replication status was studied using azide-alkyne Huisgen cycloaddition reaction ('Click chemistry'; Salic and Mitchison, 2008) according to a protocol optimised in the laboratory of Prof. Corrado Santocanale (DNA Replication and Anticancer Therapeutics Laboratory, Centre for Chromosome Biology, National University of Ireland, Galway, Ireland). Prof. Corrado Santocanale kindly provided reagents necessary to perform the experiments.

2.2.18.1 Sample preparation and EdU incorporation

Cells were cultured on glass coverslips as described in Section 2.2.17.2 and treated as indicated in particular experiments. 75 minutes before harvesting, cells were pulse-labelled with 10μM 5-ethynyl-2'-deoxyuridine (EdU, Berry & Associates), a thymidine

analogue which can be incorporated into DNA during replication (Buck et al., 2008). EdU was diluted directly in culture media as shown in Table 2.1. Cells were fixed, permeabilised and non-specific sites were blocked as described in Sections 2.2.17.2 and 2.2.17.3. Using EdU instead of BrdU removes the requirement to use harsh conditions, such as extremes of pH or temperature, in order to denature double-stranded DNA to expose the epitopes specific for the anti-BrdU antibody (Buck et al., 2008). The EdU-based approach therefore reduces protein degradation (Buck et al., 2008).

2.2.18.2 Azide-alkyne Huisgen cycloaddition reaction ('Click chemistry')

Staining with anti-phospho-Ser4/Ser8 RPA2 primary antibody (1/100 dilution) was carried out as described in 2.2.17.3.

EdU incorporation was detected by covalent linkage of a fluorochrome to the modified nucleotide in DNA, using the highly specific azide-alkyne Huisgen cycloaddition reaction ('Click chemistry') (Cappella et al., 2008). 10mM 6-carboxyfluorescein-TEG azide stock solution was prepared in DMSO and stored in -20°C. 1M sodium-L-ascorbate (Sigma) and 0.1M copper (II) sulphate (Sigma) were prepared in milliQ-H_2O immediately before the reaction. The 'click chemistry' reaction cocktail was prepared in a 1.5ml tube (Eppendorf) as shown in Table 2.10. Reagents were mixed precisely in the listed order and the tube was vortexed thoroughly before adding the next reagent. Excess primary antibody was removed from the coverslips by washing 3 times for 7 minutes each time with PBS-TX (PBS, 0.1% (v/v) Triton X-100). Coverslips were then placed on the parafilm-coated surface of a light-protected box and 100µl of the 'Click chemistry' reaction cocktail was applied per slide. EdU staining was performed for 30 minutes in room temperature. Next, coverslips were placed in 4-well plates and washed extensively, 5 times for 5 minutes in PBS-TX, with gentle rocking (Kliszczak et al., 2011).

Staining with Alexa Fluor 594-conjugated anti-rabbit secondary antibody (1/200 dilution), washing and mounting of coverslips on slides were performed according to Section 2.2.17.3.

2.2.18.3 Data analysis

Microscopic images were captured using a DeltaVision Core system (Applied Precision) controlling an interline charge-coupled device camera (Coolsnap HQ2; Roper) mounted on an inverted microscope (IX-71; Olympus). For each sample, images were collected at 2x binning using a 60x oil objective at 0.2 µm z sections, and processed as described before (Prendergast et al., 2011). Briefly, images were deconvolved and maximum intensity projected using SoftWoRx (Applied Precision).

Compound name	Stock concentration	Working concentration
PBS	10x	1x
Sodium-L-Ascorbate	1M	10mM
6-Carboxyfluorescein-TEG azide	10mM	0.1mM
Copper (II) Sulphate ($CuSO_4$)	100mM	2mM

Table 2.10 Click chemistry reagents.

For quantification, unscaled, DeltaVision images were used. EdU signal intensity was determined using ImagePro 6.3. A mask was created using the DAPI signal to define the nucleus. The 'nucleus' mask was applied to the images in the FITC channel, and the mean fluorescence intensity of at least 100 objects per sample was measured. The intensity of each individual sample was corrected for (i) background fluorescence intensity outside the nucleus mask and (ii) background fluorescence intensity from an EdU-negative nucleus. Prism v5.0 (GraphPad Software) was used to plot data as graphs.

2.2.19 Analysis of DNA replication using DNA combing

DNA replication status was studied using a DNA combing protocol (Figure 2.2) developed in the Maintenance of Genome Integrity during DNA replication laboratory of Dr. Philippe Pasero (Department of Molecular Bases of Human Diseases Laboratory, Institute of human Genetics, CNRS, Montpellier, France) (Bianco et al., 2012). Procedures described in Sections 2.2.19.3 to 2.2.19.6 were performed in the laboratory of Dr. Philippe Pasero.

2.2.19.1 Double-labelling of human cells with IdU and CldU

48h before treatment, XP30RO and TR30-2 cells were plated in 100mm dishes ($8x10^5$ cells per dish). Cells were either mock-treated or treated with the indicated doses of cisplatin and carboplatin for various times. Before harvesting, cells were pulse-labelled for 15min with 20µM iodo-deoxyuridine (IdU, Sigma), which was added directly to the culture media. At the end of the labelling period, medium was removed and replaced with 7ml of fresh, pre-warmed medium containing 200µM chloro-deoxyuridine (CldU, MP Biomedicals). Stock solutions of nucleotide analogues were prepared according to Table 2.1 Chemicals used in tissue culture:Table 2.1.

2.2.19.2 Preparation of genomic DNA plugs

Cells were harvested by trypsinisation as described in Section 2.2.2, resuspended in sterile PBS (Sigma) to a concentration of $8x10^5$ cells/ml, and gently diluted 1 in 2 in 1% (w/v) low melting point agarose (Molecular Probes). To form agarose plugs, 100µl of cells

($4x10^4$ cells) suspended in agarose were placed in plug-casting molds (Bio-Rad) and left to solidify for 30 minutes at room temperature, followed by 10 minutes in 4°C. Solid agarose plugs were placed in 14ml, round bottom tubes (BD Biosciences). Each plug was incubated in 0.5ml of proteinase K buffer (10mM Tris-HCl buffer (pH 7.5) containing 50mM EDTA (Sigma), 1% (w/v) Sarkosyl (Sigma) and 2 mg/ml proteinase K (Roche). Incubation was carried out for 48h at 50°C in the dark, with the tube cap closed. Next, buffer containing proteinase K was carefully removed by blocking the agarose plug with a plastic cell scraper to prevent damage to the plugs. Plugs were washed 5 times for 10 minutes in Tris-EDTA buffer (TE_{50}: 10mM Tris-HCl, pH 7.0; 50mM EDTA) with gentle shaking. Plugs were transferred to 2ml test tubes (Eppendorf) and stored in TE_{50} buffer at 4°C. At no time were the agarose plugs exposed to metal. Plugs were transferred to 2ml test tubes and shipped on ice to the Institute of Human Genetics in Montpellier.

2.2.19.3 Melting of genomic DNA plugs

One plug from each experimental condition was placed in a single 14ml, round bottom tube and incubated in 100µl of TE_{50} buffer and 1.5µl of YOYO-1 (stock solution, Molecular Probes) for 30 minutes at room temperature, in the dark. Next, plugs were washed 4 times for 5 minutes with 10ml of $TE_{50,}$ with gentle shaking, followed by 30min incubation in 3ml of 50mM MES pH 5.7 in a heating block set at 67°C until the plugs dissolved completely. From this time samples were manipulated with extreme care to avoid shearing the DNA. After 30 minutes, samples were checked and in cases where the shape of the plug was still visible, samples were put back at 67°C for an additional 10 minutes. The temperature of the heating block was decreased to 42°C and samples were left for 1h to equilibrate at this temperature before adding 3 units of β-agarase (New England Biolabs) and incubating overnight at 42°C. The next day, the temperature of the heating block was increased to 65°C and the samples were incubated for a further 10 minutes. Samples were stored at room temperature, in the dark, until ready to use.

2.2.19.4 DNA combing

The DNA solution, prepared as described in the previous section, was carefully placed into 2ml Teflon reservoir. A silanised coverslip was inserted into the DNA solution and left for 15 minutes at room temperature. Next the coverslip was carefully removed from the reservoir at the speed of 300µm/s. This step was repeated for all the samples to be analysed. In order to prevent cross-contamination between samples, the teflon reservoirs were extensively washed with water after each sample and any remaining liquid was eliminated using an 'air duster'. After each experiment, the teflon reservoirs were boiled in water for 20 minutes. The presence of uniformly stretched DNA fibres was confirmed using

a Leica DM6000B microscope (40X objective) on the FITC filter cube. To this end the coverslip was attached to the microscope stage and a drop of immersion oil was placed on the surface of the coverslip to visualize DNA fibres on the underside of the coverslip. Next, coverslips were placed clean side up on clean Whatman paper (VWR) and the DNA was cross-linked to the coverslip by baking in an oven for 2 hours at 60°C. Coverslips were then immobilised on SuperFrost glass slides (BDH) using cyanoacrylate glue, such that the DNA fibres were oriented horizontally. Slides were labelled using a diamond-tip engraving pen (Diversified Biotech) and stored at -20°C until staining.

2.2.19.5 Immunodetection

Slides were de-hydrated for 3 minutes in successive baths of 70%, 90% and 100% ethanol (EtOH, Sigma) in Coplin jars. DNA was denatured by incubation for precisely 25 minutes in 1M sodium hydroxide (NaOH, Sigma) as longer incubation would damage the samples (Bianco et al., 2012). Slides were extensively washed, 5 times for 1 minute each time, with PBS pH 7.4 (Sigma), in order to neutralize the NaOH. Non-specific antibody binding sites were blocked by incubation in PBS-TX (PBS pH7.4, 0.1% (v/v) Triton X-100), containing 1% (w/v) bovine serum albumin (BSA, Sigma), for 15 minutes at room temperature, in the Coplin jars. After removal of excess blocking solution, 18µl of a solution containing the primary antibodies was applied to the slides, which were then covered by a

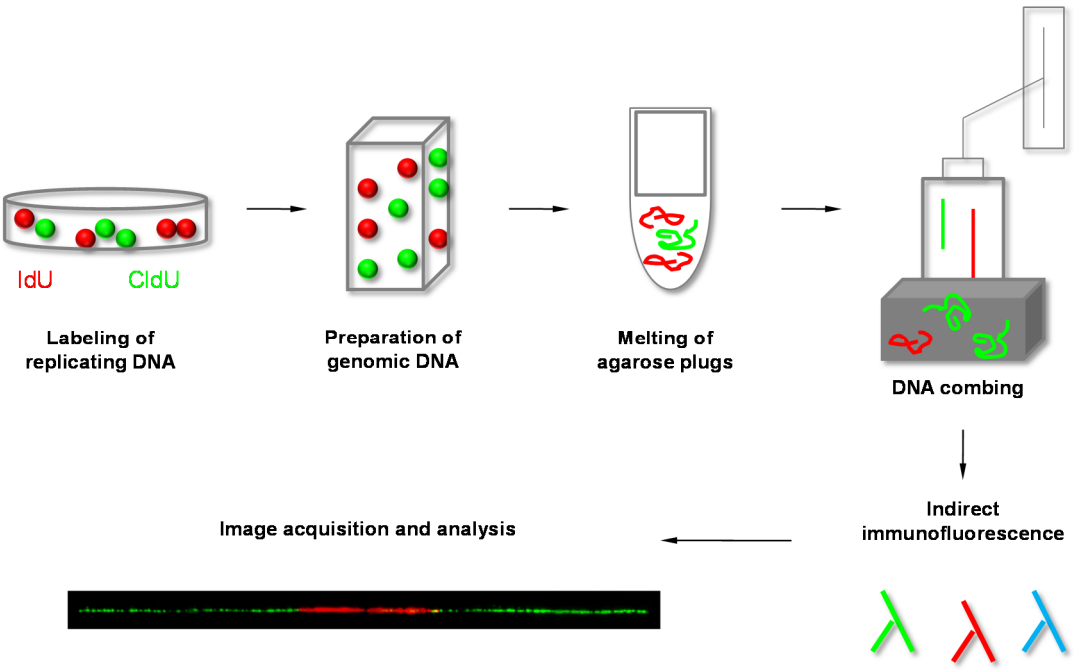

Figure 2.2 An overview of the DNA combing technique. The steps of DNA combing are outlined. Upon labelling cells in culture using nucleotide analogues cells are embedded in agarose plugs. DNA is extracted and stretched uniformly on silanised coverslips. Indirect immunofluorescence staining of samples allows for detection of individual, nascent DNA strands detection (adapted from Bianco et al., 2012).

coverslip and incubated for 45 minutes at 37°C in humidified chamber, in the dark. IdU tracks were detected using B44 mouse anti-BrdU primary antibody (Becton Dickinson), and CldU tracks were detected using BU1/75 rat anti-BrdU antibody (AbCys). Antibodies were prepared in PBS-TX as described in Table 2.9. Following incubation with the primary antibodies, slides were washed 5 times for 2 minutes in PBS-TX. Primary antibody binding was detected by incubation with 18µl of a solution containing secondary antibodies for 30 minutes at 37°C in humidified chamber, in the dark. IdU tracks were detected using Alexa Fluor 546-conjugated goat anti-mouse IgG1 secondary antibody (Molecular Probes), and CldU tracks were detected using Alexa Fluor 488-conjugated chicken anti-rat IgG secondary antibody (Molecular Probes). Secondary antibodies were prepared in PBS-TX as described in Table 2.9. Next, slides were washed 5 times for 2 minutes in PBS-TX, and single-stranded DNA was detected by incubation of the slides with 18µl of PBS-TX containing anti-ssDNA (poly dT) primary antibody (Chemicon), for 45 minutes at 37°C in humidified chamber. Slides were then washed in PBS-TX and anti-ssDNA antibody binding was detected by addition of 18 µl of PBS-TX containing Alexa Fluor 674-conjugated goat anti-mouse IgG2a secondary antibody (Molecular Probes) for 30 minutes at 37°C in humidified chamber, in the dark. After washing in PBS-TX, slides were dried and mounted using 20µl of Prolong Gold Antifade (Molecular Probes). The mounting reagent was left to polymerise overnight at room temperature in the dark, before proceeding with microscopy. Mounted coverslips were stored at 4°C.

2.2.19.6 Image acquisition and data analysis

Image acquisition was performed with a 40x objective on a motorised Leica DM6000B microscope equipped with a CoolSNAP HQ CCD camera and controlled with MetaMorph (Roper Scientific). The following equation was used to convert the pixel size to µm:

*1 pixel = pixel size of the camera (µm) / magnification of the objective * 1000*

Based on previous optimization using molecules of known size, the speed of the moving interface and the camera setup above, one pixel was calculated to equal 340 bp. Only fibres stained for both IdU and CldU were included in statistical analysis, and only the length of the CldU-labelled region was measured. To generate images, representative DNA fibres were selected from different fields and processed with Adobe Photoshop, as described previously (Pasero et al., 2002). Prism v5.0 (GraphPad Software) was used to plot data as graphs.

Origin firing analysis was performed by capturing random fields on the ssDNA fluorescence channel and then measuring at least 80Mbp of DNA fibres per experimental condition. Replication origins were scored based on fibres showing IdU incorporation or both IdU and CldU incorporation. Each incorporation was classified as an active origin. The percentage of the DNA that is derived from S-phase cells was assessed from BrdU incorporation experiments (as described in Section 2.2.7). The frequency of origin firing was calculated by multiplying the length of measured DNA by the fraction of S-phase cells, and dividing by the number of origins. Results are expressed as kb of S-phase DNA per ori [kb/ori].

2.2.20 Pulsed-Field Gel Electrophoresis (PFGE)

48h before treatment, XP30RO and TR30-2 cells were plated in 100mm dishes ($8x10^5$ cells per dish). Cells were either mock-treated or treated with the indicated doses of cisplatin and carboplatin for various times. Samples for pulsed-field gel electrophoresis (PFGE) were prepared as outlined in Section 2.2.19.2. Separation of DNA fragments was performed on a 1% agarose gel (Certified Megabase Agarose, Bio-Rad) using a CHEF DR II apparatus (Bio-Rad). 2.5l of 1x Tris-EDTA buffer (TE, 10mM Tris-HCl (Sigma), pH 7.5 1mM EDTA (Sigma) was prepared, and the electrophoresis chamber was filled with 1.5l of TE buffer and cooled to 14°C using a circulation pump. To prepare 1% agarose, 2.5g of agarose was dissolved in 250ml of 1X TE buffer by heating in a microwave on high power for 1 minute. The gel was allowed to cool to 56°C by incubation in a waterbath for one hour. Next the solution was placed in a gel casting apparatus, the desired gel comb was used and the gel was allowed to solidify for at least 30 minutes at room temperature. Agarose plugs containing DNA from the indicated samples were loaded in the wells of the agarose gel, and empty wells were filled with agarose and left to solidify. The gel was then placed in the electrophoresis chamber for 20 minutes to equilibrate.

The gel was covered by 1X TE buffer and electrophoresis was carried out at the following settings:

- Initial switch time: **60s**
- Final switch time: **240s**
- Current: **4V/cm**
- Temp: **14°C**
- Time: **20h**

The gel was stained by incubation with 0.5μg/ml of ethidium bromide (Sigma), and the DNA bands were visualised using a UV transilluminator (λ = 302 nm).

2.2.21 Molecular biology

2.2.21.1 Preparation of competent cells

Escherichia coli TOP10 or DH5α cells were used for transformation by plasmids. To prepare competent cells, cells were streaked on non-selective Luria-Bertani agar, Miller plates (LB-agar, 1% (w/v) tryptone, 0.5% (w/v) yeast extract, (w/v) 1% sodium chloride, 1.5% (w/v) agar, Fisher Scientific, BP1425-500) and incubated overnight at 37°C. A single colony from the plate was inoculated into 5ml of Luria-Bertani broth, Miller (LB, 1% (w/v) tryptone, 0.5% (w/v) yeast extract, 1% (w/v) sodium chloride, Fisher Scientific, BP1426-500) without antibiotic and grown overnight at 37°C, with vigorous shaking (190rpm). The starter culture was diluted 1:50 in 250ml of LB the following day. Cells were grown at 37°C, with vigorous shaking (190rpm). The optical density (OD) of the culture was analyzed by spectrophotometry at a wavelength 600nm, until the absorbance (A_{600}) of the culture reached an OD of 0.6. At this point the culture was chilled on ice for 10 minutes. Cells were centrifuged at 1,500rpm at 4°C for 15 minutes and then re-suspended in filter-sterilised, ice cold Buffer I containing 30mM Potassium Acetate (Sigma), 100mM $RbCl_2$ (Sigma), 10mM $CaCl_2$ (Sigma), 50mM $MnCl_2$ (Sigma) and 15% (v/v) sterile glycerol (Sigma) pH 5.8 (pH adjusted using 50% (v/v) HCl). Buffer I was added at a ratio of 40ml of Buffer I per 100ml of overnight culture. Cells were collected by centrifugation and re-suspended in filter-sterilised, ice cold Buffer II containing 10mM MOPS (Sigma), 75mM $CaCl_2$ (Sigma), 10mM $RbCl_2$ (Sigma) and 15% (v/v) glycerol, pH 6.5 (adjusted using 1M KOH). Buffer II was added at a ratio of 4ml of Buffer II per 100 ml of overnight culture. Cells were incubated on ice for 15 min, aliquoted to sterile tubes (100µl per tube, Eppendorf), snap-frozen in liquid nitrogen and stored at –80°C.

2.2.21.2 Transformation of competent cells

All procedures were carried out in a sterile environment (open flame, ethanol cleaned surfaces). One aliquot (100µl) of *E. coli* Top10 or DH5α competent cells were thawed on ice. 500ng of plasmid DNA was added to the cells and mixed very gently using a pipette tip. As a control, the same volume of water was added to 100µl of a second aliquot of competent cells. Cells were incubated on ice for 30 minutes, heat-shocked for 90 seconds at 42°C and placed back on ice for 2 minutes. 500µl of LB broth, Miller, was added and cultures were incubated with shaking at 37°C for 1 hour. 100µl of cells were streaked on an LB agar plate containing a selective antibiotic (LB ATB^+ plates, containing either 100µg/ml of ampicillin or 50µg/ml of kanamycin, Fisher Scientific). The rest of the cells were collected by centrifugation for 3 minutes at 1,200rpm, and the cell pellet was resuspended in 100 µl LB broth and streaked on another LB agar plate containing a selective antibiotic. The

same procedures were carried out with the control sample. Plates were incubated at 37°C overnight. Colonies growth was confirmed after at least 16 hours incubation in 37°C, and plates were stored at 4°C.

2.2.21.3 Plasmid DNA purification

All procedures were carried out in sterile environment (open flame, ethanol cleaned surfaces). One colony of transformed cells (Section 2.2.21.1) was picked from an LB agar plate using a sterile 200µl tip and inoculated in 5ml of LB broth, Miller, containing the desired selective antibiotic (100µg/ml of ampicillin or 50µg/ml of kanamycin, Fisher Scientific) in a sterile 50ml tube (Sarstedt). Controls samples were prepared by the inoculation of a sterile tip without a colony in LB broth, and by growing a bacterial colony in media containing antibiotic of a different resistance spectrum to the one provided by the plasmid. Cultures were grown overnight with shaking and tube lid loosely closed, for no longer than 16h at 37°C. At this point plasmid DNA purification was carried out using the Mini Prep kit from Qiagen or the GenElute™ Five-minute Plasmid Miniprep Kit from Sigma, according to the manufacturers' instructions. Alternatively, tubes were placed at 4°C to inhibit cell growth and 500µl of the culture was later used to inoculate 250ml of LB broth containing the selective antibiotic. The culture was incubated for no longer than 16h at 37°C with shaking. Plasmid DNA purification from large-scale cultures were performed using the Maxi Prep kit from Qiagen, or the GenElute™ HP Plasmid Kit, according to the manufacturers' instructions. DNA quantification and purity was determined using a NanoDrop Spectrophotometer (ND-1000, Nanodrop). The OD at 260nm and 280nm was measured. The ratio A_{260}/A_{280} provides an estimate of the purity of the nucleic acid; pure preparations of DNA have an A_{260}/A_{280} ratio values of about 1.8 (Glasel, 1995).

2.2.21.4 Restriction endonuclease digestion of DNA

Restriction endonuclease reactions were carried out by using 1µg of plasmid DNA. In a sterile test tube, DNA was mixed with the appropriate amount of enzyme (1µl) and a suitable reaction buffer, complemented with BSA (final concentration 100µg/ml) if required. MilliQ-H_2O was used to reach the required reaction volume. Reagents were carefully mixed by 'flicking' the tube, briefly spun down and incubated for 1h at 37°C, or as recommended by the manufacturer. To inactivate the enzyme, the reaction was incubated for 10-20 minutes in 65-80°C (according to manufacturers' recommendation). For double digestions involving two non-compatible enzymes, the first enzyme was heat inactivated after the reaction, prior to addition of the second restriction enzyme.

2.2.21.5 DNA gel electrophoresis and DNA extraction

To analyse restriction endonuclease digestion or ligation of DNA fragments, agarose gel electrophoresis was carried out. A 1% (w/v) agarose gel (Thermo Fisher Scientific), containing 0.01% (v/v) SYBR Safe DNA Gel Stain (Invitrogen) was prepared in 1X Tris-Acetate EDTA buffer (TAE, 40mM Tris-acetate (Sigma), 2mM Na_2EDTA (Sigma)). To prepare 1% agarose, 1g of agarose was dissolved in 100ml of the 1x TAE buffer by heating in a microwave on high power for 1 minute. The gel was allowed to cool to about 56°C and 10µl of SYBR Safe DNA Gel Stain was added. The solution was placed in a gel casting apparatus, the gel comb was inserted and the gel was allowed to solidify for at least 30 minutes in room temperature. The gel was submerged in TAE buffer. Prior to loading, DNA samples of the required concentration were prepared in 6x sample loading dye (30% (v/v) glycerol (Sigma), 0.25% (w/v) bromophenol blue (Sigma). To estimate the size of the DNA fragments, a DNA marker was analysed in parallel (100bp or 1 kb DNA Ladder; New England Biolabs, UK). Electrophoresis was carried out at 100V (current limit, 400mA) until desired separation was reached. DNA bands were visualised by transillumination with ultraviolet light (λ = 302 nm). Where necessary, the desired bands were excised from the gel using a sterile scalpel and DNA was isolated. DNA was recovered from agarose gel slices with the GeneElute Gene Extraction kit (Sigma) following the manufacturers' instructions. DNA concentration and purity was assayed as described in Section 2.2.21.3.

2.2.21.6 Polymerase-chain reaction (PCR)

Amplification of the DNA sequence encoding Replication Protein A2 (RPA2) was performed by polymerase-chain reaction (PCR). A pair of primers was designed (forward and reverse). Primer specificity towards RPA2 was checked using BLAST software. In specific cases, primers were designed to introduce a FLAG tag which consisting of the following eight amino acids, DYKDDDDK, into the final sequence. Pre-designed primers were synthesised by Sigma Company, received in a lyophilized form and re-suspended in milliQ-H_2O at a concentration of 100µM. Primers are listed in Table 2.11. KOD Hot Start DNA Polymerase (Novagene) was used in PCR. The reaction was carried out in a 50µl reaction volume, containing 10ng template DNA, 0.4µM of each primer (forward and reverse), 0.25µM of each dNTP (Sigma), 2.5mM Mg_2SO_4 (provided with the polymerase), 1X KOD buffer (provided with the polymerase), 1% (v/v) DMSO (provided with the polymerase) and 0.4µl of the KOD Hot Start DNA Polymerase. The reaction was made up to a final volume of 50µl with milliQ-H_2O. Reactions were carried out in the Eppendorf Mastercycler, under the following conditions: initial denaturation step at 95°C for 2 min, 35 cycles of: 95°C for 30s, 55°C for 40s, 70°C for 1min, and a final elongation step at 70°C for

2min. As negative controls for PCR, reactions without primers were carried out. Reaction products were analysed by separation of 5µl of the reaction on an agarose gel, as described in Section 2.2.21.5. PCR products were purified from the reaction using GeneElute PCR clean-up kit, according to manufacturers' instructions.

2.2.21.7 DNA ligation

Quick T4 DNA ligase (New England Biolabs) was used to ligate vector and insert DNA. A three-fold molar excess of the insert DNA to the linearised vector (50ng) was used in the ligation reactions. The volume of insert and vector DNA was brought up to 10µl with milliQ-H_2O, and mixed with 10µl of the Quick T4 ligation buffer prior to the addition of 1 µl (equal to 1 unit) of T4 DNA ligase. After a brief centrifugation step, the reaction was incubated for 5 minutes at room temperature, and then chilled on ice. 5µl of the reaction was transformed into competent cells, as described in Section 2.2.21.2.

Primer Name	Oligonucleotide Sequence (5' to 3')	Tm (°C)
F-EcoRI-wtRPA2	GAATTC**ATGTGGAACAGTGGATTCGAA**	71.1
R-wtRPA2(-STOP)-GC-BamHI	GGATCCGC**TTCTGCATCTGTGGATTTAAA**	74.5
F-BamHI-FLAG-wtRPA2	GGATCCATGGATTACAAGGATGACGACGACAAG **ATGTGGAACAGTGGATTCGAA**	78.9
R-wtRPA2-EcoRI	GAATTC**TTATTCTGCATCTGTGGATTTAAA**	66.4
F-BamHI-wtRPA2	GGATCC**ATGTGGAACAGTGGATTCGAA**	74.7
R-wtRPA2-FLAG-EcoRI	GAATTCTTACTTGTCGTCGTCATCCTTGTAATC**T TCTGCATCTGTGGATTTAAA**	80.9

Table 2.11 Primers used in PCR. RPA2 codons in bold, FLAG-tag codons underlined.

2.2.21.8 PCR mutagenesis

Point mutations in a plasmid expressing the GFP- or FLAG- tagged RPA2 subunit of replication protein A were introduced according to a protocol optimised in the laboratory of Dr. Andrew Flaus (Chromatin Structure and Function Laboratory, Centre for Chromosome Biology, National University of Ireland, Galway, Ireland). A schematic of the procedure is presented as Figure 2.3.

A pair of complementary primers was designed. The mutation to be introduced was placed in the centre of the primer and the flanking region was at least 16bp on each side of the mutation site. Primers had melting temperature (T_m) of at least 55°C (Table 2.12). Pre-designed primers were synthesised by Sigma Company, received in a lyophilised form and resuspended in milliQ-H_2O at a concentration of 100µM. KOD Hot Start DNA Polymerase

(Novagene) was used in the following mutagenesis procedure. PCR was carried out in a 50µl reaction volume, containing 750ng template DNA, 0.4µM of each primer (forward and reverse), 0.2µM of each dNTP (Sigma), 1.5mM Mg_2SO_4 (provided with the polymerase), 1X KOD buffer (provided with the polymerase), 5% (v/v) DMSO (provided with the polymerase) and 1µl of the KOD Hot Start DNA Polymerase. The reaction was made up to a final volume of 50µl with milliQ-H_2O. Reactions were carried out in the Eppendorf Mastercycler, under the following conditions: initial denaturation step at 95°C for 2 min, 16 cycles of: 95°C for 30s, 56°C for 20s, 68°C for 30s per 1kb (210s), and final elongation at 72°C for 5min. As PCR negative controls, reactions without primers were carried out. Reaction products were analysed by separating 5µl of the reaction on an agarose gel, as described in Section 2.2.21.5.

The fact that plasmid methylation status varies between the original plasmid which is methylated at adenines located in the sequence 5'GATC3' as a result of propagation in

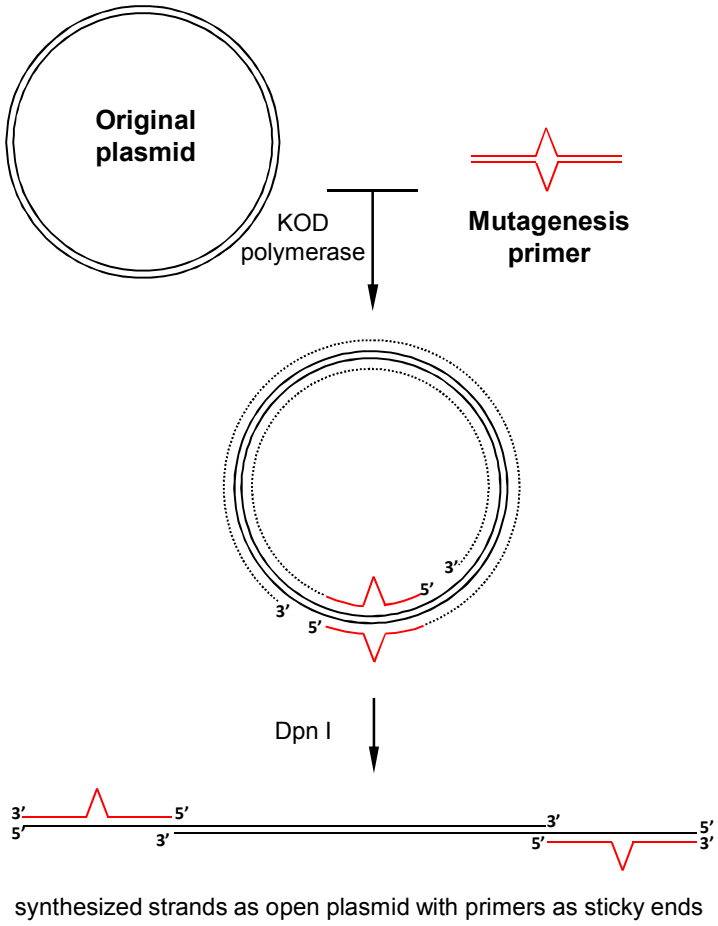

Figure 2.3 Scheme for PCR-based mutagenesis (adapted from PCR mutagenesis protocol obtained from Dr. Andrew Flaus, CCB, NUIG).

dam$^+$ bacteria, and DNA newly synthesised *in vitro*, which remains unmethylated, was used in order to remove the original plasmid DNA that does not carry the mutation, prior to transformation. Restriction endonuclease digestion with *DpnI* was carried out, since *DpnI* preferentially digests methylated DNA synthesised in *dam*$^+$ bacteria, while the PCR reaction product is resistant to *DpnI* digestion. 1.5µl of *DpnI* enzyme (New England Biolabs) was added directly to the PCR reactions and samples were further incubated for 16 hours at 37°C. The following day, 1µl of the reaction was transformed into *E. coli* competent cells according to procedure described in Section 2.2.21.2, where reaction products were ligated

Primer Name	Oligonucleotide Sequence (5' to 3')	Tm (°C)
Ser4 → Ala4		
S4A-RPA2-GFP-N1 F	TTCGAATTCATGTGGAAC**GCT**GGATTCGAAAGCTATGG	81.9
S4A-RPA2-GFP-N1 R	CCATAGCTTTCGAATCC**AGC**GTTCCACATGAATTCGAA	81.9
S4A-RPA2(C)-FLAG F	CGGATCCATGTGGAAC**GCT**GGATTCGAAAGCTATGG	83.6
S4A-RPA2(C)-FLAG R	CCATAGCTTTCGAATCC**AGC**GTTCCACATGGATCCG	83.6
FLAG-S4A-RPA2(N) F	GACGACAAGATGTGGAAC**GCT**GGATTCGAAAGCTATGG	82.2
FLAG-S4A-RPA2(N) R	CCATAGCTTTCGAATCC**AGC**GTTCCACATCTTGTCGTC	82.2
Ser8 → Ala8		
S8A-RPA2-GFP-N1 F	GGAACAGTGGATTCGAA**GCC**TATGGCAGCTCCTCATAC	81.0
S8A-RPA2-GFP-N1 R	GTATGAGGAGCTGCCATA**GGC**TTCGAATCCACTGTTCC	81.0
Ser4/Ser8 → Ala4/Ala8		
S4A/S8A-RPA2-GFP-N1 F	GCTTCGAATTCATGTGGAAC**GCT**GGATTCGAA**GCC**TAT GGCAGCTCCTCATACGG	90.1
S4A/S8A-RPA2-GFP-N1 R	CCGTATGAGGAGCTGCCATA**GGC**TTCGAATCC**AGC**GTT CCACATGAATTCGAAGC	90.1
S4A/S8A-RPA2(C)-FLAG F	AGCTCGGATCCATGTGGAAC**GCT**GGATTCGAA**GCC**TAT GGCAGCTCCTCATACGG	91.6
S4A/S8A-RPA2(C)-FLAG R	CCGTATGAGGAGCTGCCATA**GGC**TTCGAATCC**AGC**GTT CCACATGGATCCGAGCT	91.6
FLAG-S4A/S8A-RPA2(N) F	ACGACGACAAGATGTGGAAC**GCT**GGATTCGAA**GCC**TAT GGCAGCTCCTCATACGG	90.8
FLAG-S4A/S8A-RPA2(N) R	CCGTATGAGGAGCTGCCATA**GGC**TTCGAATCC**AGC**GTT CCACATCTTGTCGTCGT	90.8

Table 2.12 Primers used in PCR mutagenesis. Codons introducing mutations are marked in **red**.

and amplified. To confirm the presence of the mutation, plasmid DNA was isolated using the mini-prep procedure (as described in Section 2.2.21.3) and samples were sent for sequencing to LGC Genomics, AGOWA GmbH, Berlin, Germany. Sequencing results were analysed with Chromas lite, EMBOSS and ExPASy software, available online.

2.2.22 Transient transfection of human cell lines

36 hour prior to transfection, XP30RO cells were plated out and grown to approximately 80% confluency. FuGENE HD transfection reagent (Roche, Promega) was incubated for 15 minutes at room temperature with plasmid DNA, at a ratio of 6µl per 2µg DNA, in 100µl of serum-free MEM medium, as recommended by the manufacturer. The transfection mixture was added to cells in media containing 10% FBS. Cells were transfected for 8 or 24 hours, after which transfection media was removed and cells were treated as indicated in specific experiments.

2.3 References

Bianco, J.N., J. Poli, J. Saksouk, J. Bacal, M.J. Silva, K. Yoshida, Y.-L. Lin, H. Tourriere, A. Lengronne, and P. Pasero. 2012. Analysis of DNA replication profiles in budding yeast and mammalian cells using DNA combing. *Methods*. 57:149-157.

Buck, S.B., J. Bradford, K.R. Gee, B.J. Agnew, S.T. Clarke, and A. Salic. 2008. Detection of S-phase cell cycle progression using 5-ethynyl-2'-deoxyuridine incorporation with click chemistry, an alternative to using 5-bromo-2'-deoxyuridine antibodies. *Biotechniques*. 44:927-9.

Cappella, P., F. Gasparri, M. Pulici, and J. Moll. 2008. A novel method based on click chemistry, which overcomes limitations of cell cycle analysis by classical determination of BrdU incorporation, allowing multiplex antibody staining. *Cytometry A*. 73:626-36.

Cruet-Hennequart, S., S. Coyne, M.T. Glynn, G.G. Oakley, and M.P. Carty. 2006. UV-induced RPA phosphorylation is increased in the absence of DNA polymerase eta and requires DNA-PK. *DNA Repair (Amst)*. 5:491-504.

Gerlier, D., and N. Thomasset. 1986. Use of MTT colorimetric assay to measure cell activation. *J Immunol Methods*. 94:57-63.

Glasel, J.A. 1995. Validity of nucleic acid purities monitored by 260nm/280nm absorbance ratios. *Biotechniques*. 18:62-3.

Gorg, A., O. Drews, C. Luck, F. Weiland, and W. Weiss. 2009. 2-DE with IPGs. *Electrophoresis*. 30 Suppl 1:S122-32.

Harper, J.V. 2005. Synchronization of cell populations in G1/S and G2/M phases of the cell cycle. *Methods Mol Biol*. 296:157-66.

Kliszczak, A.E., M.D. Rainey, B. Harhen, F.M. Boisvert, and C. Santocanale. 2011. DNA mediated chromatin pull-down for the study of chromatin replication. *Sci. Rep.* 1.

Pasero, P., A. Bensimon, and E. Schwob. 2002. Single-molecule analysis reveals clustering and epigenetic regulation of replication origins at the yeast rDNA locus. *Genes Dev*. 16:2479-84.

Prendergast, L., C. van Vuuren, A. Kaczmarczyk, V. Doering, D. Hellwig, N. Quinn, C. Hoischen, S. Diekmann, and K.F. Sullivan. 2011. Premitotic assembly of human CENPs -T and -W switches centromeric chromatin to a mitotic state. *PLoS Biol*. 9:e1001082.

Richard, D.J., E. Bolderson, L. Cubeddu, R.I.M. Wadsworth, K. Savage, G.G. Sharma, M.L. Nicolette, S. Tsvetanov, M.J. McIlwraith, R.K. Pandita, S. Takeda, R.T. Hay, J. Gautier, S.C. West, T.T. Paull, T.K. Pandita, M.F. White, and K.K. Khanna. 2008. Single-stranded DNA-binding protein hSSB1 is critical for genomic stability. *Nature*. 453:677-681.

Salic, A., and T.J. Mitchison. 2008. A chemical method for fast and sensitive detection of DNA synthesis in vivo. *Proc Natl Acad Sci U S A*. 105:2415-20.

Scudiero, D.A., R.H. Shoemaker, K.D. Paull, A. Monks, S. Tierney, T.H. Nofziger, M.J. Currens, D. Seniff, and M.R. Boyd. 1988. Evaluation of a soluble tetrazolium/formazan assay for cell growth and drug sensitivity in culture using human and other tumor cell lines. *Cancer Res*. 48:4827-33.

Skop, A.R., H. Liu, J. Yates, B.J. Meyer, and R. Heald. 2004. Dissection of the Mammalian Midbody Proteome Reveals Conserved Cytokinesis Mechanisms. *Science*. 305:61-66.

Volpe, J.P.G., and J.E. Cleaver. 1995. Xeroderma pigmentosum variant cells are resistant to immortalization. *Mutation Research/DNA Repair*. 337:111-117.

Chapter 3: Human DNA polymerase η expression modulates nascent strand length and the DNA damage response following platinum-induced DNA damage

Sokol A.M.[1], Cruet-Hennequart S.[1**], Pasero P.[2], Carty M.P.[1]

Manuscript prepared for submission to *Nucleic Acid Research*

[1] DNA Damage Response Laboratory, Centre for Chromosome Biology, Biochemistry, School of Natural Sciences, National University of Ireland, Galway, Ireland
[2] Department of Molecular Basis of Human Diseases, Institute of Human Genetics, CNRS UPR 1142, Montpellier, France

[**] Present Address: Microenvironment and Pathology Laboratory (MILPAT, EA 4652), Niveau 3, Faculté de Médecine, Avenue de la Côte de Nacre, 14032 Caen cedex. France

Key words: cisplatin, carboplatin, translesion synthesis (TLS), DNA polymerase η (polη), replication protein A2 (RPA2), phosphorylation, cell cycle

3.1 Introduction

Despite recent advances in the development of targeted therapies, induction of genomic DNA damage, in particular by radiotherapy and chemotherapy using platinum-based drugs, continues to play a major role in cancer treatment. Cisplatin [cis-diamminedichloroplatinum (II)], the first platinum-based anticancer agent to be introduced, is widely used to treat various malignancies, in particular testicular and ovarian cancers, as well as small cell lung cancer (Kelland, 2007). Cisplatin analogues including carboplatin [*cis*-diammine(1,1-cyclobutanedicarboxylate)-platinum(II)] have been developed, with reduced side-effects and improved selectivity towards cancer cells (Kelland, 2007). However, further investigation of the cellular processes that modulate the response of human cells to platinum-induced DNA damage is required, in order to understand the basis of resistance in cancer cells, the development of secondary tumours in surviving cells, and to identify novel targets to potentiate the cytotoxic effects of these agents (Wernyj and Morin, 2004).

The effectiveness of cisplatin and carboplatin in cancer treatment is attributed to the induction of DNA damage, through the formation of monoadducts, intrastrand and interstrand cross-links (ICLs), primarily at guanine residues (Wang and Lippard, 2005). While the cytotoxic effects of platinum-based drugs are primarily attributable to the formation of ICLs, the majority (>90%) of platinum-DNA adducts are intrastrand adducts rather than ICLs (Chaney et al., 2005; Kartalou and Essigmann, 2001). Platinum-DNA adducts block both transcription and DNA replication, leading to cell cycle arrest and cell death (Wang and Lippard, 2005). The process of translesion synthesis (TLS), a cellular DNA damage tolerance pathway that allows cells to continue DNA replication in the presence of unrepaired damage in the genome, may contribute to tumour cell survival following platinum-induced DNA damage (Kelland, 2007).

TLS is carried out by specialized, low-fidelilty DNA polymerases, including DNA polymerase eta (polη), a 78kDa protein encoded by the human *POLH* gene (Burgers et al., 2001; Johnson et al., 1999; Masutani et al., 1999). Mutations in *POLH* underlie the skin cancer-prone genetic disease xeroderma pigmentosum variant (XPV) (Johnson et al., 1999; Masutani et al., 1999). Polη normally carries out error-free replication at sites of UV-induced dithymine cyclobutane pyrimidine dimers (CPDs) (Masutani et al., 2000). In the absence of polη in XPV patients, mutations accumulate in the genome as a result of error-prone lesion bypass carried out by other DNA polymerases (Gueranger et al., 2008; Maher et al., 1976). In addition to this major biological role, *in vitro* studies have shown that purified polη can also bypass cisplatin-induced intrastrand guanine-guanine adducts (Masutani et al., 2000; Vaisman et al., 2000). Consistent with a role for polη in cisplatin

tolerance *in vivo*, human cells lacking polη are more sensitive to platinum-based drugs (Albertella et al., 2005; Chen et al., 2006; Cruet-Hennequart et al., 2008).

Activation of the DNA damage response (DDR) plays an important role in determining the outcome of replication arrest induced by DNA damaging agents (Branzei and Foiani, 2007; Chanoux et al., 2009). Replication arrest and DNA strand break formation activate phosphatidylinositol-3-kinase-related protein kinases (PIKKs) which phosphorylate downstream target proteins to orchestrate the damage response (Chanoux et al., 2009; Jackson and Bartek, 2009; Zhou and Elledge, 2000). Following treatment with platinum-based drugs, DNA damage response signalling is enhanced in cells lacking polη as a consequence of replication arrest and fork collapse (Cruet-Hennequart et al., 2006; Cruet-Hennequart et al., 2008; Despras et al., 2010). To directly investigate the consequences of polη-deficiency for replication of genomic DNA containing cisplatin and carboplatin lesions *in vivo,* we have used DNA combing to demonstrate that in the absence of polη the length of nascent DNA strands is reduced following cisplatin- and carboplatin-induced DNA damage. We also show that damage-induced phosphorylation of the RPA2 subunit of replication protein A, a key PIKK target, directly correlates with the extent of replication inhibition in individual cells. Our data provide new insights into the role of polη and downstream signaling pathways in the processing of DNA damage induced by platinum-based anti-cancer drugs.

3.2 Results

While cisplatin and carboplatin form covalent adducts in DNA, which can block DNA synthesis by replicative DNA polymerases (Wang and Lippard, 2005), DNA replication can be completed by the process of translesion synthesis (TLS), an evolutionarily conserved mechanism which allows DNA synthesis to occur without prior lesion removal. To directly investigate the role of polη in replication of platinum-damaged DNA *in vivo,* we have used flow cytometry and DNA combing to compare the effects of cisplatin and carboplatin on DNA synthesis between polη-deficient XP30RO cells (Johnson et al., 1999; Masutani et al., 1999) and TR30-2 cells, an isogenic line derived from XP30RO cells that stably expresses polη from a *POLH* transgene.

3.2.1 Enhanced cisplatin- and carboplatin-induced replication inhibition in polη-deficient cells

XP30RO and TR30-2 cells were either mock-treated or treated with equitoxic doses of cisplatin (0.5μg/ml) and carboplatin (50μM) (Cruet-Hennequart et al., 2009), and cell cycle distribution was analysed by flow cytometry 24h after drug treatment. Consistent with our previous report that cells lacking polη strongly arrest in S-phase in response to cisplatin or carboplatin but eventually progress through the cell cycle (Cruet-Hennequart et al., 2009), it was found that, while both cell lines were arrested in S-phase in response to treatment, S-phase accumulation was significantly higher in polη-deficient XP30RO cells compared to TR30-2 cells expressing polη (Supplementary Figure 3.1). Accumulation of cells in S-phase is a result of inhibition of replication, as determined by analysis of BrdU incorporation (Figure 3.1A). Following treatment with cisplatin or carboplatin the percentage of cells in S-phase increased in both cell lines. However, consistent with a role for polη in determining the extent of replication arrest, the intensity of BrdU staining was more strongly reduced in polη-deficient XP30RO cells than in TR30-2 cells expressing polη (Figure 3.1A).

Based on comparison with mock-treated cells, two separate populations of S-phase cells could be identified by analysis of BrdU incorporation (Figure 3.1A). In addition to BrdU-positive S-phase cells, a population of cells with S-phase DNA content but showing reduced BrdU incorporation were defined (Figure 3.1A). These two populations have been termed ‘normal replication’ and ‘inhibited replication’, respectively (Figure 3.1A). After treatment of XP30RO cells with 50μM carboplatin, 26% of total S-phase cells showed inhibited replication, while this value was 43.4% in cells treated with 0.5μg/ml cisplatin (Figure 3.1B). The percentage of S-phase cells showing inhibited replication was significantly higher in polη-deficient XP30RO cells compared to TR30-2 cells expressing

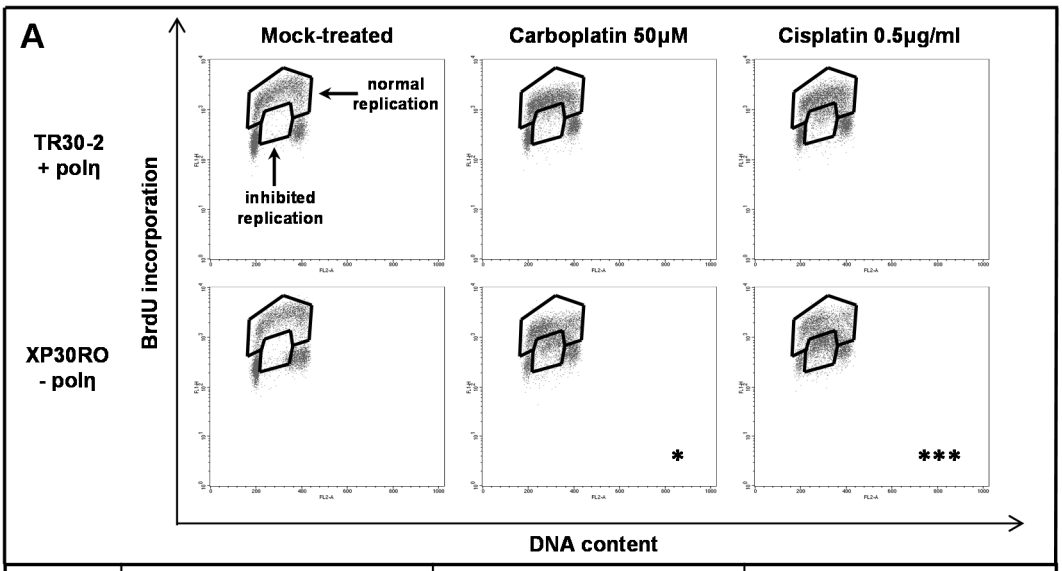

B

	Mock-treated			Carboplatin 50μM			Cisplatin 0.5μg/ml		
	% S phase population	% normal replication	% inhibited replication	% S phase population	% normal replication	% inhibited replication	% S phase population	% normal replication	% inhibited replication
TR30-2	41.3 ± 1.6	94.3 ± 1.0	5.7 ± 1.0	62.9 ± 2.0	86.4 ± 2.2	13.6 ± 2.2	61.9 ± 1.5	77.4 ± 2.7	22.6 ± 2.7
XP30RO	40.0 ± 0.5	93.7 ± 0.9	6.3 ± 0.9	69.5 ± 2.0	74.0 ± 2.2	26.0 ± 3.0	70.9 ± 2.8	56.6 ± 5.2	43.4 ± 5.2

Figure 3.1 Cell cycle progression and DNA replication analysis in carboplatin and cisplatin treated cells lacking or expressing DNA polymerase η. Cells expressing (TR30-2) or lacking (XP30RO) polη were continuously treated with the indicated doses of cisplatin and carboplatin. Cells were incubated with 10μM BrdU before fixing and staining with propidium iodide (PI) and anti-BrdU-FITC antibody as described in Materials and Methods. **A.** Representative flow cytometry PI/BrdU dot plots are presented. Populations of cells with S-phase DNA content were divided in two groups based on BrdU staining and named: normal replication and inhibited replication. Asterisks indicate statistically significant differences in the percentage of cells exhibiting replication inhibition, determined using the two-way ANOVA test. **B.** The mean percentage of cells in the indicated groups +/- SEM values, derived from four independent experiments, is presented in Table format.

polη, as determined using two-way ANOVA (Figure 3.1B). This effect was DNA damage-dependent, since polη expression did not influence the percentage of cells in S-phase in the absence of platinum treatment (Figure 3.1A, B). Thus, following exposure to platinum-based DNA damaging agents, the extent of DNA replication inhibition in S-phase cells is dependent on polη expression. It has been previously demonstrated, by analysis of cell cycle distribution at later times following exposure to platinum-based drugs that S phase-arrested XP30RO cells eventually progress into the G2/M phase (Cruet-Hennequart et al., 2008; Cruet-Hennequart et al., 2009).

3.2.2 Effect of polη expression on nascent DNA strand length following DNA damage.

To determine whether decreased BrdU incorporation in cisplatin- and carboplatin-treated XP30RO cells (Figure 3.1A, B) was due to a direct role for polη in bypass of drug-induced lesions during DNA replication *in vivo*, DNA combing was used to directly determine the length of individual nascent DNA strands synthesized in polη-expressing and

polη-deficient fibroblasts exposed to cisplatin or carboplatin (Figure 3.2). Before harvesting, cells were pulse-labeled for 15min with IdU, followed by 60min labeling with CldU (Figure 2A). Differential labeling of the DNA using two modified nucleosides allowed strands derived from newly-fired origins and from stalled replication forks to be distinguished (Figure 3.2B). For each experimental condition, individual DNA fibres were uniformly stretched of glass coverslips, and visualized by fluorescence microscopy using specific antibodies to detect IdU, CldU and total DNA (Figure 3.2B). Only fibres that were stained for both IdU (green) and CldU (red) were included in the subsequent analysis. Merged replicons and origins that fired during the second pulse (i.e. fibres stained for CldU but not for IdU) were therefore excluded from the analysis. For each fibre, only the length of the CldU track was measured (Figure 3.2C, green tracks).

In the absence of cisplatin or carboplatin, the mean fibre length in both cell lines was approximately 82kb (Figure 3.2E; Supplementary Figure 3.2A). Compared to control cells, there was no statistically significant difference in the mean length of nascent DNA strands, or in the replication fork rate, when TR30-2 cells expressing polη were treated with 0.5μg/ml cisplatin or 50μM carboplatin (Figure 3.2D, E; Supplementary Figure 3.2A). However, following treatment of polη-deficient XP30RO cells for 24h with 50μM carboplatin, the frequency of shorter fibres was increased, visible as a shift towards shorter fibre lengths on the frequency distribution graphs (Figure 3.2D). In these samples, the mean fibre length decreased to 69.1kb, compared to 82.3kb and 82.0kb in mock-treated XP30RO and TR30-2 cells, respectively. The difference in mean fibre length was greater when XP30RO cells were treated with 0.5μg/ml cisplatin (Figure 3.2E; Supplementary Figure 3.2A). In this case, the mean DNA strand length was 48.2kb in XP30RO cells, compared to 78.9kb in TR30-2 cells, representing a 39% decrease in fibre length in the absence of polη. The replication fork rate was also decreased in XP30RO cells treated with cisplatin or carboplatin (Supplementary Figure 3.2A). This data provides the first direct evidence *in vivo* that polη-deficiency results in a statistically significant reduction (Figure 3.2E; Mann-Whitney test, $p<0.0001$) in the mean length of nascent DNA strands in XP30RO cells treated with cisplatin or carboplatin.

3.2.3 Cisplatin- and carboplatin-induced DNA damage responses.

Since polη deficiency leads to replication arrest and a reduction in the length of nascent strands in cells treated with cisplatin or carboplatin, we investigated the relationship between inhibition of DNA synthesis and activation of DNA damage responses in XP30RO and in TR30-2 cells. Protein samples from mock-treated cells and cells exposed to cisplatin and carboplatin were analysed by western blotting for polη expression and for key DNA

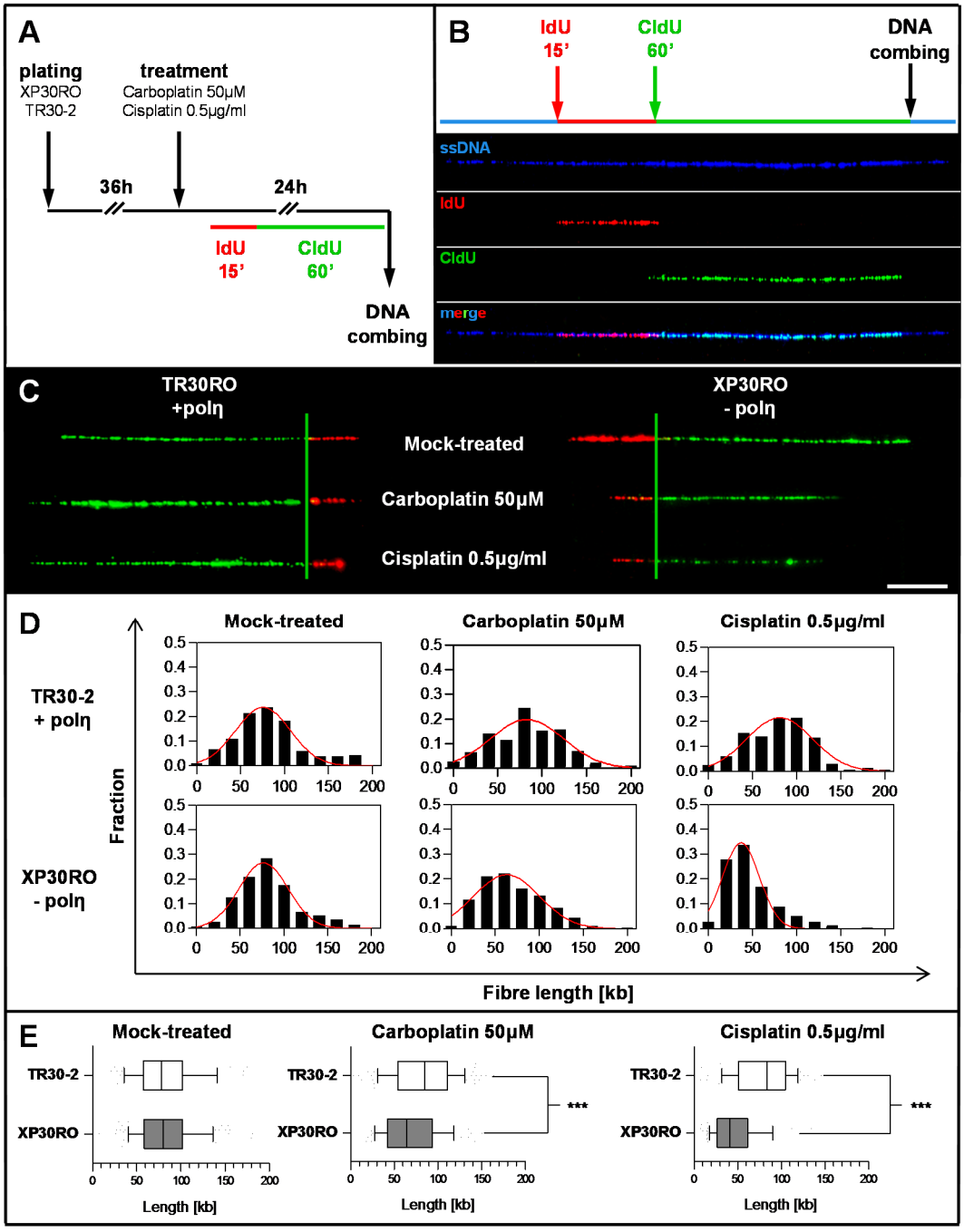

Figure 3.2 Analysis of DNA replication by DNA combing. A. A schematic outline of the DNA combing experiment is shown. **B**. DNA fibres are visualized using specific primary antibodies in conjunction with fluorescently-labelled secondary antibodies. In the image, single-stranded DNA is shown in blue, IdU-labelled DNA in red and CldU-labelled DNA in green. **C.** Representative, individual DNA fibres for each experimental condition are presented. Scale bar corresponds to 20kb DNA. **D.** The frequency distribution of fibres of particular lengths is presented as histograms plots. Data represent the population of fibres obtained by measuring at least 150 individual DNA fibres for selected experimental conditions, in two independent experiments. A Gaussian curve is fitted in red. **E.** Data are presented as inbox-and-whiskers graphs. Each box represents the 25th and 75th percentile (the lower and upper quartiles, respectively) and the median (50th percentile) is marked as the line near the middle of the box. Data not included between the whiskers were plotted as outliers (dots). Data was analysed by the use of Mann-Whitney test. Asterisks indicate statistically significant differences.

damage responses, including phosphorylation of Chk1, RPA2 and H2AX. Consistent with *POLH* being mutated in XP30RO cells (Johnson et al., 1999; Masutani et al., 1999), polη protein was expressed in TR30-2 cells, but not in XP30RO cells (Figure 3.3).

The PIKK ATR is activated in an ATRIP-dependent manner in response to single-stranded DNA generated at arrested replication forks (Olson et al., 2006; Zou and Elledge, 2003). ATR-mediated phosphorylation of Chk1 on serine 317 directly modulates the DNA damage response by regulating S-phase arrest and mitotic entry (Smith et al., 2010). Compared to mock-treated cells, Chk1 phosphoryation on Ser317 was elevated at 6h post-exposure to both cisplatin and carboplatin, and peaked at 24h post-treatment (Figure 3.3). Chk1 phosphorylation was enhanced in polη-deficient cells (Figure 3.3, Supplementary Figure 3.3), consistent with increased replication arrest in these cells. At 36h and 48h post-treatment, the level of phosphorylated Chk1 and total Chk1 decreased (Figure 3.3). While there was little evidence of apoptosis 24h after treatment of cells with 0.5μg/ml cisplatin or 50μM carboplatin (Supplementary Figure 3), the decrease in Chk1 levels at 36h and 48h post-treatment may reflect proteolytic degradation of Chk1 in cells that are undergoing apoptosis as a result of prolonged drug exposure (O'Meara et al., 2010; Wang and Lippard, 2005; Zhang et al., 2005). Following replication arrest, PIKK-dependent phosphorylation of histone 2AX on Ser139 (generating γH2AX) was found to stabilize stalled forks and prevent their collapse (Chanoux et al., 2009) as well as to function in DNA strand break signalling (Revet et al., 2011). In the present study, slight phosphorylation of H2AX was detectable at 6h post-treatment with cisplatin and carboplatin, and the level of γH2AX increased with time up to 48h post-exposure (Figure 3.3). The levels of γH2AX were elevated in polη-deficient cell lines compared to cells expressing polη. Induction of H2AX phosphorylation occurred earlier and to a higher level in response to 0.5μg/ml cisplatin compared to 50μM carboplatin (Figure 3.3). In contrast to Chk1 signalling, H2AX phosphorylation on Ser317 is a later event, and is significantly enhanced from 24h post-drug exposure, especially in XP30RO cells. This could be due to prolonged replication fork arrest, and fork collapse when polη-deficient cells attempt to progress through S-phase in the presence of damaged DNA (Branzei and Foiani, 2007).

Trimeric replication protein A (RPA), the main single-stranded DNA binding protein in human cells, plays a role in all aspects of DNA metabolism including replication, recombination and repair. Phosphorylation of the 34kDa RPA2 subunit occurs in a cell cycle-dependent manner, and in response to DNA damage (Binz et al., 2004; Cruet-Hennequart et al., 2008; Stephan et al., 2009). In cells undergoing replication stress, RPA coated single-stranded DNA activates ATRIP-dependent ATR signalling (Binz et al., 2004). Following replication arrest, ATR phosphorylates RPA2 on Ser33 (Olson et al., 2006) and

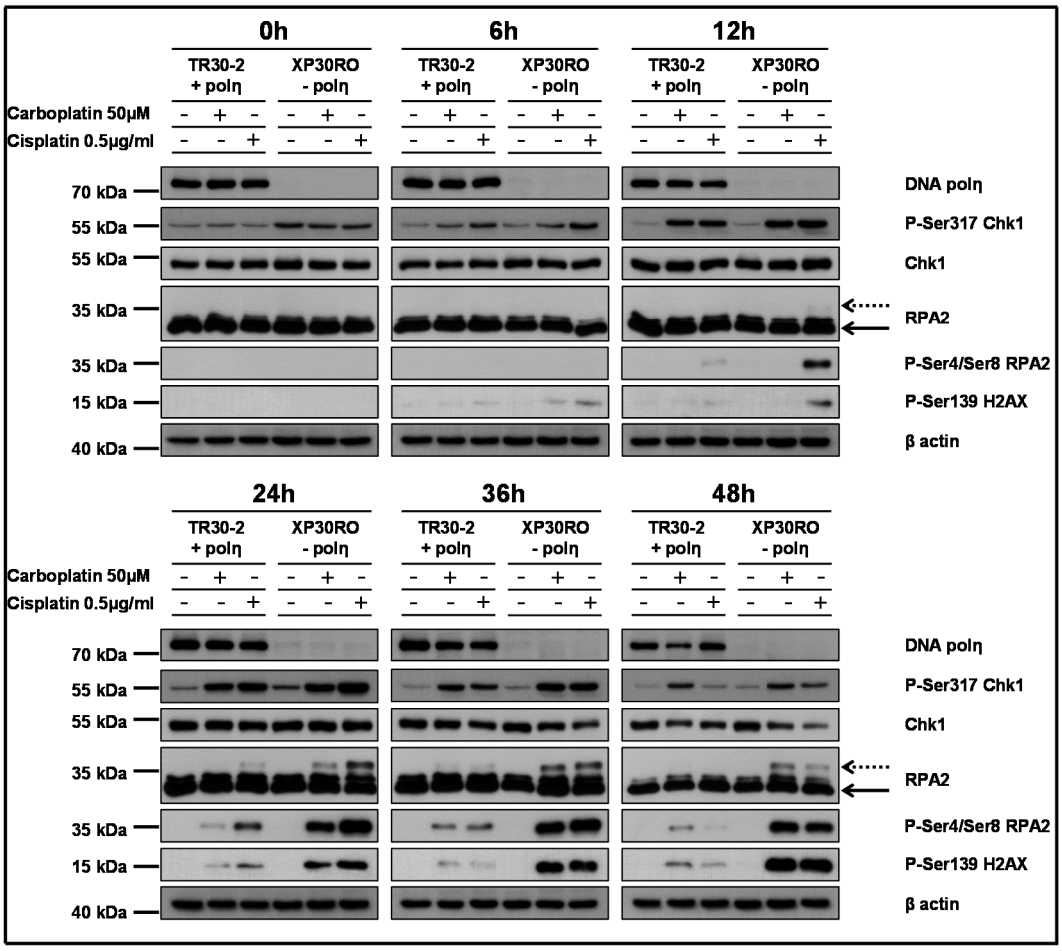

Figure 3.3 Kinetics of carboplatin- and cisplatin-induced DNA damage responses in cells lacking and expressing DNA polymerase η. Polη-deficient XP30RO cells and polη expressing TR30-2 cells were continuously treated with equitoxic doses of carboplatin and cisplatin, and harvested at the indicated times post-treatment. Expression of DNA damage response proteins and protein phosphorylation were analysed by western blotting using specific antibodies as described in Materials and Methods. For direct comparison, samples obtained from both cell lines at the same timepoint were run on the same gels.

the protein is also phosphorylated on Thr21 by other PIKKs (Binz et al., 2004). In response to UVR-, IR- and platinum-induced DNA damage, RPA2 is further phosphorylated on Ser4/Ser8 in a DNA-PK-dependent manner, generating a hyperphosphorylated form of the protein with distinct reduced mobility upon SDS-polyacrylamide gel electrophoresis (Cruet-Hennequart et al., 2006; Cruet-Hennequart et al., 2008; Liaw et al., 2011; Oakley et al., 2001). Hyperphosphorylated RPA2 can be detected using anti-RPA2 antibody as a band corresponding to a slower mobility form (Figure 3.3). We have previously shown that in response to platinum-based chemotherapeutic agents, RPA2 is also phosphorylated on Ser33 by ATR (Cruet-Hennequart et al., 2008). Here, the presence of additional RPA2 phosphorylation on Ser4/Ser8 was confirmed by the use of an anti-phospho-Ser4/Ser8 RPA2 antibody. Consistent with H2AX phosphorylation and in contrast to Chk1 phosphorylation, RPA2 phosphorylation was detected at later times post-treatment. Phosphorylation was first

detected 12h post-treatment with cisplatin, and 24h post-treatment with carboplatin, with the peak signals detected at 24h and 36h post-exposure, respectively. The level of phospho-Ser4/Ser8 RPA2 decreased slightly by 48h post-drug exposure (Figure 3.3). The timing of RPA2 phosphorylation on Ser4/Ser8 was also confirmed by quantitative immunofluorescence (data partially published in Cruet-Hennequart et al., 2009). Consistent with a role for RPA2 phosphorylation in the cellular response to replication arrest (Cruet-Hennequart et al., 2009), the level of RPA2 phosphorylated on Ser4/Ser8 was significantly higher in polη-deficient XP30RO cells compared to TR30-2 cells that express polη.

In summary, platinum-induced DNA damage leads to ATR-mediated, S-phase checkpoint activation both in DNA polη-deficient XP30RO cells and in TR30-2 cells expressing polη. Moreover, phosphorylation of downstream DNA damage response proteins including RPA2 and H2AX is greatly enhanced in polη-deficient, XP30RO cells.

3.2.4 Quantitative association between replication inhibition and phosphorylation of RPA2 on Ser4/Ser8.

Given that platinum-induced phosphorylation of RPA2 on Ser4/Ser8 was enhanced in cells lacking polη (Figure 3.3) in which replication was also strongly inhibited (Figure 3.1; 3.2), we used quantitative immunofluorescence to investigate the relationship between replication inhibition and RPA2 phosphorylation on Ser4 and Ser8 in individual cells. This was studied directly using 'click chemistry' to monitor incorporation of the modified nucleoside EdU during DNA replication, and immunofluorescence to determine the extent of RPA2 phosphorylation on Ser4/Ser8 (Figure 3.4A).

Consistent with data obtained by flow cytometry (Figure 1) it was found that the mean relative EdU intensity was reduced in cells treated with cisplatin or carboplatin, compared to mock-treated cells (Figure 3.4B and Supplementary Table 3.1A). EdU incorporation was lower in polη-deficient XP30RO cells compared to TR30-2 cells. Thus, in XP30RO cells treated with 50μM carboplatin, the mean relative EdU intensity decreased by 5.7-fold compared to mock-treated samples, while the same treatment resulted in a 2.7-fold decrease in EdU intensity in TR30-2 cells (Figure 3.4B and Supplementary Table 3.1B). Following cisplatin treatment, the difference between polη-deficient and polη-expressing cells was even larger. When compared to mock-treated samples, the mean relative EdU intensities decreased by 7.5-fold in XR30RO cells and by 3.2-fold in TR30-2 cells (Supplementary Table 3.1B). This is consistent with a role for polη in replication following platinum-induced DNA damage.

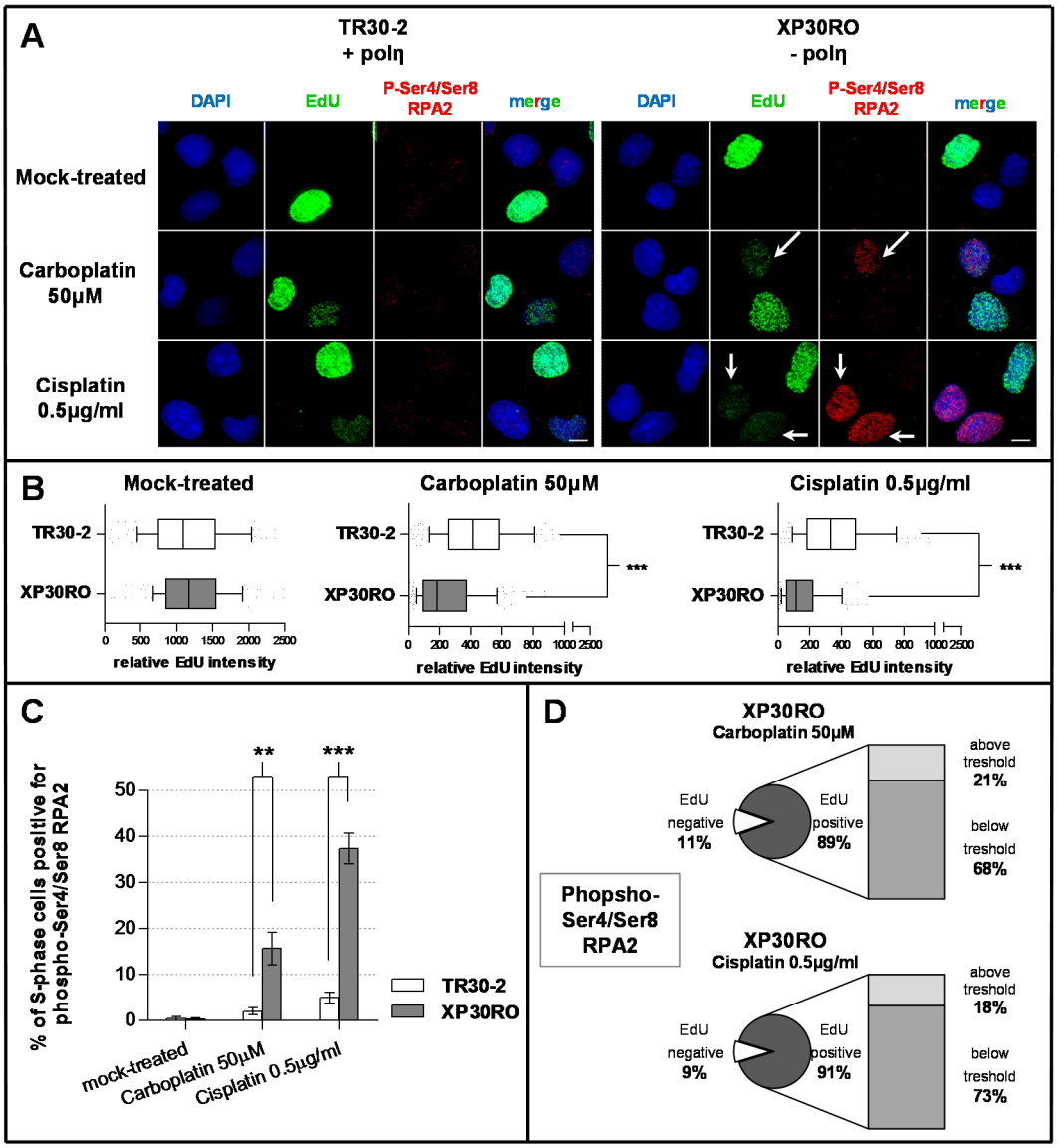

Figure 3.4 Analysis of DNA replication by quantitative immunofluorescence. Cells expressing (TR30-2) or lacking (XP30RO) polη were grown on glass coverslips and continuously treated with equitoxic doses of cisplatin or carboplatin. 75 minutes before fixing, cells were incubated with 10μM EdU. Click chemistry was used to visualise EdU incorporation, and immunofluroescence staining was performed using anti-phospho-Ser4/Ser8 RPA2 primary antibody and Alexa 594-coupled secondary antibody. DNA was counterstained with DAPI. A. Representative images from three independent experiments are presented. The scale bar corresponds to 25μm. Arrows show representative cells which exhibit a decrease in EdU incorporation and increased phospho-Ser4/Ser8 RPA2 staining. B. The EdU fluorescence signal was quantified as described in Materials and Methods. Relative EdU fluorescence values were analysed using the Mann-Whitney test and significant values are marked with asterisks. In the inbox-and-whiskers graphs, the top and bottom of each box represents the 25th and 75th percentile (the lower and upper quartiles, respectively) and the median (50th percentile) is marked as the line near the middle of the box. C. Cells positive for phospho-Ser4/Ser8 RPA2 were counted in the EdU-positive cell population. Data represent the mean from three independent experiments +/- SEM. A two–way ANOVA test was carried out and statistically significant differences are marked with asterisks. D. EdU staining in phospho-Ser4/Ser8 RPA2 positive cells was analysed under conditions where RPA2 phosphorylation on Ser4/Ser8 is enriched. The intensity of the EdU signal in phospho-Ser4/Ser8 RPA2-positive cells was further analysed and categorised into values above and below the threshold value. Threshold values were defined as the mean relative EdU intensity values in each condition, minus twice the SEM value.

It was previously reported that in polη-deficient XP30RO cells, carboplatin-induced RPA2 phosphorylation on Ser4/Ser8 occurred primarily in cells in S-phase, and to a lesser extent in G2/M-phase cells (Cruet-Hennequart et al., 2009). According to the present data, 24h treatment with cisplatin or carboplatin leads both to arrest of cells in S-phase (Figure 4.1) and to RPA2 phosphorylation on Ser4/Ser8 (Figure 3.3). In order to directly investigate the correlation between DNA replication inhibition and RPA2 phosphorylation on Ser4/Ser8, we determined the fraction of EdU-positive S-phase cells that were also positive for phospho-Ser4/Ser8 RPA2. In mock-treated cells, these values were below 0.5% for each cell line, reflecting the fact that phosphorylation of RPA2 on Ser4/Ser8 is DNA damage-dependent (Figure 3.4C). Consistent with western blotting data (Figure 3.3), cisplatin- and carboplatin-induced RPA2 phosphorylation was strongly polη-dependent (Figure 3.4C). 15% of S-phase XP30RO cells were positive for phospho-Ser4/Ser8 RPA2 following carboplatin treatment, while up to 37% of cells were positive following treatment with cisplatin (Figure 3.4C). In contrast, in polη-expressing TR30-2 cells, 24h following DNA damage only 2-5% of S-phase cells were positive for RPA2 phosphorylated on Ser4/Ser8 (Figure 3.4C).

To directly correlate DNA replication status with phosphorylation of RPA2, we determined the level of EdU incorporation in carboplatin- or cisplatin-treated XP30RO cells that were positive for phospho-Ser4/Ser8 RPA2. To carry out quantitative analysis of relative fluorescence intensities, XP30RO cells were treated under conditions that generated elevated levels of phospho-Ser4/Ser8 RPA2-positive nuclei. Around 90% of phospho-Ser4/Ser8 RPA2-positive cells were also positive for EdU incorporation (Figure 3.4D), consistent with the previous report that damage-induced RPA phosphorylation on Ser4/Ser8 occurs primarily in S-phase cells (Cruet-Hennequart et al., 2009). However, analysis of the intensity of EdU staining in individual cells revealed that RPA2 phosphorylation on Ser4/Ser8 occurred mainly in cells with the lowest level of EdU incorporation. As shown in Figure 3.4D, using the mean relative EdU staining intensity for the entire cell population as a threshold value, it was found that following carboplatin treatment, 68% of phospho-Ser4/Ser8 RPA2-positive cells had a level of EdU incorporation below this threshold (Figure 3.4D; Supplementary Table 4.1C). Similarly, following cisplatin treatment, 73% of phospho-Ser4/Ser8 RPA2-positive XP30RO cells were in the low EdU category (Figure 3.4D). This data provides the first direct evidence at the level of individual cells that RPA2 phosphorylation on Ser4/Ser8 occurs in cells where DNA replication is severely inhibited (Figure 3.4D).

3.2.5 Consequences of cisplatin- and carboplatin-induced replication arrest and RPA2 phosphorylation in polη-deficient cells.

We have shown that following cisplatin- and carboplatin-induced DNA damage, cells accumulate in S-phase (Figure 3.1), and that polη is required for completion of DNA synthesis (Figure 3.2). Furthermore, in XP30RO cells where TLS is compromised due to the absence of polη, intra-S checkpoint activation is enhanced (Figure 3.3) leading to phosphorylation of DNA damage response proteins, including H2AX and RPA2 (Figure 3.3). To further investigate the relationship between replication inhibition and phosphorylation of RPA2 on Ser4/Ser8 (Figure 3.4) we tested the hypothesis that prolonged replication fork arrest results in fork collapse and DNA double-strand break (DSB) formation. Pulsed-field gel electrophoresis was used to determine whether DNA strand breaks were induced. This technique is used to separate large fragments of damaged DNA which migrate through an agarose gel upon applying an electric field, which change periodically. Under these conditions intact mammalian chromosomes are too large to migrate through the gel. Damaged DNA was detectable by PFGE at 24 post-treatment (Figure 3.5A), and the signal was enhanced in polη-deficient XP30RO cells when compared to that in TR30-2 cells. A prominent, DNA damage-dependent band was observed on the PFGE gel (Figure 3.5A). While the origin of this major band was not further investigated in the present study, it could result from breaks occurring in abundant tandem DNA repeats, including ribosomal DNA repeat arrays or satellite DNA (Richard et al., 2008).

To further investigate the relationship between phosphorylation of RPA2 on Ser4/Ser8 and DNA strand break formation, we performed double-immunofluorescence staining with anti-phospho-Ser4/Ser8 RPA2, anti-γH2AX and anti-53BP1 antibodies. While there is debate as to whether γH2AX is a marker for DSBs only (Cleaver, 2011), p53-binding protein1 (53BP1) foci specifically form at sites of DSBs (Schultz et al., 2000). Quantitative analysis of RPA2 phosphorylation on Ser4/Ser8 revealed that 24h post-treatment with equitoxic doses of cisplatin and carboplatin, phospho-Ser4/Ser8 RPA2 staining shows small, dispersed foci, evenly distributed throughout the nucleus (Figure 3.4A). Treatment of polη-deficient cells for 24h with higher doses of cisplatin (Figure 3.5B, C) and UV-C (Cruet-Hennequart et al., 2006) generates an additional phospho-Ser4/Ser8 RPA2 staining pattern. Under these conditions, in addition to cells with evenly distributed nuclear staining, the phosphorylated form of RPA2 was also localised to large, distinct nuclear foci. Both classes of phospho-Ser4/Ser8 RPA2 foci co-localised with γH2AX staining, whereas co-localisation with 53BP1 was observed in cells where phosphorylated RPA2 was present in large foci (Figure 3.5B). This differential staining leads to the conclusion that when present in dispersed foci, phosphorylated RPA2 and γH2AX

localisation may not correspond to sites of DSBs. Alternatively, in our model system, not all DSBs are 53BP1 foci-positive.

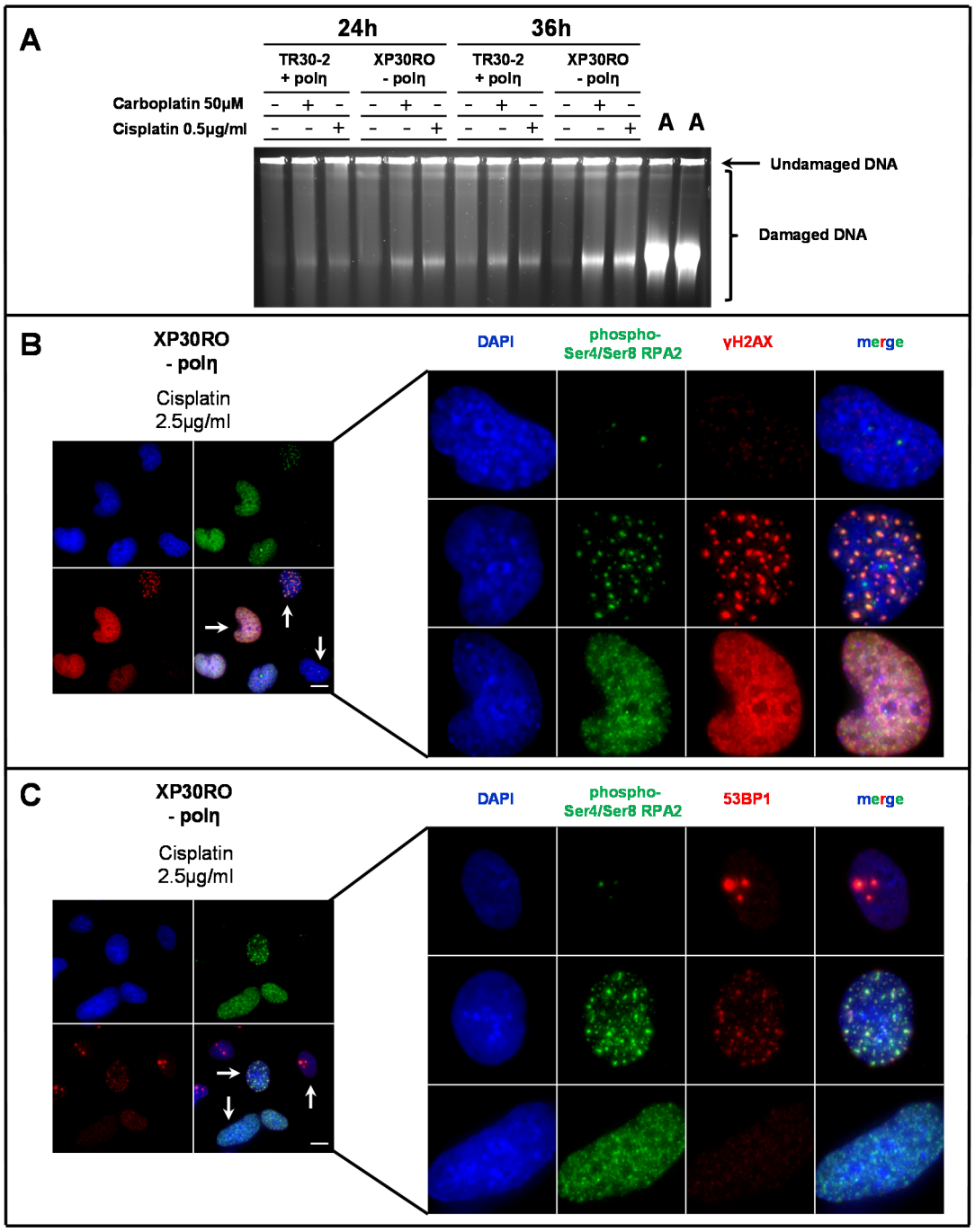

Figure 3.5 Induction of DNA double strand breaks by cisplatin and carboplatin. **A.** Cells from the indicated conditions were prepared for pulsed-field gel electrophoresis as described in Materials and Methods. As a control for apoptosis-induced DNA breaks, DNA derived from non-adherent XP30RO cells following treatment with 5μg/ml cisplatin was analysed (lanes marked with A). Ethidium bromide was used to visualise intact and damaged DNA. **B.** XP30RO cells lacking polη were treated for 24h with 2.5μg/ml cisplatin. Phospho-specific primary antibodies against γH2AX and phospho-Ser4/Ser8 RPA2 were used with with Alexa 594- and Alexa 488-labeled secondary antibodies. DNA was counterstaind with DAPI. Scale bar corresponds to 25μm. **C.** DNA strand break formation was analysed in XP30RO cells lacking polη. Cells were treated for 24h with 2.5μg/ml

cisplatin. Primary antibodies against 53BP1, a marker for double-strand breaks, and phospho-Ser4/Ser8 RPA2 were used with Alexa 594- and Alexa 488-labeled secondary antibodies. DNA was counterstaind with DAPI. Scale bar corresponds to 25μm.

3.3 Discussion

It is important to understand the role of polη in the response to platinum-induced DNA damage, since cells lacking polη are more sensitive to platinum-based chemotherapeutic drugs (Albertella et al., 2005; Chen et al., 2006; Cruet-Hennequart et al., 2008) and it has been reported that the endogenous level of polη modulates the sensitivity of non-small lung cancer and metastatic gastric adenocarcinoma cells to platinum-based drugs (Ceppi et al., 2009; Teng et al., 2010). The recent elucidation of the structure polη in the presence of an intrastrand cisplatin adduct formed between two adjacent guanines has provided a biochemical basis for these observations (Ummat et al., 2012; Zhao et al., 2012). Although the major biological role of polη is during replication of DNA containing UV-induced thymine-thymine CPDs, the open, active site cleft of polη can also accommodate a platinum adduct without major rearrangement of the structure of the protein (Ummat et al., 2012).

Consistent with previous reports (Cruet-Hennequart et al., 2008; Cruet-Hennequart et al., 2009; Pani et al., 2007), following treatment with equitoxic doses of cisplatin and carboplatin, polη-deficient XP30RO cells accumulate in S-phase while BrdU incorporation is strongly inhibited, as a consequence of replication arrest in the presence of platinum-induced DNA damage. In order to elucidate whether this decrease in DNA synthesis depends on polη expression, we used DNA combing to analyse DNA replication in detail at the level of individual nascent DNA strands. We found that, after treatment with cisplatin or carboplatin for 24h, nascent DNA fibres were up to 39% shorter in XP30RO cells lacking polη when compared to TR30-2 cells expressing polη. No difference between the mean lengths of DNA fibres was observed between mock-treated, polη-expressing cells and polη-deficient cells, consistent with previous reports that polη is not required for DNA synthesis on non-damaged templates (Despras et al., 2010; Lehmann et al., 1975). This provides the first direct evidence that polη is involved in DNA synthesis on platinum-damaged DNA in human cells *in vivo*. This and other reports raise the possibility that targeting polη-dependent TLS could improve the efficacy of platinum-based drugs in cancer therapy (Albertella et al., 2005; Alt et al., 2007; Chen et al., 2006; Ummat et al., 2012).

It was of interest to characterise the DNA damage responses activated following treatment with platinum-based chemotherapeutic agents. While drug exposure did not reduce the length of DNA strands synthesized in TR30-2 cells expressing polη, as determined by DNA combing, incorporation of halogenated nucleosides was significantly inhibited as determined using FACS analysis (Fig. 3.1) and immunofluorescence (Fig. 3.4A, B). This could reflect activation of the Chk1-mediated S-phase checkpoint (Fig. 3.2) in TR30-2 cells,

consistent with a recent report that dissociation of DNA damage-activated Chk1 is crucial for efficient recruitment of polη to sites of damage (Speroni et al., 2012). Despite continuous DNA synthesis in cells expressing polη, platinum-DNA lesions present on the template strand need to be repaired. Chk1-mediated activation of the S-phase checkpoint could provide more time for repair to take place (Bartek and Lukas, 2001; Zhou and Elledge, 2000). Active checkpoint signalling also impedes S-phase progression by preventing new origins from firing (Despras et al., 2010; Maya-Mendoza et al., 2007; Petermann et al., 2010). We found that cisplatin and carboplatin treatment reduced the frequency of origin firing, independent of polη expression, with an up to 37% reduction following cisplatin treatment (Supplementary Figure 3.2B). In polη-deficient XP30RO cells, incorporation of halogenated nucleosides is strongly inhibited upon treatment with cisplatin or carboplatin. This may be a cumulative effect of both reduced lesion bypass and checkpoint-dependent inhibition of origin firing (Despras et al., 2010). However, DNA damage-dependent increase in phosphorylation of RPA2 on Ser4/Ser8 in XP30RO cells depends on inhibition of DNA replication, since the level of damage-induced RPA2 phosphorylation is significantly lower in TR30-2 cells expressing polη. We have previously reported that platinum-induced phosphorylation of RPA2 on Ser4/Ser8 occurs predominantly in S-phase cells (Cruet-Hennequart et al., 2009). Here, we directly link RPA phosphorylation on Ser4/Ser8 with severe replication inhibition. During this analysis, EdU fluorescence intensity was determined in all S-phase cells, with no distinction between cells in early, mid- or late S-phase. Based on the frequency distribution graphs and BrdU incorporation profiles (Figure 3.1A and Supplementary Figure 3.1A) showing that under the present experimental conditions, arrested cells are distributed throughout S-phase, and the fact that the same experimental approach was used for mock-treated cells, it is unlikely that all XP30RO cells with relative EdU fluorescence intensities below the threshold value represent early S-phase cells.

Investigation of the downstream effects of the processing of damaged DNA showed that phospho-Ser4-Ser8 RPA2 was found in small, dispersed nuclear foci that co-localised with γH2AX. The kinetics of HA2X phosphorylation on Ser139 closely paralleled RPA2 phosphorylation on Ser4/Ser8, and was a relatively late event when compared to Chk1 activation. Consistent with the present observations, a similar distribution of γH2AX foci has been observed under conditions where DNA replication was inhibited by HU or UV-irradiation (Ward and Chen, 2001). Pan-nuclear distribution of γH2AX staining has been previously reported to occur in apoptotic cells (Solier et al., 2009). However, western blotting analysis of apoptotic markers, including cleaved caspase-3 and cleaved PARP show little or no evidence of apoptosis 24h after treatment of cells with 0.5μg/ml cisplatin and

50μM carboplatin (Supplementary Figure 3.3). This also supports the conclusion that double-stand breaks detectable 24h after treatment are not the result of fragmentation of DNA in apoptotic cells. However, it does not rule out the possibility that this pattern of γH2AX staining represents an early pre-apoptotic state in polη-deficient cells which will not go on to complete S-phase successfully in the presence of platinum-induced DNA damage. Since DNA damage is detectable by PFGE in both polη-expressing and polη-deficient cells 24 post-treatment with cisplatin and carboplatin, it is also possible that the damaged DNA is derived from processing of toxic interstrand adducts (ICLs).

Based on our observations, we propose that in polη-deficient cells, DNA synthesis on the leading strand is impaired by platinum-induced intrastrand DNA lesions, which can lead to uncoupling of the DNA polymerase and helicase activities at the replication fork. DNA lesions on the lagging strand may constitute a less serious barrier to replication fork progression, due to the possibility of repriming downstream of the lesion during the synthesis a new Okazaki fragment (Bell and Dutta, 2002). Uncoupling at the replication fork leads to accumulation of ssDNA, enhanced RPA binding and PIKK-mediated checkpoint signalling (Figure 3.3; Supplementary Figure 4). In support of this conclusion, cells treated with UV-irradiation, which similar to platinum-based drugs does not directly induce DSBs, show a similar pattern of accumulation of ssDNA coated by RPA (Despras et al., 2010) and γH2AX (de Feraudy et al., 2010; Despras et al., 2010) but no 53BP1 staining unless present in large, distinct foci (de Feraudy et al., 2010). Uncoupling of helicase and polymerase activities during replication of cisplatin-damaged DNA has been reported previously in the *Xenopus* egg extract system (Byun et al., 2005). UV radiation (UVR)- and cisplatin-induced inhibition of DNA synthesis in cells lacking polη also leads to accumulation of ssDNA and formation of double strand ends due to collapse of stalled replication forks (Supplementary Figure 4) (Cruet-Hennequart et al., 2006; Cruet-Hennequart et al., 2008; Despras et al., 2010).

Collectively, our data provide novel insights into the cellular processes that modulate the outcome to treatment with cisplatin and related platinum-based drugs. Inhibition of these pathways could represent one approach to potentiate the effects of these agents.

ACKNOWLEDGEMENTS

We would like to thank Dr. Seamus Coyne for development of the TR30-2 cell line and Dr. Julien Bianco for training in DNA combing. We are grateful to the DNA combing facility of Montpellier for silanised coverslips. We wish to thank to Alicja Barczyńska and Dr. Cyril Carroll (NUI Galway) for kindly providing the PFGE apparatus. The authors would like to thank Dr. Anna Kliszczak and Prof. Corrado Santocanale for reagents and assistance for the Edu labelling experiments. We thank Prof. Noel Lowndes for providing anti-53BP1 antibody.

FUNDING

The project was funded by the Irish Research Council (AMS), and Health Research Board (MPC; SC-H). DNA combing training and experiments were supported by the NUI Galway Beckman Fund Scholarship 2009 and Thomas Crawford Hayes Scholarship 2010 (AMS). Research in the laboratory of Dr. Pasero is supported by the Ligue contre le Cancer (Equipe labellisée).

3.4 References

Albertella, M.R., C.M. Green, A.R. Lehmann, and M.J. O'Connor. 2005. A role for polymerase eta in the cellular tolerance to cisplatin-induced damage. *Cancer Res*. 65:9799-806.

Alt, A., K. Lammens, C. Chiocchini, A. Lammens, J.C. Pieck, D. Kuch, K.P. Hopfner, and T. Carell. 2007. Bypass of DNA lesions generated during anticancer treatment with cisplatin by DNA polymerase eta. *Science*. 318:967-70.

Bartek, J., and J. Lukas. 2001. Mammalian G1- and S-phase checkpoints in response to DNA damage. *Curr Opin Cell Biol*. 13:738-47.

Bell, S.P., and A. Dutta. 2002. DNA replication in eukaryotic cells. *Annu Rev Biochem*. 71:333-74.

Binz, S.K., A.M. Sheehan, and M.S. Wold. 2004. Replication protein A phosphorylation and the cellular response to DNA damage. *DNA Repair (Amst)*. 3:1015-24.

Branzei, D., and M. Foiani. 2007. Interplay of replication checkpoints and repair proteins at stalled replication forks. *DNA Repair (Amst)*. 6:994-1003.

Burgers, P.M., E.V. Koonin, E. Bruford, L. Blanco, K.C. Burtis, M.F. Christman, W.C. Copeland, E.C. Friedberg, F. Hanaoka, D.C. Hinkle, C.W. Lawrence, M. Nakanishi, H. Ohmori, L. Prakash, S. Prakash, C.A. Reynaud, A. Sugino, T. Todo, Z. Wang, J.C. Weill, and R. Woodgate. 2001. Eukaryotic DNA polymerases: proposal for a revised nomenclature. *J Biol Chem*. 276:43487-90.

Byun, T.S., M. Pacek, M.C. Yee, J.C. Walter, and K.A. Cimprich. 2005. Functional uncoupling of MCM helicase and DNA polymerase activities activates the ATR-dependent checkpoint. *Genes Dev*. 19:1040-52.

Ceppi, P., S. Novello, A. Cambieri, M. Longo, V. Monica, M. Lo Iacono, M. Giaj-Levra, S. Saviozzi, M. Volante, M. Papotti, and G. Scagliotti. 2009. Polymerase eta mRNA expression predicts survival of non-small cell lung cancer patients treated with platinum-based chemotherapy. *Clin Cancer Res*. 15:1039-45.

Chaney, S.G., S.L. Campbell, E. Bassett, and Y. Wu. 2005. Recognition and processing of cisplatin- and oxaliplatin-DNA adducts. *Critical reviews in oncology/hematology*. 53:3-11.

Chanoux, R.A., B. Yin, K.A. Urtishak, A. Asare, C.H. Bassing, and E.J. Brown. 2009. ATR and H2AX Cooperate in Maintaining Genome Stability under Replication Stress. *Journal of Biological Chemistry*. 284:5994-6003.

Chen, Y.-w., J.E. Cleaver, F. Hanaoka, C.-f. Chang, and K.-m. Chou. 2006. A Novel Role of DNA Polymerase eta in Modulating Cellular Sensitivity to Chemotherapeutic Agents. *Molecular Cancer Research*. 4:257-265.

Cleaver, J.E. 2011. gammaH2Ax: biomarker of damage or functional participant in DNA repair "all that glitters is not gold!". *Photochem Photobiol*. 87:1230-9.

Cruet-Hennequart, S., S. Coyne, M.T. Glynn, G.G. Oakley, and M.P. Carty. 2006. UV-induced RPA phosphorylation is increased in the absence of DNA polymerase eta and requires DNA-PK. *DNA Repair (Amst)*. 5:491-504.

Cruet-Hennequart, S., M.T. Glynn, L.S. Murillo, S. Coyne, and M.P. Carty. 2008. Enhanced DNA-PK-mediated RPA2 hyperphosphorylation in DNA polymerase eta-deficient human cells treated with cisplatin and oxaliplatin. *DNA Repair (Amst)*. 7:582-96.

Cruet-Hennequart, S., S. Villalan, A. Kaczmarczyk, E. O'Meara, A.M. Sokol, and M.P. Carty. 2009. Characterization of the effects of cisplatin and carboplatin on cell cycle progression and DNA damage response activation in DNA polymerase eta-deficient human cells. *Cell Cycle*. 8:3039-50.

de Feraudy, S., I. Revet, V. Bezrookove, L. Feeney, and J.E. Cleaver. 2010. A minority of foci or pan-nuclear apoptotic staining of gammaH2AX in the S phase after UV damage contain DNA double-strand breaks. *Proc Natl Acad Sci U S A*. 107:6870-5.

Despras, E., F. Daboussi, O. Hyrien, K. Marheineke, and P.L. Kannouche. 2010. ATR/Chk1 pathway is essential for resumption of DNA synthesis and cell survival in UV-irradiated XP variant cells. *Hum Mol Genet*. 19:1690-701.

Gueranger, Q., A. Stary, S. Aoufouchi, A. Faili, A. Sarasin, C.-A.s. Reynaud, and J.-C. Weill. 2008. Role of DNA polymerases eta, iota and zeta in UV resistance and UV-induced mutagenesis in a human cell line. *DNA Repair*. 7:1551-1562.

Jackson, S.P., and J. Bartek. 2009. The DNA-damage response in human biology and disease. *Nature*. 461:1071-8.

Johnson, R.E., C.M. Kondratick, S. Prakash, and L. Prakash. 1999. hRAD30 mutations in the variant form of xeroderma pigmentosum. *Science*. 285:263-5.

Kartalou, M., and J.M. Essigmann. 2001. Recognition of cisplatin adducts by cellular proteins. *Mutation Research/Fundamental and Molecular Mechanisms of Mutagenesis*. 478:1-21.

Kelland, L. 2007. The resurgence of platinum-based cancer chemotherapy. *Nat Rev Cancer*. 7:573-584.

Lehmann, A.R., S. Kirk-Bell, C.F. Arlett, M.C. Paterson, P.H. Lohman, E.A. de Weerd-Kastelein, and D. Bootsma. 1975. Xeroderma pigmentosum cells with normal levels of excision repair have a defect in DNA synthesis after UV-irradiation. *Proc Natl Acad Sci U S A*. 72:219-23.

Liaw, H., D. Lee, and K. Myung. 2011. DNA-PK-Dependent RPA2 Hyperphosphorylation Facilitates DNA Repair and Suppresses Sister Chromatid Exchange. *PLoS ONE*. 6:e21424.

Maher, V.M., L.M. Ouellette, R.D. Curren, and J.J. McCormick. 1976. Frequency of ultraviolet light-induced mutations is higher in xeroderma pigmentosum variant cells than in normal human cells. *Nature*. 261:593-5.

Masutani, C., R. Kusumoto, S. Iwai, and F. Hanaoka. 2000. Mechanisms of accurate translesion synthesis by human DNA polymerase [eta]. *EMBO J*. 19:3100-3109.

Masutani, C., R. Kusumoto, A. Yamada, N. Dohmae, M. Yokoi, M. Yuasa, M. Araki, S. Iwai, K. Takio, and F. Hanaoka. 1999. The XPV (xeroderma pigmentosum variant) gene encodes human DNA polymerase eta. *Nature*. 399:700-4.

Maya-Mendoza, A., E. Petermann, D.A. Gillespie, K.W. Caldecott, and D.A. Jackson. 2007. Chk1 regulates the density of active replication origins during the vertebrate S phase. *EMBO J*. 26:2719-31.

O'Meara, E., S.v. Cruet-Hennequart, and M.P. Carty. 2010. Analysis of Protein Phosphorylation in Cisplatin-Treated Human Cells Following Annexin V-based Separation and Multi-Antibody Screening. *Cancer Genomics - Proteomics*. 7:279-286.

Oakley, G.G., L.I. Loberg, J. Yao, M.A. Risinger, R.L. Yunker, M. Zernik-Kobak, K.K. Khanna, M.F. Lavin, M.P. Carty, and K. Dixon. 2001. UV-induced hyperphosphorylation of replication protein a depends on DNA replication and expression of ATM protein. *Mol Biol Cell*. 12:1199-213.

Olson, E., C.J. Nievera, V. Klimovich, E. Fanning, and X. Wu. 2006. RPA2 is a direct downstream target for ATR to regulate the S-phase checkpoint. *J Biol Chem*. 281:39517-33.

Pani, E., L. Stojic, M. El-Shemerly, J. Jiricny, and S. Ferrari. 2007. Mismatch repair status and the response of human cells to cisplatin. *Cell Cycle*. 6:1796-802.

Petermann, E., M. Woodcock, and T. Helleday. 2010. Chk1 promotes replication fork progression by controlling replication initiation. *Proc Natl Acad Sci U S A*. 107:16090-5.

Revet, I., L. Feeney, S. Bruguera, W. Wilson, T.K. Dong, D.H. Oh, D. Dankort, and J.E. Cleaver. 2011. Functional relevance of the histone H2Ax in the response to DNA damaging agents. *Proceedings of the National Academy of Sciences*. 108:8663-8667.

Richard, G.F., A. Kerrest, and B. Dujon. 2008. Comparative genomics and molecular dynamics of DNA repeats in eukaryotes. *Microbiol Mol Biol Rev*. 72:686-727.

Schultz, L.B., N.H. Chehab, A. Malikzay, and T.D. Halazonetis. 2000. p53 binding protein 1 (53BP1) is an early participant in the cellular response to DNA double-strand breaks. *J Cell Biol*. 151:1381-90.

Smith, J., L. Mun Tho, N. Xu, D. A. Gillespie, F.V.W. George, and K. George. 2010. Chapter 3 - The ATM-Chk2 and ATR-Chk1 Pathways in DNA Damage Signaling and Cancer. *In* Advances in Cancer Research. Vol. Volume 108. 2010, editor. Academic Press. 73-112.

Solier, S., O. Sordet, K.W. Kohn, and Y. Pommier. 2009. Death receptor-induced activation of the Chk2- and histone H2AX-associated DNA damage response pathways. *Mol Cell Biol*. 29:68-82.

Speroni, J., M.B. Federico, S.F. Mansilla, G. Soria, and V. Gottifredi. 2012. Kinase-independent function of checkpoint kinase 1 (Chk1) in the replication of damaged DNA. *Proc Natl Acad Sci U S A*. 109:7344-9.

Stephan, H., C. Concannon, E. Kremmer, M.P. Carty, and H.P. Nasheuer. 2009. Ionizing radiation-dependent and independent phosphorylation of the 32-kDa subunit of replication protein A during mitosis. *Nucleic Acids Res*. 37:6028-41.

Teng, K.Y., M.Z. Qiu, Z.H. Li, H.Y. Luo, Z.L. Zeng, R.Z. Luo, H.Z. Zhang, Z.Q. Wang, Y.H. Li, and R.H. Xu. 2010. DNA polymerase eta protein expression predicts treatment response and survival of metastatic gastric adenocarcinoma patients treated with oxaliplatin-based chemotherapy. *J Transl Med*. 8:126.

Ummat, A., O. Rechkoblit, R. Jain, J. Roy Choudhury, R.E. Johnson, T.D. Silverstein, A. Buku, S. Lone, L. Prakash, S. Prakash, and A.K. Aggarwal. 2012. Structural basis for cisplatin DNA damage tolerance by human polymerase eta during cancer chemotherapy. *Nat Struct Mol Biol*. 19:628-32.

Vaisman, A., C. Masutani, F. Hanaoka, and S.G. Chaney. 2000. Efficient Translesion Replication Past Oxaliplatin and Cisplatin GpG Adducts by Human DNA Polymerase η *Biochemistry*. 39:4575-4580.

Wang, D., and S.J. Lippard. 2005. Cellular processing of platinum anticancer drugs. *Nat Rev Drug Discov*. 4:307-320.

Ward, I.M., and J. Chen. 2001. Histone H2AX is phosphorylated in an ATR-dependent manner in response to replicational stress. *J Biol Chem*. 276:47759-62.

Wernyj, R.P., and P.J. Morin. 2004. Molecular mechanisms of platinum resistance: still searching for the Achilles' heel. *Drug Resist Updat*. 7:227-32.

Zhang, Y.W., D.M. Otterness, G.G. Chiang, W. Xie, Y.C. Liu, F. Mercurio, and R.T. Abraham. 2005. Genotoxic stress targets human Chk1 for degradation by the ubiquitin-proteasome pathway. *Mol Cell*. 19:607-18.

Zhao, Y., C. Biertumpfel, M.T. Gregory, Y.J. Hua, F. Hanaoka, and W. Yang. 2012. Structural basis of human DNA polymerase eta-mediated chemoresistance to cisplatin. *Proc Natl Acad Sci U S A*. 109:7269-74.

Zhou, B.B., and S.J. Elledge. 2000. The DNA damage response: putting checkpoints in perspective. *Nature*. 408:433-9.

Zou, L., and S.J. Elledge. 2003. Sensing DNA damage through ATRIP recognition of RPA-ssDNA complexes. *Science*. 300:1542-8.

3.5 Supplementary materials

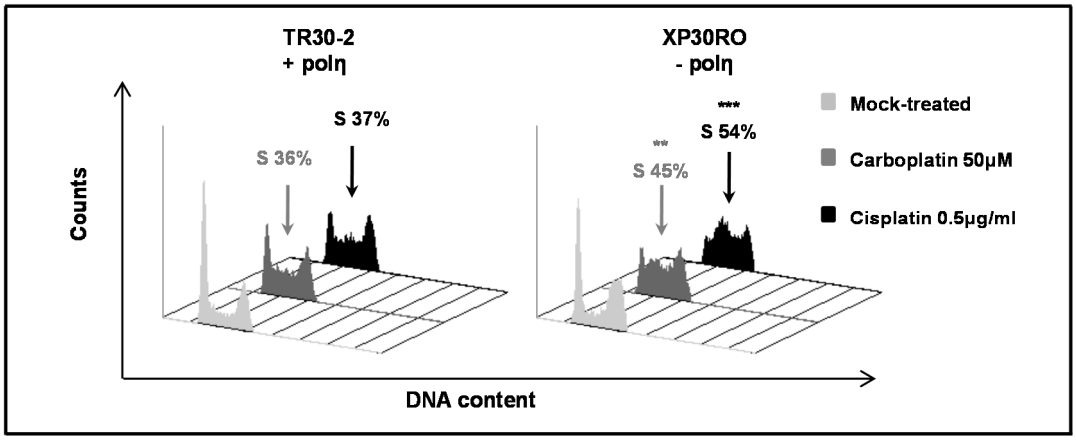

Supplementary Figure 3.1 Cell cycle progression in carboplatin- and cisplatin-treated cells lacking or expressing DNA polymerase η. Cells expressing (TR30-2) or lacking (XP30RO) polη were treated with indicated doses of cisplatin and carboplatin, and fixed for flow cytometry analysis as described in Material and Methods. Representative overlay graphs show cell cycle distribution derived from PI histograms for each experimental condition. Asterisks indicate statistically significant differences between data obtained from four independent experiments for XP30RO and TR30-2 cells, using two-way ANOVA analysis.

A

	Mock-treated			Carboplatin 50µM			Cisplatin 0.5µg/ml		
	Mean length [kb]	Mean synthesis rate [kb/min]	n	Mean length [kb]	Mean synthesis rate [kb/min]	n	Mean length [kb]	Mean synthesis rate [kb/min]	n
TR30-2	82.0 ± 2.8	1.37 ± 0.05	183	82.8 ± 2.8	1.38 ± 0.05	185	78.9 ± 2.8	1.31 ± 0.05	163
XP30RO	82.3 ± 2.1	1.37 ± 0.03	268	69.1 ± 2.6	1.15 ± 0.04	180	48.2 ± 1.6	0.80 ± 0.03	360

B

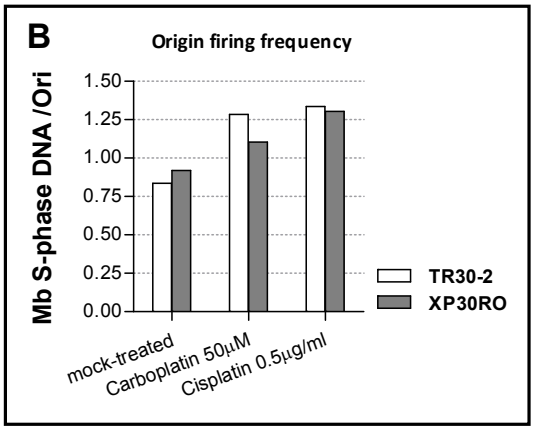

Supplementary Figure 3.2 DNA combing parameters. A Mean strand length and DNA synthesis rate values from two independent DNA combing experiments ± SEM, are presented in Table format. N stands for the number of measured objects. **B** Graph presents the frequency of origin firing based on data from DNA combing experiments carried out under the indicated conditions. BrdU incorporation data from FACS analysis was used to calculate the S-phase DNA fraction.

.

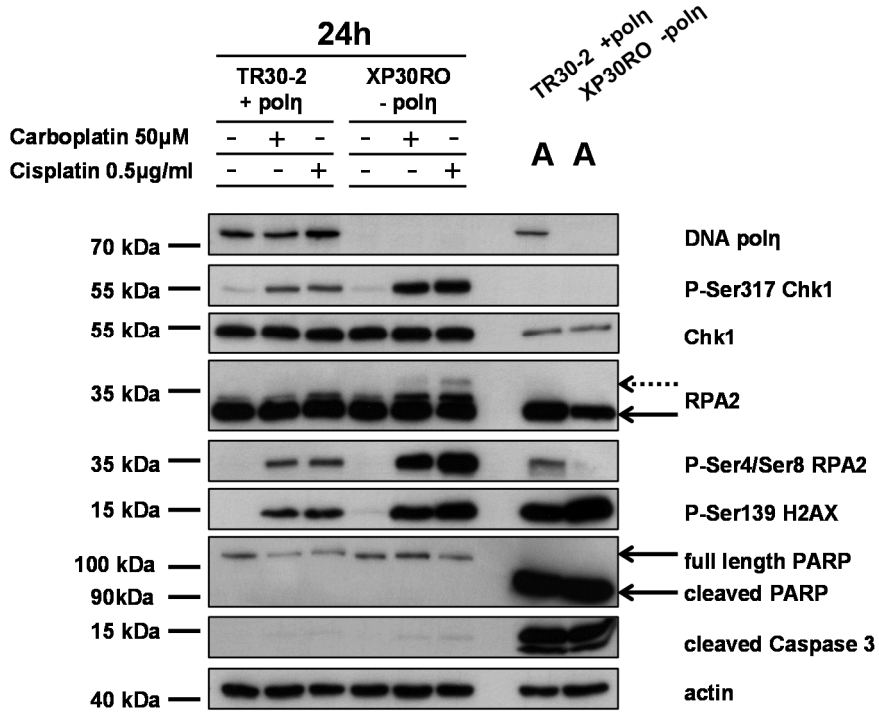

Supplementary Figure 3.3 Carboplatin- and cisplatin-induced DNA damage responses and apoptosis induction in cells lacking and expressing DNA polymerase η. Polη-deficient XP30RO cells and polη-expressing TR30-2 cells were treated with equitoxic doses of carboplatin or cisplatin and harvested 24h post treatment. Polη and DNA damage response and apoptosis-related proteins were analysed by western blotting using specific antibodies as described in Materials and Methods. As a control for apoptosis, proteins obtained from floating cells following treatment of cells with 5μg/ml cisplatin for 24h were loaded in the lanes marked A.

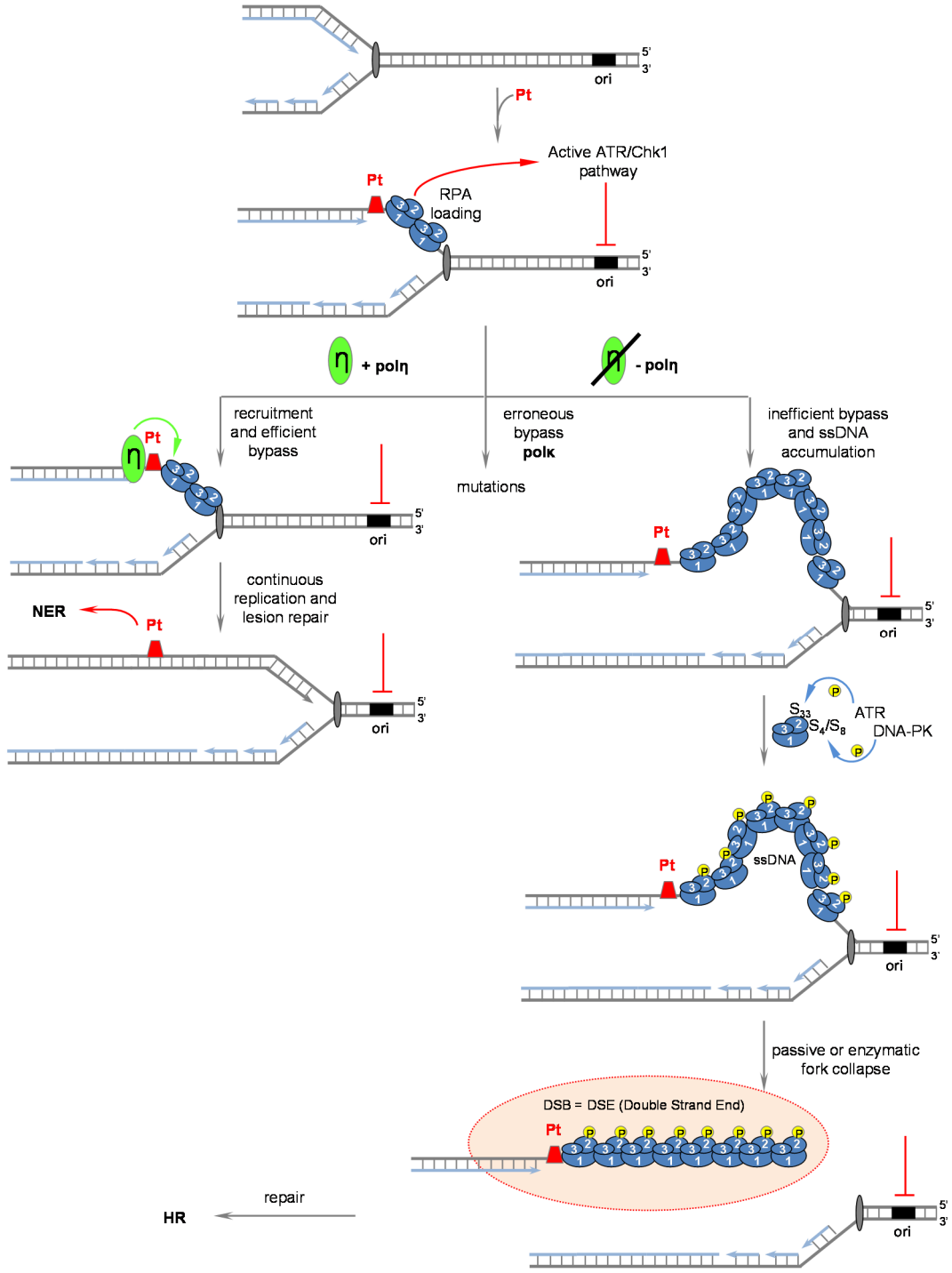

Supplementary Figure 3.4 Model of DNA replication arrest and DNA damage response activation. Platinum-DNA adducts constitute an obstacle for replicative DNA polymerases. Replication arrest activates the DNA damage response. Signalling from the active S-phase checkpoint prevents new origins from firing. In normal cells, TLS-mediated bypass of platinum-induced intrastrand adducts in DNA can occur in the presence of DNA polymerase

η. Other translesion polymerases may also be involved in DNA synthesis at sites of platinum-DNA adducts. The alternative pathway of template switching is not shown in this model. In polη-deficient cells such as XP30RO, uncoupling of the polymerase and helicase activities as a result of blocked polymerisation at intrastrand adducts could lead to the accumulation of regions of ssDNA, and phosphorylation of the RPA2 subunit of replication protein A. This may eventually lead to fork collapse, generating a double-strand end and free ssDNA.

A	Mock-treated		Carboplatin 50μM		Cisplatin 0.5μg/ml	
	Mean relative EdU intensity	n	Mean relative EdU intensity	n	Mean relative EdU intensity	n
TR30-2	1175.0 ± 31.5	394	447.9 ± 12.4	487	385.7 ± 14.1	402
XP30RO	1220.0 ± 26.7	362	255.1 ± 9.4	523	177.0 ± 9.5	489

B	Carboplatin 50μM	Cisplatin 0.5μg/ml
	Fold decrease in relative EdU intensity	Fold decrease in relative EdU intensity
TR30-2	2.7 ± 0.14	3.2 ± 0.22
XP30RO	5.7 ± 1.75	7.3 ± 1.19

C	Carboplatin 50μM	Cisplatin 0.5μg/ml
	Threshold value for EdU intensity (Mean relative EdU intensity - 2xSEM)	Threshold value for EdU intensity (Mean relative EdU intensity - 2xSEM)
XP30RO	236.7	157.9

Suppmentary Table 3.1 EdU intensity analysis by quantitative immunofluorescence. Cells expressing (TR30-2) or lacking (XP30RO) polη were grown on glass coverslips and treated with equitoxic doses of cisplatin and carboplatin. 75 minutes before fixing, cells were incubated with 10μM EdU. Click chemistry was used to visualise EdU incorporation. **A.** Mean relative EdU intensities values ± SEM from three independent experiments under the indicated conditions are presented. The number of individual values is indicated as n. **B.** Fold-decrease in EdU intensity ± SEM relative to mock-treated samples is presented. **C.** The EdU intensity threshold, obtained by subtracting double the SEM value from the mean relative EdU intensity value.

Chapter 4: Identification and characterisation of phospho-Ser4/Ser8 Replication Protein A2 (RPA2) in mitotic cells

Sokol A.M.[1], Carty M.P.[1]

[1] DNA Damage Response Laboratory, Centre for Chromosome Biology, Biochemistry, School of Natural Sciences, National University of Ireland, Galway, Ireland

Key words: Replication Protein A2 (RPA2), phosphorylation, cell cycle, mitosis, centrosome, midbody

4.1 Introduction

The cell cycle comprises a series of strictly controlled events which ensure faithful chromosomes duplication and transport into two daughter cells during cell division. The eukaryotic cell cycle is divided morphologically into the mitotic phase (M) and interphase (Norbury and Nurse, 1992). The purpose of the mitotic phase, which is further subdivided into mitosis and cytokinesis, is to correctly segregate the duplicated DNA into two genetically identical daughter cells (Norbury and Nurse, 1992). M-phase is further divided into prophase, metaphase, anaphase and telophase (Norbury and Nurse, 1992; Vermeulen et al., 2003). With the onset of early metaphase (called prometaphase), a dynamic bipolar array of microtubules, called the spindle, is assembled at two microtubule organizing centres (MTOCs), called centrosomes (Mardin and Schiebel, 2012). The spindle microtubules attach to kinetochores, specialised protein structures that are formed at the centromere of sister chromatids and govern faithful segregation of the genetic material to opposite spindle poles (Kline-Smith and Walczak, 2004). During cytokinesis the remnants of the spindle microtubules form an intracellular bridge. Abscission, the final step of cytokinesis which physically separates the two post-mitotic cells, occurs in the centre of the intracellular bridge, called the midbody (Fededa and Gerlich, 2012; Steigemann and Gerlich, 2009).

An undisturbed cell cycle is a prerequisite for the maintenance of genome integrity and is supported by tight regulation of cellular proteins in terms of their turnover, localisation and functionality (Norbury and Nurse, 1992). Replication protein A (RPA) is an abundant, heterotrimeric, single-stranded DNA binding protein that is uniformly expressed during the cell cycle in human cells (Din et al., 1990). RPA2, the second subunit of RPA, is phosphorylated in a cell cycle dependent manner by cyclin-dependent kinases (CDKs) on two serines residues located at positions 23 and 29 in the N-terminus of the protein (Figure 4.1; Din et al., 1990; Erdile et al., 1990; Kemp and Pearson, 1990; Niu et al., 1997).

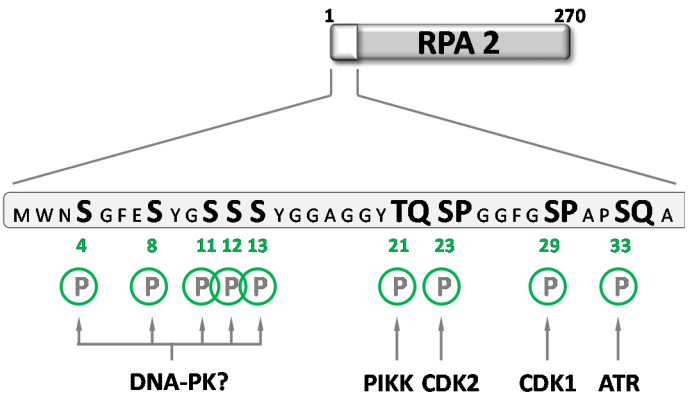

Figure 4.1 Phosphorylation map of the N-terminal domain of RPA2.

Detailed analysis of RPA2 phosphorylation throughout the cell cycle revealed that two additional forms of RPA can be distinguished by SDS-PAGE at different cell cycle stages (Anantha et al., 2007; Din et al., 1990; Dutta and Stillman, 1992; Oakley et al., 2003; Stephan et al., 2009). RPA is a component of pre-replication centres (pre-RCs) formed post-mitotically, and is involved in the early steps of the initiation of DNA synthesis at the onset of S-phase (Adachi and Laemmli, 1994), RPA is regulated by phosphorylation of RPA2 upon binding of the trimeric complex to ssDNA shortly after DNA synthesis is initiated (Din et al., 1990; Fang and Newport, 1993; Fotedar and Roberts, 1992). Phosphorylation of RPA2 at the begining of S-phase occurs on Ser23 and is carried out by the CDK2-cyclin A complex (Din et al., 1990; Dutta and Stillman, 1992; Fang and Newport, 1993; Henricksen and Wold, 1994; Stephan et al., 2009). Moreover, in normal mitotic cells, RPA2 is additionally phosphorylated on Ser29 by the CDK1-cyclinB complex (Fang and Newport, 1993; Oakley et al., 2003; Stephan et al., 2009). Phosphorylation on Ser23 and Ser29 was abolished when mitotic cells were exposed to roscovitine, a selective CDK1 and CDK2 inhibitor (Anantha et al., 2007). While phosphorylation is known to regulate protein function, mitotic phosphorylation of RPA2 did not influence ssDNA binding *in vitro*, the basic property of the purified RPA heterotrimer (Oakley et al., 2003). It is known that apart from its primary role in binding to ssDNA, RPA can also, in a less efficient manner, bind to and destabilise duplex DNA, participating in DNA unwinding prior to replication (Patrick and Turchi, 1998). Interestingly, it was reported that compared to RPA from interphase cells, mitotic RPA binds less efficiently to dsDNA (Binz et al., 2003; Oakley et al., 2003). Consistent with the limited ability of mitotic RPA to bind to dsDNA is the fact that RPA is excluded from the chromatin during normal mitosis (Stephan et al., 2009). Thus, during the normal cell cycle RPA2 is phosphorylated at the onset of S-phase on Ser23, followed by phosphorylation on Ser29 when cells enter mitosis. RPA2 is rapidly dephosphorylated in late cytokinesis, before RPA re-enters the nucleus of the two daughter cells in G1-phase (Figure 4.2) (Francon et al., 2004; Stephan et al., 2009).

It is well established that exposure of cells to DNA damaging agents such as UV-C irradiation (Carty et al., 1994; Cruet-Hennequart et al., 2006), ionising radiation (Stephan et al., 2009) and cisplatin (Cruet-Hennequart et al., 2008) or replication inhibitors like hydroxyurea (HU) (Manthey et al., 2007) and camptothecin (CPT) (Shao et al., 1999), generates forms of RPA2 that can be detected as additional bands upon SDS-PAGE and western blotting. These forms of the protein have even slower mobility compared to the S-phase and mitotic forms, and correspond to protein phosphorylation on at least four of the serine and threonine residues located in the N-terminal domain, namely Ser4, Ser8, Ser 11-13, Thr21, Ser23, Ser29 or Ser33 (Figure 4.1) (Nuss et al., 2005; Oakley et al., 2001; Zernik-

Kobak et al., 1997). The slow mobility forms of RPA2 have been termed hyperphosphorylated RPA2 (Carty et al., 1994; Nuss et al., 2005; Oakley et al., 2001).

As already described, serines 23 and 29 are phosphorylated by CDK-cyclin complexes. Ser33 and Thr21 constitute consensus sites for phosphatidylinositol 3-kinases (PIKK) including ATM, ATR and DNA-PK (Kim et al., 1999). By phosphorylation of many downstream proteins all PIKKs play crucial roles in the DNA damage signalling cascade, transducing the signal in order to activate the appropriate downstream pathways including DNA repair, transcription, checkpoint activation or apoptosis (Bakkenist and Kastan, 2004). Following genotoxic stress, ATR phosphorylates RPA2 on Ser33 (Figure 4.1) (Anantha et al., 2007; Olson et al., 2006). Thr21 was reported to be phosphorylated primarily by ATM and DNA-PK, and to a lesser extent by ATR (Figure 4.1) (Block et al., 2004; Zernik-Kobak et al., 1997). Little is known about phosphorylation of serines 11-13, originally identified by 2D peptide mapping and classified as DNA-PK-dependent phosphorylation sites (Zernik-Kobak et al., 1997). Recently, phosphorylation of Ser12 was correlated with recovery of DNA synthesis post-replication stress (Liu et al., 2012b). It is also reported that DNA-PK can phosphorylate Ser4 and Ser8 *in vitro*, despite the fact that neither residue is located in a PIKK consensus site (Figure 4.1) (Liu et al., 2012b; Zernik-Kobak et al., 1997).

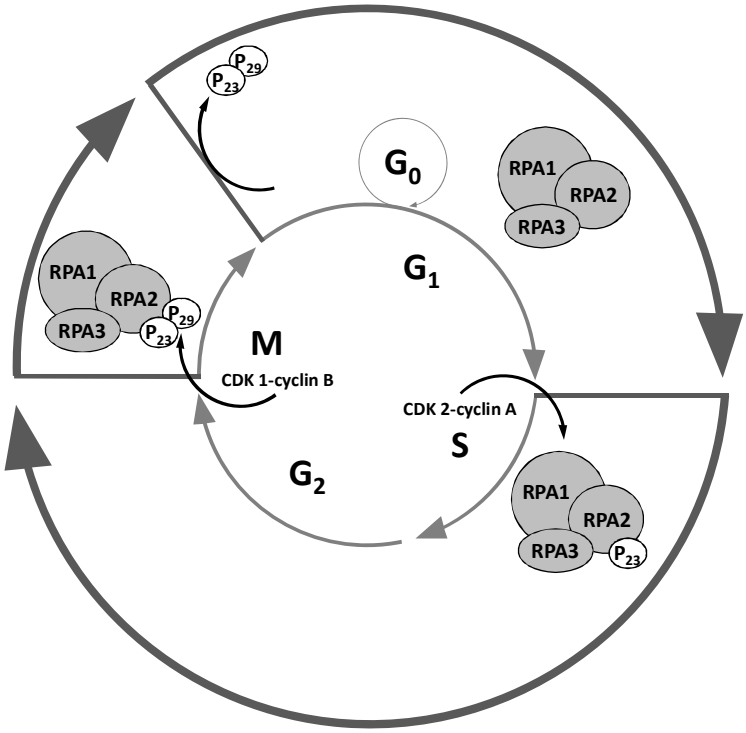

Figure 4.2 Current model of RPA2 phosphorylation and dephosphorylation during the cell cycle.

RPA2 phosphorylation can affect the function of RPA during DNA repair. For example, during the early steps of mismatch repair (MMR), unphosphorylated RPA remains tightly bound to DNA and stimulates excision of the mismatched nucleotides (Guo et al., 2006). However, the step of DNA re-synthesis is potentiated by RPA phosphorylation on so far unidentified residues, possibly by decreasing RPA-DNA interactions and making the DNA template more accessible (Guo et al., 2006).

Using a phosphospecific antibody, we have previously shown that following UV-C and cisplatin treatment of human cell lines *in vivo*, phosphorylation on Ser4/Ser8 is DNA-PK-dependent (Cruet-Hennequart et al., 2006; Cruet-Hennequart et al., 2008). While RPA2 phosphorylation on Ser4/Ser8 has been reported to occur in response to genotoxic stress (Cruet-Hennequart et al., 2006; Cruet-Hennequart et al., 2008; Nuss et al., 2005; Oakley et al., 2001; Shi et al., 2010), it has not been reported to date during the normal cell cycle. In the present report, similar to previous observations using specific antibodies against phospho-Ser23 RPA2 and phospho-Ser29 RPA (Stephan et al., 2009), we detected phospho-Ser4/Ser8 RPA2-positive immunofluorescence staining outside the chromatin in mitotic cells. Additionally, a subset of the mitotic RPA2 pool that is phosphorylated on Ser4/Ser8, was found to be localised to the centrosome, to the centromere region, and to the midbody. RPA2 was dephosphorylated during late cytokinesis before cells entered the G1-phase.

4.2 Results

4.2.1 Phospho-Ser4/Ser8 RPA2 localises to the centrosome, to the centromere region and to the midbody in mitotic cells.

The function of the human ssDNA-binding protein, RPA, is regulated by N-terminal phosphorylation of RPA2 both in a DNA damage-dependent and -independent fashion (Stephan et al., 2009). We have previously shown that in response to UV-irradiation (Cruet-Hennequart et al., 2006) and treatment with platinum-based chemotherapeutic drugs (Cruet-Hennequart et al., 2008; Cruet-Hennequart et al., 2009) RPA2 was phosphorylated on a number of sites on the N-terminus, including serines 4 and 8 and serine 33. Interestingly, indirect immunofluorescence staining using a phospho-Ser4/Ser8 RPA2 specific antibody revealed positive staining in mitotic cells (Figure 4.3A). The observed phospho-Ser4/Ser8 RPA2 staining was detectable outside the chromatin (Figure 4.3A). The majority of RPA protein is excluded from chromatin in mitotic cells, based on comparison of immunofluorescence staining for RPA and DAPI staining of genomic DNA (Francon et al., 2004; Stephan et al., 2009). Additionally, strong and discrete staining was observed in the area of the centrosome (Figure 4.3A). The centrosome, also known as the microtubule organizing centre (MTOC), is an important membraneless organelle, necessary for proper cell division in mammalian cells (Kellogg et al., 1994). It is known that in proliferating cells, the centrosome duplicates once per cell cycle, during S-phase. During mitosis, the centrosome plays a key role in the assembly and organization of the mitotic spindle and in cytokinesis, the final step of cell division (Mardin and Schiebel, 2012). The anti-centrosomal SJI antibody was used to confirm co-localisation of phospho-Ser4/Ser8 RPA2 with the centrosome (Figure 4.3A). In order to exclude the possibility that the observed staining was specific to a single human cell line, experiments were performed in XP30RO cells, derived from patients with the rare genetic disease xeroderma pigmentosum variant (XPV) (Volpe and Cleaver, 1995), the cervical adenocarcinoma HeLa cell line and in normal foreskin fibroblast (NFF) cells. Similar patterns of staining were observed in all cell lines examined (Figure 4.3A). The observed fluorescence signal was abrogated by pre-incubating the anti-phospho-Ser4/Ser8 RPA2 antibody with a blocking peptide mimicking the phospho-Ser4/Ser8 epitope on RPA2. This supports the conclusion that the observed staining is specific for phosphorylated RPA2 (Figure 4.3A). Additionally, strong detection of phospho-Ser4/Ser8 RPA2 was observed between two cells in late cytokinesis, around the region of the intracellular bridge, termed the midbody (Figure 4.3B). Interestingly, in cells at this stage of cell division phospho-Ser4/Ser8 RPA2 was no longer detected at the centrosomes (Figure 4.3B).

Double immunofluorescence staining using anti-phospho-Ser4/Ser8 RPA2 and anti-Aurora B antibody was used to confirm the localisation of phospho-RPA2 to the midbody. Aurora B, a serine/threonine kinase and a member of the chromosome passenger complex, is a key protein in mitosis, playing a role in proper chromosome condensation, kinetochore function, cytokinesis and activation of the spindle-assembly checkpoint when spindle tension is perturbed (Carmena and Earnshaw, 2003). Aurora B is known to relocate from the centromere in metaphase, through the central spindle during anaphase and finally to the midbody at the onset of telophase and during cytokinesis (Carmena and Earnshaw, 2003; Fededa and Gerlich, 2012) . Phospho-Ser4/Ser8 RPA2 staining did not directly co-localise with Aurora B in prometaphase mitotic cells. However, based on immunofluorescence

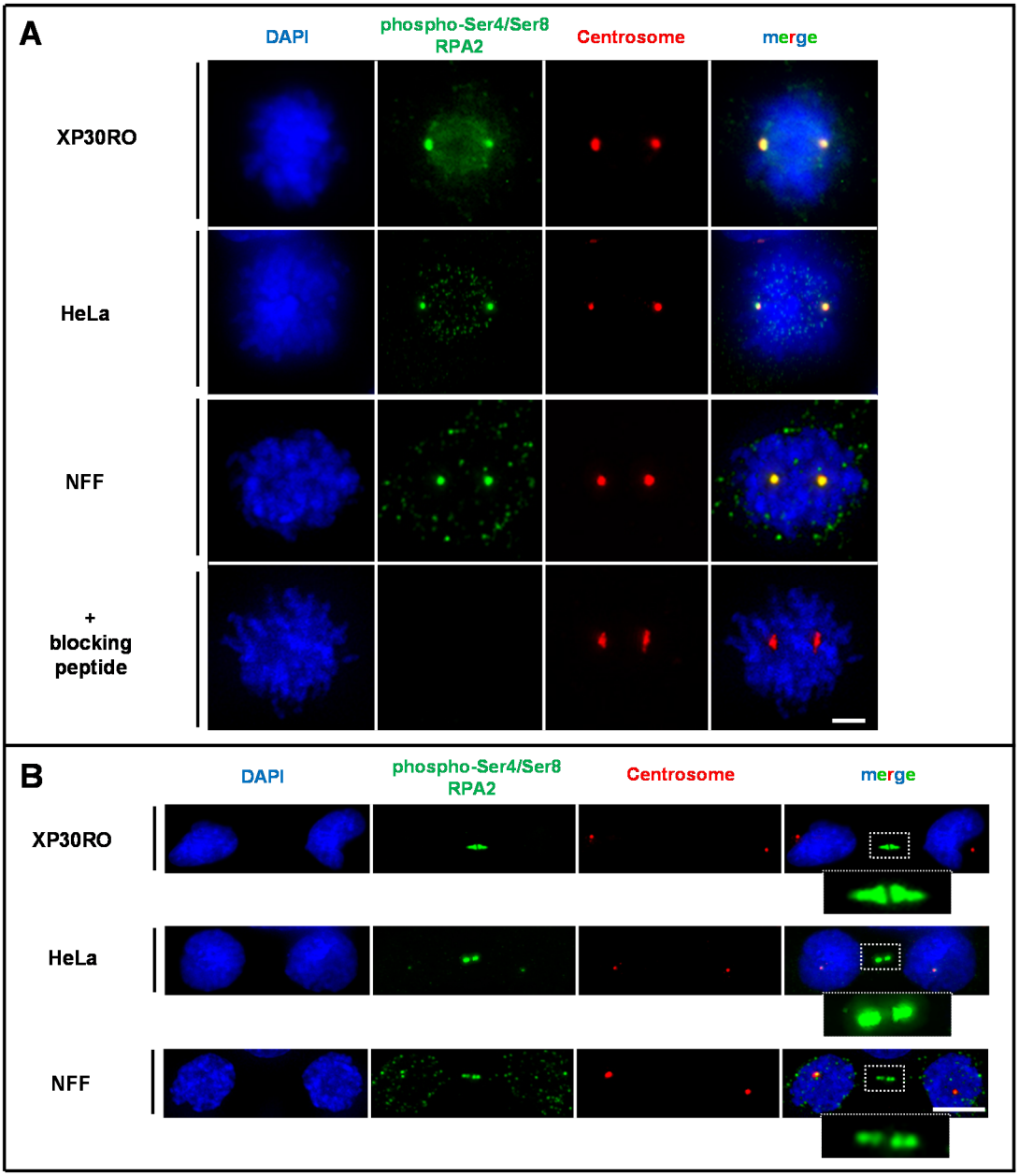

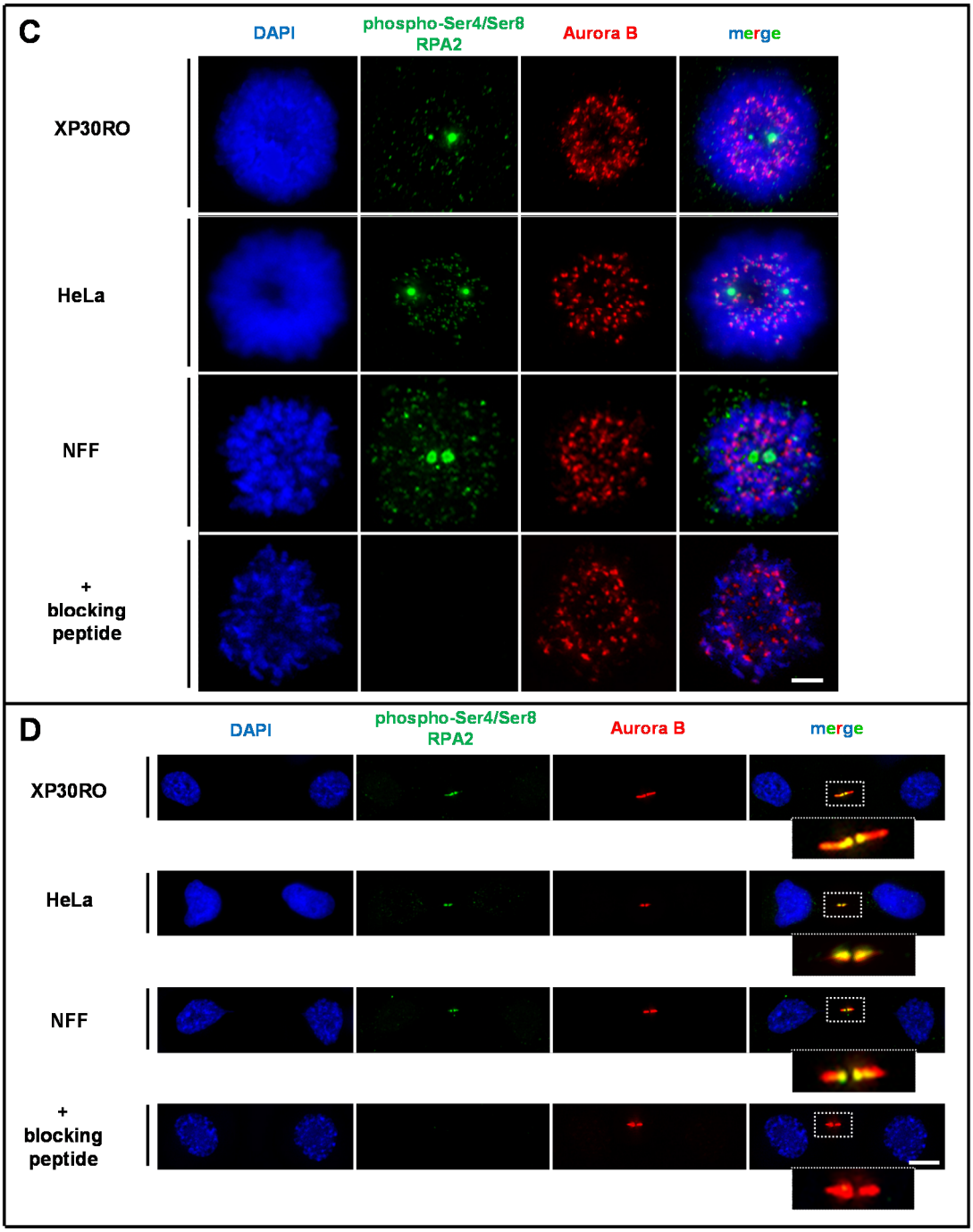

Figure 4.3 Localisation of phospho-Ser4/Ser8 RPA2 in mitosis. XP30RO, HeLa and NFF cells were grown on glass coverslips, fixed and non-specific antibody binding sites were blocked as described in Materials and Methods. Samples were stained with anti-phospho-Ser4/Ser8 RPA2 antibody, followed by Alexa 488-coupled secondary antibody. Where indicated, a blocking peptide against the anti-phospho-Ser4/Ser8 RPA2 antibody was used. Cells were subsequently stained with anti-SJI centrosomal antibody (**A, B**) or anti-Aurora B antibody (**C, D**) along with Alexa 594-coupled secondary antibody. DNA was counterstaind with DAPI. Representative cells in mitosis (**A, C**, scale bar corresponds to 5μM) and undergoing cytokinesis (**B, D**) Scale bar corresponds to 10 μM) are presented.

images, both proteins were in close proximity suggesting that this form of RPA2 localises to the centomere region of mitotic cells (Figure 4.3C). In cells undergoing cytokinesis, the signal for phospho-Ser4/Ser8 RPA2 staining was detected within the fluorescence signal of

Aurora B, supporting their co-localisation (Figure 4.3D). Consistent with our previous observations, phospho-Ser4/Ser8 RPA2 staining near the centromere region and in the midbody was observed in XP30RO, HeLa and NFF cell lines and could be abrogated using the blocking peptide (Figure 4.3C, D).

The re-localisation of phospho-RPA2 described here was detected in 100% of mitotic cells analysed, based on the observation of at least 500 cells.

4.2.2 Phospho-Ser4/Ser8 levels decrease upon mitotic exit

Given that RPA2 is phosphorylated on Ser23 and Ser29 in mitosis, and is excluded from the chromatin before being dephosphorylated and relocated to the nucleus of newly formed, G1-phase cells, we investigated whether the same pattern is observed with phospho-Ser4/Ser8 RPA2 staining. In order to follow the cells transiting mitosis, the XP30RO cell population was first enriched in mitosis by using nocodazole to arrest cell cycle progression. Nocodazole is an anti-mitotic drug which inhibits microtubule polymerisation, leading to arrest of cells in a pro-metaphase-like state (Jordan et al., 1992). The fact that adherent XP30RO cells change their morphology in mitosis, becoming round and less attached to the surface of the culture dish was used in order to shake off the nocodazole-enriched mitotic cell population. It has been shown that cells released from nocodazole arrest traverse mitosis while still in suspension, without reattachment to a culture dish (Skop et al., 2004). This approach allows cellular changes during mitosis to be monitored, without the need for trypsinisation or other methods to remove cells from the surface of a dish. This approach was used here to investigate the changes in RPA2 localisation and phosphorylation. Cells were released from nocodazole exposure by resuspension in fresh media, and allowed to resume cycling. At the indicated times post-mitotic release, samples were collected for protein analysis by immunofluorescence and western blotting (Figure 4.4A). The cytospin technique was used to obtain samples for protein localisation analysis. After fixing, slides were processed for immunofluorescence with anti-phospho-Ser4/Ser8 RPA2 and anti-α-tubulin antibodies. α-tubulin forms a heterodimer with β-tubulin to generate microtubules, dynamic structures involved in mitotic spindle formation and chromosome segregation (Kline-Smith and Walczak, 2004). Here, an anti- α-tubulin antibody was used to visualise various stages of mitosis. Immunofluorescence analysis of the T_0 sample revealed that both mitotic arrest and shake-off was successful (Figure 4.4B), as the majority of cells had pro-metaphase morphology. However, by 30 minutes after release from nocodazole arrest (T_{30}, Figure 4.4B) anaphase cells and cells undergoing cytokinesis were detectable, indicating that the cells progressed through mitosis. Subsequently, at 60 minutes post-mitotic release (T_{60}), the majority of the cells were either undergoing cytokinesis or were already in G1 phase.

Consistent with the observations described above (Figure 4.4) qualitative analysis of immunofluorescence images confirmed the presence of phospho-Ser4/Ser8 RPA2 at the centrosomes, near the centromere region, and in midbody in the cells following release from mitotic arrest.

Nocodazole treatment may lead to abnormalities such as changes in centrosome number, which can lead to faulty chromosome segregation and aneuploidy (Jordan et al., 1992; Mardin and Schiebel, 2012). It was therefore of interest to investigate the localisation of phospho-Ser4/Ser8 RPA2 during abnormal mitoses. Consistent with the observations described above, phospho-Ser4/Ser8 RPA2 was found in all overduplicated centrosomes (Supplementary Figure 4.1A) and multipolar spindle-derived midbodies (Supplementary Figure 4.1B).

Quantitative analysis of the percentages of cells in mitosis and undergoing cytokinesis confirmed that cells progressed through mitosis under these conditions. Based on the morphology, around 90% of cells were identified as mitotic just after the mitotic shake-off, with this number dropping to 20% at 60 minutes, and to 3% at 120 minutes post-nocodazole release (Figure 4.4C, left graph). Therefore, we conclude that XP30RO cells can: (i) resume cell cycle progression *in vitro* after release from nocodazole treatment, and (ii) require up to 120 minutes for all cells to complete mitosis. Consistent with these observations, the number of cells undergoing cytokinesis increased from 0% of cells immediately after mitotic shake-off, peaked at over 50% of cells at 60 minutes post-release, and then gradually decreased when cells were entering G1 phase (Figure 4.4C, left graph).

Western blotting of whole cell lysates using anti-RPA2 antibody confirmed mitotic arrest and shake-off. At T_0, where 90% of cells are in mitosis (Fig. 4.4C), RPA2 appears as a slower mobility form on SDS-PAGE (Figure 4.4D, left image, marked with *) when compared to the mobility of RPA2 from an asynchronous cell population ('As' sample). The slower mobility form of RPA2 in mitotic cells is a result of cell cycle-dependent RPA2 phosphorylation (Din et al., 1990; Dutta and Stillman, 1992; Stephan et al., 2009). Upon release from nocodazole arrest, cells transit M-phase and before entering G1 phase RPA2 is dephosphorylated, which increases the mobility of the protein on SDS-PAGE. This is supported by the observation that 60 minutes post-mitotic release (T_{60} sample), when the majority of cells have completed M-phase, RPA2 mobility was similar to that of RPA2 from asynchronous cells (Figure 4.4D, left image, marked with **).

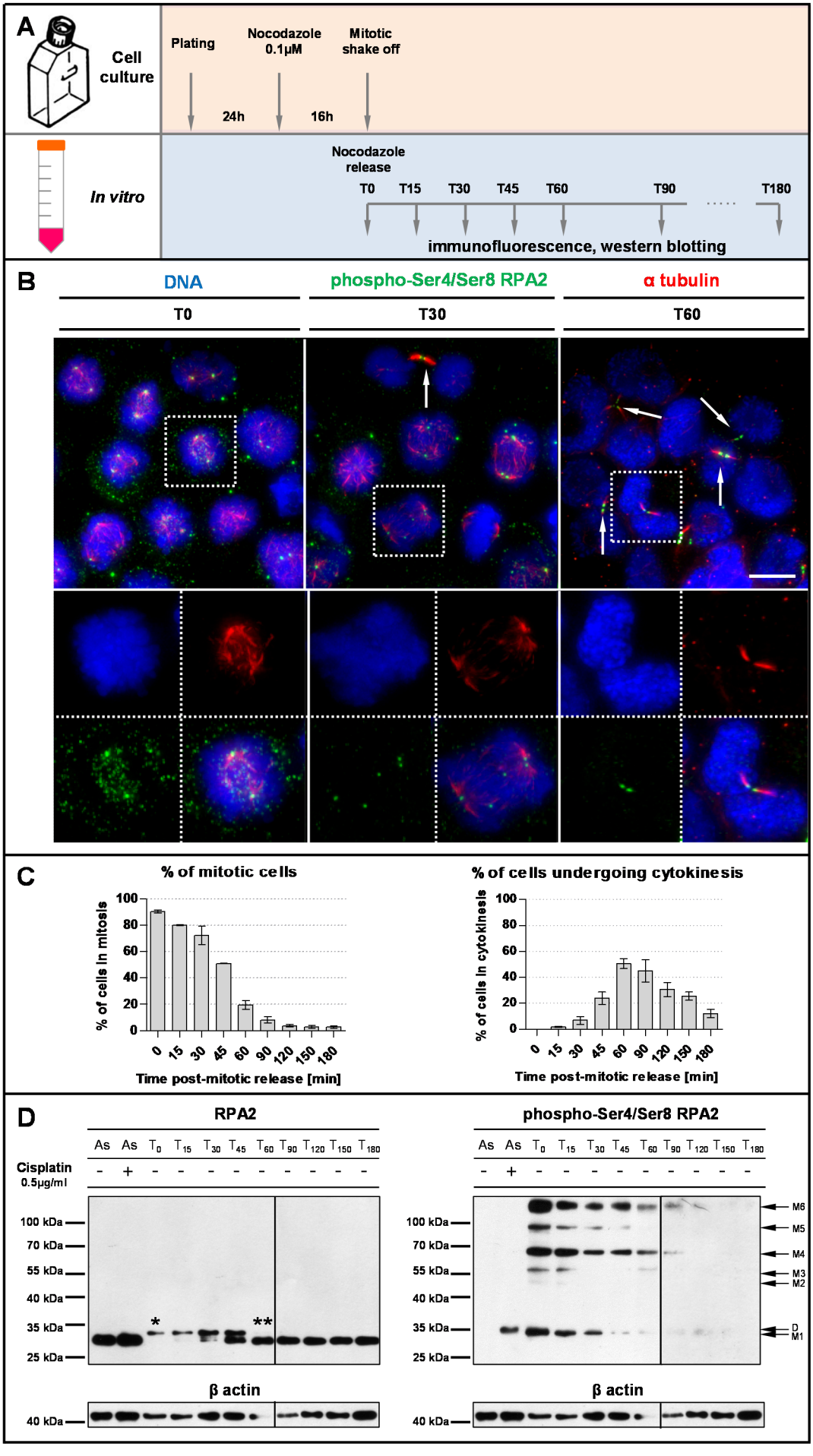
A
Cell culture
Plating
Nocodazole 0.1µM
Mitotic shake off
24h
16h
In vitro
Nocodazole release
T0 T15 T30 T45 T60 T90 T180
immunofluorescence, western blotting
B
DNA
phospho-Ser4/Ser8 RPA2
α tubulin
T0
T30
T60
C
% of mitotic cells
% of cells in mitosis
Time post-mitotic release [min]
% of cells undergoing cytokinesis
% of cells in cytokinesis
Time post-mitotic release [min]
D
RPA2
phospho-Ser4/Ser8 RPA2
As As T0 T15 T30 T45 T60 T90 T120 T150 T180
Cisplatin 0.5µg/ml
100 kDa
70 kDa
55 kDa
40 kDa
35 kDa
25 kDa
β actin
M6
M5
M4
M3
M2
D
M1

Figure 4.4 Mitotic cells and midbody enrichment. A. Schematic outline of the midbody enrichment procedure. XP30RO cells were plated 24 hours before being treated with 0.1μM nocodazole. 16 hours later, mitotic cells were collected and released from nocodazole-induced mitotic arrest. At the indicated times following mitotic release, samples were taken for immunofluorescence and western blotting (see Materials and Methods). **B.** Representative images from samples taken at 0, 30 and 60 minutes post-mitotic release are presented. Samples were stained for phospho-Ser4/Ser8 RPA2 and α-tubulin, and bound antibody was detected using Alexa 488- and Alexa 594-coupled secondary antibodies, respectively. DNA was counterstained with DAPI. Arrows indicate midbody location. Scale bar corresponds to 10μm. **C.** Percentages of cells in M-phase and undergoing cytokinesis were calculated from immunofluorescence images derived from two independent experiments. The percentage of cells undergoing cytokinesis was determined based on counting the number of midbodies. **D.** Protein samples were analysed by SDS-PAGE and western blotting. Membranes were probed with anti-RPA2 antibody followed by membrane stripping and re-probing with anti-phospho-Ser4/Ser8 RPA2 antibody. Protein lysates from either mock-treated or cells treated with cisplatin (0.5μg/ml) were used as controls. Actin was used as a loading control. Numbered arrows (M1-M6) show various bands detected using anti-phospho-Ser4/Ser8 RPA2 antibody. Asterisks indicate mitotic (*) and interphase (**) RPA2 bands. Samples from T_{90} to T_{180} were run on separate gels, marked with the vertical line.

Next, anti-phospho-Ser4/Ser8 RPA2 antibody was used to further test the hypothesis that RPA2 is phosphorylated on serines 4 and 8 during mitosis. A strong band was detected in the extract of asynchronous cells treated with cisplatin for 24h. This form of RPA2, running slower than the 35kDa size marker (Figure 4.4D, top left image, arrow marked 'D'), corresponds to the DNA damage-induced, hyperphosphorylated form of RPA2 (Cruet-Hennequart et al., 2008; Cruet-Hennequart et al., 2009). Consistent with this, no signal was detected in the mock-treated, asynchronous sample. Interestingly, several bands were detected in the extracts of mitotic cells. These are marked on the gel as forms M1 to M6 (Figure 4.4D, top left image). All the observed bands were specific to M-phase as the intensity of these bands decreased with time, in a similar timeframe to the mitotically phosphorylated RPA2 (Figure 4.4D, top left image, marked with *). Band M1 was of slightly faster mobility when compared to the hyperphosphorylated form of RPA2, suggesting that not all the sites phosphorylated in the damage-induced form of RPA2 are also phosphorylated in the M-phase-specific form (Figure 4.4D, top left image, lanes T_0 and As (+), respectively). The mobility of band M1 corresponded to the main mitotic band detected by anti-RPA2 antibody (Figure 4.4D, top right image, marked with M1 arrow and top left image, marked with *). Bands M2 to M6 run at positions corresponding to approximately 50kDa, 60kDa, 68kDa, 90kDa and 120kDa based on comparison to the size markers, with band M6 giving the strongest signal by western blotting. Since RPA2 is 34kDa, detection of slower mobility bands (M2-M6) could represent a non-specific signal on the western blot or could be due to detection of modified forms of RPA2. RPA2 phosphorylation could not by itself account for the significant decrease in mobility of the identified bands (M2-M6). Alternatively, these slow-mobility forms detected by anti-phospho-Ser4/Ser8 RPA2 antibody could be a result of covalent modification of RPA2 by,

for example, ubiquititation or SUMOylation. Conjugation of ubiquitin or small ubiquitin-like modifier (SUMO) to lysine residues of RPA2 could increase the size of the protein by 8kDa or 11kDa respectively (Hannoun et al., 2010; Hicke, 2001). Both modifications can alter protein function and addition of multiple ubiquitin residues (polyubiquitination) commonly directs proteins for proteasomal degradation, thus controlling protein turnover (Hannoun et al., 2010; Hicke, 2001). However, the presence of ubiquitin or SUMO modifications on RPA2 was not directly investigated further here.

None of the mitotic forms that show slower mobility when compared to mitotic form M1 and are detectable using the anti-phospho-Ser4/Ser8 RPA2 antibody, could be detected using the anti-RPA2 antibody (Figure 4.4D, top right versus top left image). This observation could be a result of non-specific detection by anti-phospho-Ser4/Ser8 RPA2. Alternatively, since the specificity of the anti-phospho-RPA2 antibody has been previously demonstrated using the blocking peptide, RPA2 phosphorylation in mitosis could induce a conformational change in the subunit preventing anti-RPA2 antibody from binding. Another reason for this could be that the absolute level of mitotic phospho-Ser4/Ser8 RPA2 protein is very low and does not suffice to generate a signal when using the anti-RPA2 antibody in western blotting.

It was of interest to determine if the bands detected by western blotting of mitotic whole cell lysates were present is specific cellular structures, for example the midbody. Since phospho-Ser4/Ser8 RPA2 was localised to the midbody in late cytokinesis (Figure 4.3D, Figure 4.4B), the midbody proteome was analysed. Midbodies were isolated from XP30RO cells, at 30, 45 and 60 minutes post-release from nocodazole arrest, as described in Materials and Methods. Indirect immunofluorescence analysis of extracted midbodies, using anti-phospho-Ser4/Ser8 RPA2 and anti-α-tubulin antibodies revealed that phospho-Ser4/Ser8 RPA2 staining was still detectable following isolation of midbodies (Figure 4.5A, upper panel). However, the midbody fractions obtained were not homogenous, but instead were mixed populations of isolated, individual midbodies (Figure 4.5A, lower panel) and midbodies that were still attached through one end to a G1 phase cell. This is consistent with recent reports that midbodies remain attached to one of the daughter cells before being released or internalised (Kuo et al., 2011; Pohl and Jentsch, 2009). It is also worth noting that individual, isolated midbodies can be isolated with residual DNA present, visualised in blue following DAPI staining (example in Figure 4.5B, upper panel). This is important and could help explain the presence of RPA2 in the midbody. SDS-PAGE and western blotting analysis of protein lysates revealed enrichment for Aurora B in protein samples derived from isolated midbodies and from mitotically-enriched cells, when compared to extracts of asynchronous cells (Figure 4.5B). This observation is consistent with the report

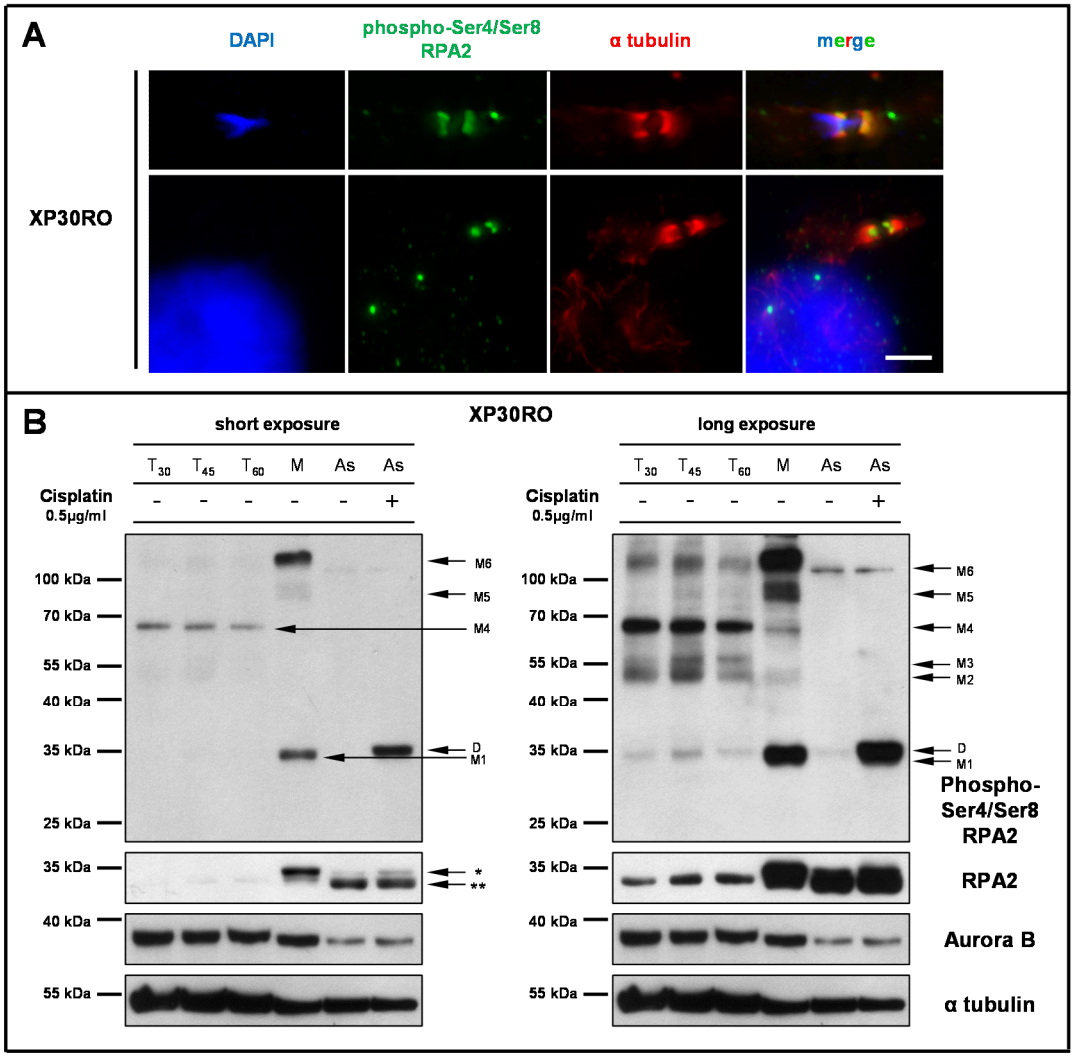

Figure 4.5 Analysis of RPA2 in isolated midbodies. XP30RO cells were plated 24 hours before being treated with 0.1μM nocodazole. 16 hours later, mitotic cells were collected and released from nocodazole-induced mitotic arrest. 30, 45 and 60 minutes post-mitotic release, samples were collected for midbody extraction (see Materials and Methods). **A.** Before protein extraction, samples from the isolated midbodies were taken for immunofluorescence analysis. Representative images of isolated midbodies, probed for phospho-Ser4/Ser8 RPA2 and α-tubulin are presented. DNA was counterstained with DAPI. **B.** Proteins were extracted from the isolated midbodies (lanes marked T_{30}, T_{45}, T_{60}), separated by SDS-PAGE and probed with the indicated antibodies. Protein lysates from mitotic cells (M) and from asynchronous (As) cells (either mock-treated or treated with cispatin for 24h) were run as controls. Arrows show the bands detected using the anti-phospho-Ser4/Ser8 RPA2 antibody. Asterisks mark mitotic (*) and interphase (**) RPA2.

that Aurora B expression peaks at the G2 to M-phase transition, and the kinase activity is maximal during mitosis (Carmena and Earnshaw, 2003). Increased α-tubulin staining in samples from isolated midbodies (Fig. 4.5B) is likely to be a consequence of α-tubulin enrichment in the intercellular bridge structure (Skop et al., 2004). Similar to previous observations (Figure 4.4D, right panel), RPA2 staining from mitotic (M) and asynchronous (As) cells showed bands of lower (*) and higher (**) mobility, respectively, corresponding to M-phase and interphase forms (Din et al., 1990; Dutta and Stillman, 1992; Stephan et al.,

2009). RPA2 staining was also detected in the lysates from isolated midbodies (Figure 4.5B).

Western blotting for phospho-Ser4/Ser8 RPA2 showed that band M4 was enriched in all the extracted midbody samples (Figure 4.5B, top left image) indicating that this is the most abundant form of phospho-RPA2 present in the midbody. Again, there was a small difference in the mobility of mitotic band M1 and the DNA damage-induced hyperphosphorylated form of RPA2 ('D') (Figure 4.5B, top left image, lanes M and As (+)), indicating that these represent differently modified forms of this protein. Longer film exposure (Figure 4.5A, top right image) confirmed that the most abundant form of phospho-RPA2 in the midbody was approximately 68kDa in size (M4). Interestingly, after longer film exposure, bands M1 and M6 were also detected in asynchronous cell lysates (Figure 4.5, top right image). Consistent with the fact that these bands are the most abundant in mitotically-enriched cells, their presence in extracts of asynchronous cells is consistent with the fact that a fraction of the cells in an asynchronous population are mitotic.

In summary, the present data support the conclusion that a phospho-Ser4/Ser8-positive form of RPA2 can be detected in mitotic cells without the addition of DNA damaging agents. The levels of this modified form of RPA2 decrease as cells progress through M-phase; phospho-Ser4/Ser8 RPA2 concentrates in the midbody just before the final cell division and is no longer detectable with the onset of G1 phase.

4.2.3 Biochemical characterisation of mitotic phospho-Ser4/Ser8 RPA2.

In order to further characterise the phospho-Ser4/Ser8-positive form of RPA2, protein lysates from mitotic cells were analysed biochemically. First, protein lysates from control and mitotic cells were treated with λ phosphatase. It was found that upon 30 minutes exposure to this enzyme, both the damage-dependent RPA2 form (D) and the mitotic forms M1, M3, M5 and M6 were no longer detectable, consistent with these bands representing phosphorylated proteins (Figure 4.6A). During this procedure not all of the previously described forms (M2 and M4) of mitotic phospho-Ser4/Ser8 RPA2 were detected. This could be the result of differences in procedure used to prepare samples for λ phosphatase treatment (see Materials and Methods). Sodium orthovanadate (Na_3VO_4) at a concentration commonly used in cell lysis buffers (1mM), did not completely inhibit λ phosphatase activity under the conditions used in the reaction; the major effect of the inhibitor was to prevent dephosphorylation of band M6 (Figure 4.6A, right lane). However, the levels of hyperphosphorylated RPA2 and mitotic form M1 decreased (Figure 4.6A) even in the absence of the inhibitor, possibly due to the action of endogenous phosphatases present

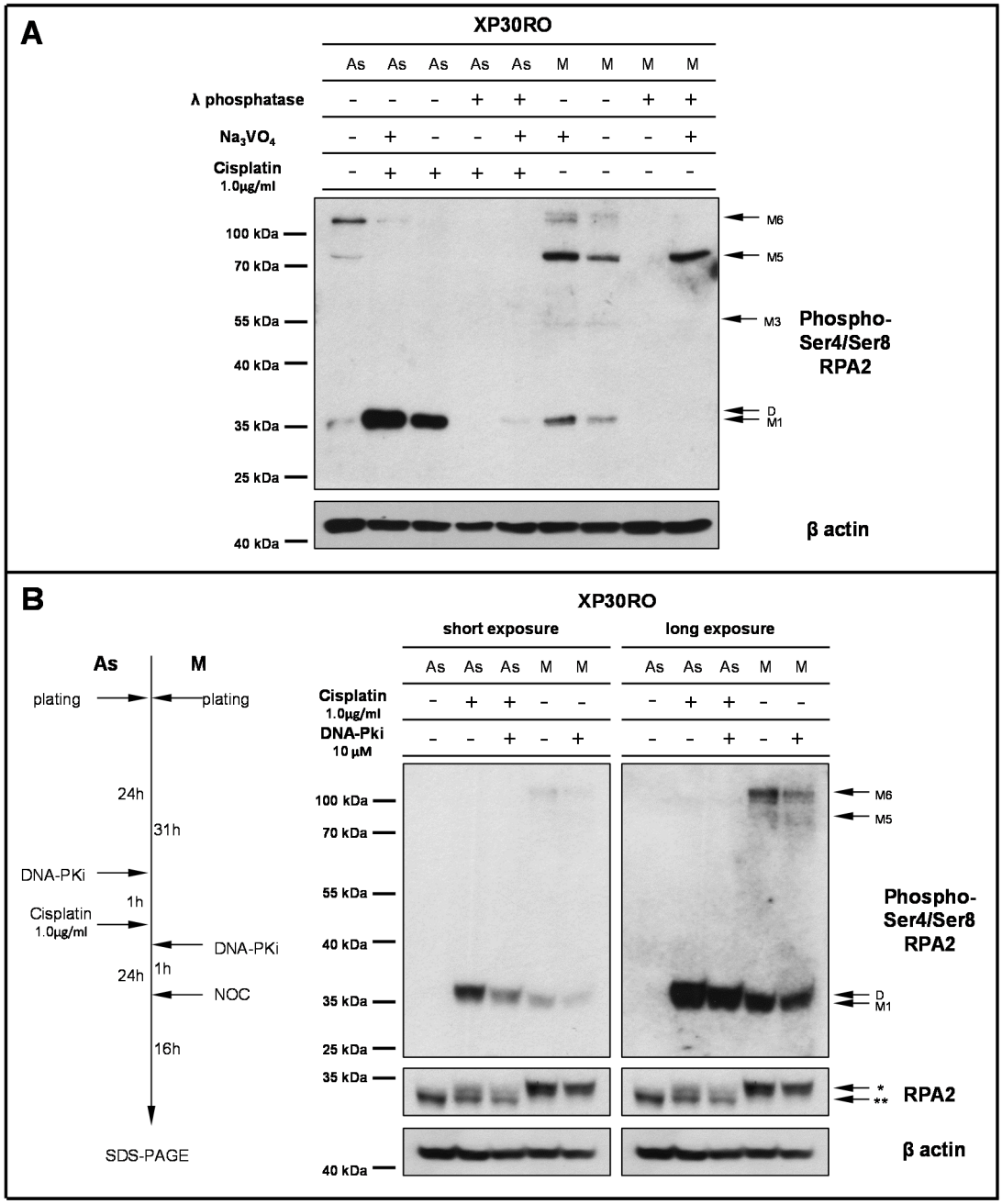

Figure 4.6 Analysis of mitotic phospho-Ser4/Ser8 RPA2 phosphorylation status. A. Mitotic XP30RO cells (M) were obtained by mitotic shake-off of cells treated for 16h with 0.1μM nocodazole. Cells were harvested for protein analysis and protein lysates were incubated in the presence or absence of λ phosphatase as described in Materials and Methods, and separated on on SDS-PAGE. Membranes were exposed to anti-phospho-Ser4/Ser8 RPA2 antibody and anti-β-actin antibody staining was used as loading control. Protein lysates from asynchronous cells (As), either mock-treated or treated with cisplatin (1μg/ml) for 24h were used as controls for phosphorylation of RPA2 on Ser4/Ser8. Sodium orthovanadate (Na_3VO_4) was used as a phosphatase inhibitor. Arrows point to bands detected using anti-phospho-Ser4/Ser8 RPA2 antibody. **B.** XP30RO cells were treated either with DMSO, or with 10μM NU7441 (DNA-PKi), 1h prior to treatment with 1μg/ml cisplatin for 24h (As) or with 0.1μM nocodazole for 16h (M). Whole cell lysates were then prepared and analysed using western blotting (as shown in the schematic outline, left). Phosphorylation of RPA2 on Ser4/Ser8 was analysed using the specific antibody. Mitotic enrichment was confirmed by using the anti-total RPA2 antibody. Protein extracts from mock-treated samples were used as controls. β actin antibody staining was used as a loading control. Arrows point to bands detected using anti-phospho-Ser4/Ser8 RPA2 antibody. Asterisks mark the position of interphase (**) and mitotic (*) RPA2.

in the lysate.

Since damage-induced phosphoryalation of RPA2 on Ser4/Ser8 is a DNA-PK-dependent process (Cruet-Hennequart et al., 2008; Liaw et al., 2011; Liu et al., 2012b) it was of interest to determine whether mitotic RPA2 phosphorylation also depends on DNA-PK activity. To test this hypothesis, XP30RO cells were exposed to the DNA-PK inhibitor, NU7741 (Leahy et al., 2004) prior to being cells exposed to cisplatin or to nocodazole treatment (Figure 4.6B, left, schematic diagram). Interestingly, both damage-induced (D) and mitotic (forms M1 and M6) phospho-Ser4/Ser8 RPA2 staining decreased in the presence of NU7741, suggesting that both processes are DNA-PK-dependent (Figure 4.6B, short and long film exposure). This provides further evidence that serines 4 and 8 of RPA2 are a target for cellular PIK kinases during mitosis (Stephan et al., 2009).

To investigate whether the mitotic phospho-Ser4/Ser8 RPA2 can form the RPA heterotrimer, immunoprecipitation using the anti-phospho-Ser4/Ser8 RPA2 antibody was carried out. SDS-PAGE and western blotting analysis using anti-phospho-Ser4/Ser8 RPA2 antibody demonstrated that phospho-Ser4/Ser8 RPA2 could be specifically immunoprecipitated from samples where this form of RPA2 protein was previously observed (Figure 4.7A, top panel, cisplatin-treated asynchronous cells and mitotic cells). . Following -immunoprecipitation, it should be noted that both the damage-dependent and the M1 phospho-Ser4/Ser8 form of RPA2 had slightly slower mobility when compared to non-immunoprecipitated samples (Figure 4.7A, top panel). This could be a result of salt present in the buffer used to elute proteins from the beads. Consistent with the presence of mitotic forms of phospho-Ser4/Ser8 RPA2 in an RPA complex, further analysis of the immunoprecipitated samples revealed that the 70kDa subunit of replication protein A (RPA1) could be immunoprecipitated using anti-phospho-Ser4/Ser8 RPA2 only from samples in which the hyperphosphorylated or mitotic forms of RPA2 had previously been detected (Figure 4.7A). In mock-treated samples, where the hyperphosphorylated form of RPA2 is completely absent, and only a relatively small fraction of cells are mitotic, no RPA1 co-immunoprecipitation was detected. The specificity of the anti-phospho-Ser4/Ser8 RPA2 antibody was confirmed by analysis of immunoprocipitates for β-actin, which was present only in whole cell protein lysates but not in the immunoprecipitates (Figure 4.7A).

In order to further distinguish the DNA damage-dependent hyperphosphorylated form of RPA2 from the mitotic, phospho-Ser4/Ser8-positive form, two-dimensional (2D) gel electrophoresis analysis was performed in the pH range of 4 to 7. Recombinant RPA2 has an isoelectric point of 5.75 (Sandoval et al., 2006). Since phosphorylation adds negative charges to a protein, the isoelectric point of phosphorylated proteins decreases. Western blot

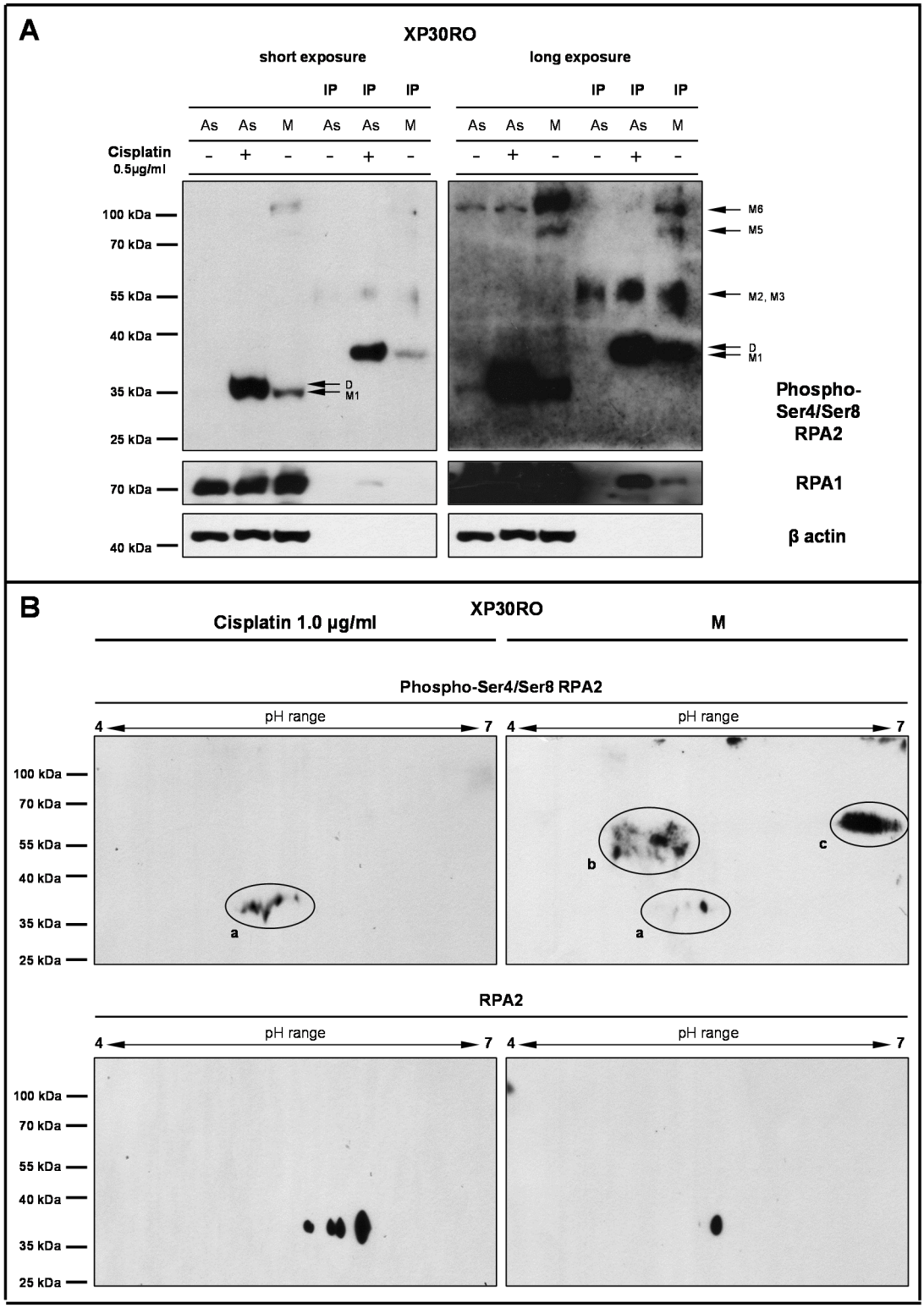

Figure 4.7 Biochemical characterisation of mitotic phospho-Ser4/Ser8 RPA2. A. Asynchronous, XP30RO cells, either mock-treated or treated continuously for 24h with 1µg/ml cisplatin, as well as mitotic cells derived from shake-off of cells exposed to 0.1µM nocodazole for 16h, were harvested for immunoprecipitation as described in Materials and Methods. Following immunoprecipitation using anti-phospho-Ser4/Ser8 RPA2, samples (IP) were analysed by SDS-PAGE and western blotting using anti-phospho-Ser4/Ser8 RPA2, anti-RPA1 and anti-β-actin antibodies. Whole cell lysates (WL) were run as controls. **B.** XP30RO protein samples from cisplatin–treated and mitotic cells were obtained as described above. Proteins were re-hydrated onto 2-D electrophoresis strips (pH range 4 to 7). Isoelectric focusing was carried out as described in Materials and Methods, followed by second-

dimension electrophoresis. Phospho-Ser4/Ser8 RPA2 was analysed using phosphospecific antibody in western blotting. Positively-stained gel regions are marked as 'a', 'b', 'c' (upper panel). Membranes were then stripped and re-probed with anti-RPA2 antibody (bottom panel). A representative blot from repeated mitotic sample is presented.

analysis of mock-treated, asynchronous cell extracts showed no staining with anti-phospho-Ser4/Ser8 RPA2 antibody using one-dimensional SDS-PAGE (Figure 4.4A). One-dimensional analysis of cisplatin-treated samples shows the band of slower mobility corresponding to damage-dependent, hyperphosphorylated form of RPA2, referred to as 'D' (see Figures 4.4D; 4.5B; 4.6). However, five spots of differing intensities were identified when cisplatin-treated samples were analysed by 2-D gel electrophoresis followed by western blotting using anti-phospho- Ser4/Ser8 RPA2 antibody (Figure 4.7B, upper panel, left image). Interestingly, when mitotic lysates were analysed by 2-D electrophoresis, three gel regions (a, b, c) were identified that showed phospho-Ser4/Ser8 RPA2-positive staining (Figure 4.7B, upper panel, right image). In the first area (a), spots localised to the same gel region as spots detected in cisplatin-treated samples. However, spots with most acidic pI identified in cisplatin-treated samples were largely absent in area (a) of the mitotic sample (Figure 4.7B, upper panel, right image). This indicates that in response to DNA damage, RPA2 is modified on more phosphorylation sites when compared to RPA2 that is modified in mitotic cells. This could account for the difference in the mobility of cisplatin-induced hyperphosphorylated RPA2 and mitotic phospho-Ser4/Ser8 RPA2 observed after one-dimensional gel electrophoresis (Figures 4.4D; 4.5B; 4.6).

Consistent with the presence of additional, slow mobility, phospho-Ser4/Ser8 RPA2 bands in mitotic extracts observed following one-dimensional SDS-PAGE (Figure 4.4D), several additional spots were detected by 2-D electrophoresis (Fig. 4.7B, right). The spots in the area marked (b) of the mitotic sample (Fig. 4.7B upper panel, right image) could account for phospho-Ser4/Ser8 RPA2 forms M2 and M3 detected on the one-dimensional gel (Figure 4.4D,). These spots appear to be shifted towards lower pI values, indicating that they represent a form of protein which contains more negative charges when compared to spots detected in area (a), again consistent with increased phosphorylation of RPA2. Strong staining within area (c), which could be correlated with form M4 on one-dimensional gel electrophoresis, is shifted towards the basic pI regions. This could lead to the conclusion that this form represents non-specific phospho-Ser4/Ser8 RPA2 staining or that it corresponds to additionally modified RPA2, and therefore is shifted towards basic pI regions. Bands M5 and M6, detected by the one dimensional electrophoresis were not clearly identified.

Stripping and re-probing of membranes with anti-RPA2 antibody resulted in RPA2 detection only in area (a) of the blot, in both cisplatin-treated and mitotic samples (Figure 4.7B, lower panel). This is consistent with previous observations using the anti-RPA2 antibody on one-dimensional SDS-PAGE (Figure 4.4D). However, more spots, corresponding to differentially phosphorylated RPA2 forms, were observed in the cisplatin treated sample (Figure 4.7B, lower panel, left image versus right image). This could mean that during mitosis total the RPA2 protein pool is phosphorylated, whereas only a subset of RPA2 is phosphorylated in response to DNA damage. This could account for the heterogenous RPA2 population observed using anti-RPA2 antibody in cisplatin-treated samples.

In conclusion, it has been shown that the mitotic M1 RPA2 form, detected using anti-phospho-Ser4/Ser8 RPA2 antibody on the one-dimensional SDS-PAGE (i) results from phosphorylation and (ii) is DNA-PK-dependent. Analysis of mitotic protein extracts revealed that mitotic phospho-Ser4/Ser8 RPA2 forms (i) exist in a complex with the RPA1 subunit and, (ii) compared to the DNA damage-induced hyperphosphorylated form, vary in phosphorylation pattern as determined by two-dimensional gel electrophoresis. Further analysis is required in order to determine the nature of the lower mobility forms of RPA2 (M2-M6), detected in whole cell mitotic extracts using the anti-phospho-Ser4/Ser8 RPA2 antibody.

4.2.4 Localisation of phospho-RPA2 in mitosis.

It has been shown that RPA2 is phosphorylated on serine 23 and serine 29 in mitotic cells (Stephan et al., 2009). To test whether the mitotic phospho-Ser4/Ser8 RPA2 described here co-localised with these mitotic phospho-Ser4/Ser8 RPA2 forms and with total RPA2, dual-staining immunofluorescence experiments using specific antibodies were performed. In order to rule out cell line specificity, studies were performed in XP30RO cells (Volpe and Cleaver, 1995) and in HeLa cells, a cervical adenocarcinoma cell line. Consistent with previous reports (Stephan et al., 2009), RPA2 was excluded from the chromatin in mitosis (Figure 4.8A, B, C). In both cell lines, phospho-Ser4/Ser8 RPA2 staining was detected within the RPA2 (Figure 4.8A), phospho-Ser23 (Figure 4.8B) or phospho-Ser29 (Figure 4.8C) signals. In the centrosome area, where phospho-Ser4/Ser8 RPA2 shows distinct and strong staining, enhanced staining with all other anti-RPA2 antibodies was also found (Figure 4.8).

Based on these observations, we conclude that, in addition to the known RPA2 phosphorylation events during the normal cell cycle (Figure 4.2) a subset of the RPA2 pool undergoes phosphorylation on Ser4/Ser8, and dynamically translocates during the phases of

mitosis. Various proteins are known to change localisation in mitosis, including Aurora B, and such differential localisation can dictate the functionality of proteins in mitotic cells leading to proper chromosome segregation (Carmena and Earnshaw, 2003). We propose a model for a phospho-Ser4/Ser8 RPA2 mitotic cycle (Figure 4.9). In prophase, the first M-phase stage during which condensation of duplicated chromosomes occurs, phospho-Ser4/Ser8 RPA2 is detectable both at the nuclei periphery and co-localised with centrosomes (Figure 4.9A). Centrosomes then disengage and start moving towards opposite cell poles where they participate in spindle microtubule organisation. Upon breakdown of the nuclear envelope at the onset of pro-metaphase, most of the phospho-Ser4/Ser8 RPA2 is excluded from chromatin. However, a subset of this form of RPA2 remains co-localised with the centrosomes (Figure 4.9A), as well as localised at the centromere region of the chromosomes, where Aurora B is also detected (Figure 4.9B). Phospho-Ser4/Ser8 RPA2 remains localised to the centrosome and to the centromere region throughout metaphase. In anaphase, this form of phospho-RPA2 starts to re-localise to the midbody. This process is finalised in late cytokinesis, where phospho-Ser4/Ser8 RPA2 is only found in the central midbody region (Figure 4.9 A, B, C). In contrast, during interphase, nuclei are positive for phospho-Ser4/Ser8 RPA2 only when cells are exposed to DNA damaging agents, including UV-irradiation (Cruet-Hennequart et al., 2006) or platinum-based chemotherapeutics (see Chapter 3).

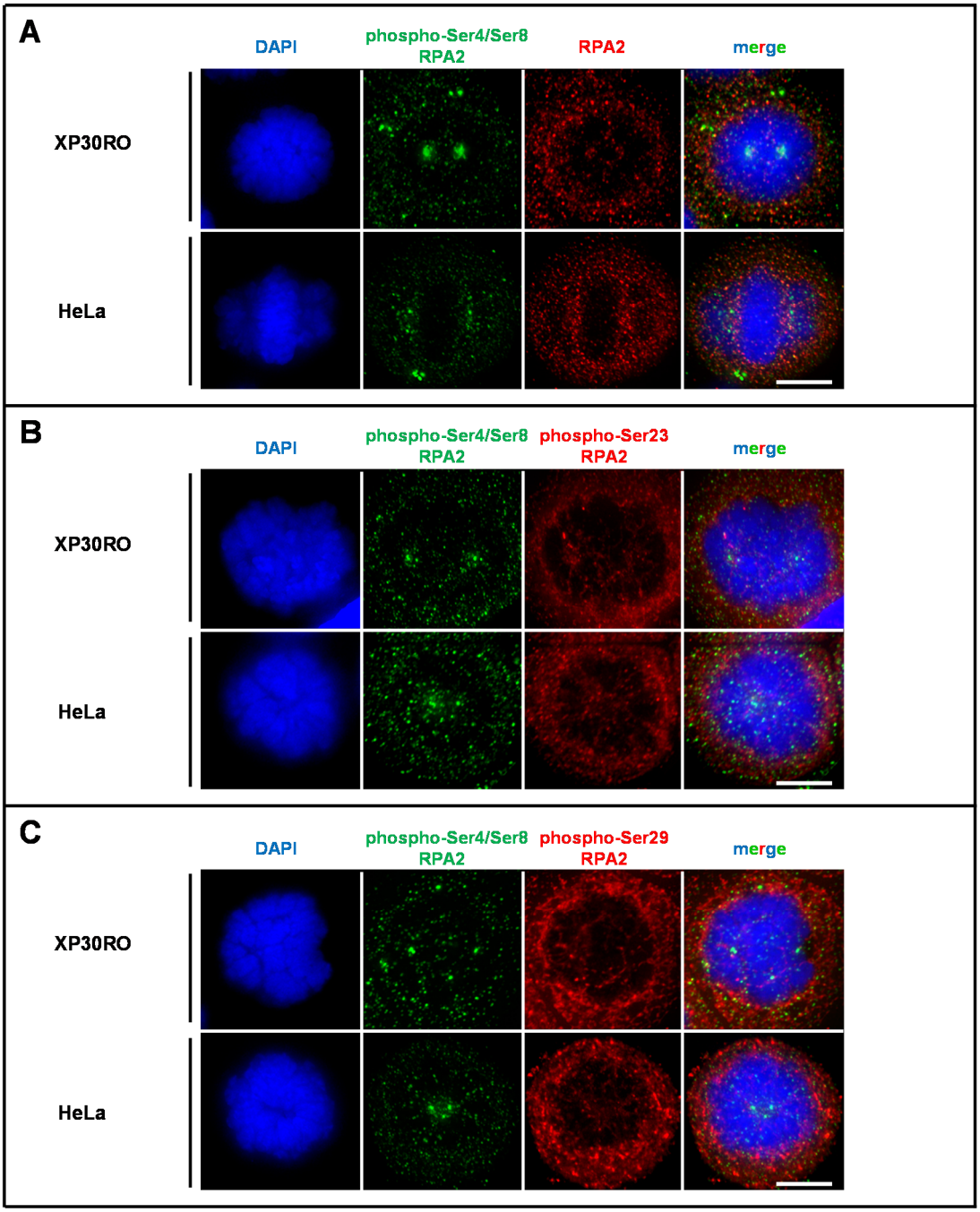

Figure 4.8 Analysis of RPA2 localisation in mitosis. XP30RO and HeLa cells were treated with 0.1μM nocodazole for 16h, to enrich for mitotic cells. Cells were harvested by mitotic shake-off. The cytospin technique was used to prepare samples for immunofluorescence staining, as described in Materials and Methods. Samples were fixed; non-specific antibody binding sites were blocked and slides were stained with anti-phospho-Ser4/Ser8 RPA2, and detected using Alexa 488-conjugated secondary antibody. Subsequently, samples were co-stained with anti-RPA2 (**A**), anti-phospho-Ser23 RPA2 (**B**) or anti-phospho-Ser29 RPA2 (**C**) primary antibodies and with Alexa 594-coupled secondary antibody. DNA was counterstained with DAPI. Scale bar corresponds to 10μM.

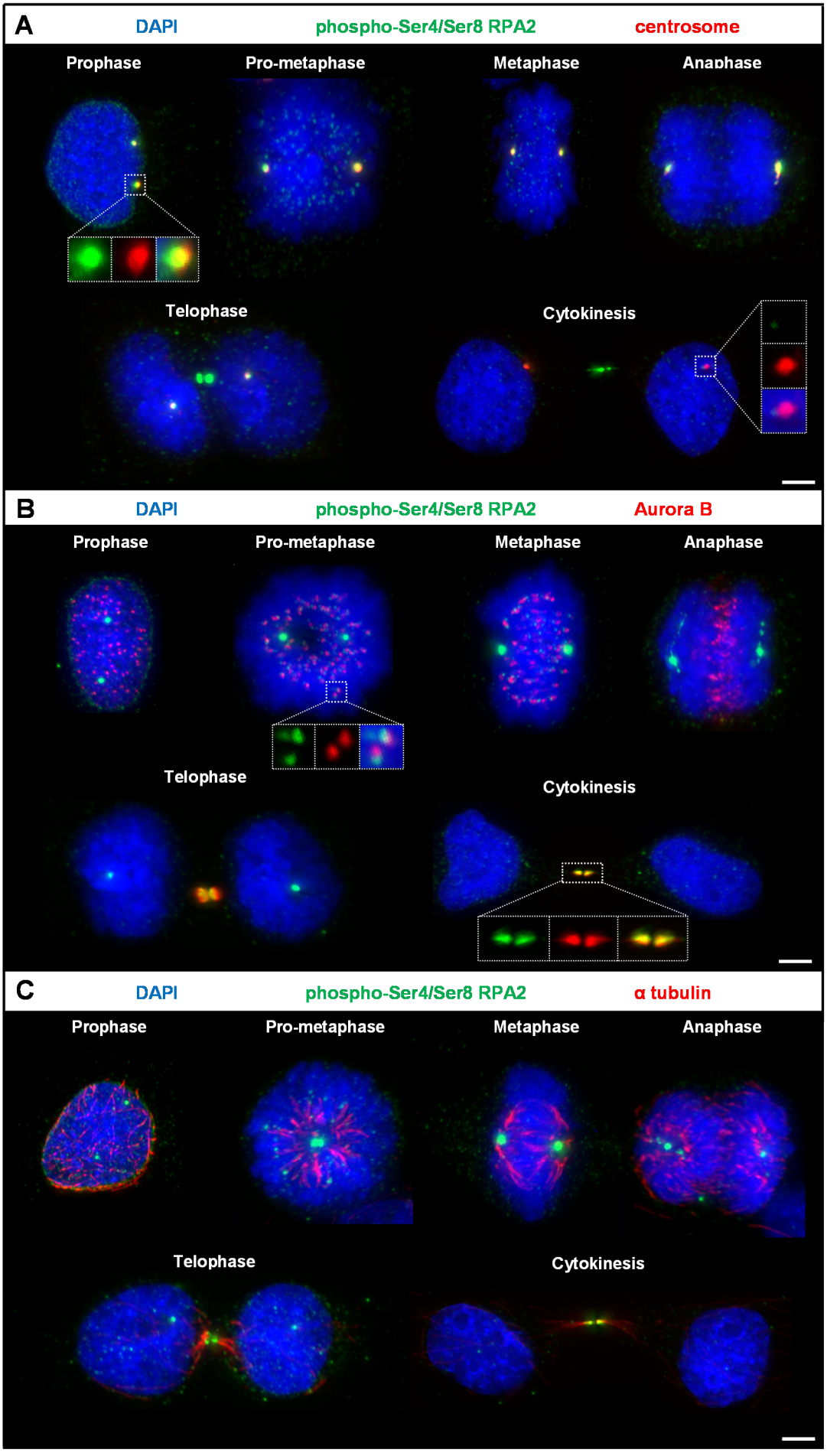
A
DAPI
phospho-Ser4/Ser8 RPA2
centrosome
Prophase
Pro-metaphase
Metaphase
Anaphase
Telophase
Cytokinesis
B
DAPI
phospho-Ser4/Ser8 RPA2
Aurora B
Prophase
Pro-metaphase
Metaphase
Anaphase
Telophase
Cytokinesis
C
DAPI
phospho-Ser4/Ser8 RPA2
α tubulin
Prophase
Pro-metaphase
Metaphase
Anaphase
Telophase
Cytokinesis

Figure 4.9 Model of phospho-Ser4/Ser8 RPA2 localisation in mitosis. Before the onset of mitosis, RPA2 is phosphorylated on Ser23 and Ser29, and is excluded from chromatin. A fraction of phospho-Ser4/Ser8 RPA2 localises to the centrosome and to the centromere region (from late G2 until anaphase), and is then detectable in the midbody (from late anaphase until cytokinesis). Cells were grown on glass coverslips, fixed and blocked as described in Materials and Methods. Dual indirect-immunofluorescence was carried out using anti-phospho-Ser4/Ser8 RPA2 antibody along with Alexa 488-coupled secondary antibody. Subsequently, cells were stained with anti-SJI centrosomal antibody (**A**), anti-Aurora B (**B**) or anti-α-tubulin (**C**) along with Alexa 594-coupled secondary antibody. DNA was counterstained with DAPI. Scale bar corresponds to 10μm.

4.3 Discussion

Maintenance of genome integrity is often supported by tight regulation of protein activity throughout the cell cycle. This is achieved either by differential protein expression, changes in protein localisation or modulation of protein activity by post-translational modifications, including phosphorylation. Replication protein A (RPA) is the major single-stranded DNA-binding protein in human cells, and plays a key role in all aspects of DNA metabolism in which ssDNA is generated (Braet et al., 2007). RPA is localised to the nucleus during interphase. However, at the onset of mitosis, RPA is excluded from the condensed chromatin (Francon et al., 2004; Stephan et al., 2009). The 34kDa RPA2 subunit is phosphorylated on Ser23 in S-phase, and is additionally phosphorylated on Ser29 by CDK-cyclin complexes when cells enter mitosis (Anantha et al., 2008; Stephan et al., 2009).

The importance of RPA2 phosphorylation on serines 23 and 29 in maintaining accurate cell division is underlined by the observation that ectopic expression of a mutated form of RPA2 in U2-OS cells, where serines 23 and 29 were both mutated to alanine and therefore could not be phosphorylated, resulted in an abnormal cell cycle distribution (Anantha et al., 2007). While it is known that CDK-dependent phosphorylation of RPA2 occurs in M-phase of a normal cell cycle, and that RPA2 undergoes dephosphorylation before the new cell enters G1-phase, the role of RPA2 phosphorylation in mitotic cells are still not fully understood (Anantha et al., 2007; Stephan et al., 2009; Zernik-Kobak et al., 1997). It is well established that RPA2 is also phosphorylated in a PIK kinase-dependent manner on serines 4 and 8 in response to a number of DNA damaging agents, including UV-irradiation (Cruet-Hennequart et al., 2006) and platinum-based chemotherapeutic drugs (see Chapter 3) (Cruet-Hennequart et al., 2008; Cruet-Hennequart et al., 2009). Phosphorylation of RPA2 on Ser4/Ser8 together with phosphorylation of a number of other sites in the N-terminus of RPA2 sites, generates a hyperphosphorylated form of the protein that is readily detected based on reduced mobility on SDS-PAGE.

Here, we report that at specific stages of mitosis, a subset of RPA2 protein is phosphorylated on serines 4 and 8, and some of this form of RPA2 localises to the centrosome, to the centromere region, and to the midbody as determined by immunofluorescence staining. Our observations have been confirmed in three different cell lines. Several lines of evidence suggest that the observed immunofluorescence staining using anti-phospho-Ser4/Ser8 RPA2 antibody is specific and reveals a cellular process that occurs during normal mitosis: (i) anti-phospho-Ser4/Ser8 RPA2 staining is epitope-specific, (ii) the RPA1 subunit of RPA can be immunoprecipitated from mitotic protein lysates using anti-phospho-Ser4/Ser8 RPA2 antibody, indicating that the novel forms of RPA2 are present in a

complex with RPA1, (iii) mitotic phospho-Ser4/Ser8 RPA2 and damage-induced hyperphosphorylated RPA2 differ in phosphorylation pattern as determined by two-dimensional gel electrophoresis.

Our observations are supported by the evidence in the literature, where RPA subunits were identified during mass-spectrometry-based proteomic analysis of centrosomal protein extracts (Andersen et al., 2003). Furthermore, previous studies using phospho-specific RPA2 antibodies indicated that RPA2 could be detected at the centrosome (Anantha and Borowiec, 2009; Stephan et al., 2009).

According to our analysis of mitotic cell lysates, phospho-Ser4/Ser8 RPA2 has been identified with multiple forms of various mobility on the SDS-PAGE, with form M1, having the most similar mobility on the gel compared to damage-induced form of RPA2. Mitotic phopho-Ser4/Ser8 RPA2 form M1 is phosphorylated in a DNA-PK-dependent manner. The observation was rather unexpected since to this point DNA-PK has been reported to be involved in DNA damage-induced phosphorylation of RPA2 on Ser4/Ser8 as opposed to modifying the protein during the normal cell cycle. However, there is increasing evidence that DNA-PK may have DNA damage- and DNA repair-independent activities, including regulation of cellular homeostasis and cell proliferation (Kong et al., 2011). Thus, it is possible that DNA-PK plays a role in phosphorylation of RPA2 during normal mitosis, especially since DNA-PK was reported to be localised to the centrosome in M-phase cells (Zhang et al., 2007). Moreover, down-regulation of DNA-PK activity was correlated with a delay in mitotic transition due to chromosome misalignment, which was associated with its role in the spindle apparatus, at both centrosomes and kinetochores (Lee et al., 2011).

The nature of the modifications of the slow mobility phosphorylated forms of RPA2 (M2-M6) in mitotic cells requires further analysis. These forms clearly represent phosphorylated forms of the protein, and a number of forms can be distinguished by 2-D electrophoresis. It is possible that the slow mobility forms detected by the anti-phospho-Ser4/Ser8 RPA2 antibody correspond to additionally modified the protein form, possibly by ubiquitination or sumoylation. While RPA2 has not been reported to be targeted for ubiquitination or SUMOylation, it is known that RPA1 can be SUMOylated (see Appendix D) (Dou et al., 2010). Further investigation of this hypothesis is required, by for example mass spectrometry-based protein modification analysis.

The role of mitotic RPA2 phosphorylation on serines 4 and 8, and the significance of the re-localisation of this form of the protein during the stages of mitosis, is still not fully clear. One possibility is that RPA2 is phosphorylated on Ser4/Ser8 in response to DNA damage in mitotic cells. It has been shown that in response DNA damage, RPA2

phosphorylation on serines 23 and 29 may facilitate further phosphorylation of RPA2 on other residues, however this event is dependent of the nature of damage (Anantha et al., 2007; Stephan et al., 2009). RPA2, extracted from the chromatin with the onset of mitosis, re-associates to the sites of damaged DNA following ionising radiation (Stephan et al., 2009) and facilitates mitotic exit (Anantha et al., 2008). These findings imply that mitotic RPA2, phosphorylated on Ser23 and Ser29, assists in mitotic damage recognition and repair. Thus, the observed phosphorylation of RPA2 on serines 4 and 8 in mitosis could serve a similar purpose at specific locations of the mitotic cell. Interestingly, a recent report shows that, during mitosis, homologous recombination protein Rad51 translocates from the centrosome to the midbody, in a manner analogous to that reported here for phospho-Ser4/Ser8 RPA2. It is suggested that Rad51, together with other HR proteins, plays a role in maintaining centrosome integrity (Cappelli et al., 2011). In response to DNA damage in mitotic cells, Rad51 translocation may indicate unrepaired damage and contribute to centrosome disruption and mitotic catastrophe (Cappelli et al., 2011). It is known that RPA interacts with Rad51 and plays an important role in HR (Golub et al., 1998). Phosphorylation of RPA on serines 4 and 8 occurs prior to Rad51 loading on to resected DNA ends, and this modification of RPA2 is therefore required for successful HR (Deng et al., 2009; Feng and Zhang, 2011; Shi et al., 2010). Thus, phospho-Ser4/Ser8 RPA2 might, by analogy with other centrosome-associated HR proteins, serve as a cellular reserve of repair proteins that can be activated in response to mitotic DNA damage. The observation that DNA is present in the midbody provides further support for the proposal that RPA and other proteins involved in maintaining DNA integrity are localised at this structure in dividing cells.

Consistent with this, it has been suggested that RPA modulates mitotic transit by silencing the spindle assembly checkpoint (SAC) (Anantha and Borowiec, 2009; Anantha et al., 2008). Anantha et. al. further propose that this could occur in a centrosome-dependent or a polo-like kinase 1 (Plk-1)-dependent manner. Plk-1 is a serine/threonine kinase that is involved in regulation of cell division, and localises to various sites throughout M-phase (Petronczki et al., 2008), including to the kinetochore, where it plays a role in silencing the spindle assembly checkpoint (SAC) (Liu et al., 2012a). Kinetochores are protein structures located within centromeres to which the spindle microtubules attach before chromosomes are segregated (Kline-Smith and Walczak, 2004). There is no previous report that RPA2 localises to the centromere region. However, recently DNA double strand breaks (DSBs) were reported to occur at the centromere (Guerrero et al., 2010). Under certain conditions, including defects in spindle function, mitotic chromosomes can be exposed to excessive forces that can lead to DNA rupture at this specific location of the chromosome. It has been proposed that a single incident of spindle-induced centromere shearing may underline a

variety of genetic defects that are found in human cancers (Guerrero et al., 2010). Given that RPA plays a role in DNA damage recognition, and phosphorylation RPA2 on serines 4 and 8 occurs during repair of damage-induced DSBs (Feng and Zhang, 2011; Serrano et al., 2012; Shi et al., 2010) one possibility is that that the observed localisation of phospho-Ser4/Ser8 RPA2 to the centromeric region plays a role in recognition, signalling and repair of DNA damage occurring at the centromere. However, direct evidence for this role is required, and it can not be ruled out that RPA is involved in other processes, or is sequestered at the centromere by interactions with other protein partners.

Clearly, based on the specificity of phosphorylation at particular residues, and the re-localisation of phosphorylated RPA2 in the mitotic cell, the RPA2 phosphorylation cycle is closely integrated with the cell cycle in dividing cells. Here, for the first time, we report that a subset of the RPA2 protein pool is phosphorylated on serines 4 and 8 during normal mitosis. While further investigation regarding (i) the DNA damage-dependence, (ii) the functional role of RPA2 phosphorylation in mitosis and (iii) the regulation of phosphorylation and dephosphorylation is required, our data provide novel insights into the relationship between phosphorylation and localisation of RPA during the mitotic phase of human cell division.

4.4 References

Adachi, Y., and U.K. Laemmli. 1994. Study of the cell cycle-dependent assembly of the DNA pre-replication centres in Xenopus egg extracts. *EMBO J*. 13:4153-64.

Anantha, R.W., and J.A. Borowiec. 2009. Mitotic crisis: the unmasking of a novel role for RPA. *Cell Cycle*. 8:357-61.

Anantha, R.W., E. Sokolova, and J.A. Borowiec. 2008. RPA phosphorylation facilitates mitotic exit in response to mitotic DNA damage. *Proc Natl Acad Sci U S A*. 105:12903-8.

Anantha, R.W., V.M. Vassin, and J.A. Borowiec. 2007. Sequential and synergistic modification of human RPA stimulates chromosomal DNA repair. *J Biol Chem*. 282:35910-23.

Andersen, J.S., C.J. Wilkinson, T. Mayor, P. Mortensen, E.A. Nigg, and M. Mann. 2003. Proteomic characterization of the human centrosome by protein correlation profiling. *Nature*. 426:570-574.

Bakkenist, C.J., and M.B. Kastan. 2004. Initiating cellular stress responses. *Cell*. 118:9-17.

Binz, S.K., Y. Lao, D.F. Lowry, and M.S. Wold. 2003. The phosphorylation domain of the 32-kDa subunit of replication protein A (RPA) modulates RPA-DNA interactions. Evidence for an intersubunit interaction. *J Biol Chem*. 278:35584-91.

Block, W.D., Y. Yu, and S.P. Lees-Miller. 2004. Phosphatidyl inositol 3-kinase-like serine/threonine protein kinases (PIKKs) are required for DNA damage-induced phosphorylation of the 32 kDa subunit of replication protein A at threonine 21. *Nucleic Acids Res*. 32:997-1005.

Braet, C., H. Stephan, I.M. Dobbie, D.M. Togashi, A.G. Ryder, Z. Foldes-Papp, N. Lowndes, and H.P. Nasheuer. 2007. Mobility and distribution of replication protein A in living cells using fluorescence correlation spectroscopy. *Exp Mol Pathol*. 82:156-62.

Cappelli, E., S. Townsend, C. Griffin, and J. Thacker. 2011. Homologous recombination proteins are associated with centrosomes and are required for mitotic stability. *Exp Cell Res*. 317:1203-13.

Carmena, M., and W.C. Earnshaw. 2003. The cellular geography of Aurora kinases. *Nat Rev Mol Cell Biol*. 4:842-854.

Carty, M.P., M. Zernik-Kobak, S. McGrath, and K. Dixon. 1994. UV light-induced DNA synthesis arrest in HeLa cells is associated with changes in phosphorylation of human single-stranded DNA-binding protein. *EMBO J*. 13:2114-23.

Cruet-Hennequart, S., S. Coyne, M.T. Glynn, G.G. Oakley, and M.P. Carty. 2006. UV-induced RPA phosphorylation is increased in the absence of DNA polymerase eta and requires DNA-PK. *DNA Repair (Amst)*. 5:491-504.

Cruet-Hennequart, S., M.T. Glynn, L.S. Murillo, S. Coyne, and M.P. Carty. 2008. Enhanced DNA-PK-mediated RPA2 hyperphosphorylation in DNA polymerase eta-deficient human cells treated with cisplatin and oxaliplatin. *DNA Repair (Amst)*. 7:582-96.

Cruet-Hennequart, S., S. Villalan, A. Kaczmarczyk, E. O'Meara, A.M. Sokol, and M.P. Carty. 2009. Characterization of the effects of cisplatin and carboplatin on cell cycle progression and DNA damage response activation in DNA polymerase eta-deficient human cells. *Cell Cycle*. 8:3039-50.

Deng, X., A. Prakash, K. Dhar, G.S. Baia, C. Kolar, G.G. Oakley, and G.E. Borgstahl. 2009. Human replication protein A-Rad52-single-stranded DNA complex: stoichiometry and evidence for strand transfer regulation by phosphorylation. *Biochemistry*. 48:6633-43.

Din, S., S.J. Brill, M.P. Fairman, and B. Stillman. 1990. Cell-cycle-regulated phosphorylation of DNA replication factor A from human and yeast cells. *Genes Dev*. 4:968-77.

Dou, H., C. Huang, M. Singh, P.B. Carpenter, and E.T. Yeh. 2010. Regulation of DNA repair through deSUMOylation and SUMOylation of replication protein A complex. *Mol Cell*. 39:333-45.

Dutta, A., and B. Stillman. 1992. cdc2 family kinases phosphorylate a human cell DNA replication factor, RPA, and activate DNA replication. *EMBO J*. 11:2189-99.

Erdile, L.F., M.S. Wold, and T.J. Kelly. 1990. The primary structure of the 32-kDa subunit of human replication protein A. *J Biol Chem*. 265:3177-82.

Fang, F., and J.W. Newport. 1993. Distinct roles of cdk2 and cdc2 in RP-A phosphorylation during the cell cycle. *J Cell Sci*. 106 (Pt 3):983-94.

Fededa, J.P., and D.W. Gerlich. 2012. Molecular control of animal cell cytokinesis. *Nat Cell Biol*. 14:440-7.

Feng, Z., and J. Zhang. 2011. A dual role of BRCA1 in two distinct homologous recombination mediated repair in response to replication arrest. *Nucleic Acids Res*. 40:726-38.

Fotedar, R., and J.M. Roberts. 1992. Cell cycle regulated phosphorylation of RPA-32 occurs within the replication initiation complex. *EMBO J*. 11:2177-87.

Francon, P., J.M. Lemaitre, C. Dreyer, D. Maiorano, O. Cuvier, and M. Mechali. 2004. A hypophosphorylated form of RPA34 is a specific component of pre-replication centers. *J Cell Sci*. 117:4909-20.

Golub, E.I., R.C. Gupta, T. Haaf, M.S. Wold, and C.M. Radding. 1998. Interaction of human rad51 recombination protein with single-stranded DNA binding protein, RPA. *Nucleic Acids Res*. 26:5388-93.

Guerrero, A.A., M.C. Gamero, V. Trachana, A. Futterer, C. Pacios-Bras, N.P. Diaz-Concha, J.C. Cigudosa, A.C. Martinez, and K.H. van Wely. 2010. Centromere-localized breaks indicate the generation of DNA damage by the mitotic spindle. *Proc Natl Acad Sci U S A*. 107:4159-64.

Guo, S., Y. Zhang, F. Yuan, Y. Gao, L. Gu, I. Wong, and G.M. Li. 2006. Regulation of replication protein A functions in DNA mismatch repair by phosphorylation. *J Biol Chem*. 281:21607-16.

Hannoun, Z., S. Greenhough, E. Jaffray, R.T. Hay, and D.C. Hay. 2010. Post-translational modification by SUMO. *Toxicology*. 278:288-93.

Henricksen, L.A., and M.S. Wold. 1994. Replication protein A mutants lacking phosphorylation sites for p34cdc2 kinase support DNA replication. *J Biol Chem*. 269:24203-8.

Hicke, L. 2001. Protein regulation by monoubiquitin. *Nat Rev Mol Cell Biol*. 2:195-201.

Jordan, M.A., D. Thrower, and L. Wilson. 1992. Effects of vinblastine, podophyllotoxin and nocodazole on mitotic spindles. Implications for the role of microtubule dynamics in mitosis. *J Cell Sci*. 102 (Pt 3):401-16.

Kellogg, D.R., M. Moritz, and B.M. Alberts. 1994. The centrosome and cellular organization. *Annu Rev Biochem*. 63:639-74.

Kemp, B.E., and R.B. Pearson. 1990. Protein kinase recognition sequence motifs. *Trends Biochem Sci*. 15:342-6.

Kim, S.T., D.S. Lim, C.E. Canman, and M.B. Kastan. 1999. Substrate specificities and identification of putative substrates of ATM kinase family members. *J Biol Chem*. 274:37538-43.

Kline-Smith, S.L., and C.E. Walczak. 2004. Mitotic spindle assembly and chromosome segregation: refocusing on microtubule dynamics. *Mol Cell*. 15:317-27.

Kong, X., Y. Shen, N. Jiang, X. Fei, and J. Mi. 2011. Emerging roles of DNA-PK besides DNA repair. *Cell Signal*. 23:1273-80.

Kuo, T.-C., C.-T. Chen, D. Baron, T.T. Onder, S. Loewer, S. Almeida, C.M. Weismann, P. Xu, J.-M. Houghton, F.-B. Gao, G.Q. Daley, and S. Doxsey. 2011. Midbody accumulation through evasion of autophagy contributes to cellular reprogramming and tumorigenicity. *Nat Cell Biol*. advance online publication.

Leahy, J.J., B.T. Golding, R.J. Griffin, I.R. Hardcastle, C. Richardson, L. Rigoreau, and G.C. Smith. 2004. Identification of a highly potent and selective DNA-dependent protein kinase (DNA-PK) inhibitor (NU7441) by screening of chromenone libraries. *Bioorg Med Chem Lett*. 14:6083-7.

Lee, K.J., Y.F. Lin, H.Y. Chou, H. Yajima, K.R. Fattah, S.C. Lee, and B.P. Chen. 2011. Involvement of DNA-dependent protein kinase in normal cell cycle progression through mitosis. *J Biol Chem*. 286:12796-802.

Liaw, H., D. Lee, and K. Myung. 2011. DNA-PK-Dependent RPA2 Hyperphosphorylation Facilitates DNA Repair and Suppresses Sister Chromatid Exchange. *PLoS ONE*. 6:e21424.

Liu, D., O. Davydenko, and M.A. Lampson. 2012a. Polo-like kinase-1 regulates kinetochore-microtubule dynamics and spindle checkpoint silencing. *J Cell Biol*. 198:491-9.

Liu, S., S.O. Opiyo, K. Manthey, J.G. Glanzer, A.K. Ashley, C. Amerin, K. Troksa, M. Shrivastav, J.A. Nickoloff, and G.G. Oakley. 2012b. Distinct roles for DNA-PK, ATM and ATR in RPA phosphorylation and checkpoint activation in response to replication stress. *Nucleic Acids Res*.

Manthey, K.C., S. Opiyo, J.G. Glanzer, D. Dimitrova, J. Elliott, and G.G. Oakley. 2007. NBS1 mediates ATR-dependent RPA hyperphosphorylation following replication-fork stall and collapse. *J Cell Sci*. 120:4221-9.

Mardin, B.R., and E. Schiebel. 2012. Breaking the ties that bind: new advances in centrosome biology. *J Cell Biol*. 197:11-8.

Niu, H., H. Erdjument-Bromage, Z.Q. Pan, S.H. Lee, P. Tempst, and J. Hurwitz. 1997. Mapping of amino acid residues in the p34 subunit of human single-stranded DNA-binding protein phosphorylated by DNA-dependent protein kinase and Cdc2 kinase in vitro. *J Biol Chem*. 272:12634-41.

Norbury, C., and P. Nurse. 1992. Animal cell cycles and their control. *Annu Rev Biochem*. 61:441-70.

Nuss, J.E., S.M. Patrick, G.G. Oakley, G.M. Alter, J.G. Robison, K. Dixon, and J.J. Turchi. 2005. DNA damage induced hyperphosphorylation of replication protein A. 1. Identification of novel sites of phosphorylation in response to DNA damage. *Biochemistry*. 44:8428-37.

Oakley, G.G., L.I. Loberg, J. Yao, M.A. Risinger, R.L. Yunker, M. Zernik-Kobak, K.K. Khanna, M.F. Lavin, M.P. Carty, and K. Dixon. 2001. UV-induced hyperphosphorylation of replication protein a depends on DNA replication and expression of ATM protein. *Mol Biol Cell*. 12:1199-213.

Oakley, G.G., S.M. Patrick, J. Yao, M.P. Carty, J.J. Turchi, and K. Dixon. 2003. RPA phosphorylation in mitosis alters DNA binding and protein-protein interactions. *Biochemistry*. 42:3255-64.

Olson, E., C.J. Nievera, V. Klimovich, E. Fanning, and X. Wu. 2006. RPA2 is a direct downstream target for ATR to regulate the S-phase checkpoint. *J Biol Chem*. 281:39517-33.

Patrick, S.M., and J.J. Turchi. 1998. Human replication protein A preferentially binds cisplatin-damaged duplex DNA in vitro. *Biochemistry*. 37:8808-15.

Petronczki, M., P. Lenart, and J.M. Peters. 2008. Polo on the Rise-from Mitotic Entry to Cytokinesis with Plk1. *Dev Cell*. 14:646-59.

Pohl, C., and S. Jentsch. 2009. Midbody ring disposal by autophagy is a post-abscission event of cytokinesis. *Nat Cell Biol*. 11:65-70.

Sandoval, J.A., J.L. Grosfeld, R.J. Hickey, and L.H. Malkas. 2006. Structural analysis of the human neuroblastoma DNA replication complex: insights into faulty proliferation. *J Pediatr Surg*. 41:266-70.

Serrano, M.A., Z. Li, M. Dangeti, P.R. Musich, S. Patrick, M. Roginskaya, B. Cartwright, and Y. Zou. 2012. DNA-PK, ATM and ATR collaboratively regulate p53-RPA interaction to facilitate homologous recombination DNA repair. *Oncogene*.

Shao, R.G., C.X. Cao, H. Zhang, K.W. Kohn, M.S. Wold, and Y. Pommier. 1999. Replication-mediated DNA damage by camptothecin induces phosphorylation of RPA by DNA-dependent protein kinase and dissociates RPA:DNA-PK complexes. *EMBO J*. 18:1397-406.

Shi, W., Z. Feng, J. Zhang, I. Gonzalez-Suarez, R.P. Vanderwaal, X. Wu, S.N. Powell, J.L. Roti Roti, and S. Gonzalo. 2010. The role of RPA2 phosphorylation in homologous recombination in response to replication arrest. *Carcinogenesis*. 31:994-1002.

Skop, A.R., H. Liu, J. Yates, B.J. Meyer, and R. Heald. 2004. Dissection of the Mammalian Midbody Proteome Reveals Conserved Cytokinesis Mechanisms. *Science*. 305:61-66.

Steigemann, P., and D.W. Gerlich. 2009. Cytokinetic abscission: cellular dynamics at the midbody. *Trends in Cell Biology*. 19:606-616.

Stephan, H., C. Concannon, E. Kremmer, M.P. Carty, and H.P. Nasheuer. 2009. Ionizing radiation-dependent and independent phosphorylation of the 32-kDa subunit of replication protein A during mitosis. *Nucleic Acids Res*. 37:6028-41.

Vermeulen, K., D.R. Van Bockstaele, and Z.N. Berneman. 2003. The cell cycle: a review of regulation, deregulation and therapeutic targets in cancer. *Cell Prolif*. 36:131-49.

Volpe, J.P.G., and J.E. Cleaver. 1995. Xeroderma pigmentosum variant cells are resistant to immortalization. *Mutation Research/DNA Repair*. 337:111-117.

Zernik-Kobak, M., K. Vasunia, M. Connelly, C.W. Anderson, and K. Dixon. 1997. Sites of UV-induced phosphorylation of the p34 subunit of replication protein A from HeLa cells. *J Biol Chem*. 272:23896-904.

Zhang, S., P. Hemmerich, and F. Grosse. 2007. Centrosomal localization of DNA damage checkpoint proteins. *J Cell Biochem*. 101:451-65.

4.5 Supplementary materials

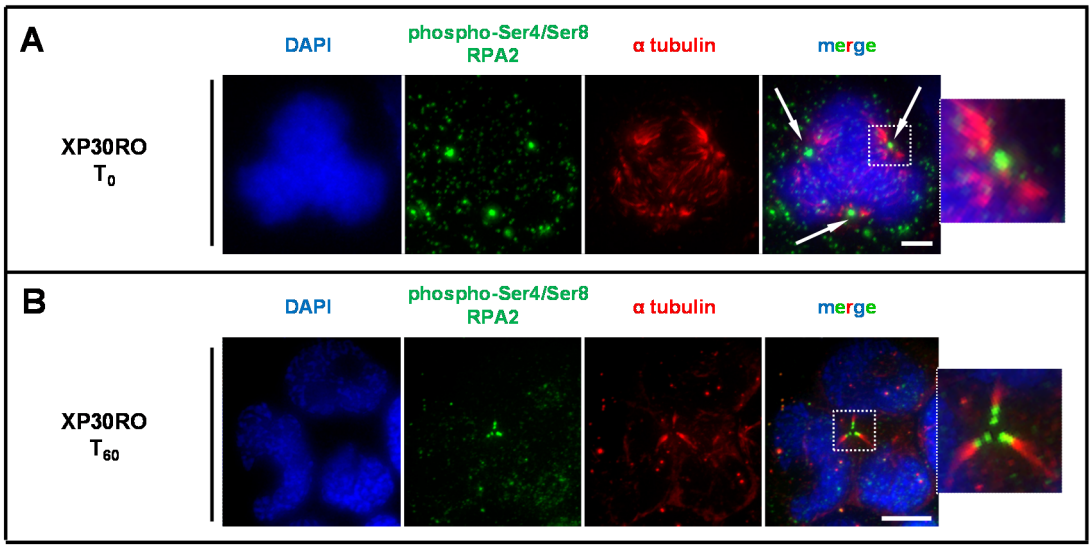

Supplementary Figure 4.1 Phospho-Ser4/Ser8 RPA2 localisation during abnormal mitosis. XP30RO cells were plated 24 hours before being treated with 0.1μM nocodazole. 16 hours later, mitotic cells were collected and released from nocodazole arrest. Immunofluorescence images show representative mitotic cells (**A**, scale bar corresponds to 10μM) and cell undergoing cytokinesis (**B**, scale bar corresponds to 10μM), from samples collected 0 and 60 minutes post-mitotic release. Samples were stained for phospho-Ser4/Ser8 RPA2 and α-tubulin, and detected using Alexa 488- and Alexa 594-coupled secondary antibodies, respectively. DNA was counterstaind with DAPI. Arrows indicate the location of the centrosome. The right panels show increased magnification of the centrosome (upper panel) and the midbody (lower panel).

Chapter 5: Conclusions and future directions

Sokol A.M.[1]

[1] DNA Damage Response Laboratory, Centre for Chromosome Biology, Biochemistry, School of Natural Sciences, National University of Ireland, Galway, Ireland

5.1 Conclusions

Cancer cells can develop resistance towards platinum-based chemotherapeutic drugs. Therefore, in order to enhance therapy success, it is important to understand the molecular mechanisms that determine the outcome of exposure to these agents. Targeting key cellular pathways involved in processing platinum-induced DNA damage may represent one way to potentiate the effects of cisplatin and related drugs (Ceppi et al., 2009; Teng et al., 2010; Ummat et al., 2012; Zhao et al., 2012). It has been proposed that polη contributes to cancer cell resistance to treatment by bypassing platinum-DNA lesions during replication, in a process called translesion synthesis (TLS) (Chaney et al., 2005; Masutani et al., 2000; Vaisman et al., 2000). In the present study, the role of polη in the replication of genomic DNA following cisplatin and carboplatin treatment was directly investigated, using XP30RO cells which do not express polη and a derivative cell line which expresses polη from a *POLH* transgene. It was found that upon treatment with equitoxic doses of cisplatin and carboplatin, the length of individual, nascent DNA strands is reduced in the absence of polη. This provides the first *in vivo* evidence that polη is involved in DNA synthesis on platinum-damaged DNA. Characterisation of the DNA damage response under these conditions provided direct evidence that phosphorylation on Ser4/Ser8 of the RPA2 subunit of the single-stranded DNA binding protein RPA is strongly dependent on severe DNA replication inhibition. These results therefore shed significant new light on the mechanisms which govern the cellular response to DNA damage by platinum-based chemotherapeutic drugs.

Furthermore, a DNA damage-independent form of phospho-Ser4/Ser8 RPA2 has been identified in mitotic cells for the first time at the centrosome, at the centromere region and at the midbody. This, together with previous findings (Anantha et al., 2008; Anantha et al., 2007; Stephan et al., 2009), supports a new role for RPA outside of S-phase. While it is known that RPA2 is phosphorylated on Ser29 at mitotic entry by the CDK1-cyclinB complex (Fang and Newport, 1993; Oakley et al., 2003a; Stephan et al., 2009), the process of RPA2 dephosphorylation during mitotic exit remains less well understood. Based on our observations, it can be speculated that in mitosis, the described locations (centrosome, centromere, midbody) serve as a channel for robust RPA2 dephosphorylation. It is also possible that phospho-Ser4/Ser8 RPA2 is sequestered with other protein partners at these locations in mitotic cells. Another possibility is that this subset of RPA2 is phosphorylated to release a protein partner from interaction with RPA, analogous to the recent report that phosphorylation of RPA2 releases p53 from interaction with RPA (Serrano et al., 2012). Furthermore, RPA may be associated with residual DNA at these described locations, and may play a role in ensuring that all DNA is correctly segregated. This is supported by the

observation that DNA can be detected in the midbody using DAPI staining (Figure 4.5A), and the report that Rad51 can also be found in the midbody (Cappelli et al., 2011).

Collectively, this research provides valuable insights into key cellular pathways which could be targeted in the future to potentiate the efficacy of platinum-based chemotherapeutic agents in cancer therapy. Additionally, novel cellular processes were identified that help unmask RPA function during the cell cycle.

5.2 Future directions

The present research identifies an important role for polη-mediated TLS and phosphorylation of RPA2 on Ser4/Ser8 in the cellular response to treatment with cisplatin and carboplatin. An exciting prospect stemming from these observations is that in the future, targeting these DNA damage response pathways in combination with platinum-based anticancer drugs could potentiate the therapeutic effect and specificity of these agents towards cancer cells.

Development of inhibitors of key proteins can be informed by biochemical studies. Recent structural studies, where polη was co-crystallised with cisplatin-damaged DNA templates, revealed a unique hydrophobic pocket between the minor groove of the platinum-damaged DNA and Trp297 of polη that can be targeted for inhibition (Zhao et al., 2012). This data, together with our observations that polη is directly involved in nascent DNA strand synthesis following treatment with cisplatin and carboplatin, provides an argument for the design of a specific inhibitor of polη-mediated translesion synthesis at sites of platinum-induced DNA damage. By knowing the precise inhibitory target a pharmacophore can be designed either by rational computational methods or by a screening process. Upon synthesis of candidate compounds their activity in bypass of genotoxic lesions on the DNA can be assayed cell-free extracts (Nikolaishvili-Feinberg and Cordeiro-Stone, 2012). In order to further characterise the potential therapeutic effect of such a polη inhibitor, the cytotoxicity of platinum-based drugs in the presence or absence of this inhibitor can be tested in cancer cell lines. The DNA combing assay described here could provide a method to investigate the effects of such compounds on DNA synthesis *in vivo*. Identification of useful inhibitors could in the future potentiate anti-cancer therapy using platinum-based drugs.

Over 90% of DNA lesions caused by cisplatin and carboplatin are 1,2-d(GpG)-intrastrand crosslinks while less than 1% are the more toxic ICLs (Eastman, 1987; Kelland, 2007). The DNA combing approach was used to measure the length of individual, nascent DNA fibres synthesised following treatment with cisplatin and carboplatin, and it was found that polη is directly involved in TLS on platinum-damaged DNA. However, there is evidence that polη also participates in DNA synthesis during repair of ICL lesions (Ho et al., 2011; Ho and Schärer, 2010; Zheng et al., 2003). In order to provide further evidence for this hypothesis, DNA combing can be used together with the model cell lines described in the present study, either lacking (XP30RO) or expressing polη (TR30-2), to measure the polη dependence of DNA synthesis upon treatment with ICL-inducing drugs, for instance mitomycin C (MMC) (Verweij and Pinedo, 1990).

Since there is evidence that polζ plays a role together with polη in the bypass of cisplatin-induced lesions, most likely by extending DNA strands after polη-mediated lesion bypass, it is important to further characterise the nature of this process (Shachar et al., 2009; Sharma et al., 2012; Ummat et al., 2012). It is also of interest to determine whether other TLS polymerases, including pol κ and polι, can play a role in the bypass of platinum-DNA adducts, and thus interfere with therapy success. To address this hypothesis, TLS polymerases can be down-regulated using the approach of short interfering RNA (siRNA) in cancer cell lines treated with platinum-based chemotherapeutic agents, and nascent DNA strand length can be measured under these conditions.

Based on the present observations, polη is a determinant of the response of cells to platinum-based drugs (Chapter 3). In cells lacking polη, DNA replication forks stall at sites of platinum-induced damage in the template. This can eventually lead to fork collapse generating DNA double strand ends (DSEs). DSEs can be further processed by homologous recombination (HR), which operates in the S- and G2/M-phases (San Filippo et al., 2008). While the role of HR in polη-deficient cells was not further investigated in the present study it can be speculated that survival of polη-deficient cells following treatment with platinum-based drugs depends on HR activity. To address this hypothesis, a siRNA-based approach could be used to knock-down proteins essential for HR (for example Rad51) in polη-deficient cells (Tsai et al., 2010). Determining cytotoxicity in control and siRNA treated cells following exposure to platinum-based chemotherapeutic using XTT-based assays or clonogenic survival assays, would provide information on the dependence of polη-deficient cells on functional HR for survival.

The present study directly correlates RPA2 phosphorylation on Ser4/Ser8 with the response to severe replication arrest in polη-deficient cells exposed to cisplatin and carboplatin. Further analysis of the role of RPA2 phosphorylation on Ser4/Ser8 in regulating RPA function is required. There is evidence that phosphorylation of RPA2 decreases the affinity of trimeric RPA for ssDNA, as well the interaction of RPA with certain protein partners, including DNA polymerase α (Oakley et al., 2003a; Oakley et al., 2003b; Patrick et al., 2005). It is hypothesised that phosphorylation may alter the ability of RPA to form complexes with key partner proteins. As RPA plays a role in almost all processes in which single-stranded DNA is generated, this can influence the cellular response to DNA damage by regulating the activation of different DNA damage signalling or repair pathways. The consequences of RPA2 phosphorylation on Ser4/Ser8 on protein-protein interactions can be studied directly, by determining the effect of mutating these residues to alanine on the interaction of RPA with protein partners *in vivo*. For that purpose, the series of constructs described here, in which serine 4 and serine 8 were mutated to

alanine, could be very useful (Appendix A). Polη-deficient cells can be transfected with vectors expressing wild-type or mutant RPA2, in which the serines of interest are mutated to alanine, and therefore can not undergo phosphorylation. To investigate the effects of mutating these phopshrylation sites, expression of endogenous RPA2 must be silenced using a short interfering RNA (siRNA) targeting the 3′-untranslated region of RPA2 (Liaw et al., 2011; Vassin et al., 2004). The conditions that strongly induce replication stress-dependent RPA2 phosphorylation on Ser4/Ser8 are now well established, and include treatment with UV-C or cisplatin. Immunoprecipitation experiments using FLAG-tagged RPA2 and a specific anti-FLAG-tag antibody can be conducted in order to isolate protein complexes formed by RPA containing the ectopically-expressed RPA2 variants. The samples obtained could be analysed by SDS-PAGE and silver staining to identify proteins that are specifically co-immunoprecipitated with along either wild-type or phosphorylation site-mutant RPA2. Upon in-gel digestion, proteins can be further analysed by mass spectrometry in order to identify protein partners that interact in a phosphorylation-dependent manner with RPA (Denis et al., 2007). Alternatively, the novel approach of stable isotope labelling with amino acids in cell culture (SILAC) could be used to identify proteins that specifically interact with wild-type or Ser4/Ser8-mutated RPA2 (Ong et al., 2003; Pimienta et al., 2009).

Since RPA2 is strongly phosphorylated on Ser4/Ser8 in polη-deficient cells exposed to platinum-based chemotherapeutic drugs, it may be of interest to determine whether inhibition of RPA, by preventing DNA damage signalling through RPA phosphorylation, would enhance the outcome of platinum-based chemotherapy (Neher et al., 2011; Shuck and Turchi, 2010). The existing RPA inhibitors target the RPA1 subunit responsible for ssDNA binding. This approach is non-specific and carries a potential risk as this essential function of RPA is required during DNA synthesis in all cells, not only in cancer cells. Understanding the role of specific phosphorylation sites on RPA2 could lead to be development of more targeted inhibitors that impact specific functions of the RPA protein, for example in the processing of platinum-induced DNA damage.

Moreover, the observation that in a situation where platinum exposure leads to severe inhibition of DNA replication, RPA2 undergoes hyperphosphorylation on Ser4/Ser8, can potentially be used in the future as a marker for the efficacy of therapy in cancer patients treated with platinum-based drugs (Manthey et al., 2010).

5.2.1 A new role for RPA in mitosis?

Our findings, described in Chapter 4, imply a novel role for phosphorylation of RPA2 on Ser4/Ser8 in mitosis. The evidence indicates that in different stages of mitosis, phospho-Ser4/Ser8 RPA2 localises to the centrosome, near the centromeres and to the midbody. While this is a novel observation, more evidence is needed to uncover both the role of RPA2 phosphorylation, and the molecular mechanisms that regulate RPA2 phosphorylation and localisation during mitosis. One approach to address this question is to perform live cell imaging using GFP-tagged RPA2 constructs. This would involve transfection of cells with the GFP-RPA2 constructs described in Appendix A, while down-regulating RPA2 expression using siRNA (Liaw et al., 2011; Vassin et al., 2004). In parallel, similar experiments could be performed where cells are transfected with a plasmid expressing an RPA2-GFP phosphorylation mutant, where serines 4 and 8 have been mutated to alanine. Live-cell imaging can be used to elucidate whether RPA2 phosphorylation is essential for normal mitosis. By measuring the duration of cytokinesis using live-cell imaging, it is possible to determine if the expression of RPA2 phosphorylation mutants impairs mitotic exit. In addition, upon treatment with DNA damaging agents it could be determined if RPA2 phosphorylation on Ser4/Ser8 during mitosis is essential for DNA damage response activation and mitotic exit (Anantha et al., 2008).

The primary function of RPA is to bind ssDNA. Another question that remains to be answered is whether the presence of phospho-RPA2 in the centrosome, near the centromere and in the midbody correlates with the presence of DNA in these locations during mitosis. A more specific method for detection of single DNA molecules is required in order to address this question, as DAPI staining is not sufficient. More specific approach to detect single DNA molecule can be applied, including immunofluorescence-based detection of ultrafine bridges (Chan and Hickson, 2011) or electron microscopy (Efcavitch and Thompson, 2010).

In the present study, western blot analysis of protein extracts from mitotic cells using the anti-phospho-Ser4/Ser8 antibody, led to identification of several RPA2 forms (M1-M6), some of which had significantly altered mobility following SDS-PAGE, as well as upon two-dimensional gel electrophoresis, when compared to the hyperphosphorylated form of RPA2. Further biochemical analysis is needed in order to characterise these additional forms of RPA2. It has been shown using λ-phosphatase treatment that these forms correspond to phosphorylated proteins. However, phosphorylation alone can not account for the mobility shift following SDS-PAGE. It is possible that these bands correspond to phosphorylated and ubiquitinated or sumoylated RPA2. In order to test whether this is the case, immunoprecipitation of mitotic RPA2 using phospho-Ser4/Ser8 antibody could be

performed followed by western blot analysis using anti-ubiquitin and anti-SUMO antibodies. Subsequently, immunoprecipitated extracts could be run on SDS-PAGE gel and upon silver staining of the gel the bands of interest could be excised from the gel for analysis of the post-translational modifications by mass-spectrometry (Denis et al., 2007).

Overall, the present research opens up new avenues into key cellular pathways that (i) modulate the outcome of exposure of human cells to DNA damage by platinum-based anticancer drugs (Chapter 3) and (ii) regulate RPA function throughout the cell cycle (Chapter 4).

5.3 References

Anantha, R.W., E. Sokolova, and J.A. Borowiec. 2008. RPA phosphorylation facilitates mitotic exit in response to mitotic DNA damage. *Proc Natl Acad Sci U S A*. 105:12903-8.

Anantha, R.W., V.M. Vassin, and J.A. Borowiec. 2007. Sequential and synergistic modification of human RPA stimulates chromosomal DNA repair. *J Biol Chem*. 282:35910-23.

Cappelli, E., S. Townsend, C. Griffin, and J. Thacker. 2011. Homologous recombination proteins are associated with centrosomes and are required for mitotic stability. *Exp Cell Res*. 317:1203-13.

Ceppi, P., S. Novello, A. Cambieri, M. Longo, V. Monica, M. Lo Iacono, M. Giaj-Levra, S. Saviozzi, M. Volante, M. Papotti, and G. Scagliotti. 2009. Polymerase eta mRNA expression predicts survival of non-small cell lung cancer patients treated with platinum-based chemotherapy. *Clin Cancer Res*. 15:1039-45.

Chan, K.L., and I.D. Hickson. 2011. New insights into the formation and resolution of ultra-fine anaphase bridges. *Semin Cell Dev Biol*. 22:906-12.

Chaney, S.G., S.L. Campbell, E. Bassett, and Y. Wu. 2005. Recognition and processing of cisplatin- and oxaliplatin-DNA adducts. *Critical reviews in oncology/hematology*. 53:3-11.

Denis, N.J., J. Vasilescu, J.P. Lambert, J.C. Smith, and D. Figeys. 2007. Tryptic digestion of ubiquitin standards reveals an improved strategy for identifying ubiquitinated proteins by mass spectrometry. *Proteomics*. 7:868-74.

Eastman, A. 1987. The formation, isolation and characterization of DNA adducts produced by anticancer platinum complexes. *Pharmacol Ther*. 34:155-66.

Efcavitch, J.W., and J.F. Thompson. 2010. Single-molecule DNA analysis. *Annu Rev Anal Chem (Palo Alto Calif)*. 3:109-28.

Fang, F., and J.W. Newport. 1993. Distinct roles of cdk2 and cdc2 in RP-A phosphorylation during the cell cycle. *J Cell Sci*. 106 (Pt 3):983-94.

Ho, T.V., A. Guainazzi, S.B. Derkunt, M. Enoiu, and O.D. Scharer. 2011. Structure-dependent bypass of DNA interstrand crosslinks by translesion synthesis polymerases. *Nucleic Acids Res*. 39:7455-64.

Ho, T.V., and O.D. Schärer. 2010. Translesion DNA synthesis polymerases in DNA interstrand crosslink repair. *Environmental and Molecular Mutagenesis*. 51:552-566.

Kelland, L. 2007. The resurgence of platinum-based cancer chemotherapy. *Nat Rev Cancer*. 7:573-584.

Liaw, H., D. Lee, and K. Myung. 2011. DNA-PK-Dependent RPA2 Hyperphosphorylation Facilitates DNA Repair and Suppresses Sister Chromatid Exchange. *PLoS ONE*. 6:e21424.

Manthey, K.C., J.G. Glanzer, D.D. Dimitrova, and G.G. Oakley. 2010. Hyperphosphorylation of replication protein A in cisplatin-resistant and -sensitive head and neck squamous cell carcinoma cell lines. *Head Neck*. 32:636-45.

Masutani, C., R. Kusumoto, S. Iwai, and F. Hanaoka. 2000. Mechanisms of accurate translesion synthesis by human DNA polymerase [eta]. *EMBO J*. 19:3100-3109.

Neher, T.M., D. Bodenmiller, R.W. Fitch, S.I. Jalal, and J.J. Turchi. 2011. Novel irreversible small molecule inhibitors of replication protein A display single-agent activity and synergize with cisplatin. *Mol Cancer Ther*. 10:1796-806.

Nikolaishvili-Feinberg, N., and M. Cordeiro-Stone. 2012. Assays of bypass replication of genotoxic lesions in cell-free extracts. *Methods Mol Biol*. 920:503-28.

Oakley, G.G., S.M. Patrick, J. Yao, M.P. Carty, J.J. Turchi, and K. Dixon. 2003a. RPA phosphorylation in mitosis alters DNA binding and protein-protein interactions. *Biochemistry*. 42:3255-64.

Oakley, G.G., S.M. Patrick, J. Yao, M.P. Carty, J.J. Turchi, and K. Dixon. 2003b. RPA Phosphorylation in Mitosis Alters DNA Binding and Protein-Protein Interactions. *Biochemistry*. 42:3255-3264.

Ong, S.E., L.J. Foster, and M. Mann. 2003. Mass spectrometric-based approaches in quantitative proteomics. *Methods*. 29:124-30.

Patrick, S.M., G.G. Oakley, K. Dixon, and J.J. Turchi. 2005. DNA damage induced hyperphosphorylation of replication protein A. 2. Characterization of DNA binding activity, protein interactions, and activity in DNA replication and repair. *Biochemistry*. 44:8438-48.

Pimienta, G., R. Chaerkady, and A. Pandey. 2009. SILAC for global phosphoproteomic analysis. *Methods Mol Biol*. 527:107-16, x.

San Filippo, J., P. Sung, and H. Klein. 2008. Mechanism of eukaryotic homologous recombination. *Annu Rev Biochem*. 77:229-57.

Serrano, M.A., Z. Li, M. Dangeti, P.R. Musich, S. Patrick, M. Roginskaya, B. Cartwright, and Y. Zou. 2012. DNA-PK, ATM and ATR collaboratively regulate p53-RPA interaction to facilitate homologous recombination DNA repair. *Oncogene*.

Shachar, S., O. Ziv, S. Avkin, S. Adar, J. Wittschieben, T. Reiszner, S. Chaney, E.C. Friedberg, Z. Wang, T. Carell, N. Geacintov, and Z. Livneh. 2009. Two-polymerase mechanisms dictate error-free and error-prone translesion DNA synthesis in mammals. *EMBO J*. 28:383-393.

Sharma, S., N.A. Shah, A.M. Joiner, K.H. Roberts, and C.E. Canman. 2012. DNA polymerase zeta is a major determinant of resistance to platinum-based chemotherapeutic agents. *Mol Pharmacol*. 81:778-87.

Shuck, S.C., and J.J. Turchi. 2010. Targeted inhibition of Replication Protein A reveals cytotoxic activity, synergy with chemotherapeutic DNA-damaging agents, and insight into cellular function. *Cancer Res*. 70:3189-98.

Stephan, H., C. Concannon, E. Kremmer, M.P. Carty, and H.P. Nasheuer. 2009. Ionizing radiation-dependent and independent phosphorylation of the 32-kDa subunit of replication protein A during mitosis. *Nucleic Acids Res*. 37:6028-41.

Teng, K.Y., M.Z. Qiu, Z.H. Li, H.Y. Luo, Z.L. Zeng, R.Z. Luo, H.Z. Zhang, Z.Q. Wang, Y.H. Li, and R.H. Xu. 2010. DNA polymerase eta protein expression predicts treatment response and survival of metastatic gastric adenocarcinoma patients treated with oxaliplatin-based chemotherapy. *J Transl Med*. 8:126.

Tsai, M.S., Y.H. Kuo, Y.F. Chiu, Y.C. Su, and Y.W. Lin. 2010. Down-regulation of Rad51 expression overcomes drug resistance to gemcitabine in human non-small-cell lung cancer cells. *J Pharmacol Exp Ther*. 335:830-40.

Ummat, A., O. Rechkoblit, R. Jain, J. Roy Choudhury, R.E. Johnson, T.D. Silverstein, A. Buku, S. Lone, L. Prakash, S. Prakash, and A.K. Aggarwal. 2012. Structural basis for cisplatin DNA damage tolerance by human polymerase eta during cancer chemotherapy. *Nat Struct Mol Biol*. 19:628-32.

Vaisman, A., C. Masutani, F. Hanaoka, and S.G. Chaney. 2000. Efficient Translesion Replication Past Oxaliplatin and Cisplatin GpG Adducts by Human DNA Polymerase η *Biochemistry*. 39:4575-4580.

Vassin, V.M., M.S. Wold, and J.A. Borowiec. 2004. Replication Protein A (RPA) Phosphorylation Prevents RPA Association with Replication Centers. *Mol. Cell. Biol.* 24:1930-1943.

Verweij, J., and H.M. Pinedo. 1990. Mitomycin C: mechanism of action, usefulness and limitations. *Anticancer Drugs*. 1:5-13.

Zhao, Y., C. Biertumpfel, M.T. Gregory, Y.J. Hua, F. Hanaoka, and W. Yang. 2012. Structural basis of human DNA polymerase eta-mediated chemoresistance to cisplatin. *Proc Natl Acad Sci U S A*. 109:7269-74.

Zheng, H., X. Wang, A.J. Warren, R.J. Legerski, R.S. Nairn, J.W. Hamilton, and L. Li. 2003. Nucleotide excision repair- and polymerase eta-mediated error-prone removal of mitomycin C interstrand cross-links. *Mol Cell Biol*. 23:754-61.

Appendicies : Supplementary report, publications, funding and contributions

Appendix A: Generation and characterisation of phosphorylation-site mutants of RPA2

Sokol A.M.[1], Carty M.P.[1]

[1] DNA Damage Response Laboratory, Centre for Chromosome Biology, Biochemistry, School of Natural Sciences, National University of Ireland, Galway, Ireland

A.1 Generation of wild-type and mutant RPA2 constructs.

A series of vectors were generated in which RPA2 was tagged at either the N- or C-terminus with eGFP (for immunofluorescence studies) or with a FLAG-tag (for biochemical studies). The phosphorylation sites at Ser4 and Ser8 were then mutated to alanine, either singly or together.

Gene expression in all constructs is under the control of the CMV promoter, allowing for protein expression in human cells. Sequence analysis of clones expressing wild-type and mutant fusion proteins is presented in Table .1.

Name	Sequence
	
wt-RPA2-eGFP-N1	CGCTACCGGACTCAGATCTCGAGCTCAAGCTTCGAATTCATGTGGAACAGTGGATTCGAAAGCTATGGCAGCTCCT CATACGGGGGAGCCGGCGGCTACACGCAGTCCCCGGGGGGCTTTGGATCGCCCGCACCTTCTCAAGCCGAAAA GAAATCAAGAGCCCGAGCCCAGCACATTGTGCCCTGTACTATATCTCAGCTGCTTTCTGCCACTTTGGTTGATGAA GTGTTCAGAATTGGGAATGTTGAGATTTCACAGGTCACTATTGTGGGGATCATCAGACATGCAGAGAAGGCTCCAA CCAACATTGTTTACAAAATAGATGACATGACAGCTGCACCCATGGACGTTCGCCAGTGGGTTGACACAGATGACAC CAGCAGTGAAAACACTGTGGTTCCTCCAGAAACATATGTGAAAGTGGCAGGCCACCTGAGATCTTTTCAGAACAAA AAGAGCCTGGTAGCCTTTAAGATCATGCCCCTGGAGGATATGAATGAGTTCACCACACATATTCTGGAAGTGATCA ATGCACACATGGTACTAAGCAAAGCCAACAGCCAGCCCTCAGCAGGGAGAGCACCTATCAGCAATCCAGGAATGA GTGAAGCAGGGAACTTTGGTGGGAATAGCTTCATGCCAGCAAATGGCCTCACTGTGGCCCAAAACCAGGTGTTGA ATTTGATTAAGGCTTGTCCAAGACCTGAAGGGTTGAACTTTCAGGATCTCAAGAACCAGCTGAAACACATGTCTGTA TCCTCAATCAAGCAAGCTGTGGATTTTCTGAGCAATGAGGGGCACATCTATTCTACTGTGGATGATGACCATTTTAA ATCCACAGATGCAGAAGCGGATCCACCGGTCGCCACCATGGTGAGCAAGGGCGAGGAGCTGTTCACCGGGGTGG TGCCCATCCTGCTCGAGCTGGACGGCGACGTAAACGGCCACAAGTTCAGCGTGTCCGGCGAGGGCGAGGG
S4A-RPA2-eGFP-N1	CGCTACCGGACTCAGATCTCGAGCTCAAGCTTCGAATTCATGTGGAACGCTGGATTCGAAAGCTATGGCAGCTCC TCATACGGGGGAGCCGGCGGCTACACGCAGTCCCCGGGGGGCTTTGGATCGCCCGCACCTTCTCAAGCCGAAAA GAAATCAAGAGCCCGAGCCCAGCACATTGTGCCCTGTACTATATCTCAGCTGCTTTCTGCCACTTTGGTTGATGAA GTGTTCAGAATTGGGAATGTTGAGATTTCACAGGTCACTATTGTGGGGATCATCAGACATGCAGAGAAGGCTCCAA CCAACATTGTTTACAAAATAGATGACATGACAGCTGCACCCATGGACGTTCGCCAGTGGGTTGACACAGATGACAC CAGCAGTGAAAACACTGTGGTTCCTCCAGAAACATATGTGAAAGTGGCAGGCCACCTGAGATCTTTTCAGAACAAA AAGAGCCTGGTAGCCTTTAAGATCATGCCCCTGGAGGATATGAATGAGTTCACCACACATATTCTGGAAGTGATCA ATGCACACATGGTACTAAGCAAAGCCAACAGCCAGCCCTCAGCAGGGAGAGCACCTATCAGCAATCCAGGAATGA GTGAAGCAGGGAACTTTGGTGGGAATAGCTTCATGCCAGCAAATGGCCTCACTGTGGCCCAAAACCAGGTGTTGA ATTTGATTAAGGCTTGTCCAAGACCTGAAGGGTTGAACTTTCAGGATCTCAAGAACCAGCTGAAACACATGTCTGTA TCCTCAATCAAGCAAGCTGTGGATTTTCTGAGCAATGAGGGGCACATCTATTCTACTGTGGATGATGACCATTTTAA ATCCACAGATGCAGAAGCGGATCCACCGGGTCGCCACCATGGTGAGCAAGGGCGAGGAGCTGTTCACCGGGGTG GTGCCCATCC
S8A-RPA2-eGFP-N1	CGCTACCGGACTCAGATCTCGAGCTCAAGCTTCGAATTCATGTGGAACAGTGGATTCGAATTCATGGCAGCTCCTC ATACGGGGGAGCCGGCGGCTACACGCAGTCCCCGGGGGGCTTTGGATCGCCCGCACCTTCTCAAGCCGAAAAGA AATCAAGAGCCCGAGCCCAGCACATTGTGCCCTGTACTATATCTCAGCTGCTTTCTGCCACTTTGGTTGATGAAGT GTTCAGAATTGGGAATGTTGAGATTTCACAGGTCACTATTGTGGGGATCATCAGACATGCAGAGAAGGCTCCAACC AACATTGTTTACAAAATAGATGACATGACAGCTGCACCCATGGACGTTCGCCAGTGGGTTGACACAGATGACACCA GCAGTGAAAACACTGTGGTTCCTCCAGAAACATATGTGAAAGTGGCAGGCCACCTGAGATCTTTTCAGAACAAAAA GAGCCTGGTAGCCTTTAAGATCATGCCCCTGGAGGATATGAATGAGTTCACCACACATATTCTGGAAGTGATCAAT GCACACATGGTACTAAGCAAAGCCAACAGCCAGCCCTCAGCAGGGAGAGCACCTATCAGCAATCCAGGAATGAGT GAAGCAGGGAACTTTGGTGGGAATAGCTTCATGCCAGCAAATGGCCTCACTGTGGCCCAAAACCAGGTGTTGAAT TTGATTAAGGCTTGTCCAAGACCTGAAGGGTTGAACTTTCAGGATCTCAAGAACCAGCTGAAACACATGTCTGTAT CCTCAATCAAGCAAGCTGTGGATTTTCTGAGCAATGAGGGGCACATCTATTCTACTGTGGATGATGACCATTTTAAA TCCACAGATGCAGAAGCGGATCCACCGGTCGCCACCATGGTGAGCAAAGGGCGAGGAGCTGTTCACCGGGGTGG
S4A/S8A-RPA2-eGFP-N1	GCGCTACCGGACTCAGATCTCGAGCTCAAGCTTCGAATTCATGTGGAACGCTGGATTCGAAGCCTATGGCAGCTC CTCATACGGGGGAGCCGGCGGCTACACGCAGTCCCCGGGGGGCTTTGGATCGCCCGCACCTTCTCAAGCCGAAA AGAAATCAAGAGCCCGAGCCCAGCACATTGTGCCCTGTACTATATCTCAGCTGCTTTCTGCCACTTTGGTTGATGA AGTGTTCAGAATTGGGAATGTTGAGATTTCACAGGTCACTATTGTGGGGATCATCAGACATGCAGAGAAGGCTCCA ACCAACATTGTTTACAAAATAGATGACATGACAGCTGCACCCATGGACGTTCGCCAGTGGGTTGACACAGATGACA CCAGCAGTGAAAACACTGTGGTTCCTCCAGAAACATATGTGAAAGTGGCAGGCCACCTGAGATCTTTTCAGAACAA AAAGAGCCTGGTAGCCTTTAAGATCATGCCCCTGGAGGATATGAATGAGTTCACCACACATATTCTGGAAGTGATC AATGCACACATGGTACTAAGCAAAGCCAACAGCCAGCCCTCAGCAGGGAGAGCACCTATCAGCAATCCAGGAATG AGTGAAGCAGGGAACTTTGGTGGGAATAGCTTCATGCCAGCAAATGGCCTCACTGTGGCCCAAAACCAGGTGTTG AATTTGATTAAGGCTTGTCCAAGACCTGAAGGGTTGAACTTTCAGGATCTCAAGAACCAGCTGAAACACATGTCTGT ATCCTCAATCAAGCAAGCTGTGGATTTTCTGAGCAATGAGGGGCACATCTATTCTACTGTGGATGATGACCATTTTA AATCCACAGATGCAGAAGCGGATCCACCGGTCGCCACCATGGTGAGCAAGGGCGAGGAGCTGTTCACCGGGGTG GTGCCCATCCTGGTCGAGCTGGACGGCGACGTAAACGGGCCACAAGTTCAGCGTGTCCGGCGAGGGCGAGG

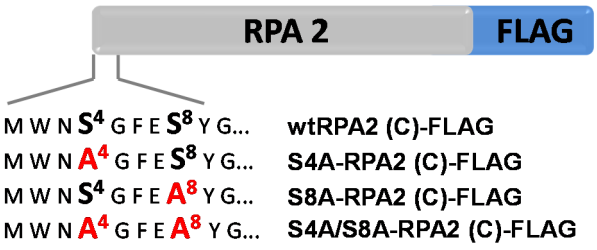

wtRPA2 (C)-FLAG	CTTGGTACCGAGCTCGGATCCATGTGGAACAGTGGATTCGAAAGCTATGGCAGCTCCTCATACGGGGGAGCCGG CGGCTACACGCAGTCCCCGGGGGGCTTTGGATCGCCCGCACCTTCTCAAGCCGAAAAGAAATCAAGAGCCCGAG CCCAGCACATTGTGCCCTGTACTATATCTCAGCTGCTTTCTGCCACTTTGGTTGATGAAGTGTTCAGAATTGGGAAT GTTGAGATTTCACAGGTCACTATTGTGGGGATCATCAGACATGCAGAGAAGGCTCCAACCAACATTGTTTACAAAA TAGATGACATGACAGCTGCACCCATGGACGTTCGCCAGTGGGTTGACACAGATGACACCAGCAGTGAAAACACTG TGGTTCCTCCAGAAACATATGTGAAAGTGGCAGGCCACCTGAGATCTTTTCAGAACAAAAAGAGCCTGGTAGCCTT TAAGATCATGCCCCTGGAGGATATGAATGAGTTCACCACACATATTCTGGAAGTGATCAATGCACACATGGTACTA AGCAAAGCCAACAGCCAGCCCTCAGCAGGGAGAGCACCTATCAGCAATCCAGGAATGAGTGAAGCAGGGAACTTT GGTGGGAATAGCTTCATGCCAGCAAATGGCCTCACTGTGGCCCAAAACCAGGTGTTGAATTTGATTAAGGCTTGTC CAAGACCTGAAGGGTTGAACTTTCAGGATCTCAAGAACCAGCTGAAACACATGTCTGTATCCTCAATCAAGCAAGC TGTGGATTTTCTGAGCAATGAGGGGCACATCTATTCTACTGTGGATGATGACCATTTTAAATCCACAGATGCAGAAG ATTACAAGGATGACGACGACAAGTAAGAATTCTGCAGATATCCAGCACAGTGGCGGCCGCTCGAGTCTAGAGGGC CCGTTTAAACCCGCTGATCAGCCTCGACTGTGCCTTCTAGTTGCCAGCCATCTGTTGTTTGCCCCTCCCCC
S4A-RPA2 (C)-FLAG	GCTTGGTACCGAGCTCGGATCCATGTGGAACGCTGGATTCGAAAGCTATGGCAGTTCCTCATACGGGGGAGCCG GCGGCTACACGCAGTCCCCGGGGGGCTTTGGATCGCCCGCACCTTCTCAAGCCGAAAAGAAATCAAGAGCCCGA GCCCAGCACATTGTGCCCTGTACTATATCTCAGCTGCTTTCTGCCACTTTGGTTGATGAAGTGTTCAGAATTGGGA ATGTTGAGATTTCACAGGTCACTATTGTGGGGATCATCAGACATGCAGAGAAGGCTCCAACCAACATTGTTTACAA AATAGATGACATGACAGCTGCACCCATGGACGTTCGCCAGTGGGTTGACACAGATGACACCAGCAGTGAAAACAC TGTGGTTCCTCCAGAAACATATGTGAAAGTGGCAGGCCACCTGAGATCTTTTCAGAACAAAAAGAGCCTGGTAGCC TTTAAGATCATGCCCCTGGAGGATATGAATGAGTTCACCACACATATTCTGGAAGTGATCAATGCACACATGGTACT AAGCAAAGCCAACAGCCAGCCCTCAGCAGGGAGAGCACCTATCAGCAATCCAGGAATGAGTGAAGCAGGGAACTT TGGTGGGAATAGCTTCATGCCAGCAAATGGCCTCACTGTGGCCCAAAACCAGGTGTTGAATTTGATTAAGGCTTGT CCAAGACCTGAAGGGTTGAACTTTCAGGATCTCAAGAACCAGCTGAAACACATGTCTGTATCCTCAATCAAGCAAG CTGTGGATTTTCTGAGCAATGAGGGGCACATCTATTCTACTGTGGATGATGACCATTTTAAATCCACAGATGCAGAA GATTACAAGGATGACGACGACAAGTAAGAATTCTGCAGATATCCAGCACAGTGGCGGCCGCTCGAGTCTAGAGGG CCCGTTTAAACCCGCTGATCAGCCTCGACTGTGCCTTCTAGTTGCCAGCCATCTGTTGTTTGCCCCTCCCCC
S8A-RPA2 (C)-FLAG	TTGGTACCGAGCTCGGATCCATGTGGAACAGTGGATTCGAAGCCTATGGCAGCTCCTCATACGGGGGAGCCGGC GGCTACACGCAGTCCCCGGGGGGCTTTGGATCGCCCGCACCTTCTCAAGCCGAAAAGAAATCAAGAGCCCGAGC CCAGCACATTGTGCCCTGTACTATATCTCAGCTGCTTTCTGCCACTTTGGTTGATGAAGTGTTCAGAATTGGGAATG TTGAGATTTCACAGGTCACTATTGTGGGGATCATCAGACATGCAGAGAAGGCTCCAACCAACATTGTTTACAAAATA GATGACATGACAGCTGCACCCATGGACGTTCGCCAGTGGGTTGACACAGATGACACCAGCAGTGAAAACACTGTG GTTCCTCCAGAAACATATGTGAAAGTGGCAGGCCACCTGAGATCTTTTCAGAACAAAAAGAGCCTGGTAGCCTTTA AGATCATGCCCCTGGAGGATATGAATGAGTTCACCACACATATTCTGGAAGTGATCAATGCACACATGGTACTAAG CAAAGCCAACAGCCAGCCCTCAGCAGGGAGAGCACCTATCAGCAATCCAGGAATGAGTGAAGCAGGGAACTTTG GTGGGAATAGCTTCATGCCAGCAAATGGCCTCACTGTGGCCCAAAACCAGGTGTTGAATTTGATTAAGGCTTGTCC AAGACCTGAAGGGTTGAACTTTCAGGATCTCAAGAACCAGCTGAAACACATGTCTGTATCCTCAATCAAGCAAGCT GTGGATTTTCTGAGCAATGAGGGGCACATCTATTCTACTGTGGATGATGACCATTTTAAATCCACAGATGCAGAAG ATTACAAGGATGACGACGACAAGTAAGAATTCTGCAGATATCCAGCACAGTGGCGGCCGCTCGAGTCTAGAGGGC CCGTTTAAACCCGCTGATCAGCCTCGACTGTGCCTTCTAGTTGCCAGCCATCTGTTGTTTGCCCCTCCCCCGTG
S4A/S8A-RPA2 (C)-FLAG	TTGGTACCGAGCTCGGATCCATGTGGAACGCTGGATTCGAAGCCTATGGCAGCTCCTCATACGGGGGAGCCGGC GGCTACACGCAGTCCCCGGGGGGCTTTGGATCGCCCGCACCTTCTCAAGCCGAAAAGAAATCAAGAGCCCGAGC CCAGCACATTGTGCCCTGTACTATATCTCAGCTGCTTTCTGCCACTTTGGTTGATGAAGTGTTCAGAATTGGGAATG TTGAGATTTCACAGGTCACTATTGTGGGGATCATCAGACATGCAGAGAAGGCTCCAACCAACATTGTTTACAAAATA GATGACATGACAGCTGCACCCATGGACGTTCGCCAGTGGGTTGACACAGATGACACCAGCAGTGAAAACACTGTG GTTCCTCCAGAAACATATGTGAAAGTGGCAGGCCACCTGAGATCTTTTCAGAACAAAAAGAGCCTGGTAGCCTTTA AGATCATGCCCCTGGAGGATATGAATGAGTTCACCACACATATTCTGGAAGTGATCAATGCACACATGGTACTAAG CAAAGCCAACAGCCAGCCCTCAGCAGGGAGAGCACCTATCAGCAATCCAGGAATGAGTGAAGCAGGGAACTTTG GTGGGAATAGCTTCATGCCAGCAAATGGCCTCACTGTGGCCCAAAACCAGGTGTTGAATTTGATTAAGGCTTGTCC AAGACCTGAAGGGTTGAACTTTCAGGATCTCAAGAACCAGCTGAAACACATGTCTGTATCCTCAATCAAGCAAGCT GTGGATTTTCTGAGCAATGAGGGGCACATCTATTCTACTGTGGATGATGACCATTTTAAATCCACAGATGCAGAAG ATTACAAGGATGACGACGACAAGTAAGAATTCTGCAGATATCCAGCACAGTGGCGGCCGCTCGAGTCTAGAGGGC CCGTTTAAACCCGCTGATCAGCCTCGACTGTGCCTTCTAGTTGCCAGCCATCTGTTGTTTGCCCCTCCCCCGTGCC TTCCTTGACCCTGG

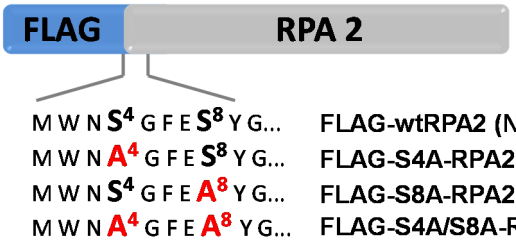

FLAG-wtRPA2 (N)	CTTGGTACCGAGCTCGGATCCATGGATTACAAGGATGACGACGACAAGATGTGGAACAGTGGATTCGAAAGCTAT GGCAGCTCCTCATACGGGGGAGCCGGCGGCTACACGCAGTCCCCGGGGGGCTTTGGATCGCCCGCACCTTCTC AAGCCGAAAAGAAATCAAGAGCCCGAGCCCAGCACATTGTGCCCTGTACTATATCTCAGCTGCTTTCTGCCACTTT GGTTGATGAAGTGTTCAGAATTGGGAATGTTGAGATTTCACAGGTCACTATTGTGGGGATCATCAGACATGCAGAG AAGGCTCCAACCAACATTGTTTACAAAATAGATGACATGACAGCTGCACCCATGGACGTTCGCCAGTGGGTTGACA CAGATGACACCAGCAGTGAAAACACTGTGGTTCCTCCAGAAACATATGTGAAAGTGGCAGGCCACCTGAGATCTTT TCAGAACAAAAAGAGCCTGGTAGCCTTTAAGATCATGCCCCTGGAGGATATGAATGAGTTCACCACACATATTCTG GAAGTGATCAATGCACACATGGTACTAAGCAAAGCCAACAGCCAGCCCTCAGCAGGGAGAGCACCTATCAGCAAT CCAGGAATGAGTGAAGCAGGGAACTTTGGTGGGAATAGCTTCATGCCAGCAAATGGCCTCACTGTGGCCCAAAAC CAGGTGTTGAATTTGATTAAGGCTTGTCCAAGACCTGAAGGGTTGAACTTTCAGGATCTCAAGAACCAGCTGAAAC ACATGTCTGTATCCTCAATCAAGCAAGCTGTGGATTTTCTGAGCAATGAGGGGCACATCTATTCTACTGTGGATGAT GACCATTTTAAATCCACAGATGCAGAATAAGAATTCTGCAGATATCCAGCACAGTGGCGGCCGCTCGAGTCTAGAG GGCCCGTTTAAACCCGCTGATCAGCCTCGACTGTGCCTTCTAGTTGCCAGCCATCTGTTGTTTGCCCCTCCCCC

FLAG-S4A-RPA2 (N)	TTGGTACCGAGCTCGGATCCATGGATTACAAGGATGACGACGACAAGATGTGGAACGCTGGATTCGAAAGCTATG GCAGCTCCTCATACGGGGGAGCCGGCGGCTACACGCAGTCCCCGGGGGGCTTTGGATCGCCCGCACCTTCTCAA GCCGAAAAGAAATCAAGAGCCCGAGCCCAGCACATTGTGCCCTGTACTATATCTCAGCTGCTTTCTGCCACTTTGG TTGATGAAGTGTTCAGAATTGGGAATGTTGAGATTTCACAGGTCACTATTGTGGGGATCATCAGACATGCAGAGAA GGCTCCAACCAACATTGTTTACAAAATAGATGACATGACAGCTGCACCCATGGACGTTCGCCAGTGGGTTGACACA GATGACACCAGCAGTGAAAACACTGTGGTTCCTCCAGAAACATATGTGAAAGTGGCAGGCCACCTGAGATCTTTTC AGAACAAAAAGAGCCTGGTAGCCTTTAAGATCATGCCCCTGGAGGATATGAATGAGTTCACCACACATATTCTGGA AGTGATCAATGCACACATGGTACTAAGCAAAGCCAACAGCCAGCCCTCAGCAGGGAGAGCACCTATCAGCAATCC AGGAATGAGTGAAGCAGGGAACTTTGGTGGGAATAGCTTCATGCCAGCAAATGGCCTCACTGTGGCCCAAAACCA GGTGTTGAATTTGATTAAGGCTTGTCCAAGACCTGAAGGGTTGAACTTTCAGGATCTCAAGAACCAGCTGAAACAC ATGTCTGTATCCTCAATCAAGCAAGCTGTGGATTTTCTGAGCAATGAGGGGCACATCTATTCTACTGTGGATGATGA CCATTTTAAATCCACAGATGCAGAATAAGAATTCTGCAGATATCCAGCACAGTGGCGGCCGCTCGAGTCTAGAGGG CCCGTTTAAACCCGCTGATCA
FLAG-S8A-RPA2 (N)	TTGGTACCGAGCTCGGATCCATGGATTACAAGGATGACGACGACAAGATGTGGAACAGTGGATTCGAAGCCTATG GCAGCTCCTCATACGGGGGAGCCGGCGGCTACACGCAGTCCCCGGGGGGCTTTGGATCGCCCGCACCTTCTCAA GCCGAAAAGAAATCAAGAGCCCGAGCCCAGCACATTGTGCCCTGTACTATATCTCAGCTGCTTTCTGCCACTTTGG TTGATGAAGTGTTCAGAATTGGGAATGTTGAGATTTCACAGGTCACTATTGTGGGGATCATCAGACATGCAGAGAA GGCTCCAACCAACATTGTTTACAAAATAGATGACATGACAGCTGCACCCATGGACGTTCGCCAGTGGGTTGACACA GATGACACCAGCAGTGAAAACACTGTGGTTCCTCCAGAAACATATGTGAAAGTGGCAGGCCACCTGAGATCTTTTC AGAACAAAAAGAGCCTGGTAGCCTTTAAGATCATGCCCCTGGAGGATATGAATGAGTTCACCACACATATTCTGGA AGTGATCAATGCACACATGGTACTAAGCAAAGCCAACAGCCAGCCCTCAGCAGGGAGAGCACCTATCAGCAATCC AGGAATGAGTGAAGCAGGGAACTTTGGTGGGAATAGCTTCATGCCAGCAAATGGCCTCACTGTGGCCCAAAACCA GGTGTTGAATTTGATTAAGGCTTGTCCAAGACCTGAAGGGTTGAACTTTCAGGATCTCAAGAACCAGCTGAAACAC ATGTCTGTATCCTCAATCAAGCAAGCTGTGGATTTTCTGAGCAATGAGGGGCACATCTATTCTACTGTGGATGATGA CCATTTTAAATCCACAGATGCAGAATAAGAATTCTGCAGATATCCAG
FLAG-S4A/S8A-RPA2 (N)	CTTGGTACCGAGCTCGGATCCATGGATTACAAGGATGACGACGGACAAGATGTGGAACGCTGGATTCGAAGCCTA TGGCAGCTCCTCATACGGGGGAGCCGGCGGCTACACGCAGTCCCCGGGGGGCTTTGGATCGCCCGCACCTTCTC AAGCCGAAAAGAAATCAAGAGCCCGAGCCCAGCACATTGTGCCCTGTACTATATCTCAGCTGCTTTCTGCCACTTT GGTTGATGAAGTGTTCAGAATTGGGAATGTTGAGATTTCACAGGTCACTATTGTGGGGATCATCAGACATGCAGAG AAGGCTCCAACCAACATTGTTTACAAAATAGATGACATGACAGCTGCACCCATGGACGTTCGCCAGTGGGTTGACA CAGATGACACCAGCAGTGAAAACACTGTGGTTCCTCCAGAAACATATGTGAAAGTGGCAGGCCACCTGAGATCTTT TCAGAACAAAAAGAGCCTGGTAGCCTTTAAGATCATGCCCCTGGAGGATATGAATGAGTTCACCACACATATTCTG GAAGTGATCAATGCACACATGGTACTAAGCAAAGCCAACAGCCAGCCCTCAGCAGGGAGAGCACCTATCAGCAAT CCAGGAATGAGTGAAGCAGGGAACTTTGGTGGGAATAGCTTCATGCCAGCAAATGGCCTCACTGTGGCCCAAAAC CAGGTGTTGAATTTGATTAAGGCTTGTCCAAGACCTGAAGGGTTGAACTTTCAGGATCTCAAGAACCAGCTGAAAC ACATGTCTGTATCCTCAATCAAGCAAGCTGTGGATTTTCTGAGCAATGAGGGCACATCTATTCTACTGTGGATGATG ACCATTTTAAATCCACAGATGCAGAATAAGAATTCTGCAGATATCCAGCACA

Table A.1 Sequencing analysis of DNA plasmids expressing tagged replication protein A2 (RPA2). The coding sequences of replication protein A2 (RPA2) are marked in blue, and for Green Fluorescent Protein (GFP) in green. The FLAG-tag sequence is marked in pink. Restriction sites for EcoRI (GAATTC) and BamHI (GAATTC) are marked in gray. Modified codons for introduction of mutations at serines 4 or 8 in RPA2 are marked in red, and stop codons in navy.

A.2 Characterisation of wild-type and mutant RPA2 tagged with eGFP.

To test the functionality of the constructs prior to site-directed mutagenesis of the two serines of interest, RPA2 tagged either at the N- or C-terminus with eGFP, was expressed in XP30RO cells. Because this cell line lacks polη, DNA damage-induced RPA2 phosphorylation on Ser4/Ser8 is strongly induced (see previous Chapters and enclosed review). Compared to the mock-transfected cells, expression of protein from both vectors was confirmed by the use of anti-GFP and anti-RPA2 antibodies in western blotting (Figure A.1). Given that RPA2 is 32kDa in size and GFP is 26.9kDa, the fusion protein was expected to run on SDS-PAGE as a protein of approximately 59kDa. Using the anti-GFP antibody two bands were detected following expression of RPA2 tagged on the N-terminus with eGFP (Figure A.1, left panel). The upper band corresponded to that of the eGFP-tagged RPA2 protein, although the size was slightly lower when compared to that of RPA2 labelled at the C-terminus with eGFP. Additionally, a lower band (of approximately 35kDa) was detected in both cases, most likely corresponding to free eGFP, cleaved from the fusion protein. In the case of the N-terminally-tagged RPA2, the size of the cleaved form did not fully correlate to the size of eGFP (~27kDa) whereas in the C-terminally tagged RPA2 the cleaved, free GFP form ran slightly above the 25kDa marker. However, when the C-terminally tagged RPA2 was expressed several other bands were detected when using either

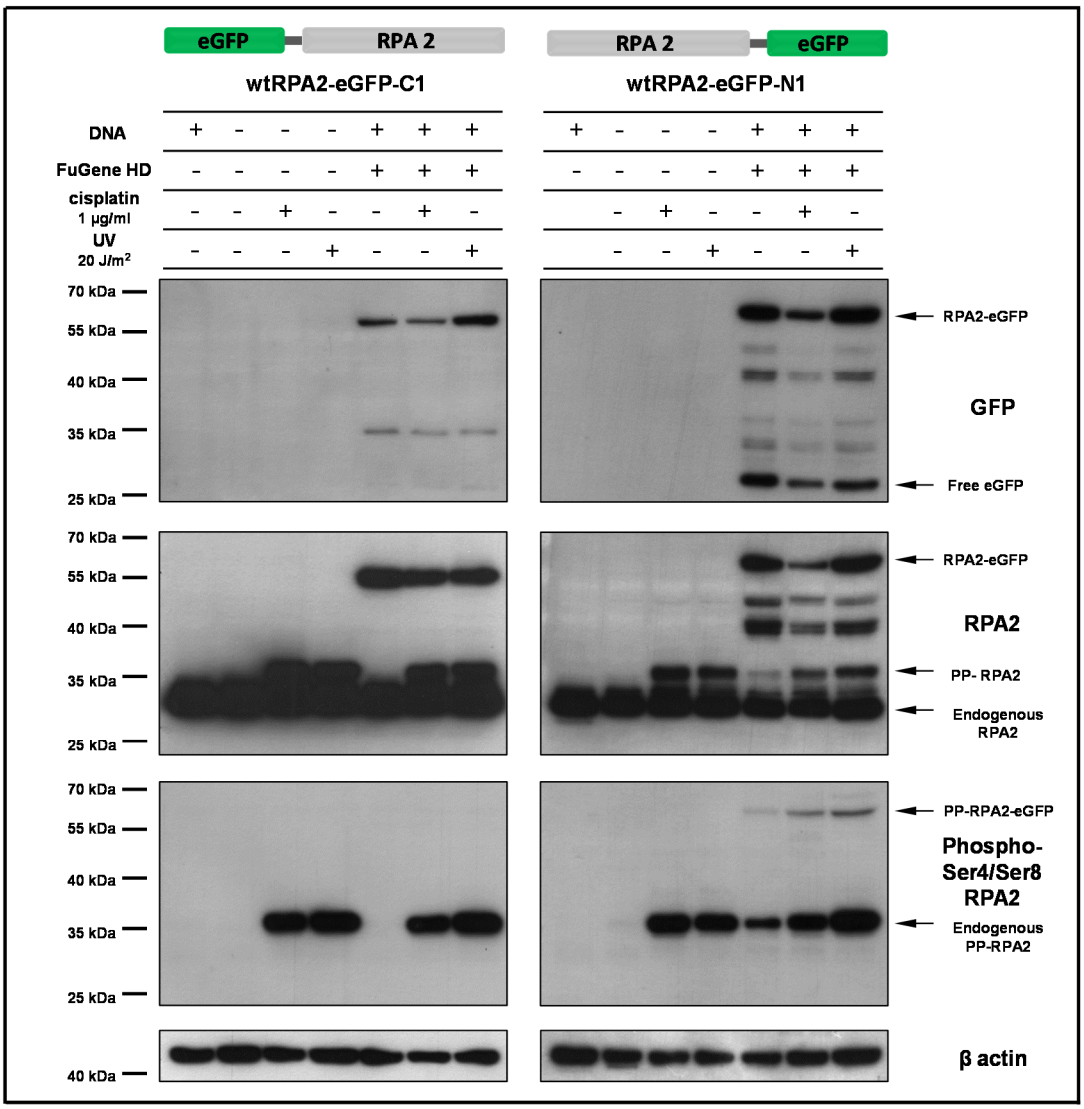

Figure A. 1 Expression of ectopic RPA2 tagged with eGFP tag on the either the N- or C-terminus. At 80% confluence, XP30RO cells were mock-transfected or transfected using wtRPA2-eGFP-C1 (left panel) or using wtRPA2-eGFP-N1 (right panel), as described in Materials and Methods. 24h later, the transfection media was removed and the cells were allowed to grow in normal media for further 24h before being treated with the indicated doses of UV-C or cisplatin. Subsequently, 6h (in the case of UV-C treatment) and 24h (in the case of cisplatin treatment) later, cells were harvested for western blotting. Protein expression was analysed by western blotting using anti-GFP and anti-RPA2 antibodies. Anti-phospho-Ser4/Ser8 RPA2 antibody was used to detect the phosphorylation status of RPA2. β-actin staining was used as loading control.

with anti-GFP or anti-RPA2 antibodies. This could be due to turnover of the RPA2 protein when it is over-expressed from the transfected plasmid; however the origin of these additional bands was not further investigated in the present study.

Interestingly, in response to genotoxic stress induced by cisplatin and UV-C treatment, only the C-terminally tagged RPA2 was phosphorylated on Ser4 and Ser8, as visualised using the phospho-Ser4/Ser8 RPA2 specific antibody (Figure A.1, bottom panel, right). No phosphorylation was detectable on Ser4/Ser8 when GFP was fused to the N-terminus of RPA2. This leads to the conclusion that the eGFP tag on the N-terminus of

RPA2 may constitute an obstacle to phosphorylation of this domain by the relevant cellular kinases. This construct is therefore not a good system in which to study the role of phosphorylation of RPA2 on Ser4/Ser8 in the response to DNA damage in human cells.

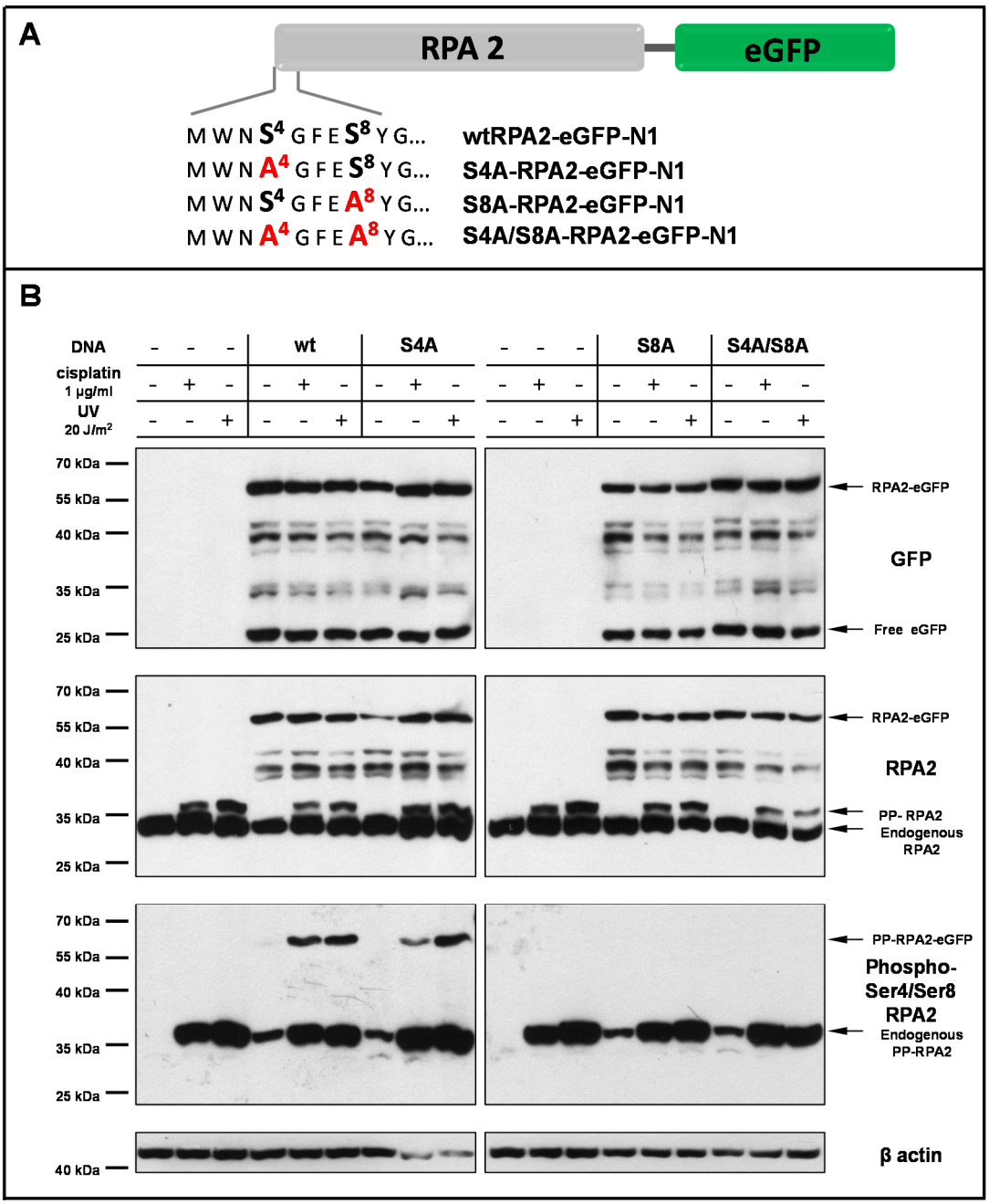

Figure A. 2 Expression of ectopic, wild-type or mutant RPA2 tagged with the eGFP tag on the C terminus. A Schematic of the DNA plasmid used with detailed analysis of the mutated sites **B** At 80% confluence, XP30RO cells were mock-transfected or transfected using the indicated DNA plasmids expressing wild-type or mutated versions of the RPA2 protein tagged on the C-terminus with a eGFP tag. 24h later, transfection media was removed and cells were allowed to grow in normal media for a further 24h (in the case of cisplatin treatment) and 42h (in the case of UV-C treatment) before being treated with cisplatin or UV-C, at the indicated doses. Subsequently, cells were harvested for western blotting analysis. Ectopic protein expression was analysed using anti-GFP and anti-RPA2 antibodies and anti-phospho-Ser4/Ser8 RPA2 antibody was used to detect phosphorylation status. β-actin staining was used as loading control.

Based on this analysis, mutations at the phosphorylation sites of interest were introduced into the vector expressing the C-terminally, eGFP-tagged RPA2 rather than into the N-terminally tagged protein. It was further noted that transfection itself caused a stress response in XP30RO cells, detectable as RPA2 phosphorylation on Ser4/Ser8 without exposure of cells to DNA damage (Figure A.1, bottom right panel, lane 5). No phosphorylation-induced mobility shift was noted when cells expressing the C-terminally, eGFP-tagged RPA2 were exposed to DNA damage. Phosphorylation induces small changes in protein mobility that can be more readily detected by SDS-PAGE and western blotting when the proteins of lower molecular weight. The absence of a change in mobility in the ectopically expressed and phosphorylated fusion protein, which is approximately 59kDa in size, could be due to insufficient resolution of unmodified and modified proteins on SDS-PAGE. It is also possible that the overall level of modified fusion protein was too low to be detected under the conditions used here.

In order to further study RPA2 phosphorylation on the serines of interest, C-terminally, eGFP-tagged RPA2 carrying single and double mutations in serine 4 or serine 8 was expressed in XP30RO cells (Figure A.2A). It was observed that DNA damage-induced phosphorylation of ectopically-expressed RPA2 was detectable only in the wild-type and the S4A-RPA2 mutant proteins (Figure A.2B). Lack of phosphorylation of the double mutant is consistent with successful mutation of both serine 4 and serine 8 to alanine. Interestingly, no DNA damage-induced phosphorylation of the eGFP-tagged RPA2 construct was observed when serine 8 was mutated to alanine. This could be a result of (i) serine 8 phosphorylation being required for phosphorylation of serine 4, or (ii) the antibody having specificity only towards phosphorylated serine 8. The primary antibody against phospho-Ser4/Ser8 RPA2 was raised against a mixture of two peptides carrying single phosphorylations on either serine 4 or serine 8. Nothing is known about whether this antibody recognises one or both phosphorylated serine residues in western blotting. Here, we provide evidence that the phospho-Ser4/Ser8 antibody can detect at least a single phosphorylation on serine 8. The absence of a phosphorylation signal in the S4A-RPA2 mutant (Figure A.2B) could be due to the lack of serine 4 phosphorylation when serine 8 is mutated. However, it is also possible that the antibody does not recognise phospho-Ser4 if this residue is present in the absence of phospho-Ser8.

It is known that upon exposure of XP30RO cells to UV-C, RPA2 is localised to DNA damage sites and forms distinct nuclear foci (Cruet-Hennequart et al., 2006). Localisation of ectopically-expressed wild-type or mutant RPA2 under DNA damage conditions was analysed using fluorescence microscopy. When UV-C treated samples were stained for anti-RPA2 it was found that the majority of the endogenous RPA2 foci co-

localised with eGFP-tagged RPA2 (Figure A.3 A). While all eGFP foci co-localised with the RPA2 signal (red), not all of the endogenous RPA2 foci co-localised with the ectopically-expressed fusion protein. This may be explained by the fact that cellular levels of endogenous RPA2 are high such that in some foci, all or the major proportion of the RPA2 present is of endogenous origin. This analysis provides strong evidence that phosphorylation of RPA2 on serines 4 and 8 is not required for localisation of the protein into damage-induced foci, since S4A/S8A-RPA2-eGFP which can not undergo phosphorylation on these sites still localises to nuclear foci upon UV-C irradiation (Figure A.3A). Thus it can be concluded that RPA recruitment to nuclear foci precedes RPA2 hyperphosphorylation on Ser4/Ser8, consistent with previous data based on chromatin fractionation (Cruet-Hennequart et al., 2006; Cruet-Hennequart et al., 2008).

Given that RPA2 phosphorylation on Ser4/Ser8 is not required for RPA localisation to DNA damage-induced foci, we tested if a subset of the GFP-positive foci were also positive for phospho-Ser4/Ser8 RPA2. Interestingly, analysis of cells in which wild-type- and S4A-RPA2-eGFP constructs were expressed revealed that, upon UV-C exposure, the vast majority of eGFP foci co-localised with the phospho-Ser4/Ser8 RPA2 signal (Figure A.3B). It should be noted, however, that a small proportion of nuclear foci showing phospho-Ser4/Ser8 staining were negative for eGFP, and that some foci that were positive for eGFP did not contain distinct phospho-Ser4/Ser8 RPA2 foci, especially when S8A-single and S4A/S8A-double RPA2 mutants were analysed (see detail of individual foci shown in Figure A.3B). The fact that in most cases the phospho-RPA2 and eGFP signals co-localised is not unexpected, as foci recruitment was demonstrated to be independent of RPA2 phosphorylation on Ser4/Ser8 (Figure A.3A).

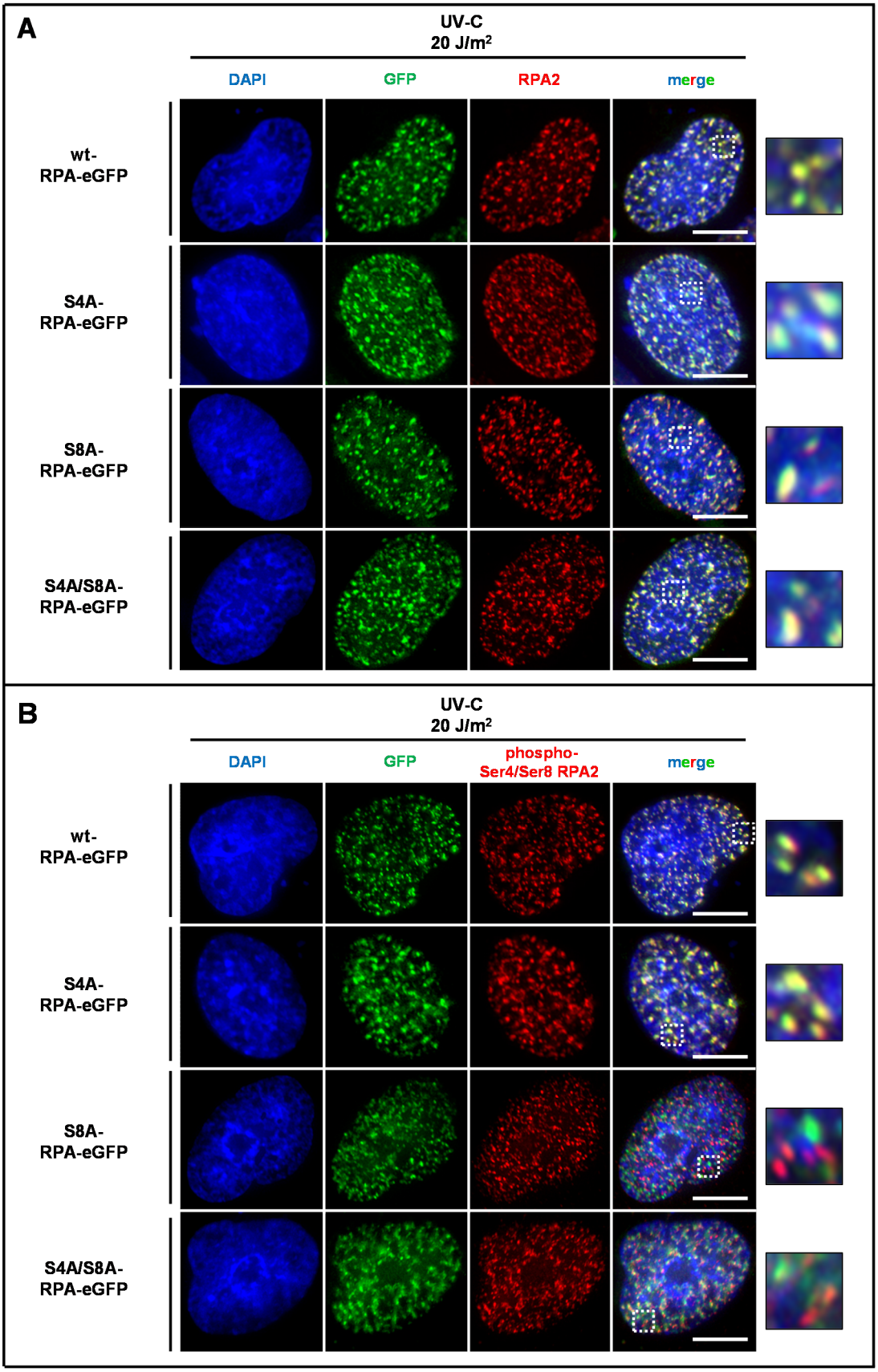

Figure A. 3 Analysis of UV-C irradiation-induced foci formation of wild-type or mutant RPA2 tagged with the eGFP tag on the C terminus. XP30RO cells were transefected using the indicated DNA plasimds expressing wild-type or mutated versions of the RPA2 protein tagged on the C-terminus with eGFP for 8hours. Transfection media was then removed and cells were allowed to grow

in normal media for further 24h before being treated with 20J/m^2 UV-C. 6h later, cells were fixed for immunofluorescence analysis with anti-RPA2 (Fig. A.3.A) or anti-phospho-Ser4/Ser8 RPA2 (Fig. A.3.B) primary antibody and Alexa-594-conjugated secondary antibody. DNA was counterstained with DAPI. Scale bar corresponds to 10μm.

A.3 Conclusions

The aim of this study was to generate and characterise a series of RPA2 constructs for expression in mammalian cells. We report that C-terminally, eGFP-tagged RPA2 and both C- and N-terminally FLAG-tagged RPA2 constructs were successfully generated. The serine 4 and serine8 residues in these constructs were mutated to alanine, generating a series of single- and double-mutants at these sites. Analysis of RPA2-eGFP phosphorylation mutants showed that:

(i) mutation of Ser4 and/or Ser8 has differential effects on damage-induced RPA2 phosphorylation;

(ii) anti-phospho-Ser4/Ser8 RPA2 antibody can detect phosphorylation on a single Ser8 residue in the absence of phosphorylation on serine 4;

(iii) RPA2 localiastion to UV-C induced DNA damage foci is independent on RPA2 phosphorylation on Ser4/Ser8.

This series of constructs and the preliminary data reported here could be used in the future to investigate the role of both damage-dependent and –independent phosphorylation of RPA2 on Ser4 and/or Ser8.

A.4 References

Cruet-Hennequart, S., S. Coyne, M.T. Glynn, G.G. Oakley, and M.P. Carty. 2006. UV-induced RPA phosphorylation is increased in the absence of DNA polymerase eta and requires DNA-PK. *DNA Repair (Amst)*. 5:491-504.

Cruet-Hennequart, S., M.T. Glynn, L.S. Murillo, S. Coyne, and M.P. Carty. 2008. Enhanced DNA-PK-mediated RPA2 hyperphosphorylation in DNA polymerase eta-deficient human cells treated with cisplatin and oxaliplatin. *DNA Repair (Amst)*. 7:582-96.

Appendix B: Characterization of the effects of cisplatin and carboplatin on cell cycle progression and DNA damage response activation in DNA polymerase eta-deficient human cells

Cruet-Hennequart S.[1], Villalan S.[1], Kaczmarczyk A.[1], O'Meara E.[1], **Sokol A.M.[1]**, Carty M.P.[1]: *Cell Cycle* 2009, 8:3039-3050

[1] DNA Damage Response Laboratory, Centre for Chromosome Biology, School of Natural Sciences, National University of Ireland, Galway, Ireland

Cell Cycle 8:18, 3043-3054; September 15, 2009; © 2009 Landes Bioscience

Characterization of the effects of cisplatin and carboplatin on cell cycle progression and DNA damage response activation in DNA polymerase eta-deficient human cells

Séverine Cruet-Hennequart, Sangamitra Villalan, Agnieszka Kaczmarczyk, Elaine O'Meara, Anna M. Sokol and Michael P. Carty*

Centre for Chromosome Biology; School of Natural Sciences; National University of Ireland Galway, Galway Ireland

Keywords: DNA damage response, replication arrest, translesion synthesis, RPA, phosphorylation, cisplatin, carboplatin, DNA polymerase eta

Abbreviations: ATM, ataxia telangiectasia mutated; ATR, ATM and Rad3-related; DNA-PK, DNA-dependent protein kinase; HR, homologous recombination; ICL, interstrand crosslink; PIKK, PI-3 kinase-related protein kinase; Polη, DNA polymerase η; RPA, replication protein A; XPV, xeroderma pigmentosum variant

Translesion synthesis by DNA polymerase eta (polη) is one mechanism by which cancer cells can tolerate DNA damage by platinum-based anti-cancer drugs. Cells lacking polη are sensitive to these agents. To help define the consequences of polη-deficiency, we characterized the effects of equitoxic doses of cisplatin and carboplatin on cell cycle progression and activation of DNA damage response pathways in a human cell line lacking polη. We show that both cisplatin and carboplatin induce strong S-phase arrest in polη-deficient XP30RO cells, associated with reduced expression of cyclin E and cyclin B. PIK kinase-mediated phosphorylation of Chk1, H2AX and RPA2 was strongly activated by both cisplatin and carboplatin, but phosphorylation of these proteins was induced earlier by cisplatin than by an equitoxic dose of carboplatin. Compared to Chk1 and H2AX phosphorylation, RPA2 hyperphosphorylation on serine4/serine8 is a late event in response to platinum-induced DNA damage. We directly demonstrate, using dual-labeling flow cytometry, that damage-induced phosphorylation of RPA2 on serine4/serine8 occurs primarily in the S and G_2 phases of the cell cycle, and show that the timing of RPA2 phosphorylation can be modulated by inhibition of the checkpoint kinase Chk1. Furthermore, Chk1 inhibition sensitizes polη-deficient cells to the cytotoxic effects of carboplatin. Both hyperphosphorylated RPA2 and the homologous recombination protein Rad51 are present in nuclear foci after cisplatin treatment, but these are separable events in individual cells. These results provide insight into the relationship between cell cycle regulation and processing of platinum-induced DNA damage in human cells when polη-mediated TLS is compromised.

Introduction

Cells are constantly exposed to environmental and metabolic insults such as radiation, chemical agents and oxidative stress. Such exposure may generate DNA lesions that lead to mutations and DNA strand breaks and cause genomic instability. DNA damage from exposure to UV radiation can lead to skin cancer, while DNA damage induced by agents such as platinum-based drugs is routinely used in chemotherapy to kill tumor cells. A number of conserved DNA repair and DNA damage tolerance pathways minimize the effects of DNA damage. A better understanding of these pathways is relevant to both cancer prevention and cancer treatment.[1] Platinum-based chemotherapeutic agents such as cisplatin and carboplatin are widely used in cancer treatment. Carboplatin has a similar range of clinical activity to cisplatin, but causes fewer side effects.[2] Cisplatin and carboplatin both induce DNA damage, primarily at guanine residues, generating monoadducts, intrastrand crosslinks and interstrand crosslinks (ICL), leading to inhibition of DNA replication and transcription, and ultimately to cell death.[2-6] The DNA adducts formed by cisplatin and carboplatin are similar, although approximately 30-fold higher doses of carboplatin are required to obtain equivalent cytotoxic effects.[3,5] However, the efficacy of both drugs is limited by the development of resistance.[7] Tumors can become resistant to platinum-based drugs by a number of mechanisms, including decreased uptake or increased efflux of the drug; increased repair of lesions in DNA, or by DNA tolerance through replication of DNA containing unrepaired damage. Processing of DNA damage induced by platinum-based drugs is complex. In the case of interstrand crosslinks, which covalently link bases on two DNA

*Correspondence to: Michael P. Carty; Email: michael.carty@nuigalway.ie
Submitted: 07/09/09; Revised: 07/14/09; Accepted: 07/25/09
Previously published online: www.landesbioscience.com/journals/cc/article/9624

strands, proteins from a number of cellular pathways, including nucleotide excision repair, mismatch repair, homologous recombination (HR) and the Fanconi anemia protein complex play a role in repair.[2,3,8] Understanding the cellular pathways by which cells process cisplatin and carboplatin-induced DNA damage is important for the design of more efficient platinum-based anticancer drugs.

The process of translesion synthesis (TLS), is one mechanism by which cells can tolerate and survive platinum-induced DNA damage, and may be particularly important in dealing with intrastrand crosslinks.[2] The *POLH* gene product, DNA polymerase η (polη) normally plays a key role in TLS at sites of UV-induced DNA damage.[9-16] Mutations in human *POLH* cause the skin cancer-prone disease xeroderma pigmentosum variant (XPV), characterized on a cellular level by a defect in bypass of UV-induced lesions in DNA,[12,17] and the accumulation of UV-induced mutations in the genome. Structural studies on purified polη demonstrate that the active site of the enzyme, unlike that of replicative polymerases, can accommodate bulky dinucleotide adducts such as the dithymine cyclobutane pyrimidine dimer (CPD), and insert two adenines opposite the lesion.[13] In addition to its main biological role in bypass of UV-induced CPDs, purified polη can bypass cisplatin-induced intrastrand guanine-guanine adducts in oligonucleotide templates in vitro.[13,18] Structural and biochemical analysis of the bypass of a cisplatin-induced guanine-guanine intrastrand crosslink by polη has revealed key features of the active site that facilitate translesion synthesis at these lesions.[19] The role of polη-mediated TLS in DNA damage tolerance in tumor cells is supported by the observation that cells lines lacking polη are more sensitive to killing by platinum-based drugs.[3,20-23]

TLS is an integral component of the network of DNA damage responses in the cell. In the absence of polη, the extent of DNA replication arrest at sites of UV-induced damage is greatly increased.[24,25] Both single-stranded DNA generated by replication fork arrest, and DNA strand break formation resulting from replication fork collapse, activate downstream DNA damage response (DDR) pathways mediated by the phosphoinositide 3-kinase (PI-3K)-related protein kinases (PIKKs)including ataxia-telangiectasia mutated (ATM), ATM and RAD3-related (ATR) and DNA-dependent protein kinase catalytic subunit (DNA-PKcs).[26-31] Polη-deficient cell lines show enhanced replication arrest following exposure to UV radiation or cisplatin,[32,33] with strong activation of the ATR-mediated checkpoint.[34] DNA damage also leads to the generation of DNA strand breaks and activation of ATM and DNA-PK, as evidenced by phosphorylation of PIKK substrates including RPA2, H2AX and Nbs1.[32,33] Thus, polη plays an important role in preventing genome instability after UV- and cisplatin-induced DNA damage.

Inhibition of TLS mediated by polη has been proposed as a potential approach to enhance the effectiveness of platinum-based anti-cancer agents.[19,22,23] However, the consequences of polη-deficiency for cell cycle progression and DDR signaling in response to platinum-based agents require further characterization. Polη-deficient human XPV cell lines represent a useful model in which to begin this investigation. The aim of the present study was to characterize cell cycle progression and DDR activation following treatment of a polη-deficient human cell line with cisplatin and carboplatin.

Results

Effects of cisplatin and carboplatin on cell cycle progression in polη-deficient XP30RO cells. Cells lacking polη are more sensitive to platinum-based anti-cancer drugs.[20-23] Inhibition of polη-mediated TLS represents a potential target for improving the efficacy of these agents.[19] However, the effects of polη-deficiency on cell cycle progression and activation of the DNA damage response (DDR) following exposure of human cells to platinum-based drugs are not well understood on a molecular level. We have characterized the effects of two widely used cancer chemotherapeutics, cisplatin and carboplatin, on cell cycle progression and DDR activation in a DNA polη-deficient human cell line. Polη-deficient XP30RO cells were treated with either 0.5 μg/ml cisplatin or 50 μM carboplatin. These doses were determined to be equitoxic, using the XTT cell viability assay (**Suppl. Fig. 1**). To investigate the effect of drug treatment on DNA replication, cells were pulse-labeled using bromodeoxyuridine (BrdU) (**Fig. 1**). The percentage of cells in S phase or the level of BrdU incorporation does not change in untreated cells over the period between 0 and 48 h (**Fig. 1A and B**, control cells). Treatment with cisplatin inhibited BrdU incorporation in XP30RO cells, as shown by a decreased intensity of BrdU staining in S-phase cells by 12 and 24 h after drug treatment (**Fig. 1A**). An equitoxic dose of carboplatin (50 μM), also inhibited BrdU incorporation in XP30RO cells (**Fig. 1A**). While the intensity of BrdU staining is decreased, the percentage of BrdU-positive cells is higher in drug-treated cells than in control cells (**Fig. 1B**), reflecting accumulation of cells in S-phase for up to 24 h after cisplatin treatment, and for 36 h after carboplatin treatment (**Fig. 1B**). By 36 h after exposure to 0.5 μg/ml cisplatin, and 48 h after exposure to 50 μM carboplatin, the extent of BrdU incorporation is greatly reduced, consistent with entry of cells that have completed replication into the G_2/M phase (**Fig. 1A and B**). Overall, these data show that exposure to cisplatin and carboplatin lead to a prolonged inhibition of DNA replication in polη-deficient XP30RO cells.

To further characterize cell cycle progression in polη-deficient XP30RO cells, cells in G_1 phase were treated with cisplatin or carboplatin, and the level of cyclins E and B, key regulators of the G_1/S and G_2/M phases respectively, was analyzed by western blotting. To generate cells in G_1 phase, cells were first arrested in mitosis using the microtubule inhibitor nocodazole (**Fig. 1C**). Cells were treated with cisplatin or carboplatin 6 hours after release from nocodazole arrest, when the majority of cells are in G_1 phase, although a proportion has not yet exited mitosis (**Fig. 1C**). At the time of treatment the expression of cyclin B is low, consistent with the majority of the cells being in G_1 phase (0 h lanes, **Fig. 1C**). 4 h after mock-treatment, as control cells progress through S phase and into G_2/M phase, expression of both cyclin E and cyclin B increases (**Fig. 1C**). Consistent with the delay in cell cycle progression observed in unsynchronized cell cultures (**Fig. 1A and B**), expression of both cyclin E and cyclin B is reduced following exposure to cisplatin or carboplatin (**Fig.**

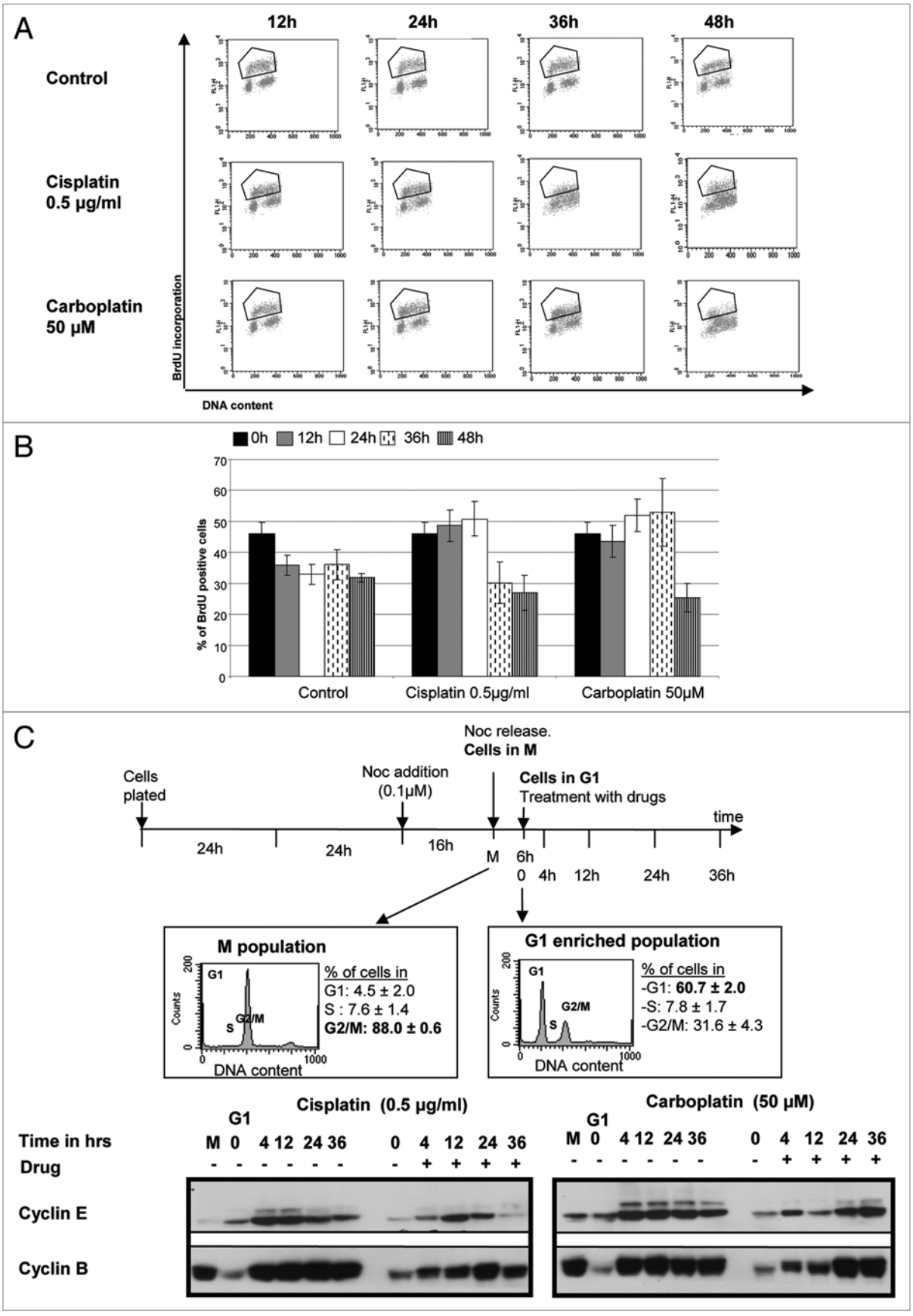

Figure 1. For figure legend, see page 3046.

Figure 1. Effects of treatment with platinum-based drugs on cell cycle progression of polη-deficient cells. (A) XP30RO cells were treated with equitoxic doses (see Suppl. Fig. 1) of cisplatin or carboplatin for the indicated times before being harvested for propidium iodide (PI) and BrdU staining (10 μM BrdU added 1 h before ethanol fixation), and analyzed by flow cytometry. Flow cytometry dot plots from a representative experiment out of three experiments, generated using Cell Quest™, are shown. (B) The percentage of cells incorporating BrdU, determined by analysing BrdU positive cells using Cell Quest™ as in (A), are indicated. Data represent the mean of three independent experiments ± STD. (C) XP30RO cells were synchronized in M phase by treatment with nocodazole (Noc), collected by mitotic shake-off, and released for 6 h to generate a cell population enriched in G_1 phase cells. PI histograms of the mitotic and G_1 cell populations are shown. Cells in G_1 phase were treated with cisplatin or carboplatin before being harvested at the indicated times for analysis of expression of cyclin E and cyclin B by western blotting.

1C). The reduction in cyclin expression reflects delayed S phase progression; no drug-induced G_1 arrest is detected as cells begin BrdU incorporation at the same time after release from nocodazole arrest, independent of drug treatment (data not shown). The lack of G_1 arrest reflects the loss of p53 function in XP30RO cells as a result of SV40 transformation.[10] The peak of cyclin E expression occurs 12 h post-cisplatin treatment, and the peak of cyclin B expression occurs 24 h post-treatment (**Fig. 1C**, left), while highest cyclin E and cyclin B expression is observed 24 to 36 h post-carboplatin treatment (**Fig. 1C**, right).

Kinetics of DDR activation by cisplatin and carboplatin. The PIK kinases ATM, ATR and DNA-PK play a key role in response to DNA damage in human cells.[31] To characterize the sequence of PIK kinase-mediated protein phosphorylation in polη-deficient XP30RO cells in response to cisplatin and carboplatin, we used western blotting with phospho-specific antibodies to analyze the kinetics of phosphorylation of the PIK kinase substrates RPA, Chk1 and H2AX.[27,35,36] RPA is the major single-stranded DNA binding protein in the cell, with numerous roles in DNA metabolism including binding ssDNA generated after replication stress leading to ATR activation.[37] ATR-mediated phosphorylation of the checkpoint kinase Chk1 regulates both replication arrest and entry into mitosis,[26] while PIK kinase-dependent phosphorylation of H2AX on serine 139 is central to the cellular response to DNA strand breaks.[38]

Chk1 ser317 phosphorylation is first detectable 6 h after cisplatin treatment, and 12 h after carboplatin treatment (**Fig. 2A**) and is sustained for up to 48 h after drug treatment (**Fig. 2A**), consistent with checkpoint activation and delayed S phase progression as determined by flow cytometry (**Fig. 1**). Phosphorylation of H2AX on ser139 is induced at 6 h post-cisplatin, and 12 h post-carboplatin, consistent with formation of DNA strand breaks. Strong induction of H2AX phosphorylation occurs 24 h and 36 h after both cisplatin and carboplatin treatment (**Fig. 2A**), possibly due to replication fork collapse when cells attempt to progress through S-phase in the presence of unrepaired DNA damage.[39,40]

In contrast to phosphorylation of Chk1 and H2AX, RPA2 modification is a late event in the response to platinum-induced DNA damage, and is preceded by phosphorylation of both Chk1 and H2AX (**Fig. 2A**). RPA2 phosphorylation on serine4/serine8 is not clearly detectable until 24 h after cisplatin treatment (**Fig. 2A**). Furthermore, in the case of phosphorylation of all three proteins, following exposure to equitoxic doses of each drug, carboplatin-induced phosphorylation is delayed compared to cisplatin-induced phosphorylation. Thus, RPA2 phosphorylation on serine4/serine8 is detectable 24 h after cisplatin treatment, but is not detected until 36 h after carboplatin treatment (**Fig. 2A**). In order to rule out an effect of the period of exposure to the drug on the timing of RPA2 phosphorylation, we compared the kinetics of RPA2 phosphorylation under conditions where cells were either continuously exposed to the drug for the duration of the experiment (**Fig. 2A**), or were treated with the drug for 18 h, with subsequent incubation in drug-free medium (**Fig. 2B**). The latter exposure protocol i.e., 18 h drug exposure followed by incubation in the absence of drug for 48 h, was also used to determine that 0.5 μg/ml cisplatin and 50 μM carboplatin were equitoxic to XP30RO cells (**Suppl. Fig. 1**). When cells were exposed to cisplatin or carboplatin for 18 h, followed by removal of the drug, RPA2 hyperphosphorylation was detectable 6 h after removal of cisplatin, and 12 h after removal of carboplatin. There was little difference in the kinetics of RPA2 phosphorylation following continuous exposure to drug for the duration of the experiment (**Fig. 2A**) compared to when cells were exposed to the drug for 18 h only (**Fig. 2B**). In both cases, RPA2 hyperphosphorylation was first detectable by western blotting 24 h after the beginning of exposure to cisplatin, and 30 h after the beginning of exposure to carboplatin. Thus, DNA damage leading to RPA2 serine4/serine8 phosphorylation has occurred by 18 h of drug exposure, and is not dependent on continued drug exposure.

Treatment of cells in G_1 phase with cisplatin or carboplatin confirms that phosphorylation of RPA2 on serine4/serine8 is a relatively late event after drug treatment, and that the timing differs between cisplatin and carboplatin. RPA2 serine4/serine8 phosphorylation is detectable 12 h after cisplatin treatment, and 24 h after carboplatin treatment (**Fig. 2C**). RPA2 serine4/serine8 phosphorylation coincides with an increase in cyclin E levels in drug-treated cells (**Fig. 1C**), consistent with RPA2 phosphorylation occurring when cells progress through S phase. The difference in the timing of RPA2 phosphorylation following exposure of XP30RO cells to cisplatin or carboplatin may reflect differences either in the rate at which cisplatin and carboplatin-induced lesions form in DNA,[2] in the processing of these lesions, or in cell cycle progression after drug treatment.

Cell cycle dependence of RPA2 hyperphosphorylation. The relationship between cell cycle stage and platinum-induced RPA2 phosphorylation on serine4/serine8 was directly addressed using dual-labeling flow cytometry. Carboplatin-treated cells were dual-labeled for DNA content using PI, and for intracellular hyperphosphorylated RPA2, and analyzed using flow cytometry (**Fig. 3A**). Analysis of DNA content by PI staining shows that cells with carboplatin-induced hyperphosphorylated RPA2 are predominantly in the S and G_2/M phases (**Fig. 3A**). Phosphorylated RPA2 staining represents specific antibody-antigen interaction rather than non-specific antibody binding, as staining is abolished by the use of a phosphoSer4/Ser8-RPA2

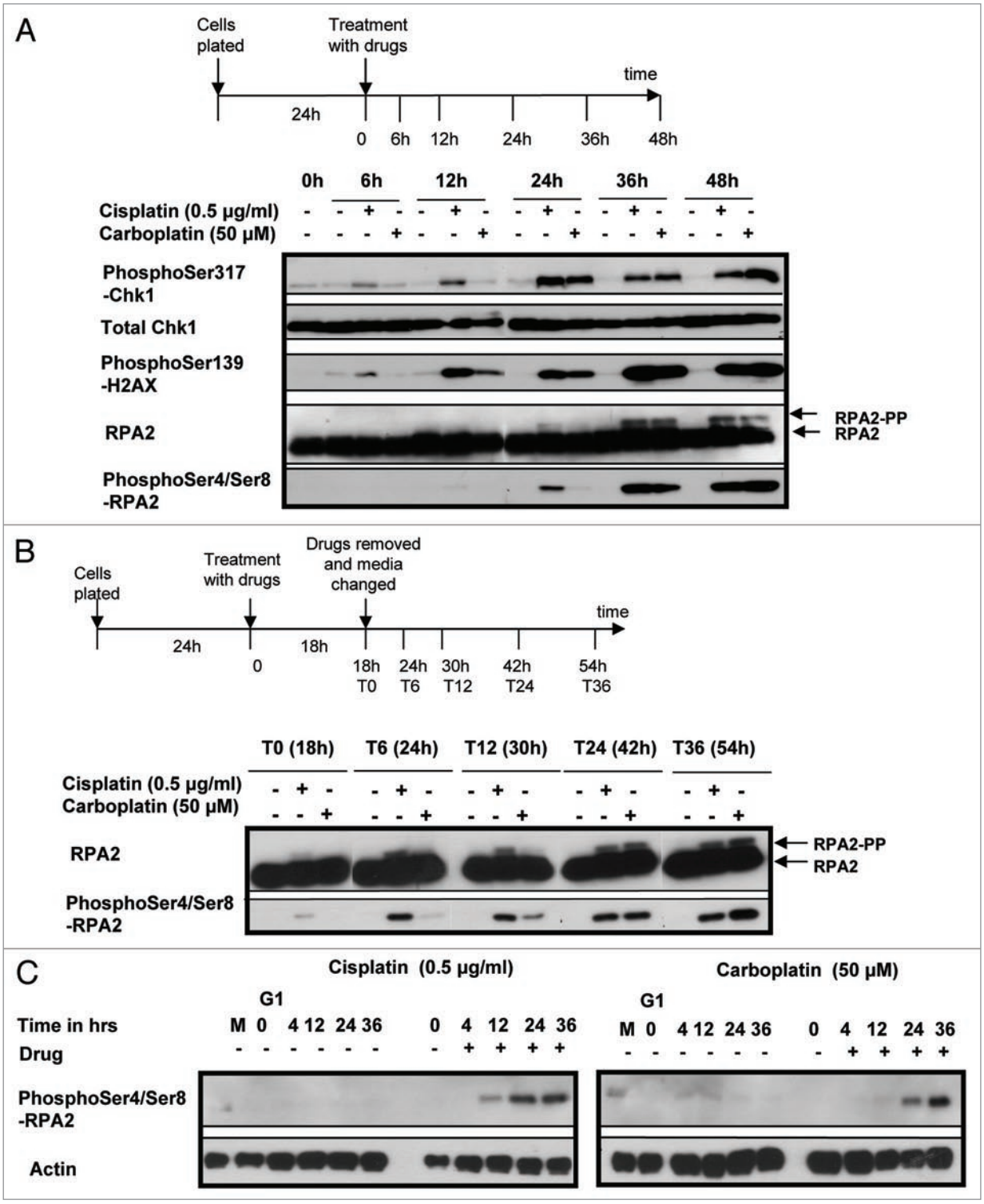

Figure 2. Effect of platinum-based drugs on activation of DNA damage responses in polη-deficient cells. (A) XP30RO cells were treated with equitoxic doses of cisplatin or carboplatin for the indicated times before being harvested for western blot. Chk1 and H2AX phosphorylation were detected using antibodies against the phosphorylated forms of the proteins, respectively Chk1 phosphorylated on serine 317, and H2AX phosphorylated on serine 139. RPA2 hyperphosphorylation was detected either as a shift to a slower mobility form of the protein (arrowed) using an anti-RPA2 antibody, or using an anti-phosphoSer4/Ser8-RPA2 antibody. (B) XP30RO cells were treated with equitoxic doses of cisplatin or carboplatin for 18 h. The drugs were removed and replaced by drug-free medium, and cells were harvested for western blot at the indicated times. RPA2 hyperphosphorylation was detected as in (A). (C) XP30RO cells in G_1 phase (see Fig. 1C and M&M for protocol) were treated with cisplatin or carboplatin. Cell extracts were prepared at the indicated times. RPA2 hyperphosphorylation was detected by western blotting using anti-phosphoSer4/Ser8-RPA2 antibody.

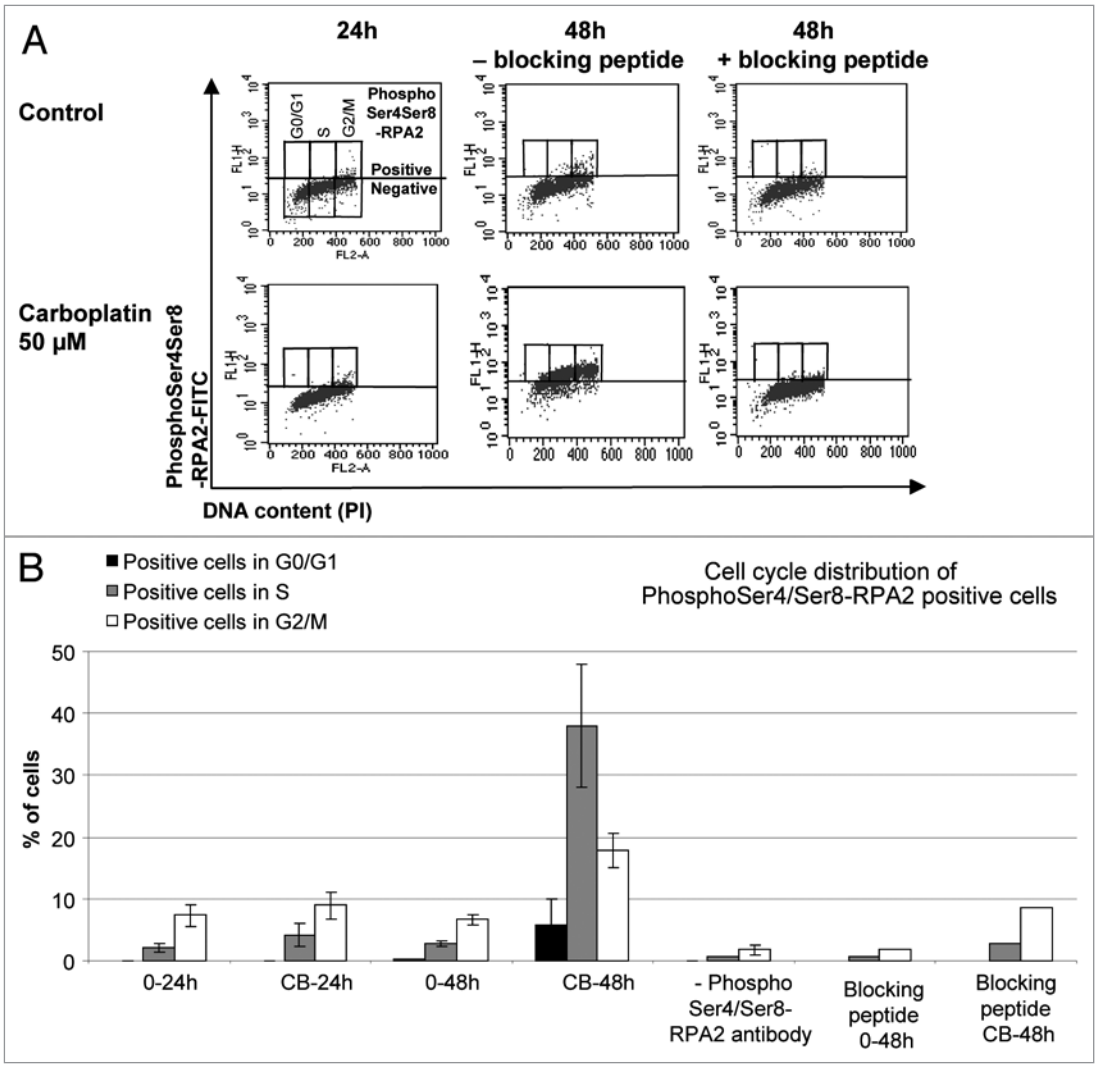

Figure 3. Flow cytometric analysis after co-staining for phosphoSer4/Ser8-RPA2 and DNA content in polη-deficient cells treated with carboplatin. (A) XP30RO cells were mock treated or treated with carboplatin for 24 h and 48 h before being harvested for co-staining for phosphoSer4/Ser8-RPA2, using the anti-phosphoSer4/Ser8-RPA2 and a secondary FITC labelled antibody, and for DNA content, using PI. Flow cytometry acquisition and analysis were performed using a FACSCalibur and Cell Quest™ software. The threshold for phosphoSer4/Ser8-RPA2 positivity was determined using a control cell population stained with the secondary FITC labelled antibody only. A phospho-RPA32 (S4/S8) blocking peptide (Bethyl Laboratories) was added during staining with the anti-phosphoSer4/Ser8-RPA2 antibody in a control and a treated population in order to determine the specificity of the staining. (B) Determination of the cell cycle distribution of the cells positive for phosphoSer4/Ser8-RPA2 was performed using the G_0/G_1, S and G_2/M boxes shown in A using Cell Quest™ software. The data are expressed as the percentages of cells positive in each phase of the cell cycle relative to the total population of cells (i.e., both the cells positive and negative for phosphoSer4/Ser8-RPA2). Data represent the mean of two independent experiments ± STD. 0, mock treated; CB, carboplatin treated.

blocking peptide (**Fig. 3A**). Mock-treated and carboplatin-treated cells present similar dot plots 24 h after treatment (**Fig. 3A**), and less than 10% of these cells are positive for phosphoSer4/Ser8-RPA2 (**Fig. 3B**). Positive cells are mostly in G_2/M (**Fig. 3B**), consistent with the detection of a low level of hyperphosphorylated RPA2 in extracts of mitotic XP30RO cells (**Fig. 2, lanes M**).[41,42] However, 48 h after carboplatin treatment, a high percentage of XP30RO cells are positive for phosphoSer4/Ser8-RPA2, as determined by a shift of cells into the positive region of the dot plot (**Fig. 3A**, compare lower panels 24h and 48h). In cells treated with carboplatin for 48 h, almost 60% of cells are positive for phosphoSer4/Ser8-RPA2, most of which are either in S phase (38%) or in G_2/M (19%) phase (**Fig. 3B**). This analysis directly demonstrates that carboplatin-induced RPA2 hyperphosphorylation occurs primarily in the S and G_2/M phases in polη-deficient XP30RO cells.

Modulation of carboplatin-induced RPA2 hyperphosphorylation using the Chk1 inhibitor UCN-01. If RPA2 hyperphosphorylation is dependent on cells progressing through S phase, inhibition of a carboplatin-induced S-phase checkpoint should accelerate the onset of RPA2 phosphorylation after drug treatment. The checkpoint kinase Chk1 is phosphorylated by ATR after DNA damage and is required for the S phase checkpoint.[43] We examined the effect of UCN-01, an established inhibitor

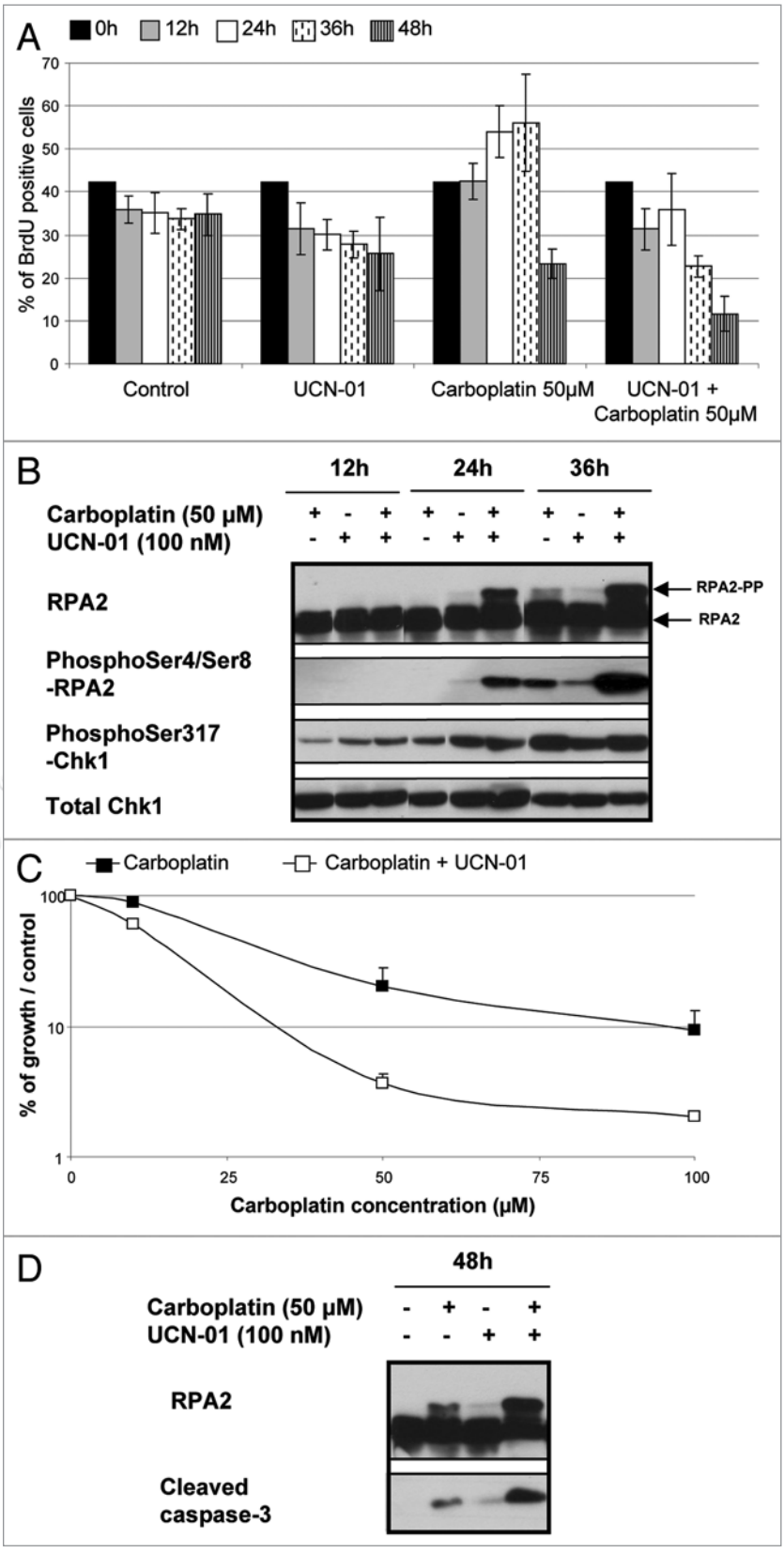

Figure 4. Effect of UCN-01 on RPA2 hyperphosphorylation and cell viability in carboplatin-treated polη-deficient XP30RO cells. (A) XP30RO cells were either mock-treated with DMSO and H_2O, or treated either with 100 nM UCN-01, with 50 μM carboplatin or with both UCN-01 and carboplatin, before being harvested for propidium iodide (PI) and BrdU staining (10 μM BrdU added 1 h before ethanol fixation), and analyzed by flow cytometry. The percentage of cells incorporating BrdU, determined using Cell Quest™, are indicated. Data represent the mean of three independent experiments ± STD for control, carboplatin and carboplatin + UCN-01, and the mean of two independent experiments ± STD for UCN-01. (B) Cell extracts were prepared for western blotting at the indicated times from XP30RO cells treated as in A. RPA2 and Chk1 phosphorylation were detected by western blotting as in Figure 2A. (C) Cells were treated for 18 h, with either 50 μM carboplatin alone or in the presence of 100 nM UCN-01. Drugs were removed and cell viability was measured 48 h later, using the XTT proliferation/toxicity assay (Roche). Data shown is the average of four experiments + one STD. (D) Cell extracts were harvested 48 h after treatment with carboplatin and UCN-01, as indicated for individual lanes. Cleaved caspase-3 and hyperphosphorylated RPA2 were detected by western blotting.

of the Chk1-mediated S phase checkpoint,[44] on carboplatin-induced RPA2 hyperphosphorylation. Carboplatin treatment leads to slowdown of cell cycle progression and accumulation of cells in S phase (**Fig. 4A**). However, UCN-01 abrogates the carboplatin-induced accumulation in S phase (**Fig. 4A**). Consistent with RPA2 hyperphosphorylation being dependent on progression through S phase, UCN-01 leads to earlier and stronger induction of RPA2 hyperphosphorylation in carboplatin-treated cells compared to cells treated with carboplatin alone (**Fig. 4B**). Thus, after 24 h neither carboplatin nor UCN-01 alone induce detectable RPA2 hyperphosphorylation, while co-treatment with carboplatin and UCN-01 strongly induces RPA2 hyperphosphorylation (**Fig. 4B**, compare lanes four, five and six). Inhibition of Chk1 reduces cell cycle arrest after carboplatin treatment and promotes progression through S phase leading to RPA2 hyperphosphorylation. Co-treatment with UCN-01 also sensitizes XP30RO cells to carboplatin, as determined using the XTT assay (**Fig. 4C**). These results are consistent with in vivo data on the effect of UCN-01 on the response to cisplatin.[44] Cleaved caspase-3, a marker of apoptosis is more strongly induced when cells are treated with both carboplatin and UCN-01, supporting the conclusion that UCN-01 sensitizes XP30RO cells to carboplatin by induction of apoptosis (**Fig. 4D**).

Dual staining for Rad51 foci and hyperphosphorylated RPA2. RPA2 hyperphosphorylation on serine4/serine8 may play a role in channeling DNA intermediates generated as a result of replication arrest into downstream repair pathways including homologous recombination (HR).[45,46] Since HR is strongly activated in

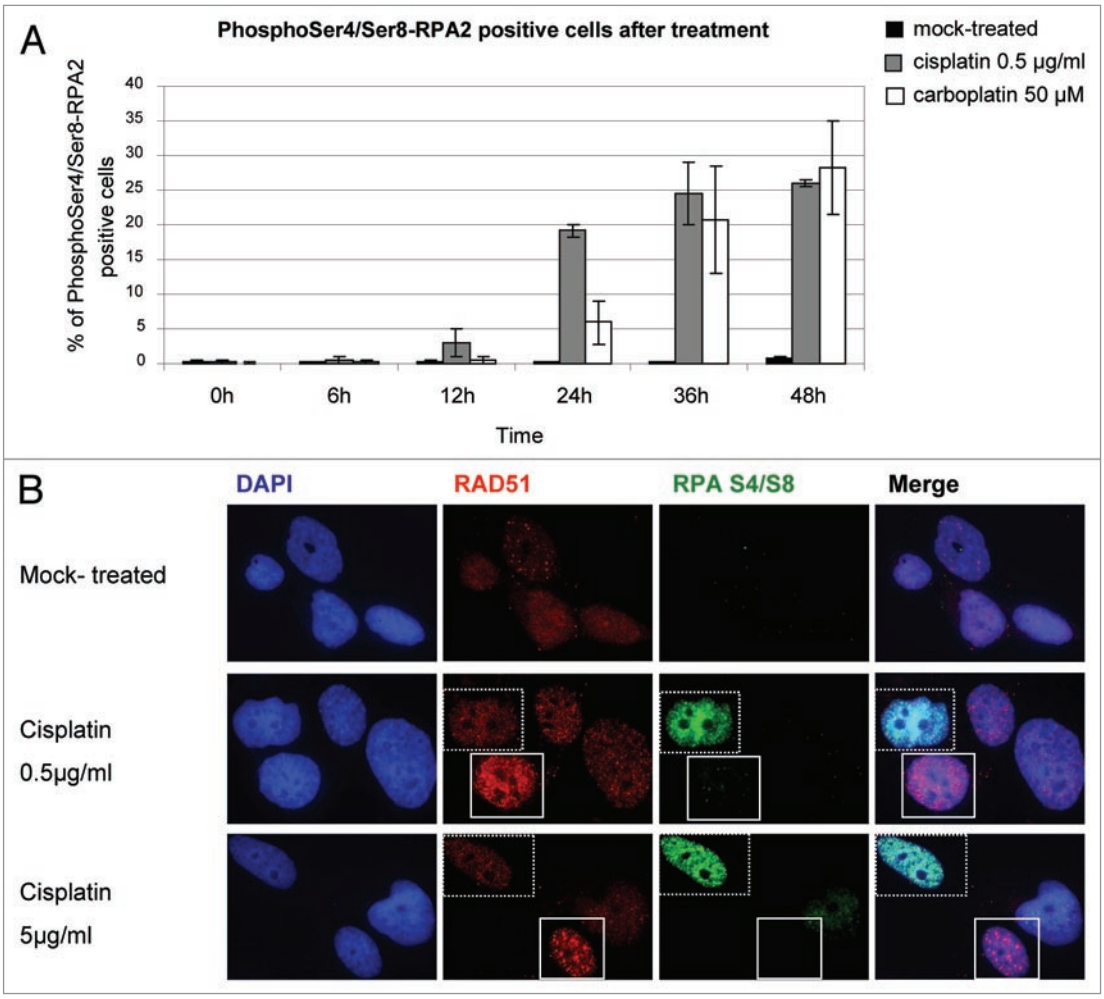

Figure 5. Detection of hyperphosphorylated RPA2 and Rad51 in cisplatin or carboplatin-treated polη-deficient cells. (A) XP30RO cells were grown on coverslips, and immunofluorescence was carried out at the indicated times after treatment with cisplatin or carboplatin. The percentage of cells positive for phosphoSer4/Ser8-RPA2 was determined by counting at least 200 cells per condition. (B) XP30RO cells were either mock-treated or treated with 0.5 or 5 µg/ml cisplatin for 24 h. Cells were stained for both Rad51 and phospho-Ser4/Ser8-RPA2 (see Materials and Methods). Rad51 was detected using a Cy3-coupled secondary anti-mouse antibody, Phospho-Ser4/Ser8-RPA2 was detected using a FITC-coupled secondary anti-rabbit antibody. DNA was counterstained using DAPI. Images were captured using an Olympus fluorescence microscope, at 100x magnification.

polη-deficient cells after DNA damage[47,48] this role of RPA may be especially important in these cells. Immunofluorescence staining confirmed that phosphorylation of RPA2 on serine4/serine8 occurred earlier following treatment with cisplatin than following carboplatin (**Fig. 5A**), consistent with western blotting data (**Fig. 2**). To investigate the relationship between drug-induced RPA2 hyperphosphorylation, and homologous recombination (HR) in XP30RO cells, dual-labeling immunofluorescence was carried out to detect Rad51 foci, and phosphoserine4/serine8 RPA2 in individual cisplatin-treated cells (**Fig. 5B**). 24 h following cisplatin treatment, RPA2 phosphorylated on serine4/serine8, and Rad51 foci were only observed in cisplatin-treated cells (**Fig. 5B**). However, dual-labeling immunofluorescence (**Fig. 5B**) indicates that RPA2 hyperphosphorylation and formation of Rad51 foci are separable events, as individual cells were found to stain strongly for either phosphoSer4/Ser8-RPA2 or for Rad51 foci, but not for both.

Discussion

DNA damage tolerance by translesion synthesis may contribute to the ability of cancer cells to survive replication-blocking lesions induced by platinum-based anti-cancer drugs such as cisplatin and carboplatin.[49] The TLS enzyme DNA polη can bypass lesions induced by platinum-based chemotherapeutic drugs, and polη-deficient human cells are more sensitive than normal cells to both cisplatin and carboplatin (**Suppl. Fig. 1**).[3,20-22] Although the adducts formed by cisplatin and carboplatin are structurally identical, we find that, compared to cisplatin, an approximately thirty-fold higher concentration of carboplatin is required to obtain equivalent cytotoxicity in XP30RO cells.[2,50] Inhibition of polη-mediated TLS may be a potential approach to enhancing the effectiveness of platinum-based anti-cancer agents.[19,22,23] However, the consequences of polη-deficiency for cell cycle pro-

gression and activation of downstream DNA damage responses in platinum-treated cells is not understood in detail.

In the present study, we have characterized cell cycle progression and activation of DNA damage response pathways in a human cell line lacking DNA polη[12,17] following exposure to equitoxic doses of cisplatin and carboplatin. We show that both cisplatin and carboplatin induce a strong S-phase arrest in polη-deficient XP30RO cells, associated with reduced expression of cyclin E and cyclin B. PIK kinase-mediated DNA damage responses, including phosphorylation of Chk1, H2AX and RPA2 are strongly activated. The DNA damage response to equitoxic doses of cisplatin (0.5 μg/ml; 1.7 μM) and carboplatin (50 μM; 18.6 μg/ml) differs, in that PIK kinase-mediated phosphorylation of Chk1, H2AX and RPA2 is activated earlier following cisplatin than following carboplatin treatment. Using dual-labeling flow cytometry we directly demonstrate that RPA2 phosphorylation on serine4 and serine8 occurs primarily in the S and G_2 phases of the cell cycle, and show that the timing of RPA2 hyperphosphorylation can be modulated by altering cell cycle progression using UCN-01, an established inhibitor of the checkpoint kinase Chk1. Furthermore, UCN-01 sensitizes polη-deficient XP30RO cells to carboplatin, indicating that checkpoint activation protects these cells against the cytotoxic effects of platinum-based drugs. Consistent with a role for homologous recombination in repair of cisplatin-induced DNA damage, nuclear Rad51 foci are induced in cisplatin-treated cells. However, formation of Rad51 foci is separable from damage-induced phosphorylation of RPA2 on serine4/serine8, since individual nuclei stain strongly for either Rad51 foci or hyperphosphorylated RPA2.

The delay in S phase progression and the accumulation of cells in S phase, observed following treatment of asynchronously growing XP30RO cells, is consistent with previous reports that cisplatin induces S-phase arrest, and that arrest is more prolonged in polη-deficient cells than in cells expressing polη.[33,51] This is the first demonstration that carboplatin results in a delay in S-phase progression in polη-deficient human cells, and confirms a role for polη in S-phase progression in response to both cisplatin and carboplatin in vivo. Expression of cyclins E and B is delayed and reduced when XP30RO cells in G_1 phase are treated with either cisplatin or carboplatin, consistent with a drug-induced delay in S-phase progression. It has been consistently observed that the S-phase delay following carboplatin treatment occurs later than after cisplatin treatment. This may be due in part to the fact that carboplatin-induced DNA adducts, including interstrand cross-links, form more slowly than cisplatin-induced adducts.[50] Differences in the distribution of adducts in the DNA or in the rate of repair may also contribute to the difference between the two agents. In the present study, the extent of carboplatin-induced S-phase arrest is reduced when XP30RO cells are treated with UCN-01, a known inhibitor of Chk1.[52-56] Chk1 plays a number of roles in the response to DNA damage, including inhibition of replication fork progression and stabilization of arrested forks, as well as inhibition of new origin firing.[57] While UCN-01 may have non-specific effects on other kinases, at the doses used in the present experiments it should show specificity for Chk1 (IC_{50}, 5–30 nM) rather than Chk2 (IC_{50}, 1 μM).[52,58] UCN-01 increases the sensitivity of XP30RO cells to carboplatin (**Fig. 4C and D**), consistent with a role for Chk1-induced replication arrest in protecting cells against the cytotoxic effects of platinum-based drugs. A similar effect of UCN-01 on the toxicity of nucleoside analogues gemcitabine in human leukemia cell lines has also been reported.[59] However, the capacity of individual platinum-based drugs to induce both common and unique cellular responses requires further investigation, since for example, cisplatin-induced cytotoxicity and cell cycle arrest in human fibroblasts and U20S osteosarcoma cells were found to require ATR, while the response to oxaliplatin was ATR-independent.[60]

TLS by polymerases including polη, plays an important role in determining the extent of replication inhibition by platinum-based agents.[7,23] Despite the absence of polη in XP30RO cells, cells eventually progress through S phase. In absence of polη, TLS at sites of intrastrand cisplatin lesions may be carried out in a slow, error-prone process by pol kappa.[61] Thus, the transient cell cycle arrest observed here after cisplatin and carboplatin treatment could result from DNA replication being impaired at intrastrand crosslinks due to the absence of polη-mediated cells TLS, followed by resumption of replication fork progression in a process dependent on recruitment of other TLS polymerases such as pol kappa.[61] Alterations in TLS and consequently replication fork arrest at damage sites will affect the extent of activation of the DDR, mediated by protein phosphorylation by PIK kinases.[26-31] Our analysis of the timing of induction of phosphorylation of key PIK kinase substrates including Chk1, H2AX and RPA2 in polη-deficient in response to both cisplatin and carboplatin is consistent with both platinum-based drugs inducing a common DDR response. However, DDR activation is delayed after carboplatin treatment compared to cisplatin treatment, possibly due to differences in the rates of adduct formation, DNA repair or lesion bypass.[2] Both cisplatin and carboplatin induce ATR-mediated phosphorylation of Chk1 on serine 317, and the timing of Chk1 activation is consistent with S-phase arrest (**Figs. 1 and 2**). H2AX phosphorylation also occurs in response to both drugs, consistent with DNA strand break formation. While cisplatin does not directly induce DNA strand breaks, γ–H2AX formation has been shown to be dependent on DNA replication in cisplatin-treated human and rodent cells, rather than reflecting cross-link repair.[40] The formation of strand breaks is probably due to fork stalling at platinum adducts and fork collapse.[39,40]

Hyperphosphorylation of RPA2 on serine4/serine8 is a late event after cisplatin- and carboplatin-induced DNA damage. Thus, it can not account for the initial checkpoint response observed in treated cells. Although RPA is required for recruitment of TLS polymerases to sites of replication fork arrest in a Rad6/18-dependent process,[62] the present data show that hyperphosphorylation of RPA2 does not play a role in the initial step of the damage response. Comparison between the induction of RPA2 hyperphosphorylation and the kinetics of S phase accumulation show that S phase accumulation is paralleled by the induction of RPA2 hyperphosphorylation (**Figs. 1–3**). Moreover, dual-labeling experiments for DNA content and hyperphosphorylated RPA2 shows that cells with hyperphosphorylated RPA2

after carboplatin exposure are predominantly in S and G_2/M phases, consistent with RPA2 hyperphosphorylation occurring when cells are progressing through S and into G_2/M. The dependence of RPA2 hyperphosphorylation on S-phase progression is supported by strong increase in RPA2 phosphorylation on serine4/serine8 when Chk1 is inhibited using UCN-01. This is consistent with previous demonstration that UCN-01 increases gemcitabine-induced H2AX phosphorylation.[59]

RPA2 is phosphorylated at a number of sites in the N-terminal in a cell cycle-dependent manner,[45,63,64] and following DNA damage.[41,45,65-71] The observation that H2AX phosphorylation precedes RPA2 hyperphosphorylation, is consistent with DSB induction by cisplatin and carboplatin and subsequent activation of PIK kinase activation which in turn phosphorylate RPA2. We have previously shown that cisplatin-induced RPA2 hyperphosphorylation is DNA-PK-dependent.[33] As noted above, cisplatin does not directly induce DNA strand breaks.[40] However, double-strand breaks could result from fork collapse at intrastrand crosslinks in the absence of polη to carry out efficient TLS. Alternatively, or in addition, replication-dependent repair of interstrand crosslinks in DNA[4,72] generates strand breaks as intermediates in the repair process, and requires homologous recombination, as well as the activity of the NER factor ERCC1/XPF.[73] The observation that Rad51 foci are formed following cisplatin treatment, and that, as shown by our dual-labeling experiments, RPA2 hyperphosphorylation occurs in the S and G_2 phases when HR can occur,[74] supports a model in which Rad51 foci and hyperphosphorylated RPA2 are markers of HR-mediated double-strand break repair. This would be consistent with the increased level of RPA2 serine4/serine8 phosphorylation seen in polη-deficient cells,[33] since homologous recombination is highly activated in polη-deficient cells in response to DNA damage, as cells attempt to deal with replication forks arrested at sites of DNA damage.[48,75,76] Our immunofluorescence data shows that individual nuclei stain strongly for either Rad51 foci or RPA2 phosphorylated on serine4/serine8 suggesting that the two events may not be involved in a common DNA damage response. An alternative is that phosphorylation of RPA2 on serine4/serine8 and formation of Rad51 foci represent distinct steps in the HR process, such that for example phosphorylation of RPA2 is required for its interaction with Rad52, which promotes loading of Rad51 at the site of the strand break and subsequent Rad51-mediated repair.[77,78] Further investigation is required to characterize the role of RPA2 phosphorylation and Rad51 in the response to platinum-induced DNA damage when polη-mediated TLS is compromised.

Materials and Methods

Cell culture. Human skin-derived SV40-transformed XP30RO (GM03617A) fibroblast cells, which lack functional polη as a result of a 13-base pair deletion in exon 2 of *POLH*[12,17] were grown in Minimal Essential Medium Eagle-Earle BSS (MEM), supplemented with 15% uninactivated fetal bovine serum (FBS), 2X essential and non-essential amino acids, and vitamins, with 2 mM L-glutamine.[32]

Cell treatment. 48 h before treatment, 4 x 10^5 cells were plated in 60 mm dishes. Cells were treated either with cisplatin ('Ebewe' 1 mg/ml solution), or with carboplatin, from a 20 μM stock solution prepared in distilled water and stored at 4°C. Cisplatin or carboplatin was added directly to the cell culture medium at the indicated doses, and the cells were incubated in the presence of the drug as described for individual experiments. Where indicated, cells were also treated with 100 nM UCN-01 (Sigma) from a stock solution of 1 mM in DMSO, alone or in the presence of 50 μM carboplatin. Control cell cultures were treated with equivalent volumes of water or DMSO. Cells were subsequently harvested for western blot, immunofluorescence and FACS analysis, as described for individual experiments.

Cell toxicity assay. For determination of equitoxic doses of cisplatin and carboplatin, normal GM00637I and polη-deficient XP30RO (GM03617A) fibroblast cells were used. GM00637I cells were grown under the same conditions as XP30RO cells. Cells were seeded in triplicate in 96-well plates at 5 x 10^3 cells per well. After treatment for 18 h with 0–1 μg/ml (0–3.3 μM) of cisplatin or 0–100 μM (0–37.1 μg/ml) of carboplatin, media was removed and cells were allowed to recover for 48 h. Cell viability was measured using the XTT assay (Roche). To determine the effect of UCN-01 on carboplatin toxicity, XP30RO cells were treated 0–100 μM carboplatin for 18 h, in the presence or absence of 100 nM UCN-01. After drug removal, cells were incubated in fresh medium for 48 h, and cell viability was determined using the XTT assay.

Cell cycle analysis. Cell cycle progression following treatment with cisplatin or carboplatin, was analyzed using flow cytometry using a FACSCalibur system after PI staining of the cells, as described.[32] Where indicated, cells were pulse-labelled with 10 μM bromodeoxyuridine (BrdU) 1 h before being harvested, and analyzed by flow cytometry for BrdU/PI using a FACSCalibur (BD) as described previously.[32] Data was analyzed using Cell Quest™ software.

Mitotic arrest. XP30RO cells were treated with the microtubule inhibitor nocodazole (0.1 μM) dissolved in DMSO, for 16 h. Cells in M phase were collected by mitotic shake-off, and nocodazole was removed by washing with medium. 6 x 10^5 cells were replated on 60 mm dishes. Mitotic cells were released for 6 h to generate cells in G_1 phase, before being treated with cisplatin (Sigma; 0.5 μg/ml, in DMSO) or carboplatin (50 μM). Cells were harvested for flow cytometry or western blotting at intervals as indicated in individual experiments.

Dual-labeling and flow cytometric analysis of cell cycle stage and RPA2 hyperphosphorylation. After drug exposure, cells were fixed and permeabilized using Fix and Perm® solution (ADG, Bio Research GMBH), and were then incubated with 100 μl of a 1/500 dilution of anti-phosphoSer4/Ser8-RPA2 antibody (Bethyl Laboratories) for 1 h at room temperature. Cells were washed with PBS, and stained with secondary antibody, anti-rabbit-FITC at a 1/1,000 dilution for 45 min at room temperature in the dark. After washing in PBS, the cells were incubated in PI/RNase staining solution (BD Biosciences) for 45 min, before being analyzed by flow cytometry using a FASCalibur (BD Pharmingen). As a control for the specificity of antibody binding, an excess of

phospho-RPA32 (S4/S8) blocking peptide (Bethyl Laboratories, 3 μg of blocking peptide per 0.2 μg of antibody) was added during primary antibody staining step. Data analysis was carried out using Cell Quest™ software.

Immunoblotting. Whole cell lysates were prepared in PBS containing 1% Triton X-100, 0.5% DOC, 0.1% SDS, and protease and phosphatase inhibitors as described previously.[32] Protein concentration was determined using the DC assay (BioRad). Proteins were separated by SDS-PAGE, transferred to PVDF membrane, and analyzed by western immunoblotting. Where indicated, membranes were probed overnight at 4°C with one of the following antibodies: anti-phosphoSer4/Ser8-RPA2 (1/4,000, Bethyl Laboratories), anti-phosphoSer317Chk1 (1/1,000, Cell Signalling), anti-Chk1 (1/1,000, Sigma), anti-phosphoSer139-H2AX (1/1,000, UpstateTechnologies), anti-cyclin E (1/1,000, Sigma), anti-cyclin B (1/1,000, ThermoScientific), anti-actin (1/5,000, Sigma), and anti-cleaved caspase-3 (1/1,000, Cell Signalling). Blots were incubated with horseradish peroxidase-linked secondary antibody (Jackson Immunochemicals) and visualized using the ECL+ chemiluminescence method (Amersham).

Immunofluorescence. Cells grown on glass coverslips were treated with the drugs. After treatment, cells were pre-permeabilized with a hypotonic solution (20 mM HEPES (pH 8), 20 mM NaCl, 5 mM $MgCl_2$, 1 mM ATP, 0.1 mM Na_3VO_4, 1 mM NaF and 0.5% NP40) for 15 min on ice before fixation in 4% paraformaldehyde (w/v) in PBS for 10 min.[79] Cells were then permeabilized with 0.1% Triton X-100 in PBS, and blocked using PBS containing 1% BSA and 0.1% Triton X-100 for 30 min at room temperature. Cells were then stained using mouse anti-Rad51 (1/1,000, AbCam) detected by a Cy3-labelled anti-mouse antibody (Jackson Immunochemicals), followed by a rabbit anti-phosphoSer4/Ser8-RPA2 antibody (1/4,000, Bethyl Laboratories) detected using a FITC-labelled anti-rabbit antibody. Nuclear DNA was subsequently stained with DAPI, and the cells were mounted on slides in SlowFade (Invitrogen). Images were captured using an Olympus fluorescence microscope, at 100x magnification. The percentage of cells positive for phosphoSer4/Ser8-RPA2 was determined by scoring at least 200 cells, in different fields, for each experimental condition.

Acknowledgements

We thank Dr. C. Morrison and Dr. H.P. Nasheuer for gifts of anti-cyclins antibodies. We thank Sarah Conmy for her help in the optimization of the dual labeling PI/Ser4-Ser8-FITC experiment for FACS.

This research was supported by a Health Research Board research grant (M.P.C., S.C.-H.), by the Irish Research Council for Science Engineering and Technology (IRCSET) (A.S., E.O'.M.), by a NUI Galway College of Science postgraduate fellowship (S.V.).

Note

Supplementary materials can be found at:
www.landesbioscience.com/supplement/Cruet-HennequartCC8-18-Sup.pdf

References

1. Bartek J, Lukas J, Bartkova J. DNA damage response as an anti-cancer barrier: damage threshold and the concept of 'conditional haploinsufficiency'. Cell Cycle 2007; 6:2344-7.
2. Kelland L. The resurgence of platinum-based cancer chemotherapy. Nat Rev Cancer 2007; 7:573-84.
3. Chaney SG, Campbell SL, Bassett E, Wu Y. Recognition and processing of cisplatin- and oxaliplatin-DNA adducts. Crit Rev Oncol Hematol 2005; 53:3-11.
4. Dronkert ML, Kanaar R. Repair of DNA interstrand cross-links. Mutat Res 2001; 486:217-47.
5. Kartalou M, Essigmann JM. Recognition of cisplatin adducts by cellular proteins. Mutat Res 2001; 478:1-21.
6. McHugh PJ, Spanswick VJ, Hartley JA. Repair of DNA interstrand crosslinks: molecular mechanisms and clinical relevance. Lancet Oncol 2001; 2:483-90.
7. Stewart DJ. Mechanisms of resistance to cisplatin and carboplatin. Crit Rev Oncol Hematol 2007; 63:12-31.
8. Wang D, Lippard SJ. Cellular processing of platinum anticancer drugs. Nat Rev Drug Discov 2005; 4:307-20.
9. Carty MP, Glynn M, Maher M, Smith T, Yao J, Dixon K, et al. The RAD30 cancer susceptibility gene. Biochem Soc Trans 2003; 31:252-6.
10. Cleaver JE, Bartholomew J, Char D, Crowley E, Feeney L, Limoli CL. Polymerase [eta] and p53 jointly regulate cell survival, apoptosis and Mre11 recombination during S phase checkpoint arrest after UV irradiation. DNA Repair 2002; 1:41-57.
11. Cordeiro-Stone M, Nikolaishvili-Feinberg N. Asymmetry of DNA replication and translesion synthesis of UV-induced thymine dimers. Mutat Res 2002; 510:91-106.
12. Johnson RE, Kondratick CM, Prakash S, Prakash L. hRAD30 mutations in the variant form of xeroderma pigmentosum. Science 1999; 285:263-5.
13. Masutani C, Kusumoto R, Iwai S, Hanaoka F. Mechanisms of accurate translesion synthesis by human DNA polymerase eta. EMBO J 2000; 19:3100-9.
14. Stary A, Kannouche P, Lehmann AR, Sarasin A. Role of DNA polymerase eta in the UV mutation spectrum in human cells. J Biol Chem 2003; 278:18767-75.
15. Thakur M, Wernick M, Collins C, Limoli CL, Crowley E, Cleaver JE. DNA polymerase eta undergoes alternative splicing, protects against UV sensitivity and apoptosis, and suppresses Mre11-dependent recombination. Genes Chromosomes Cancer 2001; 32:222-35.
16. Yao J, Dixon K, Carty MP. A single (6-4) photoproduct inhibits plasmid DNA replication in xeroderma pigmentosum variant cell extracts. Environ Mol Mutagen 2001; 38:19-29.
17. Masutani C, Kusumoto R, Yamada A, Dohmae N, Yokoi M, Yuasa M, et al. The XPV (xeroderma pigmentosum variant) gene encodes human DNA polymerase eta. Nature 1999; 399:700-4.
18. Vaisman A, Masutani C, Hanaoka F, Chaney SG. Efficient translesion replication past oxaliplatin and cisplatin GpG adducts by human DNA polymerase eta. Biochemistry 2000; 39:4575-80.
19. Alt A, Lammens K, Chiocchini C, Lammens A, Pieck JC, Kuch D, et al. Bypass of DNA lesions generated during anticancer treatment with cisplatin by DNA polymerase eta. Science 2007; 318:967-70.
20. Yamada K, Takezawa J, Ezaki O. Translesion replication in cisplatin-treated xeroderma pigmentosum variant cells is also caffeine-sensitive: features of the error-prone DNA polymerase(s) involved in UV-mutagenesis. DNA Repair 2003; 2:909-24.
21. Bassett E, King NM, Bryant MF, Hector S, Pendyala L, Chaney SG, Cordeiro-Stone M. The role of DNA polymerase eta in translesion synthesis past platinum-DNA adducts in human fibroblasts. Cancer Res 2004; 64:6469-75.
22. Chen YW, Cleaver JE, Hanaoka F, Chang CF, Chou KM. A novel role of DNA polymerase eta in modulating cellular sensitivity to chemotherapeutic agents. Mol Cancer Res 2006; 4:257-65.
23. Albertella MR, Green CM, Lehmann AR, O'Connor MJ. A role for polymerase eta in the cellular tolerance to cisplatin-induced damage. Cancer Res 2005; 65:9799-806.
24. Boyer JC, Kaufmann WK, Brylawski BP, Cordeiro-Stone M. Defective postreplication repair in xeroderma pigmentosum variant fibroblasts. Cancer Res 1990; 50:2593-8.
25. Cordeiro-Stone M, Zaritskaya LS, Price LK, Kaufmann WK. Replication fork bypass of a pyrimidine dimer blocking leading strand DNA synthesis. J Biol Chem 1997; 272:13945-54.
26. Cimprich KA, Cortez D. ATR: an essential regulator of genome integrity. Nat Rev Mol Cell Biol 2008; 9:616-27.
27. Abraham RT. PI3-kinase related kinases: 'big' players in stress-induced signaling pathways. DNA Repair 2004; 3:883-7.
28. Bakkenist CJ, Kastan MB. Initiating cellular stress responses. Cell 2004; 118:9-17.
29. Branzei D, Foiani M. Regulation of DNA repair throughout the cell cycle. Nat Rev Mol Cell Biol 2008; 9:297-308.
30. Durocher D, Jackson SP. DNA-PK, ATM and ATR as sensors of DNA damage: variations on a theme? Curr Opin Cell Biol 2001; 13:225-31.
31. Harper JW, Elledge SJ. The DNA damage response: ten years after. Mol Cell 2007; 28:739-45.
32. Cruet-Hennequart S, Coyne S, Glynn MT, Oakley GG, Carty MP. UV-induced RPA phosphorylation is increased in the absence of DNA polymerase eta and requires DNA-PK. DNA Repair 2006; 5:491-504.

33. Cruet-Hennequart S, Glynn MT, Murillo LS, Coyne S, Carty MP. Enhanced DNA-PK-mediated RPA2 hyperphosphorylation in DNA polymerase eta-deficient human cells treated with cisplatin and oxaliplatin. DNA Repair 2008; 7:582-96.
34. Bomgarden RD, Lupardus PJ, Soni DV, Yee MC, Ford JM, Cimprich KA. Opposing effects of the UV lesion repair protein XPA and UV bypass polymerase eta on ATR checkpoint signaling. EMBO J 2006; 25:2605-14.
35. Zhou BB, Elledge SJ. The DNA damage response: putting checkpoints in perspective. Nature 2000; 408:433-9.
36. Matsuoka S, Ballif BA, Smogorzewska A, McDonald ER, III, Hurov KE, Luo J, et al. ATM and ATR substrate analysis reveals extensive protein networks responsive to DNA damage. Science 2007; 316:1160-6.
37. Binz SK, Sheehan AM, Wold MS. Replication protein A phosphorylation and the cellular response to DNA damage. DNA Repair 2004; 3:1015-24.
38. Chanoux RA, Yin B, Urtishak KA, Asare A, Bassing CH, Brown EJ. ATR and H2AX cooperate in maintaining genome stability under replication stress. J Biol Chem 2008; 806739200.
39. Branzei D, Foiani M. Interplay of replication checkpoints and repair proteins at stalled replication forks. DNA Repair 2007; 6:994-1003.
40. Olive PL, Banath JP. Kinetics of H2AX phosphorylation after exposure to cisplatin. Cytometry B Clin Cytom 2009; 76:79-90.
41. Anantha RW, Sokolova E, Borowiec JA. RPA phosphorylation facilitates mitotic exit in response to mitotic DNA damage. Proc Natl Acad Sci USA 2008; 105:12903-8.
42. Stephan H, Concannon C, Kremmer E, Carty MP, Nasheuer HP. Ionizing radiation-dependent and independent phosphorylation of the 32 kDa subunit of replication protein A during mitosis. Nucleic Acids Res 2009; In Press.
43. Paulsen RD, Cimprich KA. The ATR pathway: Fine-tuning the fork. DNA Repair 2007; 6:953-66.
44. Perez RP, Lewis LD, Beelen AP, Olszanski AJ, Johnston N, Rhodes CH, et al. Modulation of cell cycle progression in human tumors: a pharmacokinetic and tumor molecular pharmacodynamic study of cisplatin plus the Chk1 inhibitor UCN-01 (NSC 638850). Clin Cancer Res 2006; 12:7079-85.
45. Oakley GG, Loberg LI, Yao J, Risinger MA, Yunker RL, Zernik-Kobak M, et al. UV-induced hyperphosphorylation of replication protein a depends on DNA replication and expression of ATM protein. Mol Biol Cell 2001; 12:1199-213.
46. Wu X, Yang Z, Liu Y, Zou Y. Preferential localization of hyperphosphorylated replication protein A to double-strand break repair and checkpoint complexes upon DNA damage. Biochem J 2005; 391:473-80.
47. Limoli CL, Giedzinski E, Bonner WM, Cleaver JE. UV-induced replication arrest in the xeroderma pigmentosum variant leads to DNA double-strand breaks, gammaH2AX formation and Mre11 relocalization. Proc Natl Acad Sci USA 2002; 99:233-8.
48. Limoli CL, Giedzinski E, Cleaver JE. Alternative recombination pathways in UV-irradiated XP variant cells. Oncogene 2005; 24:3708-14.
49. Kelland L. Broadening the clinical use of platinum drug-based chemotherapy with new analogues. Satraplatin and picoplatin. Expert Opin Investig Drugs 2007; 16:1009-21.
50. Knox RJ, Friedlos F, Lydall DA, Roberts JJ. Mechanism of cytotoxicity of anticancer platinum drugs: Evidence that cis-diamminedichloroplatinum(II) and cis-diammine-(1,1-cyclobutanedicarboxylato)platinum(II) differ only in the kinetics of their interaction with DNA. Cancer Res 1986; 46:1972-9.
51. Pani E, Stojic L, El-Shemerly M, Jiricny J, Ferrari S. Mismatch repair status and the response of human cells to cisplatin. Cell Cycle 2007; 6:1796-802.
52. Busby EC, Leistritz DF, Abraham RT, Karnitz LM, Sarkaria JN. The radiosensitizing agent 7-hydroxystaurosporine (UCN-01) inhibits the DNA damage checkpoint kinase hChk1. Cancer Res 2000; 60:2108-12.
53. Graves PR, Yu L, Schwarz JK, Gales J, Sausville EA, O'Connor PM, Piwnica-Worms H. The Chk1 protein kinase and the Cdc25C regulatory pathways are targets of the anticancer agent UCN-01. J Biol Chem 2000; 275:5600-5.
54. Kohn EA, Ruth ND, Brown MK, Livingstone M, Eastman A. Abrogation of the S phase DNA damage checkpoint results in S phase progression or premature mitosis depending on the concentration of 7-hydroxystaurosporine and the kinetics of Cdc25C activation. J Biol Chem 2002; 277:26553-64.
55. Seiler JA, Conti C, Syed A, Aladjem MI, Pommier Y. The intra-S-phase checkpoint affects both DNA replication initiation and elongation: single-cell and -DNA fiber analyses. Mol Cell Biol 2007; 27:5806-18.
56. Shao RG, Cao CX, Shimizu T, O'Connor PM, Kohn KW, Pommier Y. Abrogation of an S-phase checkpoint and potentiation of camptothecin cytotoxicity by 7-hydroxystaurosporine (UCN-01) in human cancer cell lines, possibly influenced by p53 function. Cancer Res 1997; 57:4029-35.
57. Enders GH. Expanded Roles for Chk1 in Genome Maintenance. J Biol Chem 2008; 283:17749-52.
58. Jackson JR, Gilmartin A, Imburgia C, Winkler JD, Marshall LA, Roshak A. An indolocarbazole inhibitor of human checkpoint kinase (Chk1) abrogates cell cycle arrest caused by DNA damage. Cancer Res 2000; 60:566-72.
59. Ewald B, Sampath D, Plunkett W. H2AX phosphorylation marks gemcitabine-induced stalled replication forks and their collapse upon S-phase checkpoint abrogation. Mol Cancer Ther 2007; 6:1239-48.
60. Lewis KA, Lilly KK, Reynolds EA, Sullivan WP, Kaufmann SH, Cliby WA. Ataxia telangiectasia and rad3-related kinase contributes to cell cycle arrest and survival after cisplatin but not oxaliplatin. Mol Cancer Ther 2009; 8:855-63.
61. Shachar S, Ziv O, Avkin S, Adar S, Wittschieben J, Reiszner T, et al. Two-polymerase mechanisms dictate error-free and error-prone translesion DNA synthesis in mammals. EMBO J 2009; 28:383-93.
62. Davies AA, Huttner D, Daigaku Y, Chen S, Ulrich HD. Activation of ubiquitin-dependent DNA damage bypass is mediated by replication protein a. Mol Cell 2008; 29:625-36.
63. Fotedar R, Roberts JM. Cell cycle regulated phosphorylation of RPA-32 occurs within the replication initiation complex. EMBO J 1992; 11:2177-87.
64. Niu H, Erdjument-Bromage H, Pan ZQ, Lee SH, Tempst P, Hurwitz J. Mapping of amino acid residues in the p34 subunit of human single-stranded DNA-binding protein phosphorylated by DNA-dependent protein kinase and Cdc2 kinase in vitro. J Biol Chem 1997; 272:12634-41.
65. Carty MP, Zernik-Kobak M, McGrath S, Dixon K. UV light-induced DNA synthesis arrest in HeLa cells is associated with changes in phosphorylation of human single-stranded DNA-binding protein. EMBO J 1994; 13:2114-23.
66. Liu VF, Weaver DT. The ionizing radiation-induced replication protein A phosphorylation response differs between ataxia telangiectasia and normal human cells. Mol Cell Biol 1993; 13:7222-31.
67. Oakley GG, Patrick SM, Yao J, Carty MP, Turchi JJ, Dixon K. RPA phosphorylation in mitosis alters DNA binding and protein-protein interactions. Biochemistry 2003; 42:3255-64.
68. Olson E, Nievera CJ, Klimovich V, Fanning E, Wu X. RPA2 is a direct downstream target for ATR to regulate the S-phase checkpoint. J Biol Chem 2006; 281:39517-33.
69. Patrick SM, Oakley GG, Dixon K, Turchi JJ. DNA damage induced hyperphosphorylation of replication protein A2. Characterization of DNA binding activity, protein interactions and activity in DNA replication and repair. Biochemistry 2005; 44:8438-48.
70. Zernik-Kobak M, Vasunia K, Connelly M, Anderson CW, Dixon K. Sites of UV-induced phosphorylation of the p34 subunit of replication protein A from HeLa cells. J Biol Chem 1997; 272:23896-904.
71. Anantha RW, Vassin VM, Borowiec JA. Sequential and synergistic modification of human RPA stimulates chromosomal DNA repair. J Biol Chem 2007; 282:35910-23.
72. Bessho T. Induction of DNA replication-mediated double strand breaks by psoralen DNA interstrand cross-links. J Biol Chem 2003; 278:5250-4.
73. Niedernhofer LJ, Odijk H, Budzowska M, van Drunen E, Maas A, Theil AF, et al. The structure-specific endonuclease Ercc1-Xpf is required to resolve DNA interstrand cross-link-induced double-strand breaks. Mol Cell Biol 2004; 24:5776-87.
74. McIlwraith MJ, Vaisman A, Liu Y, Fanning E, Woodgate R, West SC. Human DNA polymerase eta promotes DNA synthesis from strand invasion intermediates of homologous recombination. Mol Cell 2005; 20:783-92.
75. Limoli CL, Giedzinski E, Morgan WF, Cleaver JE. Inaugural article: polymerase eta deficiency in the xeroderma pigmentosum variant uncovers an overlap between the S phase checkpoint and double-strand break repair. Proc Natl Acad Sci USA 2000; 97:7939-46.
76. Limoli CL, Laposa R, Cleaver JE. DNA replication arrest in XP variant cells after UV exposure is diverted into an Mre11-dependent recombination pathway by the kinase inhibitor wortmannin. Mutat Res 2002; 510:121-9.
77. Deng X, Prakash A, Dhar K, Baia GS, Kolar C, Oakley GG, Borgstahl GE. Human replication protein A-Rad52-single-stranded DNA complex: stoichiometry and evidence for strand transfer regulation by phosphorylation. Biochemistry 2009; 48:6633-43.
78. Sleeth KM, Sørensen CS, Issaeva N, Dziegielewski J, Bartek J, Helleday T. RPA mediates recombination repair during replication stress and is displaced from DNA by checkpoint signalling in human cells. J Mol Biol 2007; 373:38-47.
79. Richard DJ, Bolderson E, Cubeddu L, Wadsworth RIM, Savage K, Sharma GG, et al. Single-stranded DNA-binding protein hSSB1 is critical for genomic stability. Nature 2008; 453:677-81.

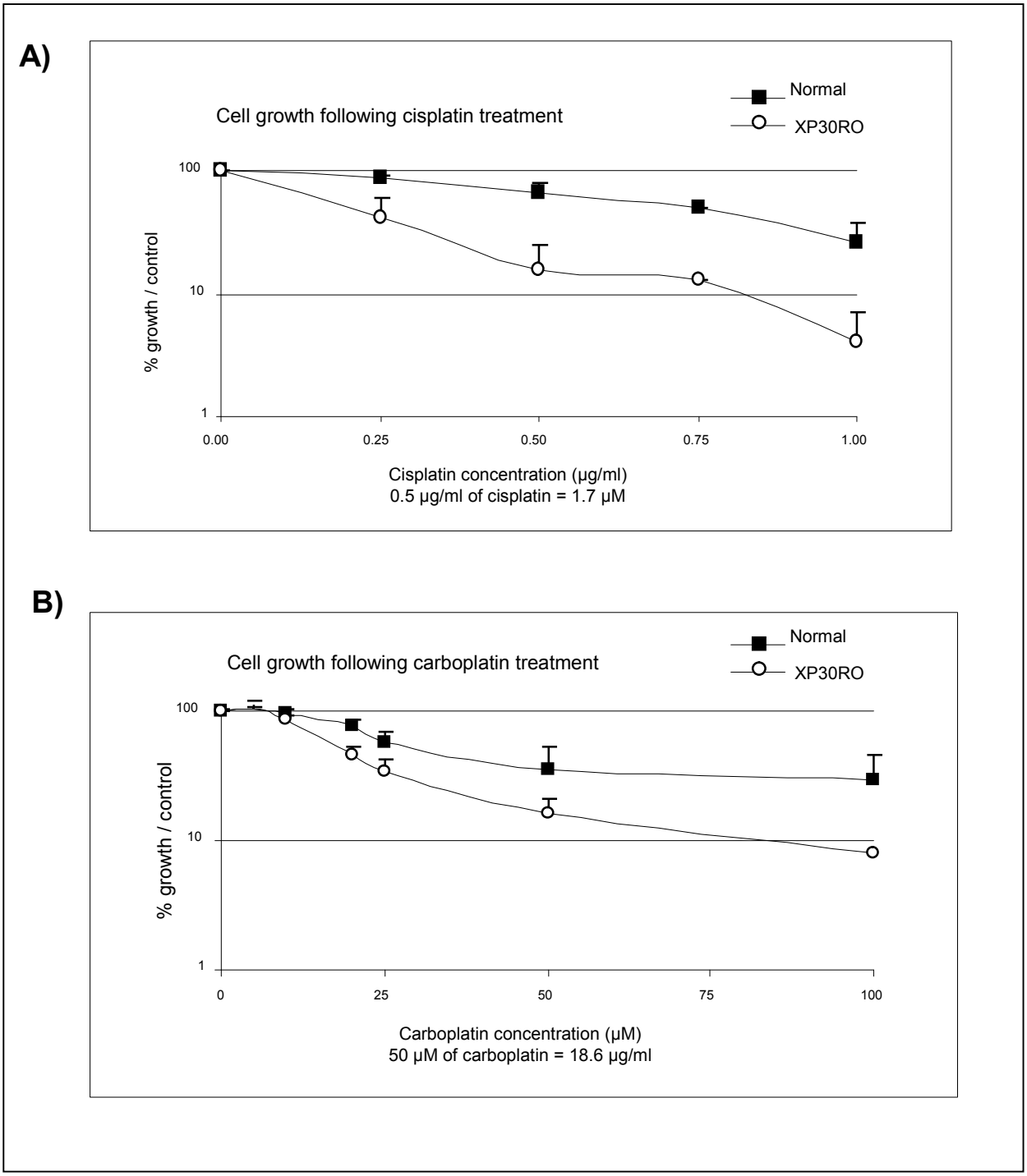

Supplementary Figure 1: Cisplatin and carboplatin sensitivity of polη-deficient XP30RO cells and normal GM00637I cells. GM00637I and XP30RO cells were seeded in triplicate in 96-well plates at 5000 cells per well. After treatment for 18h with the indicated doses of cisplatin (A) and carboplatin (B), media and drugs were removed, and cells were incubated in fresh medium for 48h. Cell viability was measured using the XTT assay. Data is the average of three to six experiments for each condition; error bars represent + one STD.

Appendix C: DNA polymerase eta, a key protein in translesion synthesis in human cells

Cruet-Hennequart S.[1], Gallagher K.[1], **Sokol A.M.[1]**, Villalan S.[1], Prendergast A.M.[1], Carty M.P.[1]: *Subcell Biochem* 2010, 50:189-209

[1] DNA Damage Response Laboratory, Centre for Chromosome Biology, Biochemistry, School of Natural Sciences, National University of Ireland, Galway, Ireland

The following pages, from 173 to 193, are available here:
http://link.springer.com/chapter/10.1007%2F978-90-481-3471-7_10

Appendix D: Replication protein A modification and function in the DNA damage response

Sokol A.M.[1], Conmy S. [1], Carty M.P. [1]

Review prepared for submission to *The International Journal of Molecular Sciences*

[1] DNA Damage Response Laboratory, Centre for Chromosome Biology, Biochemistry, School of Natural Sciences, National University of Ireland, Galway, Ireland

1. RPA structure

1.1 Background

The generation of single-stranded DNA (ssDNA) is a common feature of many aspects of DNA metabolism, not only DNA replication but also DNA repair and recombination, as well as activation of cell cycle checkpoints. Replication protein A (RPA) is the major single-stranded DNA binding protein in eukaryotic cells and therefore plays a central role in most of the biochemical pathways that carry out these transactions. RPA was first identified from HeLa cell extracts as a protein essential for simian virus 40 (SV40) origin-dependent replication of plasmid DNA *in vitro* (Fairman and Stillman, 1988; Wobbe et al., 1987; Wold and Kelly, 1988). Human RPA is a heterotrimeric protein, composed of RPA1, RPA2 and RPA3 subunits, having molecular weights of 70, 32 and 14kDa respectively (Fairman and Stillman, 1988; Wold and Kelly, 1988). The genes encoding the three human RPA subunits, RPA1, RPA2 and RPA3 have been mapped to chromosomes 17p13.3, 1p35 and 7p22 respectively (Ozawa et al., 1993; Umbricht et al., 1994). In addition, a fourth human RPA gene, RPA4, has been identified as a homologue of RPA2 (Haring et al., 2010). RPA4 is an intronless gene found on the X chromosome (Haring et al., 2010). Homologues of human RPA have been found in all eukaryotes investigated (Brill and Stillman, 1989; Fang and Newport, 1993b; Nasheuer et al., 1992). While highly homologous at the DNA sequence level, RPA subunits from different organisms are not interchangeable in DNA metabolic processes, including DNA replication (Ishiai et al., 1996; Matsumoto et al., 1990). However, it has been shown that human recombinant RPA can rescue the function of RPA-depleted *Xenopus* extracts (Lee et al., 2003; Recolin et al., 2012).

1.2 RPA structure

Although the three-dimensional structure of full-length trimeric RPA remains unsolved, a number of studies have elucidated structural elements within the various RPA subunits that, along with biochemical and computational studies, have allowed a predicted structure-function relationship of RPA to be described. The primary structural feature of RPA is the oligonucleotide/oligosaccharide binding-fold (OB-fold). OB-folds, a structural element commonly found in ssDNA binding proteins, consist of beta-barrels which facilitate ssDNA binding by wrapping around ssDNA (Murzin, 1993). X-ray crystallography has elucidated that ssDNA binding by RPA is stabilised by hydrogen bonding, between residues in the OB-folds with both the phosphate backbone and bases of the DNA, and stacking interactions, between aromatic residues in the OB-folds and the DNA bases (Bochkarev et al., 1997).

1.2.1 RPA1

RPA1 contains four DBDs, termed DBD-F, -A, -B and –C. The crystal structure of DBD–A and –B, located in the central region of the RPA1 subunit, consisting of amino acids 181-290 and 301-422 respectively, were the first to be described (Bochkarev et al., 1997). DBD-A and -B are the primary mediators of the ssDNA binding activity of RPA (Bochkarev

et al., 1997). Along with its role in ssDNA binding, DBD-A has also been shown to mediate RPA-protein interactions with for example Rad51 (Golub et al., 1998a) and XPA (Daughdrill et al., 2003). DBD-C of RPA1, composed of amino acids 436-616, is located at the C-terminal of RPA1 (Brill and Bastin-Shanower, 1998). DBD-C is involved mainly in RPA subunit interactions but the highly conserved zinc-finger domain located within DBD-C has also been shown to modulate ssDNA binding (Bochkareva et al., 2000). DBD-F is located at the N-terminal of RPA1 and comprises amino acids 1-110 (Daughdrill et al., 2001). Due to its low affinity for ssDNA DBD-F is not thought to be involved in ssDNA binding, this is further supported by NMR studies of trimeric RPA bound ssDNA showing no role DBD-F or the C-terminus of RPA2 in ssDNA binding (Brosey et al., 2009). DBD-F is also dispensable in DNA replication as RPA mutants lacking DBD-F can still support SV40 DNA replication (Gomes and Wold, 1996). However, DBD-F contains a basic cleft region which is required for RPA-protein interactions (Daughdrill et al., 2001). Many proteins, including p53, have been shown to interact with DBD-F region of RPA1 suggesting this region of the protein is important in damaged DNA processing and signalling. Structural data from NMR studies suggest that helical regions in the N-terminus of p53 mimic ssDNA allowing RPA1 binding via DBD-F (Bochkareva et al., 2005). Interestingly in the same study the authors also show that ssDNA and a phosphomimetic peptide of the RPA2 N-terminus compete with p53 for binding to the RPA1 DBD-F (Bochkareva et al., 2005). This potential competition for binding to RPA1 suggests a novel way in which signals and DNA processing could be regulated at the sites of RPA-bound ssDNA, where local area concentrations of competitors could dictate the outcome of the interaction.

1.2.2 RPA2

The central region of RPA2, amino acids 43-171, comprises DBD-D which facilitates ssDNA binding and is also essential for RPA complex formation (Bochkarev et al., 1999; Bochkareva et al., 1998). The C-terminal of RPA2 contains a winged-helix domain that is important for RPA-protein interactions. Consistent with the role of RPA in multiple DNA processing pathways, RPA2 has been shown to physically interact with a number of proteins involved in DNA repair pathways including XPA (He et al., 1995), UNG1 (Nagelhus et al., 1997) and Rad52 (Park et al., 1996). The N-terminus of RPA2 is reported to be intrinsically disordered in structure (Deng et al., 2007), it is rich in serine and threonine residues that are phosphorylated in a cell cycle- and DNA damage-dependent manner. The role of phosphorylation of the N-terminal of RPA2 in regulating RPA structure and function in DNA processing and signalling will be discussed below.

1.2.3 RPA3

The entire RPA3 subunit, 121 amino acids, comprises of DBD-E (Bochkarev et al., 1999). RPA3 is essential for stable heterotrimer formation but other functions of the subunit are still not completely understood.

1.2.4 RPA complex formation

The assembly of the trimeric RPA complex is an ordered process, with RPA2 and RPA3 first forming a stable complex, followed by binding of RPA1 (Henricksen et al., 1994; Stigger et al., 1994). Trimerisation of the RPA complex involves DBD-C of RPA1, DBD-D of RPA2 and DBD–E of RPA3. The 50 amino acids to the extreme C-terminus of RPA1 have been shown by deletion analysis to be essential for RPA1-RPA3 interaction and the 60 amino acids upstream of this are required for RPA1-RPA2 interactions (Kim et al., 1996). Once formed the RPA timer is very stable and has been shown to be resistant to dissociation by 6M urea (Wold and Kelly, 1988).

1.2.5 RPA4

A homologue of human RPA2, RPA4, was originally identified in a yeast two-hybrid screen (Keshav et al., 1995). RPA4 shares 47% amino acid identity to RPA2 (Keshav et al., 1995). RPA4 was found either to be expressed at low levels or not expressed in most established human cell lines; however, the protein was expressed in human placental and colon tissue. RPA4 can form a complex with RPA1 and RPA3, known as alternative RPA (aRPA). aRPA is unable to support SV40 origin-dependent DNA replication *in vitro* (Mason et al., 2009a), due to lack of ability to support priming by polα-primase and weakened stimulatory effect of polα-mediated strand extension (Mason et al., 2010). RPA4 has also been shown to inhibit canonical RPA function in DNA replication (Mason et al., 2009a). RPA4 is unable to support cell cycle progression in Hela cells (Haring et al., 2010). Since aRPA cannot support DNA replication, inhibits the canonical form of RPA and is expressed mainly in non-proliferating tissues, it has been suggested that aRPA may play a role in maintaining cellular quiescence. A role for RPA4 in DNA repair has also been described. RPA4 has been shown to co-localise in nuclear foci with γH2AX and phosphorylated Chk2 following camptothecin treatment (Haring et al., 2010). RPA4 can support HR *in vitro*, as aRPA interacts with Rad51 and Rad52 and can support Rad51-mediated strand exchange (Kemp et al., 2010). aRPA was also shown to support the incision step of NER *in vitro* suggesting a possible role for aRPA in NER (Kemp et al., 2010). Although aRPA cannot support polα-mediated DNA synthesis, it has been shown to support strand elongation by polδ (Mason et al., 2010). Taken together these results suggest aRPA could play a role in the DNA repair and maintenance of the genome of non-proliferating cells.

2. Single stranded DNA binding by RPA in replication, repair and recombination

2.1 Single-stranded DNA binding by RPA

RPA mediates its essential function in DNA metabolic processes by binding to ssDNA, generated as a result of replication or repair. Binding of RPA to ssDNA prevents nucleolytic degradation of the DNA and hairpin formation and coordinates DNA processing through interaction of ssDNA-bound RPA with other proteins. RPA binds ssDNA with high affinity, with an observed dissociation constant (Ka) of between 10^8 - 10^{11} M^{-1} (Fairman and

Stillman, 1988; Kim et al., 1994; Wobbe et al., 1987; Wold and Kelly, 1988). A number of studies have shown that RPA binds ssDNA with distinct polarity, such that DBD-A binds to the 5' end of the ssDNA and DBD-B binds toward the 3' end (de Laat et al., 1998b; Iftode and Borowiec, 2000; Kolpashchikov et al., 2001). Human RPA binds ssDNA in at least three binding modes, characterised by the length of the nucleotide sequence; 8-10, 12-23 and 28-30 nucleotides. The binding of RPA to ssDNA occurs in a sequential manner (Fanning et al., 2006b). First DBD-A and –B bind a tract of 8 nucleotides with DBD-A positioned at the 5' end of the ssDNA (Blackwell and Borowiec, 1994; Bochkarev et al., 1997). This 8-10 nucleotide binding mode was visualised by X-ray crystallography and showed that each DBD encapsulates three nucleotides with a two nucleotide gap between DBD-A and DBD-B (Bochkarev et al., 1997). The second mode of RPA binding to ssDNA involves the binding of DBD-A, -B and –C to a sequence of 12-23 nucleotides with an approximately four nucleotide space between DBD-B and -C (Cai et al., 2007). The third 28-30 nucleotide binding mode represents binding of RPA via DBDs A-D (Blackwell and Borowiec, 1994; Cai et al., 2007; Kim et al., 1992).

Binding of RPA to ssDNA leads to conformational changes in the RPA complex which has been elucidated by a number of studies. Scanning transmission electron microscopy analysis provides evidence that RPA in solution adopts a globular structure (Blackwell et al., 1996). The authors show that when bound in 8-10 nucleotide binding mode RPA subunits were found to have many intermolecular interactions leading to a tight association of the subunits. When bound in the 28-30 nucleotide binding mode however fewer intermolecular interactions are evident and the subunits exist in a more extended confirmation, this is consistent with the sequential binding of the RPA DBDs to longer ssDNA sequences.

There is accumulating evidence that hyperphosphorylation of the N-terminus of RPA2 can affect the positioning of the N-terminus of RPA2 relative to the RPA trimer and this has implications on RPA-ssDNA binding and RPA-protein interactions. NMR studies provide evidence that upon ssDNA binding, the N-terminal of RPA2 undergoes structural rearrangement and is positioned away from the RPA trimer (Brosey et al., 2009). Mass spectrometry footprinting analysis revealed evidence that upon hyperphosphorylation the N-terminus of RPA2 undergoes structural rearrangements and the authors suggest that the then highly negatively charged N-terminus could be attracted to the basic DBD-B residues (Liu et al., 2005a). Similarly, a phosphomimetic peptide representing the hyperphosphorylated RPA2 N-terminus, but not the unphosphorylated peptide, was shown to interact with RPA1 DBD-F (Bochkareva et al., 2005). Taken together these data suggest that at the very least hyperphosphorylation of RPA2 results in structural changes, possibly leading to a closer association of the RPA2 N-terminus with RPA1. This may provide a mechanism by which hyperphosphorylation of RPA2 regulates RPA-ssDNA and RPA-protein interactions during the DNA damage processing.

RPA has also been shown to interact with dsDNA but with much lower affinity that with ssDNA (Wold and Kelly, 1988). However, the affinity of RPA for dsDNA increases when the DNA is damaged by cisplatin (Patrick and Turchi, 1998b) or UV-irradiation

(Burns et al., 1996). The binding of RPA to cisplatin-damaged DNA was shown to be mediated through the formation of ssDNA by the DNA duplex unwinding properties of RPA (Patrick and Turchi, 1999). Further evidence for the role of RPA in the repair of damaged DNA will be discussed below.

2.2 Role of RPA in DNA replication

Studies of SV40 DNA replication in reconstituted cell-free systems have described an essential role for RPA in both the initiation and elongation steps of DNA replication. The SV40 viral genome is replicated using the virally-encoded large T antigen helicase and replication proteins provided by the host cell. RPA is recruited to the origin of replication by the large T antigen where it stimulates DNA unwinding (Wold and Kelly, 1988). Both its ability to bind ssDNA (Wold and Kelly, 1988) and to denature duplex DNA (Treuner et al., 1996) is thought to be essential to mediate unwinding of the DNA by RPA, in conjunction with the large T antigen helicase activity. RPA is also required for the recruitment of DNA polymerase α-primase complex to the origins of replication (Melendy and Stillman, 1993b). RPA interacts directly with polα-primase complex through the N-terminal of the RPA1 subunit and this interaction is essential for polα activity (Braun et al., 1997; Dornreiter et al., 1992b). The ssDNA binding property of RPA, along with polα interaction, was shown to be essential for stimulating processivity of polα (Braun et al., 1997). The essential role of RPA in the elongation phase of DNA replication is less well characterised. However, RPA stimulates the PCNA-dependent activity of polymerase δ (Kenny et al., 1989). Phosphorylation of the RPA2 subunit in response to DNA damage is known to inhibit DNA replication (Carty et al., 1994a) and disrupt the interaction of RPA with polα (Patrick et al., 2005b). This suggests an important role for phosphorylation of the RPA complex in regulating DNA replication.

2.3 Role of RPA in DNA repair

Cells are constantly being exposed to agents that damage the DNA. Damaged DNA poses a threat to the integrity of the genome and so cells have evolved mechanisms which aim to remove specific DNA damage types. Along with its essential role in DNA replication, RPA has been identified as an integral component of many DNA repair pathways which will be discussed below.

2.3.1 Nucleotide excision repair

Bulky DNA lesions, arising from various sources of genotoxic stress, like UV irradiation-induced cyclobutane pyrimdine dimers (CPDs) or cisplatin-induced intrastrand crosslinks, constitute an obstacle for transcription and replication. In order to maintain genome integrity these lesions are removed by the process of nucleotide excision repair (NER) (Lindahl and Wood, 1999; Riedl et al., 2003). NER is divided into two related subpathways depending on the way in which damage in the genome is initially recognised.

Global genome repair (GGR) removes helix-distorting DNA lesions from non-transcribed regions of the genome, while transcription-coupled repair (TCR) occurs on actively transcribed DNA (Lindahl and Wood, 1999; Mullenders and Berneburg, 2001; Riedl et al., 2003). Over 30 proteins involved in various stages of NER have been identified, and mutations in genes encoding these proteins may result in a severe phenotype, often associated with cancer predisposition (Wood et al., 2001). One example is xeroderma pigmentosum, a genetic disease characterised by increased sun sensitivity and enhanced skin cancer incidence. Seven XP complementation groups, A-G, have been identified, that result from mutations in genes encoding proteins in the NER pathway (Berneburg and Lehmann, 2001; Cleaver, 1968; Wood et al., 2001). An additional complementation group, termed XP variant (XPV), results from a mutation in *POLH*, encoding the lesion bypass polymerase, DNA polymerase eta (Johnson et al., 1999; Masutani et al., 1999). During NER-dependent processing of damaged DNA, NER factors are sequentially assembled at the site of damage (Riedl et al., 2003). TCR is strictly dependent on damage-induced inhibition of RNA polymerase II (Tornaletti, 2009). Lesion recognition in GGR requires the XPC and XPE proteins, which recognise distortions in the double helix caused by bulky lesions in the DNA (Rechkunova and Lavrik, 2010). Completion of NER involves (i) lesion recognition and DNA unwinding, (ii) double incision of the damaged DNA strand at the 3' and 5' ends of the lesion and (iii) replication-coupled gap filling and ligation of the remaining nick (Rechkunova and Lavrik, 2010; Riedl et al., 2003). Described steps are common between TCR and GGR.

RPA has a dual function in NER. Firstly, RPA is involved in the early stages of DNA lesion sensing through its specific interactions with XPA protein (Matsuda et al., 1995) and in recruiting and directing NER nucleases, XPG and XPF-EERCC1, for the incision step (de Laat et al., 1998a; Riedl et al., 2003; Thoma and Vasquez, 2003). This is supported by the observation that RPA has a greater affinity for binding to cisplatin-damaged DNA rather than to undamaged dsDNA *in vitro* (Patrick and Turchi, 1998a) and that deletion of domains within RPA1 and RPA2 that are responsible for interactions with XPA, significantly reduces the efficiency of NER *in vitro* and *in vivo* (Li et al., 1995; Stigger et al., 1998). Secondly, upon removal of the lesion-containing DNA fragment by NER nucleases, RPA remains bound to the ssDNA gap initiating the assembly of replication factors to fill the remaining gap (Riedl et al., 2003) ((Iftode and Borowiec, 1998). This is achieved by the ssDNA-binding activity of RPA and protein-protein interactions between RPA and other proteins involved in DNA synthesis, including PCNA and DNA polymerase α (Iftode and Borowiec, 1998). The effect of post-translational modifications of RPA on the NER pathway has been investigated. RPA2 is phosphorylated in a cell cycle-dependent manner and this phosphorylation decreases the ability of the heterotrimeric complex to bind ssDNA and to interact with polα (Liu et al., 2005b; Patrick et al., 2005a). However, it was found that this phosphorylation did not influence DNA replication or NER *in vitro* (Lee and Kim, 1995; Pan et al., 1995). In support of this, phosphorylation of RPA during the normal cell cycle does not change its interaction with XPA protein (Oakley et al., 2003). Furthermore, hyperphosphorylated RPA2 was found to have no impact on XPA interactions or NER functionality *in vitro* (Patrick et al., 2005b). However, a recent report by Jiang et al.

(2012) indicates that in response to UV-irradiation, the interaction between XPA and RPA is significantly decreased as a result of RPA2 hyperphosphorylation. Interestingly, treatment with HU and CPT, drugs which, like UV radiation, induce replication inhibition, but in contrast do not cause DNA damage that is repaired by NER, lead to the same observations of limited XPA-RPA interactions. Moreover, upon accumulation of ssDNA in human lung adenocarcinoma cells (A549) undergoing replication inhibition and checkpoint signalling, hyperphosphorylated RPA binds preferably to ssDNA regions. In this situation, ssDNA outcompetes XPA for binding to RPA *in vivo* (Jiang et al., 2012), resulting in disruption of the XPA-RPA complex. RPA is directed to a different DNA damage processing pathway, possibly to repair of double strand breaks arising from collapsed replication forks. The authors conclude that in this cellular context, hyperphosphorylation of RPA2 plays a critical role in regulation of the XPA-RPA complex, thus modulating NER (Jiang et al. 2012).

2.3.2 Base excision repair

The base excision repair (BER) pathway is the primary repair pathway by which DNA bases damaged by oxidation, alkylation, deamination, depurination or depyrimidination are removed from the genome. There are two BER pathways characterised by the number of nucleotides incorporated into the excision tract: short-patch BER, which involves the insertion of a single nucleotide, and long-patch BER, which involves the insertion of multiple nucleotides. RPA has been shown to be involved in both the recognition of the damaged bases and in DNA re-synthesis during long-patch BER. The N-terminus of RPA2 has been shown to interact with DNA glycosylase (UNG) (Nagelhus et al., 1997), which recognises uracil bases in DNA and functions to cleave the N-glycosidic bond removing the uracil base and creating an abasic (AP) site and thus initiating BER. RPA has also been shown to stimulate the final stages of long patch BER (DeMott et al., 1998). Genetic evidence in yeast also supports a role for RPA in BER where rfa1 mutant strains with mutation in conserved residues were shown to be sensitive to methyl methane sulfonate (MMS) treatment (Umezu et al., 1998).

2.3.3 DNA Mismatch Repair

Mismatch repair (MMR) is the process by which mismatched bases and insertion/deletion loops, usually resulting from DNA replication errors, are removed from the genome. Similar to its multiple functions in DNA replication, NER and BER, RPA is required for the excision and re-synthesis steps of MMR (Ramilo et al., 2002).

Interestingly phosphorylation of RPA2 subunit has been shown to regulate RPA function in MMR (Guo et al., 2006). In the early excision stages of MMR unphosphorylated RPA was shown to be tightly bound to DNA and stimulates excision of the mismatched nucleotides. RPA2 then becomes phosphorylated, as detected by a slow mobility band on a western blot using a RPA2 specific antibody, at the time of DNA re-synthesis. Phosphorylation of RPA2 was shown to reduce the affinity of the RPA complex for DNA making the template available for re-synthesis (Guo et al., 2006). However the exact sites phosphorylated on RPA2 were not identified in this study. In addition to the role for RPA

phosphorylation in MMR this study utilised kinetic binding assays to describe a role for RPA in nick sensing prior to the binding of the MMR proteins.

3. Post-translational modification of RPA

Post-translational modification (PTM) of proteins is a key mechanism by which cellular processes are mediated and controlled. Since RPA is known to be involved in most, if not all, DNA metabolic processes, it is suggested that PTM of RPA regulates RPA-ssDNA binding and RPA-protein interactions and thus the function of RPA. Both RPA1 and RPA2 subunits are known to be modified by phosphorylation. RPA1 is also modified by SUMOylated and RPA2 has been shown to be poly (ADP-rybosylated). The function of the post-translational modification of the RPA subunits will now be discussed.

3.1 RPA1

3.1.1 RPA1 phosphorylation

While most of the studies on RPA phosphorylation have concentrated on the phosphorylation of the RPA2 subunit, some work has suggested that the RPA1 subunit is also subject to phosphorylation. In S. cerevisiae, RPA1 is phosphorylated on S178 by the ATR-homologue, MEC1 (Kim and Brill, 2003). Human RPA1 was shown to be phosphorylated *in vitro* in Hela cell extracts on a number of residues (C-terminal sites; S560, S585, T580 and T590, and N-terminal between amino acids 112-163 which contains a number of potential phosphorylation sites) (Nuss et al., 2005b). In this study, it was shown using HPLC-MS that a single phosphorylation event in a peptide containing amino acids 122-157 was induced by HU treatment *in vivo* (Nuss et al., 2005b). While the exact site of phosphorylation remained unidentified, this phosphorylation region is located in the linker region between DBD-A and –F and the authors suggest that phosphorylation of this domain of RPA1 could influence the interaction of RPA1 with DNA or with other proteins (Nuss et al., 2005b). Interestingly, the MEC1 phosphorylation site on S178 in yeast RPA1 is also located in this linker region (Kim and Brill, 2003). In another study, the N-terminal of human RPA1 was shown to be phosphorylated by ATR in an *in vitro* kinase assay, although this phosphorylation event, like the phosphorylation of yeast RPA1 by MEC1, had no effect of RPA1 ssDNA binding (Liu et al., 2006). In the same study RPA1 was shown to be phosphorylated in DBD-B by Chk1 *in vitro*. It was shown that phosphorylation of RPA1 by Chk1 leads to a decrease in ssDNA binding and that RPA bound to ssDNA is resistant to Chk1 phosphorylation. The authors suggest that, in response to DNA damage, Chk1 and ssDNA compete for the RPA1 ssDNA binding domain. It is suggested that activated Chk1 phosphorylates soluble RPA, negatively regulating RPA-mediated DNA unwinding, while chromatin bound RPA is protected from Chk1 phosphorylation, so active replication forks remain protected (Liu et al., 2006). However, this study did not identify the RPA1 phosphorylation *in vivo*. Large scale phosphosite screens for DNA damage-inducible phosphorylation of ATM and ATR substrates identified RPA1 T180 as a phosphorylation site *in vivo* in response to UV and IR (Matsuoka et al., 2007b; Stokes et al., 2007).

However, the functional consequence of this phosphorylation of RPA1 is not yet known. Neither of the mass spectrometry-based screens identified any other phosphorylated form of RPA1 or RPA2.

3.1.2 RPA1 SUMOylation

Along with phosphorylation, the RPA1 subunit has been shown to be modified by SUMOylation (Dou et al., 2010b). SUMOylation of proteins is known to regulate cellular localisation, protein activity and stability (Geiss-Friedlander and Melchior, 2007). Through mutational analysis, RPA1 was show to be SUMOylated on K449 and K577, with K449 being the major site of SUMOylation. SUMO-specific antibodies showed that RPA1 is modified by SUMO2/3, but not SUMO1 (Dou et al., 2010b). RPA1 was also shown to interact with the sentrin/SUMO specific protease-6 (SENP6), which specifically cleaves SUMO2/3 containing substrates (Yeh, 2009), during S phase, keeping RPA1 in a hypo-SUMOylated state. Upon the induction of DNA strand breaks by campothecin (CPT) or IR, SENP6 was shown to dissociate from RPA1 leading to an increase in SUMOylation of RPA1 on chromatin (Dou et al., 2010b). The SUMOylation of RPA1 was shown to be important for efficient HR since SUMOylation of RPA1 mediates the interaction between RPA1 and Rad51. Consistent with this, cells expressing a K449R K577R double mutant of RPA1 (RPA1(ΔSUMO) which can not by SUMOylated, experience a decrease in the rate of Rad51 nucleofilament formation and a delay in Rad51 foci formation following CPT treatment (Dou et al., 2010b). However, Rad51-RPA co-localisation was not abolished in RPA1(ΔSUMO) cells suggesting that RPA1 SUMOylation enhances the efficiency of, but is not absolutely required for, Rad51 recruitment during HR. The involvement of other modifications of RPA, including phosphorylation of RPA2, in Rad51 recruitment to sites of DNA strand breaks will be discussed below.

3.2 RPA2

Phosphorylation of RPA2, the second RPA subunit, is the best studied post-translational modification of RPA. The N-terminal domain of RPA2 is an established target for phosphorylation *in vitro* and *in vivo* (Nuss et al., 2005a). This RPA2 domain is rich in serine/threonine residues which are phosphorylated in a cell cycle-dependent manner (Anantha et al., 2007; Din et al., 1990; Dutta and Stillman, 1992; Fotedar and Roberts, 1992; Niu et al., 1997; Stephan et al., 2009) as well as in response to DNA damage (Binz et al., 2004; Carty et al., 1994b; Cruet-Hennequart et al., 2008; Liu and Weaver, 1993; Oakley et al., 2001). 2D-phosphopeptide mapping and mass spectrometry analysis revealed that in total, there are nine potential phosphorylation sites within the first 33 amino-acid N-terminal tail of RPA2 (Fig. 1) (Niu et al., 1997; Nuss et al., 2005a; Zernik-Kobak et al., 1997). Deletion of the first 33 amino-acid residues from human RPA2 abolishes RPA phosphorylation (Henricksen et al., 1996). Interestingly, attempts to reveal the crystal structure of the N-terminal region of human RPA2 were not fully successful. Deng et al

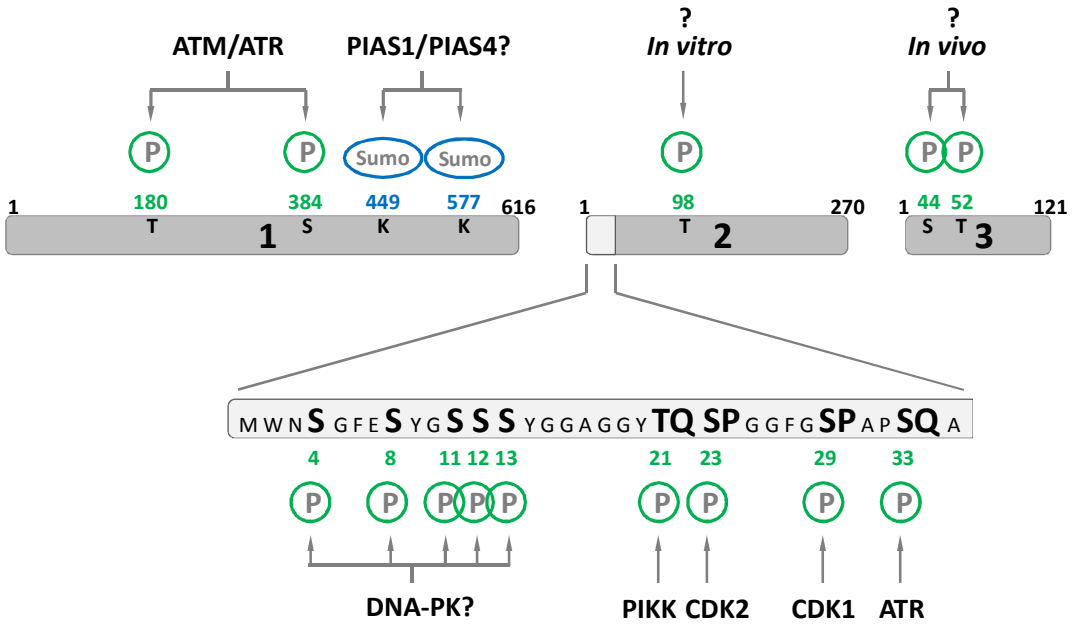

Figure 1. Diagram of the three RPA subunits with established and potential sites targeted for post-translational modifications.

reported that, while performing structural analysis of the soluble RPA2-RPA3 heterodimer, the N-terminal domain of RPA2 is attached by a flexible linker to the rest of the protein and was found to be intrinsically disordered while in the non-phosphorylated state (Deng et al., 2007). This intrinsically disordered N-terminus of RPA2, found to be characteristic of phosphoryalation domains (Iakoucheva et al., 2004), may dictate RPA2 participation in high-specificity and low-affinity interactions with structurally variable partner proteins, including kinases and other DNA damage response proteins (Deng et al., 2007; Iakoucheva et al., 2001). Phosphorylation of the N-terminal domain of RPA2 is crucial for RPA functions in DNA damage responses, DNA recombination and repair rather than in DNA synthesis. For example, expression and purification of an RPA2 hybrid protein that contained the N-terminal domain of RPA4, an alternative form of RPA2 that does not support DNA synthesis, show wild-type levels of DNA replication *in vitro* (Mason et al., 2009b). Even though the ability of RPA1 to non-specifically and tightly bind to ssDNA suffices to substitute for the heterotrimer in unwinding a new replication origin *in vitro* (Borowiec et al., 1990; Wold et al., 1987), specific protein-protein interactions between various DNA replication factors and the two other RPA subunits, provided partially by the C-terminal domain of RPA2, are crucial in proper assembly and function of the DNA synthesis initiation complex (Dornreiter et al., 1992a; Lee and Kim, 1995; Mason et al., 2009b; Melendy and Stillman, 1993a). The conformational alterations in the heterotrimer triggered by RPA2 phosphorylation include (i) intersubunit interaction between the negative charges, present on the N-terminal of RPA2 upon phosphorylation and the basic cleft of the DNA binding domain F (DBD-F) of RPA1 (Binz et al., 2003) and (ii) re-arrangements resulting from interaction of hyperphosphorylated RPA2 with the DBD-B motif located within RPA1 (Liu et al., 2005b). As noted, the N-terminal domain of RPA2 may act as a flexible hinge region that, upon phosphorylation, interacts with DNA binging motifs present within the heterotrimer and reduces the core property of RPA, binding to single-stranded

DNA (Liu et al., 2005b; Patrick et al., 2005a) and double helix destabilisation (Binz et al., 2003; Liu et al., 2005b). There is evidence that the phosphorylation-derived negative charge on the N-terminal of RPA2 changes the DNA binding mode of the heterotrimer, from compact to extended (Fanning et al., 2006a). This RPA conformation would favour DNA repair, where RPA, tightly bound to long stretches of ssDNA, functions to protect against nucleases and resolves DNA secondary structures until the repair process is complete. This RPA conformation would account for RPA extraction from replicating chromatin as during replication, RPA would preferably bind in the compact mode, favouring the fast RPA cycling on and off the replicating DNA (Fanning et al., 2006a). These predictions are supported by studies where hyperphosphorylated RPA was found to bind equally tightly to ssDNA (Binz et al., 2003; Oakley et al., 2003).

In vitro phosphorylation of threonine 98, located outside the N-terminus of RPA2, has been recently described. However, little is known on how this modification impacts RPA function (Nuss et al., 2005a). In addition to phosphorylation, RPA has also been reported to be poly (ADP-ribosylated) *in vitro*, and *in vivo* during DNA replication (Eki and Hurwitz, 1991).

3.2.1 Cell cycle-dependent phosphorylation of RPA2

Maintenance of genome integrity is often supported by tight regulation of protein activity throughout the cell cycle, either by differential protein expression, changes in protein localisation or modulation of protein activity by post-translational modifications, including phosphorylation. RPA is uniformly expressed during the cell cycle in human cells (Din et al., 1990). Interestingly, analysis of human and yeast cell extracts from S- and G2/M cell population revealed two additional bands corresponding to forms of RPA2 having significantly decreased gel mobility, suggesting that there is a conformational change in the polypeptide (Din et al., 1990). 32P-labeled RPA2 protein bands were sensitive to alkaline phosphatase treatment as well as acid hydrolysis, providing the first evidence that the slower mobility RPA2 forms resulted from phosphorylation of serine residues (Din et al., 1990). The serines of interest were identified to be localised in the N-terminal domain of RPA2 in the position of residues 23 and 29 (Fig. 1) (Erdile et al., 1990). Both serine residues are followed by a proline, constituting consensus sites for Cdc2-cyclin dependent kinases (Fig. 1) (Kemp and Pearson, 1990; Niu et al., 1997). Detailed analysis of RPA2 phosphorylation throughout the cell cycle revealed a number of phosphorylated forms of RPA at different cell cycle stages (Anantha et al., 2007; Din et al., 1990; Dutta and Stillman, 1992; Oakley et al., 2003; Stephan et al., 2009). As RPA is involved in the early steps of the initiation of DNA synthesis it is suspected that it is regulated by phosphorylation at the onset of S-phase, upon RPA binding to ssDNA (Fang and Newport, 1993a), shortly after DNA synthesis replication is initiated but not before (Din et al., 1990; Fotedar and Roberts, 1992). In fact, at the beginning of S-phase, RPA2 is phosphorylated on Ser23 by the CDK2-cyclin A complex (Din et al., 1990; Dutta and Stillman, 1992; Fang and Newport, 1993a; Henricksen and Wold, 1994; Stephan et al., 2009), and the activity of the kinase was found to stimulate DNA replication *in vitro* (Dutta and Stillman, 1992). In contrast, studies in cell-free extracts showed no significant change in the efficiency of unperturbed DNA replication in the

presence of phosphorylated or non-phosphorylated RPA (Pan et al., 1995). Furthermore, *in vitro* studies, using a RPA2 mutant lacking the phosphorylation domain had no effect on SV40-origin dependent plasmid DNA replication (Henricksen and Wold, 1994; Lee and Kim, 1995). This provided evidence that RPA2 phosphorylation had no direct effect on DNA synthesis. However, it could be speculated that *in vivo* phosphorylation of RPA2 on Ser23 at the onset of S-phase can function as an additional signalling factor for DNA synthesis to occur only once per cell cycle, in S-phase cells as opposed to in G1 phase cells. Analysis of RPA2 modifications from nocodazole-treated cells, a drug which arrests cells at the G2/M boundary due to disruption of microtubule formation (Cooper et al., 2006), revealed that the total fraction of RPA2 is phosphorylated when cells enter mitosis and corresponds to the lowest mobility form of RPA2 in protein extracts derived from normally cycling human cells (Din et al., 1990). For comparison, ~40% of RPA2 was phosphorylated in an interphase cell population (Din et al., 1990). Moreover, it was reported that all of the phosphorylated form of RPA2 from interphase cells was found to co-exist with other RPA subunits forming the heterotrimer, while free fractions of the RPA2 subunit were not phosphorylated, underlining that cell cycle-dependent phosphorylation of RPA2 is dependent on its association with subunits 1 and 3 (Din et al., 1990). In normal mitotic cells, RPA2 is additionally phosphorylated on Ser29 by the CDK1-cyclinB complex (Fang and Newport, 1993a; Oakley et al., 2003; Stephan et al., 2009) with phosphorylation on Ser23 and Ser29 being abolished when mitotically enriched cells were exposed to roscovitine, a selective CDK1 and CDK2 inhibitor (Anantha et al., 2007). *In vitro* experiments with a purified, mitotic fraction of RPA revealed no difference in the ability of mitotic RPA to bind to ssDNA when compared to recombinant, unphosphorylated RPA (Oakley et al., 2003). It is known that apart from its primary role in binding to ssDNA, RPA can also, in a less efficient manner, bind to and destabilize duplex DNA, participating in DNA unwinding prior to replication (Patrick and Turchi, 1998a). Interestingly, it was reported that mitotic RPA binds less efficiently to dsDNA (Binz et al., 2003; Oakley et al., 2003). Consistent with the limited ability of mitotic RPA to bind to dsDNA is the fact that RPA is excluded from the chromatin in normal mitosis (Stephan et al., 2009). Furthermore, unlike S-phase phosphorylation, RPA2 phosphorylation in mitosis is not dependent on DNA binding (Fang and Newport, 1993a).

Trimeric RPA interacts with various protein partners involved in all aspects of DNA metabolism, mainly through the RPA1 subunit but also via the C-terminal of RPA2 (Mer et al., 2000). It is of interest whether mitotic phosphorylation of RPA2 alters protein-protein interactions. *In vitro* assays showed that mitotic RPA has reduced potential to interact with DNA polymerase α, possibly acting as an additional control point by preventing DNA synthesis from occuring during cell division (Oakley et al., 2003). Mitotically phosphorylated RPA has a decreased ability to interact with ATM and DNA-PK, while having no influence on the RPA-XPA interaction which is essential in nucleotide excision repair (NER) (Oakley et al., 2003). Various aspects of RPA2 phosphorylation and their effect on interactions with DNA damage signaling and repair proteins are discussed later.

In conclusion, during the normal cell cycle, RPA2 is phosphorylated by the onset of S-phase on Ser23, followed by Ser29 phosphorylation when cells enter mitosis. RPA2 is

rapidly dephosphorylated in late cytokinesis, before RPA re-enters to the nucleus of the two daughter cells in G1 phase (Fig. 2). Ectopic expression of a mutated form of RPA2, where serines 23 and 29 were both mutated to alanine and therefore could not be phosphorylated, resulted in an abnormal cell cycle distribution, underlining a role for RPA2 phosphorylation in maintaining an accurate cell division (Anantha et al., 2007). Clearly, the RPA phosphorylation cycle is integrated with the cell biology via cell cycle regulation (Fig. 2). However, it is established that CDK-dependent phosphorylation of RPA on Ser23 and Ser29 occurs not only in normal cell cycle but also in response to DNA damage (Anantha et al., 2007; Zernik-Kobak et al., 1997) (see below).

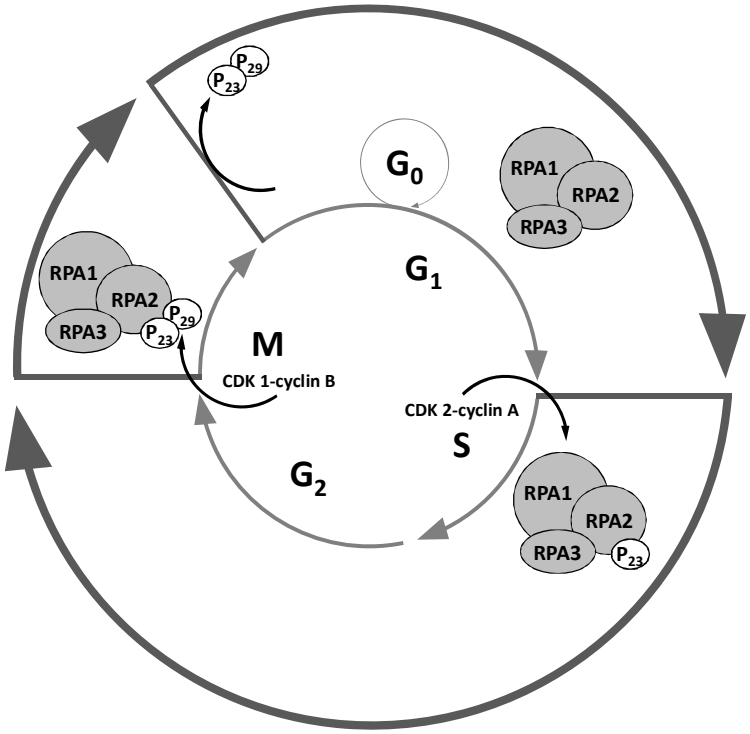

Figure 2. RPA phosphorylation during the normal cell cycle.

3.2.2 DNA damage-induced phosphorylation of the N-terminal domain of RPA2

It is well established that exposure of cells to DNA damaging agents such as UV-C irradiation (Carty et al., 1994b; Cruet-Hennequart et al., 2006), ionizing radiation (Stephan et al., 2009) and cisplatin (Cruet-Hennequart et al., 2008) or replication inhibitors like hydroxyurea (HU) (Manthey et al., 2007) and camptothecin (CPT) (Shao et al., 1999), results in additional RPA2 bands upon SDS-PAGE, of even lower mobility compared to the mitotic form. These forms of RPA2 correspond to protein phosphorylation on at least four residues located in the N-terminal domain, Ser4, Ser8, Ser 11-13, Thr21, Ser23, Ser29 or Ser33 (Nuss et al., 2005a; Oakley et al., 2001; Zernik-Kobak et al., 1997). This form has been termed hyperphosphorylated RPA2 (Nuss et al., 2005a; Oakley et al., 2001).

As described previously, serines 23 and 29 are phosphorylated by CDK-cyclin complexes. Ser33 and Thr21 constitute consensus sites for phosphatidylinositol 3-kinases (PIKK) including ATM, ATR and DNA-PK (Kim et al., 1999). It is established that following genotoxic stress ATR phosphorylates RPA2 on Ser33 (Anantha et al., 2007; Olson et al., 2006). Thr21 was reported to be phosphorylated primarily by ATM and DNA-PK, and to a lesser extent by ATR (Block et al., 2004; Zernik-Kobak et al., 1997). While little is known about phosphorylation of serines 11-13, it is reported that DNA-PK can phosphorylate Ser4 and Ser8 *in vitro* (Zernik-Kobak et al., 1997). *In vivo*, this phosphorylation event was reported to be DNA-PK-dependent following UV-C and cisplatin treatment (Cruet-Hennequart et al., 2006; Cruet-Hennequart et al., 2008).

DNA damage-induced activation of PIK-kinases play crucial role in the cascade of DNA damage signalling by phosphorylation of many downstream proteins, transducing the signal to activate the appropriate DNA repair pathway (Bakkenist and Kastan, 2004). ATM is activated in response to DNA double-strand breaks. Activation is dependent on its interaction with the Mre11/Rad50/NBS (MRN) complex and induces phosphorylation of a variety of proteins including H2AX, Chk2 and BRCA-1 (Bakkenist and Kastan, 2004; Matsuoka et al., 2007a). The ATR-ATRIP complex is recruited to sites of DNA replication inhibition due to its interaction with RPA-coated single-stranded DNA generated as a result of replication fork stalling (Namiki and Zou, 2006; Zou and Elledge, 2003). ATR phosphorylates downstream signalling proteins including RPA and Chk1 and activates the intra-S checkpoint (Zhao and Piwnica-Worms, 2001). DNA-PK plays a central role in repair of DSBs by non-homologous end joining (Kurimasa et al., 1999). All these kinases have been reported to phosphorylate the N-terminus of RPA2.

It has been proposed that in response to DNA damage occurring in interphase cells, RPA2 is primarily phosphorylated on Ser33 by the ATR-ATRIP complex early in the damage response and this phosphorylation is required for subsequent phosphorylation of other N-terminally located sites (Anantha et al., 2007). Even though multiple phosphorylation events are needed for RPA2 hyperphosphorylation to occur, the actual residues, responsible kinases and the sequence of phosphorylation events seem to vary depending on the type of DNA damage and the cell cycle phase (Anantha et al., 2007; Cruet-Hennequart et al., 2008; Sakasai et al., 2006; Stephan et al., 2009). In addition to its role during the normal cell cycle, CDK-cyclin-dependent phosphorylation of RPA2 on Ser23 and Ser29 was found to play a role in DSB repair in interphase cells treated with bleomycin or CPT (Anantha et al., 2007). In contrast to these observations, phosphorylation of Ser23 and Ser29 was dispensable for RPA2 hyperphosphorylation to occur in IR-treated interphase cells, suggesting that type of DNA damage dictates RPA2 modification sites (Stephan et al., 2009). Anantha et al. (2007) reported that phosphorylation of Ser23 and Ser29 during mitosis is required for the N-terminal domain of RPA2 to undergo additional phosphorylation events when mitotic cells are exposed to bloemycin. The importance of this hyperphosphorylation event in DNA damage processing, cell cycle progression and viability has been emphasised by the fact that in response to mitotic DNA damage, cells in which endogenous RPA2 is replaced with a RPA2 mutant, where Ser23 and Ser29 were mutated to alanines, show a severe delay in exiting mitosis into G1 phase, increased spindle assembly

checkpoint (SAC) assembly and elevated apoptosis-related lethality (Anantha et al., 2008). The authors conclude that stress-induced RPA hyperphosphorylation in mitosis can be governed through the spindle assembly checkpoint (SAC) and enhanced mitotic exit can function as a passage for the damaged DNA to be repaired my mechanisms operating in G1 (Anantha and Borowiec, 2009). This hypothesis is supported by the prediction that in mitosis, DNA breaks could not be repaired efficiently due to chromatin condensation.

As RPA function is indispensible for DNA replication, there is growing evidence supporting the hypothesis that RPA is most rapidly hyperphosphorylated in response to inhibition of DNA replication (Anantha et al., 2007; Liaw et al., 2011; Rodrigo et al., 2000; Shi et al., 2010). DNA polymerase eta-deficient cells, treated with a chemotherapeutic drug cisplatin, accumulate hyperphosphorylated RPA2 (Cruet-Hennequart et al 2008, 2009) at sites where DNA replication was significantly inhibited, due to dysfunctional translesion synthesis (unpublished data). Recent studies on a novel RPA inhibitor, TDLR-505, used in joint treatment with cisplatin show their synergy in cellular toxicity, underlying RPA role in rescuing effects of replication-dependent DNA damage (Shuck and Turchi, 2010). Sakasai et al, reported that differences in the kinase-dependence and dynamics of RPA2 hyperphosphorylation during inhibited DNA synthesis can be explained by the ability of the drug to cause direct or indirect replication coupled-DSBs (or DSEs) (Sakasai et al., 2006). Thus, while both ATR and DNA-PK were reported to participate in RPA2 hyperphosphorylation in response to CPT, a drug that causes direct, synthesis-coupled DSBs, RPA2 hyperphosphorylation post-HU, which induces DSBs indirectly, was found to be independent of DNA-PK activation (Sakasai et al., 2006). The hypothesis that hyperphosphorylated RPA2 further inhibits DNA replication is supported by findings that hyperphosphorylated RPA (i) binds less efficiently to ssDNA (Binz et al., 2003; Liu et al., 2005b; Patrick et al., 2005a), (ii) has decreased ability to interact with DNA polymerase α *in vitro* (Patrick et al., 2005a) and (iii) is excluded from DNA replication foci (Vassin et al., 2004). Conversly, *in vitro* experiments show that RPA2 hyperphosphorylation has no impact on interaction with proteins involved in DNA repair (XPA) (Oakley et al., 2003; Patrick et al., 2005a) or recombination (Rad51, Rad52) (Jackson et al., 2002). In fact, there is increasing evidence that RPA2 hyperphosphorylation can dictate RPA function in DNA damage signalling and repair, both through a change in RPA-DNA binding and RPA-protein interactions (Mer et al., 2000). Additionally, DNA-PK- and CDK-cyclin-dependent RPA hyperphosphorylation occurs on a subset of the RPA pool in cells in the early stages of apoptosis (O'Meara et al., 2010; Treuner et al., 1999).

4. Role of RPA2 post-translational modifications in regulating protein function in DNA DSB repair

As noted above, generation of single-stranded DNA is a common feature of most aspects of DNA metabolism, and RPA therefore plays a central in most of the biochemical pathways that carry out these transactions. Consistent with this, RPA was found not only to localise to replication foci during S-phase (Dimitrova and Gilbert, 2000) but also is localised

to repair foci at sites of DNA damage (Golub et al., 1998b), where it plays a role in damage recognition, processing and signalling. Above we described how post-translational modifications of RPA regulate its function in specific DNA repair pathways, here we further extent this discussion to the role of RPA2 PTMs in the regulating RPA function in the repair of DNA double strand breaks.

4.1 Homologous Recombination (HR)

Homologous recombination is one of two major pathways for processing of DNA double-strand breaks (DSBs), arising either directly from exposure to ionizing irradiation or indirectly as a consequence of replication arrest-induced double strand ends (DSE) (San Filippo et al., 2008). Recently, it has been shown that HR proteins are also involved in repair of ssDNA gaps resulting from replication stalling before their conversion to DSEs (Feng and Zhang, 2011). Unlike error-prone DNA repair by the non-homologous end joining pathway (NHEJ), HR is considered error-free, due to the fact that homologous DNA sequences in the form of sister chromatid DNA are utilised as a template for repair (San Filippo et al., 2008). The existence of homologous sequences limits HR to operate mainly in S and G2 phases of the cell cycle. Depending on the nature of the DNA lesion, different HR mechanisms are activated (Helleday, 2003). The sequence of HR steps in repair of classic DSBs include: (i) MRN-mediated damage sensing and DNA strand resection, (ii) Rad51 recombinase filament formation, (iii) homologous sequence search and invasion and (iv) synthesis-coupled gap filling and strands ligation (San Filippo et al., 2008). Recent attention has focused on the involvement of HR in processing of DNA lesions arising from replication blockage and fork collapse, which leads to formation of ssDNA gaps and one-ended DSBs (DSEs) (Feng and Zhang, 2011). Although less is known about the precise role of HR in these processes, they clearly rely on the activity of proteins involved in HR (Feng and Zhang, 2011). Many proteins of various enzymatic activities have been identified to be crucial in HR-mediated DNA repair. The importance of this pathway in maintaining genome stability is clearly demonstrated in the case of mutations in the BRCA1 and BRCA2 genes which predispose the affected individual for breast and ovarian cancer (Feng and Zhang, 2011). The products of these genes play a role in mediating recombination and HR protein complex assembly.

The role of RPA in HR is complex, dictated by its strong affinity for ssDNA as well as interaction with HR proteins, including Rad51, Rad52 and BRCA2 (Deng et al., 2009; Sugiyama and Kowalczykowski, 2002). There is increasing evidence that RPA function in HR is controlled by damage-dependent hyperphosphorylation. Thus, RPA hyperphospohrylation was found to occur predominantly in S and G2 phases, where HR preferentially operates (Anantha et al., 2007; Cruet-Hennequart et al., 2009). Additionally, hyperphosphorylated RPA preferentially localizes to repair foci following UV-C and camptothecin treatment of human lung adenocarcinoma cells (A549) (Wu et al., 2005).

The key step of HR-mediated DSB repair is the formation of a Rad51 nucleofilament in order for the recombinase to initiate the homologous strand search (San Filippo et al., 2008). RPA as the most abundant ssDNA-binding protein in the nucleus plays

an important role in this step, by binding to ssDNA generated during DNA strand resection in the early stages of HR, thereby reducing the secondary structure of the ssDNA. At this stage, RPA outcompetes Rad51 for binding to ssDNA ends, and initially inhibits presynaptic complex formation (Deng et al., 2009). This inhibition is alleviated by the recruitment of Rad52 to the site of damage where it acts as a mediator between RPA-coated ssDNA-and Rad51, since Rad52 can interact with both Rad51 and RPA as well as with ssDNA (Deng et al., 2009). RPA2 hyperphosphorylation facilitates the displacement of RPA from ssDNA by Rad51 and the activation of further HR steps (Deng et al., 2009; Golub et al., 1998b). Hyperphosphorylated RPA was reported to directly interact with Rad51 *in vitro* (Wu et al., 2005). Upon Rad51 nucleofilament formation, RPA was found to accelerate later steps in HR, including homologous pairing and strand exchange *in vitro* (Golub et al., 1998b).

Although there is increasing evidence that damage-dependent RPA2 hyperphospohrylation is specifically required for replication arrest-coupled HR, its precise role in this process remains elusive. Recently, Shi et al. reported that RPA2 phosphorylation is essential in HR in response to DNA lesions resulting from replication arrest rather that those arising as direct DSBs caused by IR (Shi et al., 2010). In support of this model, expression of an RPA2 mutant that cannot undergo N-terminal phosphorylation resulted in (i) decreased Rad51 foci formation (ii) increased chromosomal aberrations and (iii) loss of cell viability when cells were exposed to chemotherapeutic agents that inhibit replication, but not when DSBs were directly induced (Shi et al., 2010). Additionally, it was found that RPA2 hyperphosphorylation in response to HR-mediated processing of DNA replication arrested sites depended on functional BRCA-1. This BRCA-1-related modification of RPA2 provides further evidence thatRPA2 hyperphosphorylation functions in efficient HR-mediated resolution of stalled forks (Feng and Zhang, 2011).

DNA damage-induced hyperphosphorylation of RPA2 leads to disassociation of RPA from complexes formed with various protein partners and possibly directs the heterotrimer to sites of HR-mediated repair. One example is the previously described XPA-RPA complex (see 2.3.1). Moreover, a recent report by Serrano et al., revealed that checkpoint-mediated RPA2 hyperphosphorylation severely impairs the interaction of the heterotrimer with p53 (Serrano et al., 2012). In the normal cell environment, RPA binds to p53 (Dutta et al., 1993) and sequesters it in order for normal cellular processes to proceed. In response to replication stress induced by CPT treatment, RPA2 is hyperphosphorylated by PIK kinases, no longer binds to p53 and is able to relocate to lesion sites and facilitate HR-mediated lesion processing, additionally releasing p53 to orchestrate the DNA damage response (Serrano et al., 2012). The hypothesis arising from the above observation is that at the cellular level, DSBs constitute the most lethal DNA lesions and thus have priority in processing and final removal by HR, and an additional pool of free hyperphosphorylated RPA facilitates this process.

In addition to phosphorylation of RPA2, recent evidence indicates that additional PTMs also modulate RPA activity in response to DNA damage. As noted above, in response to genotoxins which directly induce DSBs (CPT and IR), RPA1 is SUMOylated *in vivo* (Dou et al., 2010a). SUMOylation was found to be critical in Rad51 recruitment to

repair foci and in the displacement of RPA from the DNA allowing for efficient HR, having no influence on the hererotrimer stability or ssDNA binding at the same time (Dou et al., 2010a). Thus, in addition to RPA2 phosphorylation, SUMOylation of the RPA1 subunit of RPA also regulates DNA repair by the HR pathway. Since, in contrast to RPA2 phosphorylation, RPA1 SUMOylation appears to occur only in response to IR and CPT, it is hypothesized that the nature of lesion, by activating different signalling pathways, might dictate which type of post-translational modification of RPA occurs, and thereby how the protein functions in HR.

5. Role of dephosphorylation of RPA2

So far the effect of RPA2 phosphorylation on RPA function and localisation during the normal cell cycle and in response to DNA damage has been discussed. The process of RPA dephosphorylation is also of interest as the status of cellular RPA is a result of the two antagonistic processes. As discussed before, during the normal cell cycle RPA2 is phosphorylated during S-phase and mitosis. Mitotic RPA is excluded from the chromatin and RPA2 is dephosphorylated before RPA re-enters the nucleus of the G1 phase daughter cell. Although no specific cell cycle-specific phosphatase has been identified as participating in RPA2 dephosphorylation at this stage, it appears to be a necessary and efficient process. While the role of damage-induced phosphorylation of RPA2 in DNA lesion detection, DNA damage signal transduction, cell cycle regulation and final lesion repair was the focus of this and other (Binz et al., 2004; Patrick et al., 2005a) reviews, less is known about the biological significance of RPA dephosphorylation. Recently, damage-induced RPA2 phosphorylation was reported to be reversed by a dimeric complex of PP4 (protein phosphatase 4) and PP4R2 (regulatory subunit 2). Lee et al., reported that RPA can interact with this PP4 complex *in vitro*, and that, *in vivo*, the level of hyperphosphorylated RPA2 is elevated upon silencing of PP4 activity using siRNA (Lee et al., 2010). The authors provide evidence for the importance of RPA2 dephosphorylation in effective DNA damage signalling, HR and normal cell cycle resumption. Firstly, cells with impaired RPA dephosphorylation show increased G2/M checkpoint signalling in response to IR. Secondly, premature RPA2 hyperphosphorylation led to a delay in RPA localisation to repair foci and impaired HR as a result of inefficient formation of Rad51 nucleofilaments. Thirdly, expression of hyperphospho-mimetic RPA2 mutants significantly impedes DNA synthesis upon DNA damage induction by IR. This suggests that dephosphorylation of RPA is necessary for resumption of DNA replication post-damage and for release of cell cycle arrest (Lee et al., 2010). Fourthly, cells with persistent levels of damage-induced, hyperphosphorylated RPA show increased sensitivity to DNA damaging agents (Feng et al., 2009; Lee et al., 2010). Additionally, PP2A-mediated RPA2 dephosphorylation was reported for efficient repair of replication-coupled DSEs (Feng et al., 2009).

There is increasing evidence that specific and sequential RPA phosphorylation and dephosphorylation events regulate efficient DNA repair by HR. Premature hyperphosphorylation of RPA2 in response to DNA damage impedes RPA localisation to

repair centres, consistent with delayed RPA localisation to repair foci when the PP4 complex is inactive (Lee et al., 2010). Possible scenarios for the role of RPA2 phosphorylation and dephosphorylation in regulation of HR are as follows. In response to DNA damage, pools of hyperphosphorylated RPA available from, for example, RPA disassociation from protein complexes, including XPA and p53 requires dephosphorylation for its efficient association with HR repair foci where it binds to DNA and eliminates secondary DNA structures. Next, RPA2 is phosphorylated to facilitate Rad52-mediated exchange for Rad51 on the DNA and in this form RPA participates in later HR steps until it is dephosphorylated when DNA synthesis is ready to restart.

6. References

Anantha, R.W., and J.A. Borowiec. 2009. Mitotic crisis: the unmasking of a novel role for RPA. Cell Cycle. 8:357-361.

Anantha, R.W., E. Sokolova, and J.A. Borowiec. 2008. RPA phosphorylation facilitates mitotic exit in response to mitotic DNA damage. Proc Natl Acad Sci U S A. 105:12903-12908.

Anantha, R.W., V.M. Vassin, and J.A. Borowiec. 2007. Sequential and synergistic modification of human RPA stimulates chromosomal DNA repair. J Biol Chem. 282:35910-35923.

Bakkenist, C.J., and M.B. Kastan. 2004. Initiating cellular stress responses. Cell. 118:9-17.

Berneburg, M., and A.R. Lehmann. 2001. Xeroderma pigmentosum and related disorders: defects in DNA repair and transcription. Adv Genet. 43:71-102.

Binz, S.K., Y. Lao, D.F. Lowry, and M.S. Wold. 2003. The phosphorylation domain of the 32-kDa subunit of replication protein A (RPA) modulates RPA-DNA interactions. Evidence for an intersubunit interaction. J Biol Chem. 278:35584-35591.

Binz, S.K., A.M. Sheehan, and M.S. Wold. 2004. Replication protein A phosphorylation and the cellular response to DNA damage. DNA Repair (Amst). 3:1015-1024.

Blackwell, L.J., and J.A. Borowiec. 1994. Human Replication Protein A Binds Single-Stranded DNA in Two Distinct Complexes. Molecular and Cellular Biology. 14:3993-4001.

Blackwell, L.J., J.A. Borowiec, and I.A. Mastrangelo. 1996. Single-stranded-DNA binding alters human replication protein A structure and facilitates interaction with DNA-dependent protein kinase. Molecular and Cellular Biology. 16:4798-4807.

Block, W.D., Y. Yu, and S.P. Lees-Miller. 2004. Phosphatidyl inositol 3-kinase-like serine/threonine protein kinases (PIKKs) are required for DNA damage-induced phosphorylation of the 32 kDa subunit of replication protein A at threonine 21. Nucleic Acids Res. 32:997-1005.

Bochkarev, A., E. Bochkareva, L. Frappier, and A.M. Edwards. 1999. The crystal structure of the complex of replication protein A subunits RPA32 and RPA14 reveals a mechanism for single-stranded DNA binding. EMBO J. 18:4498-4504.

Bochkarev, A., R.A. Pfuetzner, A.M. Edwards, and L. Frappier. 1997. Structure of the single-stranded-DNA-binding domain of replication protein A bound to DNA. Nature. 385:176-181.

Bochkareva, E., L. Frappier, A.M. Edwards, and A. Bochkarev. 1998. The RPA32 Subunit of Human Replication Protein A Contains a Single-stranded DNA-binding Domain. Journal of Biological Chemistry. 273:3932-3936.

Bochkareva, E., L. Kaustov, A. Ayed, G.-S. Yi, Y. Lu, A. Pineda-Lucena, J.C.C. Liao, A.L. Okorokov, J. Milner, C.H. Arrowsmith, and A. Bochkarev. 2005. Single-stranded DNA mimicry in the p53 transactivation domain interaction with replication protein A. Proceedings of the National Academy of Sciences of the United States of America. 102:15412-15417.

Bochkareva, E., S. Korolev, and A. Bochkarev. 2000. The Role for Zinc in Replication Protein A. Journal of Biological Chemistry. 275:27332-27338.

Borowiec, J.A., F.B. Dean, P.A. Bullock, and J. Hurwitz. 1990. Binding and unwinding--how T antigen engages the SV40 origin of DNA replication. Cell. 60:181-184.

Braun, K.A., Y. Lao, Z. He, C.J. Ingles, and M.S. Wold. 1997. Role of Protein−Protein Interactions in the Function of Replication Protein A (RPA): RPA Modulates the Activity of DNA Polymerase α by Multiple Mechanisms. Biochemistry. 36:8443-8454.

Brill, S.J., and S. Bastin-Shanower. 1998. Identification and Characterization of the Fourth Single-Stranded-DNA Binding Domain of Replication Protein A. Molecular and Cellular Biology. 18:7225-7234.

Brill, S.J., and B. Stillman. 1989. Yeast replication factor-A functions in the unwinding of the SV40 origin of DNA replication. Nature. 342:92-95.

Brosey, C.A., M.-E. Chagot, M. Ehrhardt, D.I. Pretto, B.E. Weiner, and W.J. Chazin. 2009. NMR Analysis of the Architecture and Functional Remodeling of a Modular Multidomain Protein, RPA. Journal of the American Chemical Society. 131:6346-6347.

Burns, J.L., S.N. Guzder, P. Sung, S. Prakash, and L. Prakash. 1996. An Affinity of Human Replication Protein A for Ultraviolet-damaged DNA. Journal of Biological Chemistry. 271:11607-11610.

Cai, L., M. Roginskaya, Y. Qu, Z. Yang, Y. Xu, and Y. Zou. 2007. Structural Characterization of Human RPA Sequential Binding to Single-Stranded DNA Using ssDNA as a Molecular Ruler†. Biochemistry. 46:8226-8233.

Carty, M.P., M. Zernik-Kobak, S. McGrath, and K. Dixon. 1994a. UV light-induced DNA synthesis arrest in HeLa cells is associated with changes in phosphorylation of human single-stranded DNA-binding protein. EMBO J. 13:2114-2123.

Carty, M.P., M. Zernik-Kobak, S. McGrath, and K. Dixon. 1994b. UV light-induced DNA synthesis arrest in HeLa cells is associated with changes in phosphorylation of human single-stranded DNA-binding protein. EMBO J. 13:2114-2123.

Cleaver, J.E. 1968. Defective repair replication of DNA in xeroderma pigmentosum. Nature. 218:652-656.

Cooper, S., G. Iyer, M. Tarquini, and P. Bissett. 2006. Nocodazole does not synchronize cells: implications for cell-cycle control and whole-culture synchronization. Cell Tissue Res. 324:237-242.

Cruet-Hennequart, S., S. Coyne, M.T. Glynn, G.G. Oakley, and M.P. Carty. 2006. UV-induced RPA phosphorylation is increased in the absence of DNA polymerase eta and requires DNA-PK. DNA Repair (Amst). 5:491-504.

Cruet-Hennequart, S., M.T. Glynn, L.S. Murillo, S. Coyne, and M.P. Carty. 2008. Enhanced DNA-PK-mediated RPA2 hyperphosphorylation in DNA polymerase eta-deficient human cells treated with cisplatin and oxaliplatin. DNA Repair (Amst). 7:582-596.

Cruet-Hennequart, S., S. Villalan, A. Kaczmarczyk, E. O'Meara, A.M. Sokol, and M.P. Carty. 2009. Characterization of the effects of cisplatin and carboplatin on cell cycle progression and DNA damage response activation in DNA polymerase eta-deficient human cells. Cell cycle. 8:3039-3050.

Daughdrill, G.W., J. Ackerman, N.G. Isern, M.V. Botuyan, C. Arrowsmith, M.S. Wold, and D.F. Lowry. 2001. The weak interdomain coupling observed in the 70 kDa subunit of human replication protein A is unaffected by ssDNA binding. Nucleic Acids Research. 29:3270-3276.

Daughdrill, G.W., G.W. Buchko, M.V. Botuyan, C. Arrowsmith, M.S. Wold, M.A. Kennedy, and D.F. Lowry. 2003. Chemical shift changes provide evidence for overlapping single-stranded DNA- and XPA-binding sites on the 70 kDa subunit of human replication protein A. Nucleic Acids Research. 31:4176-4183.

de Laat, W.L., E. Appeldoorn, K. Sugasawa, E. Weterings, N.G. Jaspers, and J.H. Hoeijmakers. 1998a. DNA-binding polarity of human replication protein A positions nucleases in nucleotide excision repair. Genes Dev. 12:2598-2609.

de Laat, W.L., E. Appeldoorn, K. Sugasawa, E. Weterings, N.G.J. Jaspers, and J.H.J. Hoeijmakers. 1998b. DNA-binding polarity of human replication protein A positions nucleases in nucleotide excision repair. Genes & Development. 12:2598-2609.

DeMott, M.S., S. Zigman, and R.A. Bambara. 1998. Replication Protein A Stimulates Long Patch DNA Base Excision Repair. Journal of Biological Chemistry. 273:27492-27498.

Deng, X., J.E. Habel, V. Kabaleeswaran, E.H. Snell, M.S. Wold, and G.E. Borgstahl. 2007. Structure of the full-length human RPA14/32 complex gives insights into the mechanism of DNA binding and complex formation. J Mol Biol. 374:865-876.

Deng, X., A. Prakash, K. Dhar, G.S. Baia, C. Kolar, G.G. Oakley, and G.E. Borgstahl. 2009. Human replication protein A-Rad52-single-stranded DNA complex: stoichiometry and evidence for strand transfer regulation by phosphorylation. Biochemistry. 48:6633-6643.

Dimitrova, D.S., and D.M. Gilbert. 2000. Stability and nuclear distribution of mammalian replication protein A heterotrimeric complex. Exp Cell Res. 254:321-327.

Din, S., S.J. Brill, M.P. Fairman, and B. Stillman. 1990. Cell-cycle-regulated phosphorylation of DNA replication factor A from human and yeast cells. Genes Dev. 4:968-977.

Dornreiter, I., L.F. Erdile, I.U. Gilbert, D. von Winkler, T.J. Kelly, and E. Fanning. 1992a. Interaction of DNA polymerase alpha-primase with cellular replication protein A and SV40 T antigen. EMBO J. 11:769-776.

Dornreiter, I., L.F. Erdile, I.U. Gilbert, D. von Winkler, T.J. Kelly, and E. Fanning. 1992b. Interaction of the DNA polymerase alpha-primase with cellular replication protein A and SV40 T antigen. EMBO J. 11:769-776.

Dou, H., C. Huang, M. Singh, P.B. Carpenter, and E.T. Yeh. 2010a. Regulation of DNA repair through deSUMOylation and SUMOylation of replication protein A complex. Mol Cell. 39:333-345.

Dou, H., C. Huang, M. Singh, P.B. Carpenter, and E.T.H. Yeh. 2010b. Regulation of DNA Repair through DeSUMOylation and SUMOylation of Replication Protein A Complex. Molecular Cell. 39:333-345.

Dutta, A., J.M. Ruppert, J.C. Aster, and E. Winchester. 1993. Inhibition of DNA replication factor RPA by p53. Nature. 365:79-82.

Dutta, A., and B. Stillman. 1992. cdc2 family kinases phosphorylate a human cell DNA replication factor, RPA, and activate DNA replication. EMBO J. 11:2189-2199.

Eki, T., and J. Hurwitz. 1991. Influence of poly(ADP-ribose) polymerase on the enzymatic synthesis of SV40 DNA. J Biol Chem. 266:3087-3100.

Erdile, L.F., M.S. Wold, and T.J. Kelly. 1990. The primary structure of the 32-kDa subunit of human replication protein A. J Biol Chem. 265:3177-3182.

Fairman, M.P., and B. Stillman. 1988. Cellular factors required for multiple stages of SV40 DNA replication in vitro. EMBO J. 7:1211-1218.

Fang, F., and J.W. Newport. 1993a. Distinct roles of cdk2 and cdc2 in RP-A phosphorylation during the cell cycle. J Cell Sci. 106 (Pt 3):983-994.

Fang, F., and J.W. Newport. 1993b. Distinct roles of cdk2 and cdc2 in RP-A phosphorylation during the cell cycle. Journal of Cell Science. 106:983-994.

Fanning, E., V. Klimovich, and A.R. Nager. 2006a. A dynamic model for replication protein A (RPA) function in DNA processing pathways. Nucleic Acids Res. 34:4126-4137.

Fanning, E., V. Klimovich, and A.R. Nager. 2006b. A dynamic model for replication protein A (RPA) function in DNA processing pathways. Nucleic Acids Research. 34:4126-4137.

Feng, J., T. Wakeman, S. Yong, X. Wu, S. Kornbluth, and X.F. Wang. 2009. Protein phosphatase 2A-dependent dephosphorylation of replication protein A is required for the repair of DNA breaks induced by replication stress. Mol Cell Biol. 29:5696-5709.

Feng, Z., and J. Zhang. 2011. A dual role of BRCA1 in two distinct homologous recombination mediated repair in response to replication arrest. Nucleic Acids Res. 40:726-738.

Fotedar, R., and J.M. Roberts. 1992. Cell cycle regulated phosphorylation of RPA-32 occurs within the replication initiation complex. EMBO J. 11:2177-2187.

Geiss-Friedlander, R., and F. Melchior. 2007. Concepts in sumoylation: a decade on. Nat Rev Mol Cell Biol. 8:947-956.

Golub, E.I., R.C. Gupta, T. Haaf, M.S. Wold, and C.M. Radding. 1998a. Interaction of human Rad51 recombination protein with single-stranded DNA binding protein, RPA. Nucleic Acids Research. 26:5388-5393.

Golub, E.I., R.C. Gupta, T. Haaf, M.S. Wold, and C.M. Radding. 1998b. Interaction of human rad51 recombination protein with single-stranded DNA binding protein, RPA. Nucleic Acids Res. 26:5388-5393.

Gomes, X.V., and M.S. Wold. 1996. Functional Domains of the 70-Kilodalton Subunit of Human Replication Protein A†. Biochemistry. 35:10558-10568.

Guo, S., Y. Zhang, F. Yuan, Y. Gao, L. Gu, I. Wong, and G.-M. Li. 2006. Regulation of Replication Protein A Functions in DNA Mismatch Repair by Phosphorylation. Journal of Biological Chemistry. 281:21607-21616.

Haring, S.J., T.D. Humphreys, and M.S. Wold. 2010. A naturally occurring human RPA subunit homolog does not support DNA replication or cell-cycle progression. Nucleic Acids Research. 38:846-858.

He, Z., L.A. Henricksen, M.S. Wold, and C.J. Ingles. 1995. RPA involvement in the damage-recognition and incision steps of nucleotide excision repair. Nature. 374:566-569.

Helleday, T. 2003. Pathways for mitotic homologous recombination in mammalian cells. Mutat Res. 532:103-115.

Henricksen, L.A., T. Carter, A. Dutta, and M.S. Wold. 1996. Phosphorylation of human replication protein A by the DNA-dependent protein kinase is involved in the modulation of DNA replication. Nucleic Acids Res. 24:3107-3112.

Henricksen, L.A., C.B. Umbricht, and M.S. Wold. 1994. Recombinant replication protein A: expression, complex formation, and functional characterization. Journal of Biological Chemistry. 269:11121-11132.

Henricksen, L.A., and M.S. Wold. 1994. Replication protein A mutants lacking phosphorylation sites for p34cdc2 kinase support DNA replication. J Biol Chem. 269:24203-24208.

Iakoucheva, L.M., A.L. Kimzey, C.D. Masselon, J.E. Bruce, E.C. Garner, C.J. Brown, A.K. Dunker, R.D. Smith, and E.J. Ackerman. 2001. Identification of intrinsic order and disorder in the DNA repair protein XPA. Protein Sci. 10:560-571.

Iakoucheva, L.M., P. Radivojac, C.J. Brown, T.R. O'Connor, J.G. Sikes, Z. Obradovic, and A.K. Dunker. 2004. The importance of intrinsic disorder for protein phosphorylation. Nucleic Acids Res. 32:1037-1049.

Iftode, C., and J.A. Borowiec. 1998. Unwinding of origin-specific structures by human replication protein A occurs in a two-step process. Nucleic Acids Res. 26:5636-5643.

Iftode, C., and J.A. Borowiec. 2000. 5‘ → 3‘ Molecular Polarity of Human Replication Protein A (hRPA) Binding to Pseudo-Origin DNA Substrates†. Biochemistry. 39:11970-11981.

Ishiai, M., J.P. Sanchez, A.A. Amin, Y. Murakami, and J. Hurwitz. 1996. Purification, Gene Cloning, and Reconstitution of the Heterotrimeric Single-stranded DNA-binding Protein from Schizosaccharomyces pombe. Journal of Biological Chemistry. 271:20868-20878.

Jackson, D., K. Dhar, J.K. Wahl, M.S. Wold, and G.E. Borgstahl. 2002. Analysis of the human replication protein A:Rad52 complex: evidence for crosstalk between RPA32, RPA70, Rad52 and DNA. J Mol Biol. 321:133-148.

Jiang, G., Y. Zou, and X. Wu. 2012. Replication-mediated disassociation of replication protein A-XPA complex upon DNA damage: implications for RPA handing off. Cell Biol Int. 36:713-720.

Johnson, R.E., C.M. Kondratick, S. Prakash, and L. Prakash. 1999. hRAD30 mutations in the variant form of xeroderma pigmentosum. Science. 285:263-265.

Kemp, B.E., and R.B. Pearson. 1990. Protein kinase recognition sequence motifs. Trends Biochem Sci. 15:342-346.

Kemp, M.G., A.C. Mason, A. Carreira, J.T. Reardon, S.J. Haring, G.E.O. Borgstahl, S.C. Kowalczykowski, A. Sancar, and M.S. Wold. 2010. An Alternative Form of Replication Protein A Expressed in Normal Human Tissues Supports DNA Repair. Journal of Biological Chemistry. 285:4788-4797.

Kenny, M.K., S.H. Lee, and J. Hurwitz. 1989. Multiple functions of human single-stranded-DNA binding protein in simian virus 40 DNA replication: single-strand stabilization and stimulation of DNA polymerases alpha and delta. Proceedings of the National Academy of Sciences. 86:9757-9761.

Keshav, K.F., C. Chen, and A. Dutta. 1995. Rpa4, a homolog of the 34-kilodalton subunit of the replication protein A complex. Molecular and Cellular Biology. 15:3119-3128.

Kim, C., B.F. Paulus, and M.S. Wold. 1994. Interactions of human replication protein A with oligonucleotides. Biochemistry. 33:14197-14206.

Kim, C., R.O. Snyder, and M.S. Wold. 1992. Binding properties of replication protein A from human and yeast cells. Molecular and Cellular Biology. 12:3050-3059.

Kim, D.-K., E. Stigger, and S.-H. Lee. 1996. Role of the 70-kDa Subunit of Human Replication Protein A (I). Journal of Biological Chemistry. 271:15124-15129.

Kim, H.-S., and S.J. Brill. 2003. MEC1-dependent phosphorylation of yeast RPA1 in vitro. DNA Repair. 2:1321-1335.

Kim, S.T., D.S. Lim, C.E. Canman, and M.B. Kastan. 1999. Substrate specificities and identification of putative substrates of ATM kinase family members. J Biol Chem. 274:37538-37543.

Kolpashchikov, D.M., S.N. Khodyreva, D.Y. Khlimankov, M.S. Wold, A. Favre, and O.I. Lavrik. 2001. Polarity of human replication protein A binding to DNA. Nucleic Acids Research. 29:373-379.

Kurimasa, A., S. Kumano, N.V. Boubnov, M.D. Story, C.S. Tung, S.R. Peterson, and D.J. Chen. 1999. Requirement for the kinase activity of human DNA-dependent protein kinase catalytic subunit in DNA strand break rejoining. Mol Cell Biol. 19:3877-3884.

Lee, D.H., Y. Pan, S. Kanner, P. Sung, J.A. Borowiec, and D. Chowdhury. 2010. A PP4 phosphatase complex dephosphorylates RPA2 to facilitate DNA repair via homologous recombination. Nat Struct Mol Biol. 17:365-372.

Lee, S.H., and D.K. Kim. 1995. The role of the 34-kDa subunit of human replication protein A in simian virus 40 DNA replication in vitro. J Biol Chem. 270:12801-12807.

Lee, J., A. Kumagai, and W.G. Dunphy. 2003. Claspin, a Chk1-regulatory protein, monitors DNA replication on chromatin independently of RPA, ATR, and Rad17. Mol Cell. 11:329-40.

Li, L., X. Lu, C.A. Peterson, and R.J. Legerski. 1995. An interaction between the DNA repair factor XPA and replication protein A appears essential for nucleotide excision repair. Mol Cell Biol. 15:5396-5402.

Liaw, H., D. Lee, and K. Myung. 2011. DNA-PK-Dependent RPA2 Hyperphosphorylation Facilitates DNA Repair and Suppresses Sister Chromatid Exchange. PLoS ONE. 6:e21424.

Lindahl, T., and R.D. Wood. 1999. Quality control by DNA repair. Science. 286:1897-1905.

Liu, J.-S., S.-R. Kuo, and T. Melendy. 2006. Phosphorylation of replication protein A by S-phase checkpoint kinases. DNA Repair. 5:369-380.

Liu, V.F., and D.T. Weaver. 1993. The ionizing radiation-induced replication protein A phosphorylation response differs between ataxia telangiectasia and normal human cells. Mol Cell Biol. 13:7222-7231.

Liu, Y., M. Kvaratskhelia, S. Hess, Y. Qu, and Y. Zou. 2005a. Modulation of Replication Protein A Function by Its Hyperphosphorylation-induced Conformational Change Involving DNA Binding Domain B. Journal of Biological Chemistry. 280:32775-32783.

Liu, Y., M. Kvaratskhelia, S. Hess, Y. Qu, and Y. Zou. 2005b. Modulation of replication protein A function by its hyperphosphorylation-induced conformational change involving DNA binding domain B. J Biol Chem. 280:32775-32783.

Manthey, K.C., S. Opiyo, J.G. Glanzer, D. Dimitrova, J. Elliott, and G.G. Oakley. 2007. NBS1 mediates ATR-dependent RPA hyperphosphorylation following replication-fork stall and collapse. J Cell Sci. 120:4221-4229.

Mason, A.C., S.J. Haring, J.M. Pryor, C.A. Staloch, T.F. Gan, and M.S. Wold. 2009a. An Alternative Form of Replication Protein A Prevents Viral Replication in Vitro. Journal of Biological Chemistry. 284:5324-5331.

Mason, A.C., S.J. Haring, J.M. Pryor, C.A. Staloch, T.F. Gan, and M.S. Wold. 2009b. An alternative form of replication protein a prevents viral replication in vitro. J Biol Chem. 284:5324-5331.

Mason, A.C., R. Roy, D.T. Simmons, and M.S. Wold. 2010. Functions of Alternative Replication Protein A in Initiation and Elongation. Biochemistry. 49:5919-5928.

Masutani, C., R. Kusumoto, A. Yamada, N. Dohmae, M. Yokoi, M. Yuasa, M. Araki, S. Iwai, K. Takio, and F. Hanaoka. 1999. The XPV (xeroderma pigmentosum variant) gene encodes human DNA polymerase eta. Nature. 399:700-704.

Matsuda, T., M. Saijo, I. Kuraoka, T. Kobayashi, Y. Nakatsu, A. Nagai, T. Enjoji, C. Masutani, K. Sugasawa, F. Hanaoka, and et al. 1995. DNA repair protein XPA binds replication protein A (RPA). J Biol Chem. 270:4152-4157.

Matsumoto, T., T. Eki, and J. Hurwitz. 1990. Studies on the initiation and elongation reactions in the simian virus 40 DNA replication system. Proceedings of the National Academy of Sciences. 87:9712-9716.

Matsuoka, S., B.A. Ballif, A. Smogorzewska, E.R. McDonald, 3rd, K.E. Hurov, J. Luo, C.E. Bakalarski, Z. Zhao, N. Solimini, Y. Lerenthal, Y. Shiloh, S.P. Gygi, and S.J. Elledge. 2007a. ATM and ATR substrate analysis reveals extensive protein networks responsive to DNA damage. Science. 316:1160-1166.

Matsuoka, S., B.A. Ballif, A. Smogorzewska, E.R. McDonald, K.E. Hurov, J. Luo, C.E. Bakalarski, Z. Zhao, N. Solimini, Y. Lerenthal, Y. Shiloh, S.P. Gygi, and S.J. Elledge. 2007b. ATM and ATR Substrate Analysis Reveals Extensive Protein Networks Responsive to DNA Damage. Science. 316:1160-1166.

Melendy, T., and B. Stillman. 1993a. An interaction between replication protein A and SV40 T antigen appears essential for primosome assembly during SV40 DNA replication. J Biol Chem. 268:3389-3395.

Melendy, T., and B. Stillman. 1993b. An interaction between replication protein A and SV40 T antigen appears essential for primosome assembly during SV40 DNA replication. J. Biol. Chem. 268:3389-3395.

Mer, G., A. Bochkarev, R. Gupta, E. Bochkareva, L. Frappier, C.J. Ingles, A.M. Edwards, and W.J. Chazin. 2000. Structural basis for the recognition of DNA repair proteins UNG2, XPA, and RAD52 by replication factor RPA. Cell. 103:449-456.

Mullenders, L.H., and M. Berneburg. 2001. Photoimmunology and nucleotide excision repair: impact of transcription coupled and global genome excision repair. J Photochem Photobiol B. 65:97-100.

Murzin, A. 1993. OB (oligonucleotide/oligosaccharide binding)-fold: common structural and functional solution for non-homologous sequences. EMBO J. 12:861-867.

Nagelhus, T.A., T. Haug, K.K. Singh, K.F. Keshav, F. Skorpen, M. Otterlei, S. Bharati, T. Lindmo, S. Benichou, R. Benarous, and H.E. Krokan. 1997. A Sequence in the N-terminal Region of Human Uracil-DNA Glycosylase with Homology to XPA Interacts with the C-terminal Part of the 34-kDa Subunit of Replication Protein A. Journal of Biological Chemistry. 272:6561-6566.

Namiki, Y., and L. Zou. 2006. ATRIP associates with replication protein A-coated ssDNA through multiple interactions. Proc Natl Acad Sci U S A. 103:580-585.

Nasheuer, H.-P., D. von Winkler, C. Schneider, I. Dornreiter, I. Gilbert, and E. Fanning. 1992. Purification and functional characterization of bovine RP-A in an<i>in vitro SV40 DNA replication system. Chromosoma. 102:S52-S59.

Niu, H., H. Erdjument-Bromage, Z.Q. Pan, S.H. Lee, P. Tempst, and J. Hurwitz. 1997. Mapping of amino acid residues in the p34 subunit of human single-stranded DNA-binding protein phosphorylated by DNA-dependent protein kinase and Cdc2 kinase in vitro. J Biol Chem. 272:12634-12641.

Nuss, J.E., S.M. Patrick, G.G. Oakley, G.M. Alter, J.G. Robison, K. Dixon, and J.J. Turchi. 2005a. DNA damage induced hyperphosphorylation of replication protein A. 1. Identification of novel sites of phosphorylation in response to DNA damage. Biochemistry. 44:8428-8437.

Nuss, J.E., S.M. Patrick, G.G. Oakley, G.M. Alter, J.G. Robison, K. Dixon, and J.J. Turchi. 2005b. DNA Damage Induced Hyperphosphorylation of Replication Protein A. 1. Identification of Novel Sites of Phosphorylation in Response to DNA Damage†. Biochemistry. 44:8428-8437.

O'Meara, E., S.v. Cruet-Hennequart, and M.P. Carty. 2010. Analysis of Protein Phosphorylation in Cisplatin-Treated Human Cells Following Annexin V-based Separation and Multi-Antibody Screening. Cancer Genomics - Proteomics. 7:279-286.

Oakley, G.G., L.I. Loberg, J. Yao, M.A. Risinger, R.L. Yunker, M. Zernik-Kobak, K.K. Khanna, M.F. Lavin, M.P. Carty, and K. Dixon. 2001. UV-induced hyperphosphorylation of replication protein a depends on DNA replication and expression of ATM protein. Mol Biol Cell. 12:1199-1213.

Oakley, G.G., S.M. Patrick, J. Yao, M.P. Carty, J.J. Turchi, and K. Dixon. 2003. RPA phosphorylation in mitosis alters DNA binding and protein-protein interactions. Biochemistry. 42:3255-3264.

Olson, E., C.J. Nievera, V. Klimovich, E. Fanning, and X. Wu. 2006. RPA2 is a direct downstream target for ATR to regulate the S-phase checkpoint. J Biol Chem. 281:39517-39533.

Ozawa, K., F.B. Dean, M. Chen, S.-H. Lee, A. Shiratori, Y. Murakami, T. Sakakura, J. Hurwitz, and T. Eki. 1993. Mapping of the 70 kDa, 34 kDa, and 11 kDa Subunit Genes of the Human Multimeric Single-stranded DNA Binding Protein (hSSB/RPA) to Chromosome Bands 17p13, 1p35-p36.1, and 7p21-p22. Cell Structure and Function. 18:221-230.

Pan, Z.Q., C.H. Park, A.A. Amin, J. Hurwitz, and A. Sancar. 1995. Phosphorylated and unphosphorylated forms of human single-stranded DNA-binding protein are equally active in simian virus 40 DNA replication and in nucleotide excision repair. Proc Natl Acad Sci U S A. 92:4636-4640.

Park, M.S., D.L. Ludwig, E. Stigger, and S.-H. Lee. 1996. Physical Interaction between Human RAD52 and RPA Is Required for Homologous Recombination in Mammalian Cells. Journal of Biological Chemistry. 271:18996-19000.

Patrick, S.M., G.G. Oakley, K. Dixon, and J.J. Turchi. 2005a. DNA damage induced hyperphosphorylation of replication protein A. 2. Characterization of DNA binding activity, protein interactions, and activity in DNA replication and repair. Biochemistry. 44:8438-8448.

Patrick, S.M., G.G. Oakley, K. Dixon, and J.J. Turchi. 2005b. DNA Damage Induced Hyperphosphorylation of Replication Protein A. 2. Characterization of DNA Binding Activity, Protein Interactions, and Activity in DNA Replication and Repairâ€ Biochemistry. 44:8438-8448.

Patrick, S.M., and J.J. Turchi. 1998a. Human replication protein A preferentially binds cisplatin-damaged duplex DNA in vitro. Biochemistry. 37:8808-8815.

Patrick, S.M., and J.J. Turchi. 1998b. Human Replication Protein A Preferentially Binds Cisplatin-Damaged Duplex DNA in Vitro†. Biochemistry. 37:8808-8815.

Patrick, S.M., and J.J. Turchi. 1999. Replication Protein A (RPA) Binding to Duplex Cisplatin-damaged DNA Is Mediated through the Generation of Single-stranded DNA. Journal of Biological Chemistry. 274:14972-14978.

Ramilo, C., L. Gu, S. Guo, X. Zhang, S.M. Patrick, J.J. Turchi, and G.-M. Li. 2002. Partial Reconstitution of Human DNA Mismatch Repair In Vitro: Characterization of the Role of Human Replication Protein A. Molecular and Cellular Biology. 22:2037-2046.

Rechkunova, N.I., and O.I. Lavrik. 2010. Nucleotide excision repair in higher eukaryotes: mechanism of primary damage recognition in global genome repair. Subcell Biochem. 50:251-277.

Recolin, B., S. Van der Laan, and D. Maiorano. 2012. Role of replication protein A as sensor in activation of the S-phase checkpoint in *Xenopus* egg extracts. Nucleic Acids Res. 40:3431-42.

Riedl, T., F. Hanaoka, and J.M. Egly. 2003. The comings and goings of nucleotide excision repair factors on damaged DNA. EMBO J. 22:5293-5303.

Rodrigo, G., S. Roumagnac, M.S. Wold, B. Salles, and P. Calsou. 2000. DNA replication but not nucleotide excision repair is required for UVC-induced replication protein A phosphorylation in mammalian cells. Mol Cell Biol. 20:2696-2705.

Sakasai, R., K. Shinohe, Y. Ichijima, N. Okita, A. Shibata, K. Asahina, and H. Teraoka. 2006. Differential involvement of phosphatidylinositol 3-kinase-related protein kinases in hyperphosphorylation of replication protein A2 in response to replication-mediated DNA double-strand breaks. Genes Cells. 11:237-246.

San Filippo, J., P. Sung, and H. Klein. 2008. Mechanism of eukaryotic homologous recombination. Annu Rev Biochem. 77:229-257.

Serrano, M.A., Z. Li, M. Dangeti, P.R. Musich, S. Patrick, M. Roginskaya, B. Cartwright, and Y. Zou. 2012. DNA-PK, ATM and ATR collaboratively regulate p53-RPA interaction to facilitate homologous recombination DNA repair. Oncogene.

Shao, R.G., C.X. Cao, H. Zhang, K.W. Kohn, M.S. Wold, and Y. Pommier. 1999. Replication-mediated DNA damage by camptothecin induces phosphorylation of RPA by DNA-dependent protein kinase and dissociates RPA:DNA-PK complexes. EMBO J. 18:1397-1406.

Shi, W., Z. Feng, J. Zhang, I. Gonzalez-Suarez, R.P. Vanderwaal, X. Wu, S.N. Powell, J.L. Roti Roti, and S. Gonzalo. 2010. The role of RPA2 phosphorylation in homologous recombination in response to replication arrest. Carcinogenesis. 31:994-1002.

Shuck, S.C., and J.J. Turchi. 2010. Targeted inhibition of Replication Protein A reveals cytotoxic activity, synergy with chemotherapeutic DNA-damaging agents, and insight into cellular function. Cancer Res. 70:3189-3198.

Stephan, H., C. Concannon, E. Kremmer, M.P. Carty, and H.P. Nasheuer. 2009. Ionizing radiation-dependent and independent phosphorylation of the 32-kDa subunit of replication protein A during mitosis. Nucleic Acids Res. 37:6028-6041.

Stigger, E., F.B. Dean, J. Hurwitz, and S.H. Lee. 1994. Reconstitution of functional human single-stranded DNA-binding protein from individual subunits expressed by recombinant baculoviruses. Proceedings of the National Academy of Sciences. 91:579-583.

Stigger, E., R. Drissi, and S.H. Lee. 1998. Functional analysis of human replication protein A in nucleotide excision repair. J Biol Chem. 273:9337-9343.

Stokes, M.P., J. Rush, J. MacNeill, J.M. Ren, K. Sprott, J. Nardone, V. Yang, S.A. Beausoleil, S.P. Gygi, M. Livingstone, H. Zhang, R.D. Polakiewicz, and M.J. Comb. 2007. Profiling of UV-induced ATM/ATR signaling pathways. Proceedings of the National Academy of Sciences. 104:19855-19860.

Sugiyama, T., and S.C. Kowalczykowski. 2002. Rad52 protein associates with replication protein A (RPA)-single-stranded DNA to accelerate Rad51-mediated displacement of RPA and presynaptic complex formation. J Biol Chem. 277:31663-31672.

Thoma, B.S., and K.M. Vasquez. 2003. Critical DNA damage recognition functions of XPC-hHR23B and XPA-RPA in nucleotide excision repair. Mol Carcinog. 38:1-13.

Tornaletti, S. 2009. DNA Repair in Mammalian Cells. Cellular and Molecular Life Sciences. 66:1010-1020.

Treuner, K., A. Okuyama, R. Knippers, and F.O. Fackelmayer. 1999. Hyperphosphorylation of replication protein A middle subunit (RPA32) in apoptosis. Nucleic Acids Res. 27:1499-1504.

Treuner, K., U. Ramsperger, and R. Knippers. 1996. Replication Protein A Induces the Unwinding of Long Double-stranded DNA Regions. Journal of Molecular Biology. 259:104-112.

Umbricht, C.B., C.A. Griffin, A.L. Hawkins, K.H. Grzeschik, P. O'Connell, R. Leach, E.D. Green, and T.J. Kelly. 1994. High-Resolution Genomic Mapping of the Three Human Replication Protein A Genes (RPA1, RPA2, and RPA3). Genomics. 20:249-257.

Umezu, K., N. Sugawara, C. Chen, J.E. Haber, and R.D. Kolodner. 1998. Genetic Analysis of Yeast RPA1 Reveals Its Multiple Functions in DNA Metabolism. Genetics. 148:989-1005.

Vassin, V.M., M.S. Wold, and J.A. Borowiec. 2004. Replication Protein A (RPA) Phosphorylation Prevents RPA Association with Replication Centers. Mol. Cell. Biol. 24:1930-1943.

Wobbe, C.R., L. Weissbach, J.A. Borowiec, F.B. Dean, Y. Murakami, P. Bullock, and J. Hurwitz. 1987. Replication of simian virus 40 origin-containing DNA in vitro with purified proteins. Proceedings of the National Academy of Sciences. 84:1834-1838.

Wold, M.S., and T. Kelly. 1988. Purification and characterization of replication protein A, a cellular protein required for in vitro replication of simian virus 40 DNA. Proceedings of the National Academy of Sciences. 85:2523-2527.

Wold, M.S., J.J. Li, and T.J. Kelly. 1987. Initiation of simian virus 40 DNA replication in vitro: large-tumor-antigen- and origin-dependent unwinding of the template. Proc Natl Acad Sci U S A. 84:3643-3647.

Wood, R.D., M. Mitchell, J. Sgouros, and T. Lindahl. 2001. Human DNA repair genes. Science. 291:1284-1289.

Wu, X., Z. Yang, Y. Liu, and Y. Zou. 2005. Preferential localization of hyperphosphorylated replication protein A to double-strand break repair and checkpoint complexes upon DNA damage. Biochem J. 391:473-480.

Yeh, E.T.H. 2009. SUMOylation and De-SUMOylation: Wrestling with Life's Processes. Journal of Biological Chemistry. 284:8223-8227.

Zernik-Kobak, M., K. Vasunia, M. Connelly, C.W. Anderson, and K. Dixon. 1997. Sites of UV-induced phosphorylation of the p34 subunit of replication protein A from HeLa cells. J Biol Chem. 272:23896-23904.

Zhao, H., and H. Piwnica-Worms. 2001. ATR-mediated checkpoint pathways regulate phosphorylation and activation of human Chk1. Mol Cell Biol. 21:4129-4139.

Zou, L., and S.J. Elledge. 2003. Sensing DNA damage through ATRIP recognition of RPA-ssDNA complexes. Science. 300:1542-1548.

Appendix E: Authors funding and contributions

FUNDING

Personal studentship award from the Irish Research Council (IRC, formerly IRCSET) for pursuing PhD degree (2008-2011).

The Beckman Fund Scholarship, National University of Ireland Galway (2009).

Travel Award for the Irish Association for Cancer Research (IACR) annual conference (2010).

The Thomas Crawford Hayes Trust Fund Scheme Award, National University of Ireland Galway (2010).

The Beckman Fund Scholarship, National University of Ireland Galway (2011).

The Thomas Crawford Hayes Trust Fund Scheme Award, National University of Ireland Galway (2011).

National University of Ireland, Galway write-up bursary 2012

ORAL PRESENTATIONS (presenter underlined)

Selected for oral presentation at the EMBO Young Scientists Forum 2011, International Institute of Molecular and Cell Biology, Warsaw, Poland, June 30th – July 1st, 2011:
Sokol A.M., Bianco J., Cruet-Hennequart S., Pasero P. and Carty M.P. *Analysis of cisplatin- and carboplatin-induced DNA replication arrest in DNA polymerase η-deficient human cells.*

Selected for oral poster presentation at the Responses to DNA damage: from molecular mechanism to human disease 2011 Conference, Egmond aan Zee, The Netherlands, April 3rd – 8th, 2011:
Sokol A.M., Bianco J., Cruet-Hennequart S., Pasero P. and Carty M.P. *Analysis of cisplatin- and carboplatin-induced DNA replication arrest in DNA polymerase η-deficient human cells.*

POSTER PRESENTATIONS

Maintenance of Genome Stability 2010 Conference, Antigua, March 8th – 11th, 2010:
Sokol A.M., Bianco J., Cruet-Hennequart S., Pasero P. and Carty M.P. *Translesion synthesis by human DNA polymerase η in the cellular response to DNA damage by cisplatin and carboplatin.*

* Irish Association for Cancer Research, 2010 Annual Conference, Galway, Ireland, March 3rd – 5th, 2010:
Sokol A.M., Bianco J., Cruet-Hennequart S., Pasero P. and Carty M.P. *Characterisation of the role of translesion synthesis by DNA polymerase η and DNA damage signalling in the cellular response to cisplatin and carboplatin.*

(*) Award winning poster